

**Microalgae as candidate for phenol  
bioremediation and biofuel production**

**A Thesis**

**Submitted in Partial**

**Fulfillment of the Requirements for the Degree of**

**DOCTOR OF PHILOSOPHY**

**By**

**BHASKAR DAS**




**CENTRE FOR THE ENVIRONMENT**

**INDIAN INSTITUTE OF TECHNOLOGY GUWAHATI**

**GUWAHATI-781039, ASSAM, INDIA**

**February 2016**

The logo of Indian Institute of Technology Guwahati is a circular emblem. It features a central stylized 'S' or '3' shape composed of three interlocking circles. The text 'Indian Institute of Technology Guwahati' is written in English around the bottom half of the circle, and its Hindi equivalent 'भारतीय प्रौद्योगिकी संस्थान गुवाहाटी' is written along the top half.

**DEDICATED  
TO  
MY PARENTS  
AND  
MY TEACHERS**



INDIAN INSTITUTE OF TECHNOLOGY GUWAHATI

CENTRE FOR THE ENVIRONMENT

## STATEMENT

I do hereby declare that the matter embodied in this thesis entitled “*Microalgae as candidate for phenol bioremediation and biofuel production*” is the result of investigations carried out by me in the Centre for the Environment, Indian Institute of Technology Guwahati, India under the supervision of Dr. Sanjukta Patra and co-supervision of Dr. Tapas K Mandal.

In keeping with the general practice of reporting scientific observations due acknowledgements have been made wherever the work described is based on the findings of other investigators.

February 2016

Mr. Bhaskar Das

Roll No: 09615205



**INDIAN INSTITUTE OF TECHNOLOGY GUWAHATI**  
**CENTRE FOR THE ENVIRONMENT**

**CERTIFICATE**

It is certified that the work described in the thesis entitled “*Microalgae as candidate for phenol bioremediation and biofuel production*” by Bhaskar Das (Roll No: 09615205) for the award of degree of Doctor of Philosophy is an authentic record of the results obtained from the research work carried out under our supervision in the Centre for the Environment, Indian Institute of Technology Guwahati, India and this work has not been submitted elsewhere for a degree.

**Dr. Sanjukta Patra**

Associate Professor

Dept. of Biosciences and Bioengineering

Indian Institute of Technology Guwahati

Guwahati-781039, India.

**(Thesis Supervisor)**

**Dr. Tapas K Mandal**

Associate Professor

Dept. of Chemical Engineering

Indian Institute of Technology Guwahati

Guwahati-781039, India

**(Thesis Co-supervisor)**

## Acknowledgements

I take this opportunity to express my sincere thanks to everyone who has been with me through this entire journey. Firstly, I would like to extend my heartfelt thanks to my thesis supervisor Dr.Sanjukta Patra and my thesis co-supervisor Dr.Tapas K Mandal for their constant guidance and inspiration through the entire period of research. I feel myself fortunate to work under their esteemed guidance as their knowledge made my work fruitful. Without them the dissertation would not have been possible.

I would also like to extend my heartfelt gratitude to my doctoral committee members Dr.Vikash Kumar Dubey, Dr Venkata V. Dasu, Dr.Vishal Trivedi and Dr.Chandan Mahanta for evaluating my work, giving critical comments and valuable guidance.

I am grateful to Indian Institute of Technology Guwahati, India for providing the best lab facilities to carry out my doctoral research. I am also grateful to the successive heads of the Centre for the Environment, IIT Guwahati, Dr. Chandan Mahanta, Dr. Gopal Das and Dr. Vikash Kumar Dubey for providing me the departmental facilities for carrying out my doctoral research. I also owe my thanks to Scientific Officer Dr.Deepmoni Deka and Technical Assistant Partha Pratim Bakal as well as office staff of the centre.

I am thankful to my lab members Gowtham Selvaraj, Dr. P. Saravanan, Debomitra Chakraborty, Nivedita Singh, Mohd. Faheem Khan and Nitendra Yadav for their support, help and encouragement.

I take this opportunity to express my heartfelt thanks especially to Gowtham Selvaraj, Mohd. Faheem Khan and Nitendra Yadav who had been with me in my difficult times. They made my stay in the campus enjoyable and a memorable one.

I dedicate this work to my father, Mr. Bhupen Das, my mother Mrs. Chitra Das and my grandma Late. Mrs. Bhagawati Bala Das for their unconditional love, support encouragement, blessings and belief in me which motivated me to achieve my goals.

Finally, I extend my gratitude to the almighty God for giving me the opportunity, strength and blessings to carry out my work properly.

*Bhaskar Das.*

*February 2016*



## Abstract

Phenol is a xenobiotic released in wastewaters of industries as coal industries, phenol manufacturing, pharmaceuticals, dying, petrochemicals, pulp mill etc. Owing to high ecological toxicity risks of phenol it is considered a priority pollutant requiring efficient phenol removal technologies from industrial wastewater. Biological treatment of phenol has gained wide interest owing to its advantages of complete phenol mineralization and cost effectiveness. Phenol degradation capabilities of bacteria and fungi have been profoundly studied compared to that in algae. Six algal strains were screened for phenol degradation ability of which Spirogyra, Closterium and two unidentified algae were isolated from sewage wastewater, one diatom strain BD1IITG was isolated from petroleum refinery wastewater and *Chlorella Pyrenoidosa* (NCIM 2738) was obtained from National Collection of Industrial Microorganisms, Pune. Out of the six microalgal isolates, *C.pyrenoidosa* and diatom BD1IITG showed significant capability for phenol degradation showing prospective application for phenol remediation. The growth and phenol degradation dynamics of two potent algal strains *C.pyrenoidosa* and diatom BD1IITG was analyzed by growth kinetic modeling. The practical applicability of the strain for degradation of phenol in petroleum refinery wastewater was also evaluated. Owing to the complete phenol degradation ability of *C.pyrenoidosa*, the strain was used to develop an efficient phenol degradation process that could remediate phenol concentration in the range of 50-1200 mg/l within a short time period. Pre adaptation of *C.pyrenoidosa* to the target phenol concentration is being used as a strategy to further enhance growth ( $0.078 \text{ h}^{-1}$ ) and phenol degradation rate ( $0.636 \text{ h}^{-1}$ ). Pre adaptation of *C.pyrenoidosa* leads to higher  $\mu_{\max}$  value ( $0.22 \text{ h}^{-1}$ ),  $K_s$  value (500.54 mg/l) and  $K_i$  value (900.41 mg/l) resulting in efficient growth at high phenol concentration. Pre adapted biomass after phenol degradation showed prominent enhancement in total lipid and neutral lipid productivity suggesting exciting possibility to be used as biodiesel feedstock. The ability of pre adapted cells to completely degrade 10 mg/l and 250 mg/l phenol in petroleum refinery wastewater with high growth kinetic parameters adds to practical applicability of the process. High lipid as well as neutral lipid productivities obtained in spent biomass after treatment of phenol containing

refinery wastewater qualifies the process as a source of algal biodiesel feedstock. The lipid extracted biomass from *C.pyrenoidosa* was used as substrate for bioethanol fermentation further enhancing its economic feasibility for biofuel applications. The metabolic pathways involved in phenol biodegradation have not been well studied in microalgae. This present work reports for the first time the complete pathway of phenol degradation in *Chlorella pyrenoidosa* and diatom BD1IITG using HPLC, LC-MS and UV-Visible spectrophotometry. Both the algal strains degrades phenol by both ortho and meta pathway with prominence of ortho over meta pathway. Phenol hydroxylase is the first enzyme causing initial attack on phenol in the phenol degradation pathway. There is scarcity of information regarding characterization of kinetic properties of any microalgal phenol hydroxylases. In the present study, microalgal phenol hydroxylase from *C.pyrenoidosa* has been purified and characterized. The phenol utilization by the purified enzyme followed Michealis Menten kinetics with apparent Michealis constant ( $K_m$ ) for oxidation of phenol estimated to be 1.71  $\mu\text{M}$  and the maximal velocity ( $V_{max}$ ) of 0.4  $\mu\text{M}/\text{min}$ . The optimal pH and temperature for enzyme activity was found to be pH 7 and 35°C respectively. Phenanthroline and sodium arsenate (chelator  $\text{Fe}^{2+}$ ) showed inhibition of phenol hydroxylation suggesting presence of Fe-S clusters. The inhibitory effect of heavy metals, denaturants and oxidizing agents on phenol hydroxylation activity of the purified enzyme have been verified. The enzyme has broad substrate specificity against isomeric diphenols (catechol, resorcinol, quinol), isomeric methylphenols (o- cresol, m-cresol, p-cresol), halogen substituted phenols (2-chlorophenol, 4-chlorophenol, 2,4- chlorophenol, p-bromophenol,), amino substituted phenols (2-aminophenol, 3-aminophenol),4-nitrophenol, p- hydroxybenzaldehyde ,m-hydroxybenzaldehyde and p-hydroxylbenzoic acid. The enzyme shows remarkable storage stability at room temperature and at 4°C with approximately no loss of activity till 3<sup>rd</sup> day and 5<sup>th</sup> day respectively. The characterization of properties of microalgal phenol hydroxylase gains importance as the information could be instrumental in developing enzyme based phenol remediation technology or phenol biosensor.



# Graphical Abstract

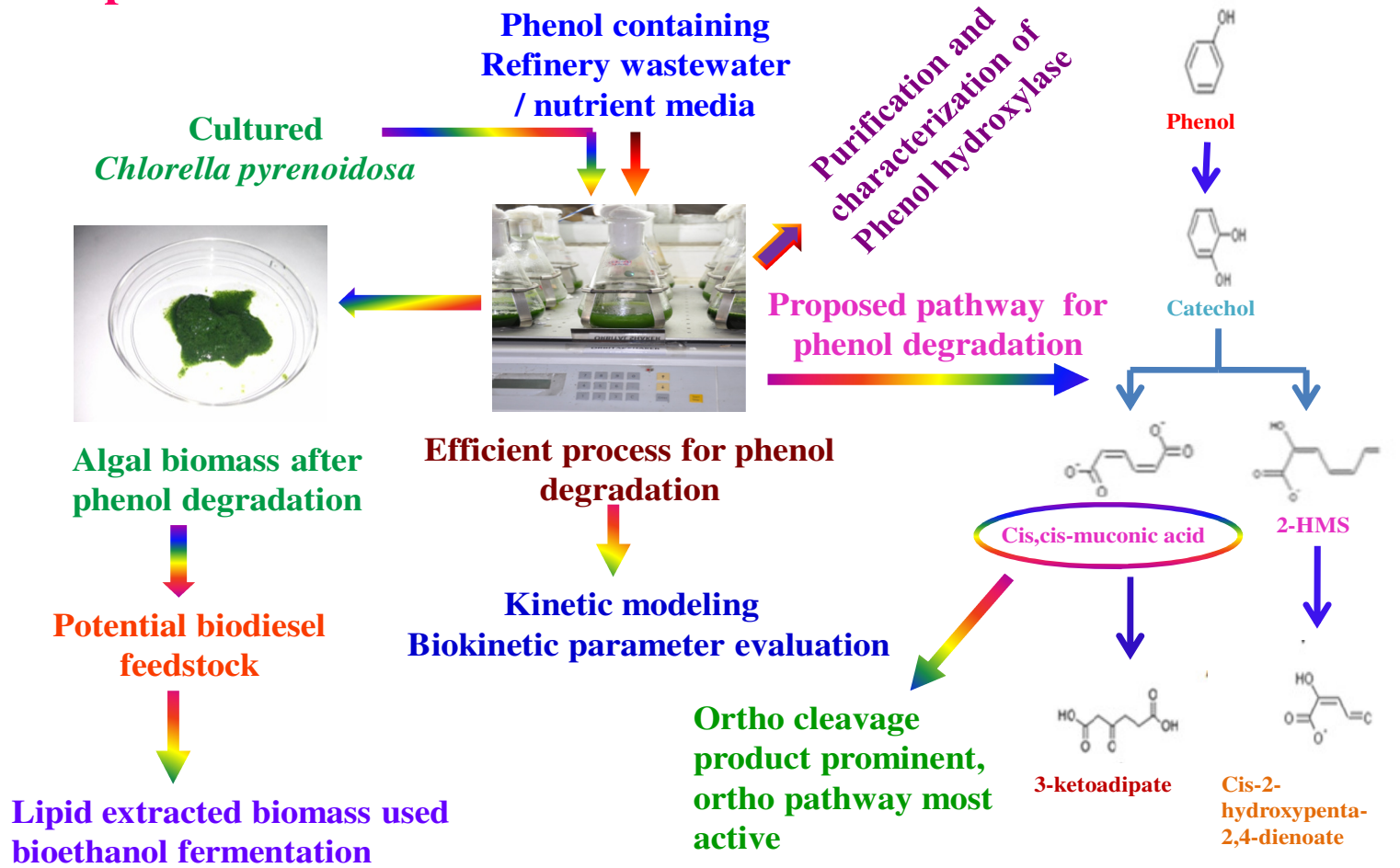


## Table of Contents

| <b>Contents</b>  | <b>Page</b> |
|--|-------------|
| Abstract   | i-ii        |
| Graphical abstract   | iii         |
| Table of Contents  | iv-ix       |
| List of Tables   | x-xi        |
| List of Figures  | xii-xviii   |
| <b>Chapter I: Introduction and Literature Review</b>                                   | <b>1-45</b> |
| <b>1.1</b> Abstract  | 2           |
| <b>1.2</b> Introduction  | 3-8         |
| <b>1.3</b> Phenol as a pollutant   | 8-10        |
| <b>1.4</b> Ecological Toxicity of Phenol   | 11-14       |
| <b>1.5</b> Methods for treatment of phenol pollution                                   | 14-28       |
| <b>1.5.1</b> Solvent extraction  | 15          |
| <b>1.5.2</b> Photodecomposition  | 15          |
| <b>1.5.3</b> Advanced oxidation processes  | 15          |
| <b>1.5.4</b> Adsorption  | 16          |
| <b>1.5.5</b> Electro-Fenton method   | 16          |
| <b>1.5.6</b> Biological Treatment  | 16-28       |
| <b>1.6</b> Microalgal wastewater treatment: Future of sustainable wastewater treatment | 29-33       |
| <b>1.7</b> Mechanism of aerobic phenol biodegradation                                  | 33-36       |
| <b>1.8</b> Phenol hydroxylase enzymes: Characteristics and potential applications      | 37-43       |
| <b>1.9</b> Significance of the work  | 44-45       |

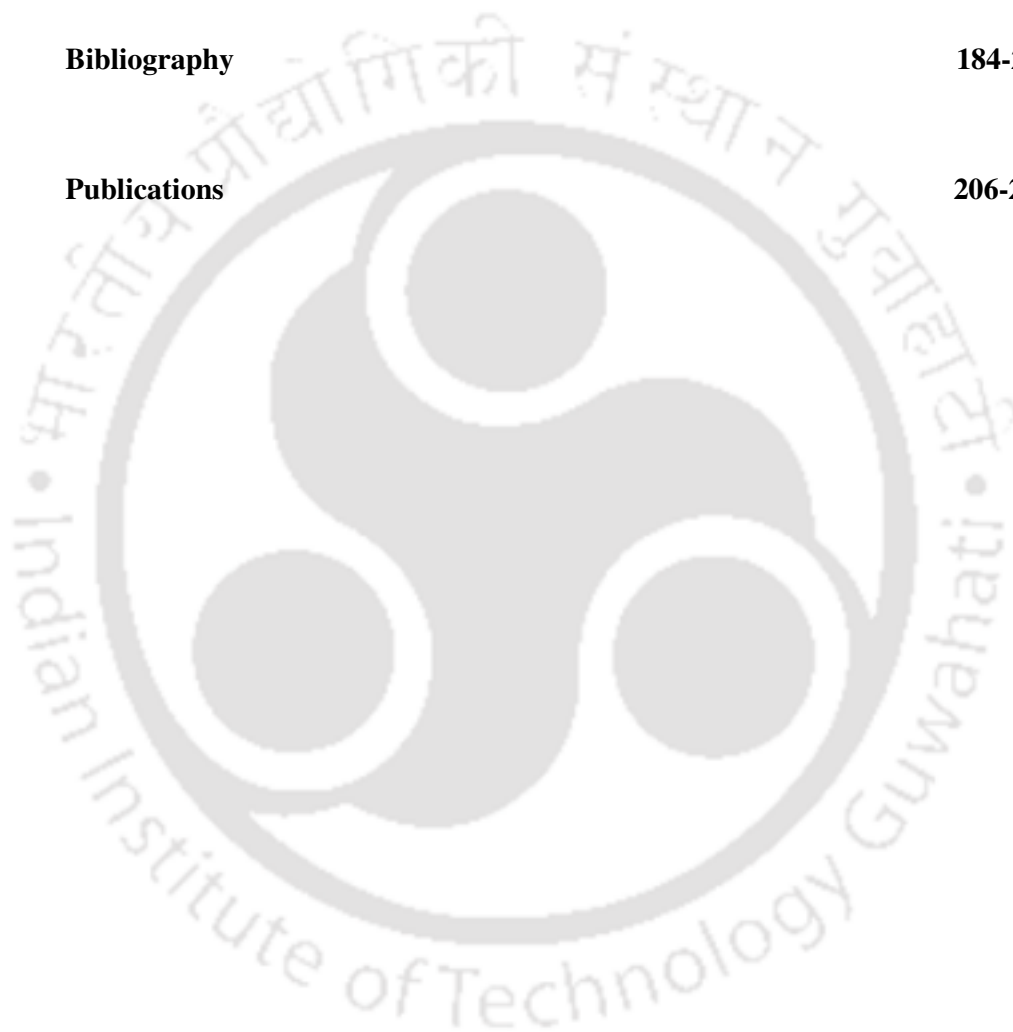
|  |              |
|--|--------------|
| <b>Chapter II: Materials and Methods</b>   | <b>46-61</b> |
| <b>2.1 Screening and characterization of phenol degradation by potent algal strains</b>                          | <b>47-50</b> |
| 2.1.1 Isolation and identification of algal strains  | 47-48        |
| 2.1.2 Screening of potent phenol degrading algal strains   | 48           |
| 2.1.3 Growth kinetics and phenol degradation by potent algal strains   | 48-49        |
| 2.1.4 Analysis of biosurfactant production   | 50           |
| 2.1.5 Analysis of effect of phenol on cell surface morphology  | 50           |
| <b>2.2 Generation of microalgae based process for efficient phenol remediation as well as biofuel production</b> | <b>50-55</b> |
| 2.2.1 Analysis of growth kinetics and phenol degradation by phenol acclimatized cells of <i>C.pyrenoidosa</i>    | 50-51        |
| 2.2.2 Effect of physical parameters on phenol degradation rate   | 51-52        |
| 2.2.3 Growth kinetics and phenol degradation by pre adapted cells  | 52-53        |
| 2.2.4 Practical application of pre adapted microalgae for phenol degradation                                     | 53           |
| 2.2.5 Biochemical characterization of phenol degrading biomass   | 53-54        |
| 2.2.6 Bioethanol fermentation of lipid extracted residual biomass  | 54-55        |
| <b>2.3 Elucidation of pathway of phenol degradation</b>  | <b>55-56</b> |
| 2.3.1 Preparation of crude enzyme extract  | 55-56        |
| 2.3.2 Characterization of the phenol degradation pathway   | 56           |

|  |               |
|--|---------------|
| <b>2.4 Purification and characterization of phenol hydroxylase from <i>Chlorella pyrenoidosa</i></b> | <b>57-61</b>  |
| 2.4.1 Purification of phenol hydroxylase   | 57            |
| 2.4.2 Electrophoresis: enzyme homogeneity, molecular weight determination                            | 57            |
| 2.4.3 Peptide mass fingerprinting of the purified protein  | 58            |
| 2.4.4 Absorption characteristics of flavoproteins  | 58            |
| 2.4.5 Effect of NADH as cofactor on phenol hydroxylation activity                                    | 58            |
| 2.4.6 Stoichiometry of reaction with phenol  | 59            |
| 2.4.7 Substrate affinity of purified enzyme towards phenol   | 59            |
| 2.4.8 Effect of pH and temperature on enzyme activity  | 59            |
| 2.4.9 Effect of chealators, heavy metals, denaturant and oxidizing agent on enzyme activity          | 60            |
| 2.4.10 Multisubstrate specificity of purified enzyme   | 60            |
| 2.4.11 Storage stability of phenol hydroxylase   | 61            |
| <br>   |               |
| <b>Chapter III: Results and Discussion</b>   | <b>62-175</b> |
| <br>   |               |
| <b>3.1 Abstract</b>  | <b>63</b>     |
| <br>   |               |
| <b>3.2 Screening and characterization of phenol degradation by potent algal strains</b>              | <b>65-86</b>  |
| 3.2.1 Identification of isolated algal strains   | 65-67         |
| 3.2.2 Screening of potent phenol degrading algal strains   | 68            |
| 3.2.3 Growth kinetics and phenol degradation by potent algal strains                                 | 69-86         |

|  |                |
|--|----------------|
| 3.2.3.1 Biomass growth and phenol degradation in <i>C. pyrenoidosa</i>   | 69-78          |
| 3.2.3.2 Biomass growth, phenol degradation and growth kinetic modeling in diatom BD1IITG   | 79-86          |
| <b>3.3 Generation of microalgae based process for efficient phenol remediation as well as biofuel production</b>                                   | <b>87-135</b>  |
| 3.3.1 Growth kinetics and phenol degradation by phenol acclimatized cells of <i>C.pyrenoidosa</i>  | 88-102         |
| 3.3.2 Effect of phenol stress on cell morphology   | 103            |
| 3.3.3 Biochemical characterization of the phenol degrading biomass   | 103-114        |
| 3.3.4 Effect of physical parameters on phenol degradation rate   | 114-120        |
| 3.3.5 Pre adaptation as a strategy for rapid phenol degradation  | 120-124        |
| 3.3.5.1 Growth kinetics and phenol degradation by pre adapted cells  | 120-122        |
| 3.3.5.2 Analysis of biochemical variation of pre adapted <i>C.pyrenoidosa</i> biomass during phenol degradation process                            | 123-125        |
| 3.3.6 Analysis of practical applicability of <i>C.pyrenoidosa</i> based process for phenol degradation and biofuel production                      | 125-132        |
| 3.3.7 Bioethanol fermentation of lipid extracted biomass   | 133-134        |
| 3.3.8 Proposed methodology for an environmentally sustainable algal process for remediation of phenol pollution coupled to clean energy generation | 135            |
| <b>3.4 Elucidation of pathway of phenol degradation</b>  | <b>136-152</b> |
| 3.4.1 Phenol degradation pathway in <i>Chlorella pyrenoidosa</i>   | 136-144        |
| 3.4.2 Phenol degradation pathway in diatom BD1IITG   | 145-152        |

|   |                |
|---|----------------|
| <b>3.5 Purification and characterization of phenol hydroxylase from <i>Chlorella pyrenoidosa</i></b>          | <b>153-175</b> |
| 3.5.1 Induction and extraction of crude enzyme extract with phenol hydroxylation activity                     | 153-155        |
| 3.5.2 Purification of phenol hydroxylase  | 155-157        |
| 3.5.3 Peptide mass fingerprinting of the purified enzyme  | 158-159        |
| 3.5.4 Spectral properties of the purified enzyme  | 159-160        |
| 3.5.5 Effect of NADH as cofactor on phenol hydroxylation activity   | 160-161        |
| 3.5.6 Stoichiometry of the reaction with phenol   | 161-164        |
| 3.5.7 Substrate affinity of purified enzyme towards phenol  | 164            |
| 3.5.8 Effect of pH and temperature on phenol hydroxylase activity   | 165-166        |
| 3.5.9 Effect of chelators on phenol hydroxylation activity  | 166-168        |
| 3.5.10 Effect of heavy metals on phenol hydroxylation activity  | 168-170        |
| 3.5.11 Effect of denaturant on phenol hydroxylation activity  | 171-172        |
| 3.5.12 Effect of oxidizing agents on phenol hydroxylation activity  | 172-173        |
| 3.5.13 Multisubstrate specificity of purified enzyme  | 173-174        |
| 3.5.14 Storage stability of the enzyme  | 174-175        |
| <br>  |                |
| <b>Chapter IV: Conclusion and Future perspective</b>  | <b>176-183</b> |
| <br>  |                |
| <b>4.1 Conclusion</b>   | <b>177-182</b> |
| 4.1.1 Introduction and Literature review  | 177-178        |
| 4.1.2 Screening and characterization of phenol degradation by potent algal strains                            | 178-179        |
| 4.1.3 Generation of a microalgae based process for efficient phenol remediation as well as biofuel production | 180-181        |

|  |                |
|--|----------------|
| 4.1.4 Elucidation of pathway of phenol degradation   | 181            |
| 4.1.5 Purification and characterization of phenol hydroxylase from<br><i>C.pyrenoidosa</i> | 182            |
| 4.2 Research Findings  | 183            |
| 4.3 Future perspective   | 183            |
| <b>Bibliography</b>  | <b>184-205</b> |
| <b>Publications</b>  | <b>206-209</b> |



## List of Tables

| Table No. | Description   | Page    |
|-----------|---|---------|
| 1.1       | Various microorganisms reported for phenol degradation  | 18-22   |
| 1.2       | Growth kinetic models available in literature   | 25      |
| 1.3       | Properties of purified phenol hydroxylase from various microorganisms   | 39-41   |
| 3.1       | Phenol degradation potential of the algal isolates  | 68      |
| 3.2       | Estimated value of growth kinetic parameters of <i>C.pyrenoidosa</i> in phenol  | 77      |
| 3.3       | Estimated growth kinetic parameters of <i>C. pyrenoidosa</i> in refinery wastewater   | 77      |
| 3.4       | Estimated value of growth kinetic parameters of diatom BD11ITG in phenol containing nutrient media                                | 82      |
| 3.5       | Estimated value of growth kinetic parameters of diatom BD11ITG in refinery wastewater   | 84      |
| 3.6       | Estimated value of growth kinetic parameters of <i>C. pyrenoidosa</i> in phenol   | 100     |
| 3.7       | Growth kinetic parameters obtained by various researchers using eukaryotic, prokaryotic and mixed cultures for phenol degradation | 101-102 |
| 3.8       | Growth kinetic parameters of pre adapted <i>C. pyrenoidosa</i> cultures in 250 mg/l phenol  | 122     |

Continued



Continued

| <b>Table No.</b> | <b>Description</b>  | <b>Page</b> |
|------------------|---|-------------|
| 3.9              | Growth kinetic parameters of <i>C. pyrenoidosa</i> in 10 mg/l phenol in refinery wastewater                             | 126         |
| 3.10             | Growth kinetic parameters of <i>C. pyrenoidosa</i> in 250 mg/l phenol in refinery wastewater                            | 128         |
| 3.11             | Enzyme activities in <i>C.pyrenoidosa</i> (NCIM 2738) cell lysate grown in phenol containing media.                     | 140         |
| 3.12             | Specific activity of active ammonium sulphate fractions   | 156         |
| 3.13             | MASCOT search based identification of purified 25 kD protein band using peptide fragment spectra obtained by MALDI TOF. | 159         |
| 3.14             | Stoichiometry of phenol hydroxylase reaction  | 162-163     |

## List of Figures

| Figure No. | Description  | Page  |
|------------|--|-------|
| 1.1        | Different sources of industrial residual wastes  | 3     |
| 1.2        | Organic pollutant dispersion in environment  | 6     |
| 1.3        | Pathway of contaminant in the food web   | 6     |
| 1.4        | Magnification of pesticide DDT along the food chain  | 7     |
| 1.5        | Pathway of pesticide movement in the food chain  | 7     |
| 1.6        | Chemical structure of some common phenolics causing environmental pollution  | 8     |
| 1.7        | Phenol burn on skin  | 14    |
| 1.8        | Necrosis of mucosa by phenol   | 14    |
| 1.9        | Biological treatment of industrial wastewater using activated sludge process   | 28    |
| 1.10       | Pathway for carbon capture and enhanced lipid production during mixotrophic growth   | 30    |
| 1.11       | Integrated wastewater based algae cultivation system for wastewater treatment and production of biofuels and bio based chemicals   | 33    |
| 1.12       | General pathway of phenol degradation in aerobic microbes  | 35-36 |
| 1.13       | Hydroxylation of phenol to catechol by phenol hydroxylase  | 37    |
| 3.1        | Bright field microscopic images of algal isolates: <b>a)</b> <i>Spirogyra</i> <b>b)</b> <i>Closterium</i> <b>c)</b> Unidentified Sample 1 <b>d)</b> Unidentified Sample 2 <b>e)</b> <i>Chlorella pyrenoidosa</i> | 66    |

| Figure No. | Description   | Page  |
|------------|---|-------|
| 3.2        | <b>a)</b> Single colony of diatom BD1IITG (colony marked by red circle) isolated by streak plate method. <b>b)</b> Phylogenetic tree constructed using Robust Phylogenetic tree for the non-specialist.   | 67    |
| 3.3        | <b>a)</b> Biomass growth profile of <i>Chlorella pyrenoidosa</i> in various initial phenol concentrations <b>b)</b> Variation in specific growth rate of <i>Chlorella pyrenoidosa</i> in various initial phenol concentrations <b>c)</b> Phenol degradation profile of <i>Chlorella pyrenoidosa</i> <b>d)</b> Specific degradation rate of <i>C.pyrenoidosa</i> for different phenol concentrations | 71-72 |
| 3.4        | Biomass growth and phenol degradation profile of <i>C.pyrenoidosa</i> in dark.  | 73    |
| 3.5        | <b>a)</b> Biomass growth and phenol degradation by <i>C.pyrenoidosa</i> in refinery wastewater <b>b)</b> Oil characteristics of refinery wastewater before (Day 0) and after treatment (Day 8) with <i>C.pyrenoidosa</i>  | 74-75 |
| 3.6        | Growth kinetic model fitted to experimental batch growth data of <i>C.pyrenoidosa</i> .   | 76    |
| 3.7        | <b>a)</b> Biomass growth profile of diatom BD1IITG <b>b)</b> Phenol degradation profile of diatom BD1IITG <b>c)</b> Specific growth and degradation rate for various concentrations of phenol <b>d)</b> Experimental and growth kinetic model predicted specific growth rates.  | 80-81 |
| 3.8        | <b>a)</b> Biomass growth as well as phenol degradation of diatom BD1IITG in refinery wastewater <b>b)</b> Characterization of oil components in refinery wastewater before (Day 0) and after (Day 6) treatment with diatom BD1IITG.   | 83-84 |
| 3.9        | Emulsification index (E 24) of diatom BD1IITG in phenol containing culture.   | 86    |

| Figure No. | Description   | Page    |
|------------|---|---------|
| 3.10       | Biomass growth and phenol degradation profile of <i>Chlorella pyrenoidosa</i> in various initial concentrations of phenol: <b>a)</b> 50 mg/l phenol <b>b)</b> 100 mg/l phenol <b>c)</b> 150 mg/l phenol <b>d)</b> 200 mg/l phenol <b>e)</b> 250 mg/l phenol <b>f)</b> 300 mg/l phenol <b>g)</b> 350 mg/l phenol <b>h)</b> 400 mg/l phenol <b>i)</b> 450 mg/l phenol <b>j)</b> 500 mg/l phenol <b>k)</b> 550 mg/l phenol <b>l)</b> 600 mg/l phenol <b>m)</b> 650 mg/l phenol <b>n)</b> 700 mg/l phenol <b>o)</b> 750 mg/l phenol <b>p)</b> 800 mg/l phenol <b>q)</b> 850 mg/l phenol <b>r)</b> 900 mg/l phenol <b>s)</b> 950 mg/l phenol <b>t)</b> 1000 mg/l phenol <b>u)</b> 1050 mg/l phenol <b>v)</b> 1100 mg/l phenol <b>w)</b> 1150 mg/l phenol <b>x)</b> 1200 mg/l phenol <b>y)</b> 1250 mg/l phenol <b>z)</b> Control | 90-99   |
| 3.11       | <b>a)</b> Experimental specific growth and degradation rate of <i>C.pyrenoidosa</i> in various initial phenol concentrations <b>b)</b> Growth kinetic models fitted to experimental batch growth data   | 99-100  |
| 3.12       | <b>a)</b> SEM image of <i>C.pyrenoidosa</i> cell (control)<br><b>b)</b> SEM image of <i>C.pyrenoidosa</i> cell cultured in 200 mg/l phenol  | 103     |
| 3.13       | Biochemical profile of <i>C.pyrenoidosa</i> in different initial concentrations of phenol: <b>a)</b> 50 mg/l phenol <b>b)</b> 100 mg/l phenol <b>c)</b> 150 mg/l phenol <b>d)</b> 200 mg/l phenol <b>e)</b> 250 mg/l phenol <b>f)</b> 300 mg/l phenol <b>g)</b> 350 mg/l phenol <b>h)</b> 400 mg/l phenol <b>i)</b> 450 mg/l phenol <b>j)</b> 500 mg/l phenol <b>k)</b> 550 mg/l phenol <b>l)</b> 600 mg/l phenol <b>m)</b> 650 mg/l phenol <b>n)</b> 700 mg/l phenol <b>o)</b> 750 mg/l phenol <b>p)</b> 800 mg/l phenol <b>q)</b> 850 mg/l phenol <b>r)</b> 900 mg/l phenol <b>s)</b> 950 mg/l phenol <b>t)</b> 1000 mg/l phenol <b>u)</b> 1050 mg/l phenol <b>v)</b> 1100 mg/l phenol <b>w)</b> 1150 mg/l phenol <b>x)</b> 1200 mg/l phenol <b>y)</b> 1250 mg/l phenol <b>z)</b> Control                                 | 105-114 |
| 3.14       | Lipid and protein productivity of <i>C.pyrenoidosa</i> in various phenol concentrations   | 114     |

| <b>Figure No.</b> | <b>Description</b>   | <b>Page</b> |
|-------------------|--|-------------|
| 3.15              | <b>a)</b> Effect of inoculum concentration on growth profile <b>b)</b> Effect of inoculum concentration on phenol degradation <b>c)</b> Effect of inoculum concentration on specific growth and degradation profile of <i>C.pyrenoidosa</i>  | 115-116     |
| 3.16              | <b>a)</b> Effect of light:dark periodicity on growth profile <b>b)</b> Effect of light:dark periodicity on phenol degradation profile <b>c)</b> Effect of light:dark periodicity on specific growth and degradation profile of <i>C.pyrenoidosa</i>  | 117-118     |
| 3.17              | <b>a)</b> Effect of pH on biomass growth profile <b>b)</b> Effect of pH on phenol degradation <b>c)</b> Effect of pH on specific growth and degradation profile of <i>C.pyrenoidosa</i> .  | 119-120     |
| 3.18              | Biomass growth and phenol degradation profile of pre adapted cells (adapted in 250 mg/l phenol) under experimentally derived optimum physical parameters.  | 121         |
| 3.19              | <b>a)</b> Biochemical profile of pre adapted cells of <i>C.pyrenoidosa</i> in 250 mg/l phenol. <b>b)</b> Lipid and protein productivity of pre adapted cells of <i>C.pyrenoidosa</i> in 250 mg/l phenol. <b>c)</b> Neutral lipid accumulation profile for pre adapted <i>C.pyrenoidosa</i> cells in 250 mg/l phenol. | 124-125     |
| 3.20              | Biomass growth and phenol degradation profile of pre adapted cells (adapted in 250 mg/l phenol) in 10 mg/l phenol containing refinery wastewater.  | 126         |

| Figure No. | Description   | Page    |
|------------|---|---------|
| 3.21       | Biomass growth and phenol degradation profile of pre adapted cells (adapted in 250 mg/l phenol) in 250 mg/l phenol containing refinery wastewater.  | 127     |
| 3.22       | <b>a)</b> Biochemical profile of pre adapted cells of <i>C.pyrenoidosa</i> in 10 mg/l phenol containing refinery wastewater. <b>b)</b> Biochemical profile of pre adapted cells of <i>C.pyrenoidosa</i> in 250 mg/l phenol containing refinery <b>c)</b> Comparison of lipid and protein productivity of pre adapted cells of <i>C.pyrenoidosa</i> in 250 mg/l media, 10 mg/l and 250 mg/l phenol containing wastewater. <b>d)</b> Comparison of neutral lipid productivity of pre adapted <i>C.pyrenoidosa</i> in 250 mg/l media, 10 mg/l and 250 mg/l phenol containing wastewater. | 130-132 |
| 3.23       | Bioethanol fermentation of lipid extracted biomass of <i>C.pyrenoidosa</i> : <b>a)</b> Utilization of reducing sugar released by saccharification of lipid extracted biomass <b>b)</b> Production of bioethanol in the fermentation broth   | 134     |
| 3.24       | Algal process for phenol remediation along with biofuel generation.   | 135     |
| 3.25       | <b>a)</b> HPLC chromatogram day 0 <b>b)</b> HPLC chromatogram at 3 <sup>rd</sup> day (phenol degradation and catechol accumulation in media)  | 137     |
| 3.26       | <b>a)</b> Hydroxylation of phenol to catechol by phenol hydroxylase activity. <b>b)</b> Ortho cleavage of catechol to cis,cis-muconic acid by catechol-1,2-dioxygenase activity. <b>c)</b> Meta cleavage of catechol to 2-hydroxymuconic semialdehyde (2-HMS) by catechol-2,3-dioxygenase activity.   | 139-140 |

| <b>Figure No.</b> | <b>Description</b>  | <b>Page</b> |
|-------------------|---|-------------|
| 3.27              | LC-MS analysis of catechol dioxygenase assay mixture <b>a)</b> 0 min (before incubation) <b>b)</b> 20 min (after incubation)  | 142         |
| 3.28              | Proposed pathway of phenol degradation in <i>Chlorella pyrenoidosa</i> (NCIM 2738).   | 144         |
| 3.29              | <b>a)</b> HPLC chromatogram at day 0 <b>b)</b> HPLC chromatogram at day 4   | 145-146     |
| 3.30              | <b>a)</b> Phenol hydroxylase activity assay <b>b)</b> Catechol-1,2-dioxygenase activity assay <b>c)</b> Catechol-2,3-dioxygenase activity assay   | 147-148     |
| 3.31              | Metabolite identification by LC-MS (0 min) <b>b)</b> Metabolite identification by LC-MS (20 min)  | 150-151     |
| 3.32              | Proposed pathway for phenol degradation in diatom BD11ITG.  | 152         |
| 3.33              | <b>a)</b> Phenol hydroxylase activity of crude extract <b>b)</b> Autooxidation of NADPH   | 154-155     |
| 3.34              | <b>a)</b> Phenol hydroxylase activity of 25% Ammonium Sulphate fraction. <b>b)</b> Silver stained SDS PAGE image of ammonium sulphate fractions (10-45%). <b>c)</b> Molecular weight determination of purified enzyme by log molecular weight (log MW) versus relative mobility plot. | 156-157     |
| 3.35              | Peptide fragment spectra of Phenol hydroxylase obtained by MALDI TOF.   | 158         |
| 3.36              | UV-Visible spectrum of purified phenol hydroxylase  | 160         |
| 3.37              | Phenol hydroxylase assay using NADH as cofactor.  | 161         |

---

| <b>Figure No.</b> | <b>Description</b>  | <b>Page</b> |
|-------------------|---|-------------|
| 3.38              | Substrate affinity of purified phenol hydroxylase towards phenol.   | 164         |
| 3.39              | Effect of pH on phenol hydroxylase activity   | 165         |
| 3.40              | Effect of temperature on phenol hydroxylase activity.   | 166         |
| 3.41              | Effect of chelators on phenol hydroxylase activity: <b>a)</b> phenanthroline (chelator of Fe <sup>2+</sup> ) <b>b)</b> Sodium arsenate (chelator of Fe <sup>2+</sup> ) <b>c)</b> Sodium diethyldithiocarbamate (Cu chealator) | 167-168     |
| 3.42              | Effect of heavy metals on phenol hydroxylase activity: a) FeSO <sub>4</sub> b) CuSO <sub>4</sub> c) AgCl <sub>2</sub> d) HgCl <sub>2</sub>  | 169-170     |
| 3.43              | <b>a)</b> Effect of denaturant SDS on Phenol hydroxylase activity <b>b)</b> Effect of denaturant Urea on phenol hydroxylase activity  | 171-172     |
| 3.44              | Effect of oxidizing agent H <sub>2</sub> O <sub>2</sub> on phenol hydroxylase activity.   | 173         |
| 3.45              | Multisubstrate specificity of Phenol hydroxylase  | 174         |
| 3.46              | Storage stability of phenol hydroxylase   | 175         |

---



The logo of the Indian Institute of Technology Guwahati is a circular emblem. It features a central stylized figure with three rounded protrusions, resembling a '3' or a traditional symbol. The figure is surrounded by a circular border containing text in both Hindi and English. The Hindi text at the top reads 'भारतीय प्रौद्योगिकी संस्थान गुवाहाटी' and the English text at the bottom reads 'Indian Institute of Technology Guwahati'.

**Introduction and Literature review**

## Chapter I

### Introduction

#### 1.1. Abstract

Phenol is a xenobiotic released in wastewaters of industries as coal industries, phenol manufacturing, pharmaceuticals, dying, petrochemicals, pulp mill etc. Owing to high ecological toxicity risks of phenol it is considered a priority pollutant requiring efficient phenol removal technologies from industrial wastewater. Biological treatment of phenol has gained wide interest owing to its advantages of complete phenol mineralization and cost effectiveness. The present chapter reviews the current scientific knowledge in the area of biological removal of phenol from wastewaters and highlights the existing knowledge gap that requires further study. Phenol degradation of microalgae has been less explored compared to other microbial strains and thus deserves further attention. Phenol metabolizing pathway comprising of a cascade enzymes is responsible for microbial phenol degradation. There is scarcity of information on metabolic mechanism of phenol degradation in green unicellular algae calls for adequate research in this direction. Apart from use in phenol bioremediation, purified phenol hydroxylase has generated wide interest for application as phylogenetic markers, organic dye synthesis and phenol biosensor. The prospective applications of phenol hydroxylase calls for knowledge of its kinetic properties There is a serious lack of information on kinetic properties of microalgal phenol hydroxylase and calls for research to fulfill this lacuna in scientific knowledge.

#### ***Research Output:***

Biodegradation of phenol: Current Status and Future Prospects (Manuscript under preparation)

## 1.2 Introduction

Xenobiotics are persistent toxic pollutants released in the aquatic ecosystems mostly due to anthropogenic activities. This has been a matter of serious concern for the ecologists as xenobiotics cause disturbance to the ecological balance by deteriorating the ground water quality, climate change, global warming and depletion of ozone layer by photochemical oxidation (Varsha et al. 2011). The most common source of anthropogenic pollution is in the form of industrial emissions or sometimes accidental in the form of chemical or oil spills (Varsha et al. 2011). Modern lifestyle is highly dependent on commodities and processes that release toxic xenobiotics at concentrations that would not normally be present in the environment. Figure 1.1 shows prime direct source of xenobiotics is wastewater and solid residues released from industries like petrochemical, pharmaceuticals, paints and dye, paper and pulp mills etc.

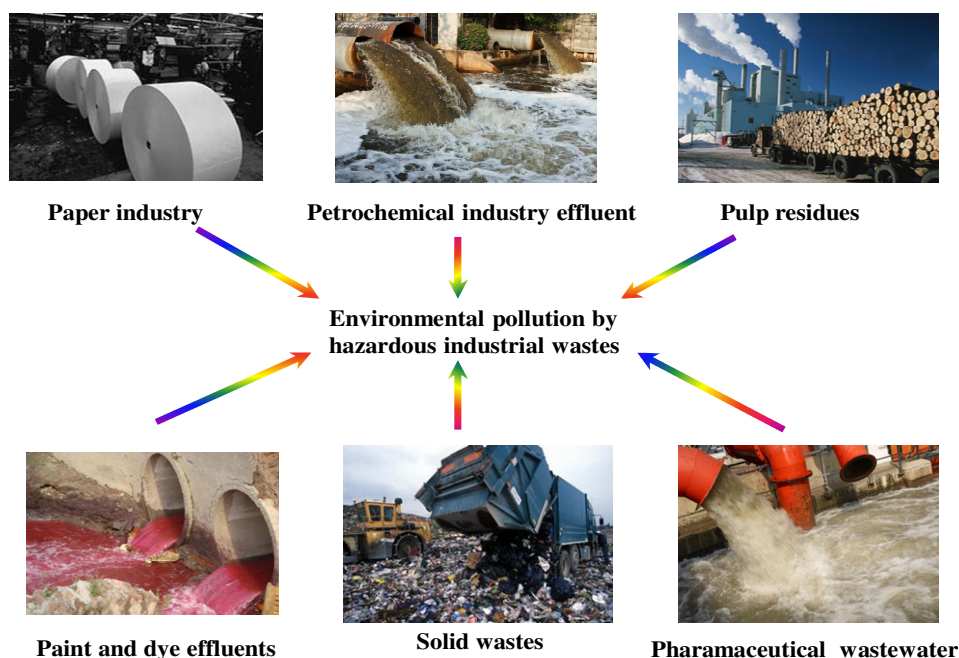


**Figure 1.1** Different sources of industrial residual wastes (Varsha et al. 2011, [www.indiamart.com](http://www.indiamart.com), [www.flowserve.com](http://www.flowserve.com), [www.rsc.org](http://www.rsc.org))

The xenobiotics can have profound harmful effect on organisms and ecosystem (Donner et al. 2010). The potential of xenobiotics as health hazard arises from its properties of toxicity, environmental persistence as well as its presence in high lethal concentrations in the ecosystem (Varsha et al. 2011). The modern civilization with existence highly dependent on processes and commodities that release hazardous artificially synthesized chemicals and metals at high concentrations that is not present in the environment. Items of daily use as toothpastes, laundry detergents, cars, cosmetics, mobile phones, disinfectants, pesticides, petrochemicals and numerous other such commodities of daily use are potential sources of xenobiotics, Although the extent and hazardous nature of xenobiotic released from these different sources vary, each one is an environmental pollutant and matter of concern for environmental management. The current daunting challenge is to exploit the beneficial uses of xenobiotics while limiting its emission into the environment. Thus, evaluating the xenobiotic toxicity to ecological flora as well as fauna and devising techniques to minimize the release of toxic xenobiotics to the environment has been a highly intriguing topic to environmental researchers. The behavior of different xenobiotics released to the environment varies according to properties of the xenobiotic as solubility, volatility and biodegradability which complicates the process of environmental management. To further complicate the application of xenobiotic remediation technologies, the xenobiotic released from a point source may be in a mixture of different pollutants or may be released in different forms as ionic species, degradation products, metabolites etc. An appropriate knowledge of the spatial distribution of the xenobiotic and the scale of the pollutant released from point source is important for risk assessment and thus form a basis for pollution monitoring, exposure assessment and design control strategies for minimizing emission of the xenobiotic to the environment (Donner et al. 2010). On the account of the extraordinary diversity of xenobiotics, a more structured approach to design ways to minimize xenobiotic emission to the environment is required. For designing control strategies for xenobiotics it is essential to identify the important xenobiotic release sources, determine sources feasible for application of on site treatment technologies, mobility of the pollutant source and rate of emission of pollutant from the source etc.

This knowledge is an essential input to determine the pattern and pathway of flow of the target xenobiotic in the environment and choosing the correct xenobiotic remediation technology. Finally, knowledge of breadth of use of a target xenobiotic i.e. if the substance is the basis of a number of key industrial process on which livelihood of thousands of people would help in assessing the environmental risk of the xenobiotic. Such a xenobiotic poses high risk of environmental deterioration and requires efficient control strategies to minimize its release into environment in high toxic limits. Figure 1.2 shows the movement of desorbed persistent organic pollutants in the the environment. Desorbed pollutants are bioavailable and can move into food chain, contaminate ground or surface water and reach atmosphere through volatilization leading to its random dissemination in the biosphere (Lagenbach 2013). Another reason which demands xenobiotic remediation before release into the environment is biomagnification of pollutants in the food chain. When persistent organic pollutants are exposed to the environment they generally end up in aquatic ecosystems by direct release of toxic effluents in water bodies, by runoff or atmospheric transport. Small organisms ingest the pollutants by bottom feeding. The pollutants accumulate in the fatty tissues of living organisms as they are not degraded by animal digestive systems. Thus, through the food chain the pollutants accumulate in the bodies of higher animals and finally in human beings (web1.cnre.vt.edu). Figure 1.3 shows the pathways that contaminant follow as they move through the food web. Xenobiotic concentration increase with each step in the food chain leading to higher concentration of xenobiotics in the predator compared to that in prey which is related to increased lipid at higher trophic levels (Gobas 2001; Gray 2002). Figure 1.4 shows that DDT contamination accumulates through the food chain in animal fat and biomagnified to 10 million times at higher trophic levels.

Soil contaminated with pesticides or other persistent organic pollutant pollutes the food chain by direct uptake in leaves during pesticide application and uptake of pollutants in soil water through roots. This results in bioaccumulation of pesticides in the crops which were consumed by animals and humans leading to biomagnifications of pollutants as shown in Figure 1.5. Phenol is one such xenobiotic which is released

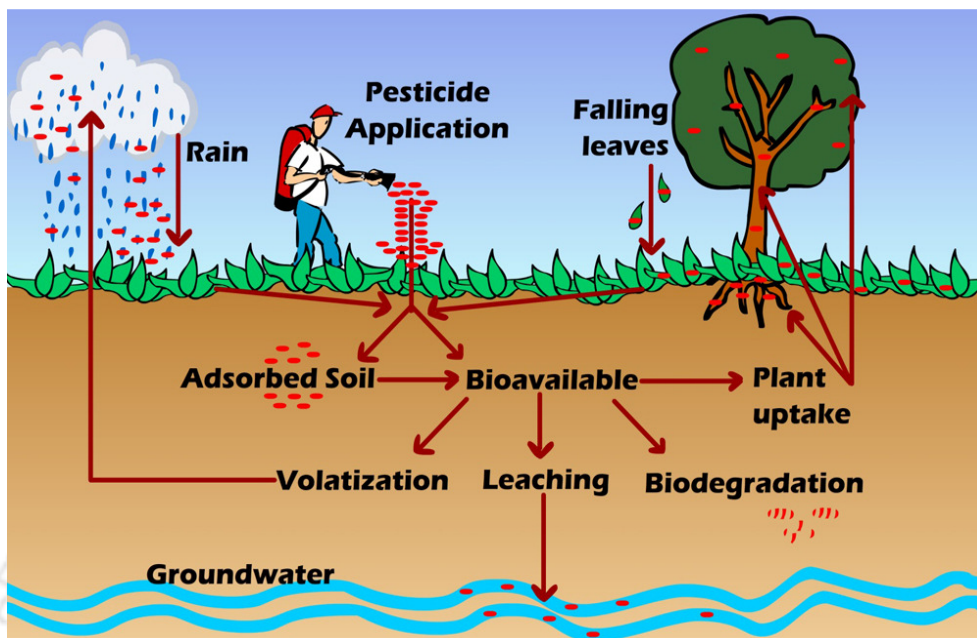


Figure 1.2 Organic pollutant dispersion in environment (Lagenbach 2013)

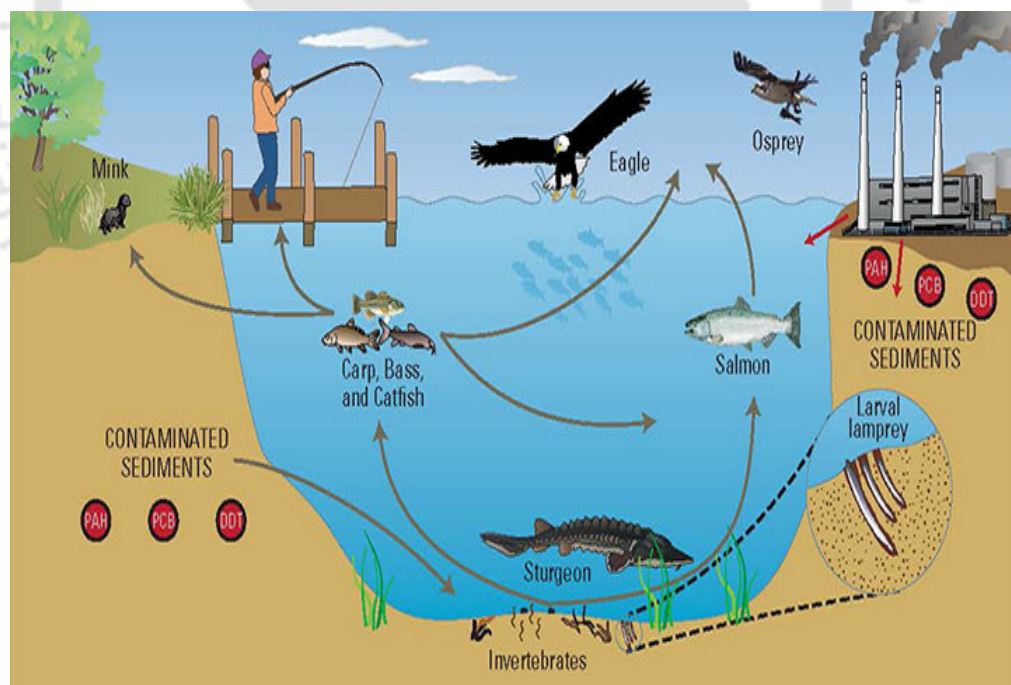
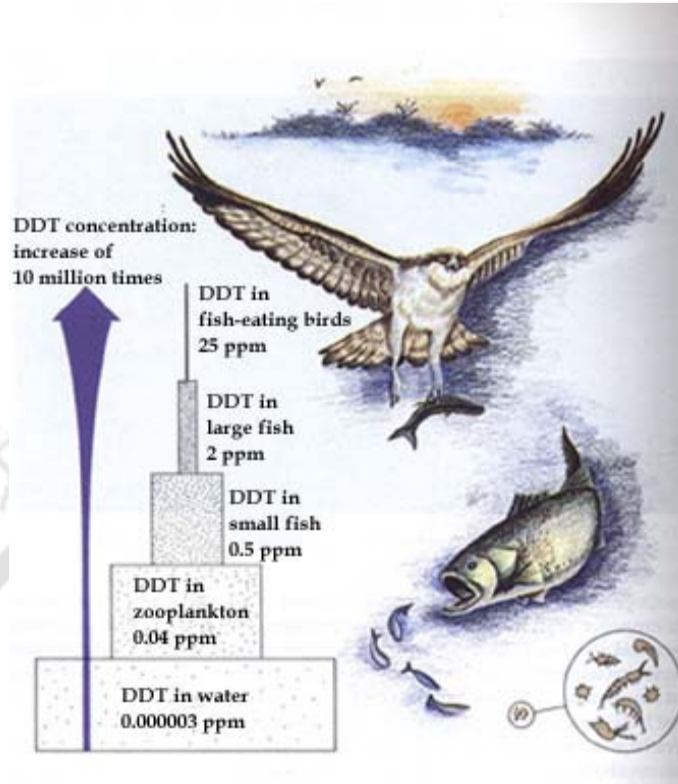


Figure 1.3 Pathway of contaminant in the food web (Portland Harbour Trustee Council <http://response.restoration.noaa.gov>)



**Figure 1.4** Magnification of pesticide DDT along the food chain (U.S. Fish and Wildlife Service; <http://response.restoration.noaa.gov>)



**Figure 1.5** Pathway of pesticide movement in the food chain (Lagenbach 2013)

in industrial wastewaters accounting for harmful effects on aquatic flora and fauna as well as humans.

### 1.3 Phenol as a pollutant

Phenol is known by many synonyms as carboic acid, hydroxybenzene, phenic acid, phenylic acid, phenyl hydroxide, monophenol, phenyl hydrate and phenic acid. It is an aromatic organic compound with molecular formula  $C_6H_5OH$ . The chemical structure of phenol and some other phenolics commonly responsible for environmental pollution is shown in Figure 1.3. It is mildly acidic in nature requiring careful handling to avoid chemical burns. It is hygroscopic in nature with a sweet and tarry odor. Phenol has a molecular mass  $94.11 \text{ g mol}^{-1}$  with a density of  $1.07 \text{ g/cm}^3$ , melting point of  $40.5^\circ\text{C}$  and boiling point of  $181.7^\circ\text{C}$ . Phenol is appreciably soluble in water with a solubility of  $8.3 \text{ gm/100 ml}$  of water at  $20^\circ\text{C}$ . The water soluble nature of phenol increases the associated environmental risk as it can easily reach downstream water sources from the point of emission.

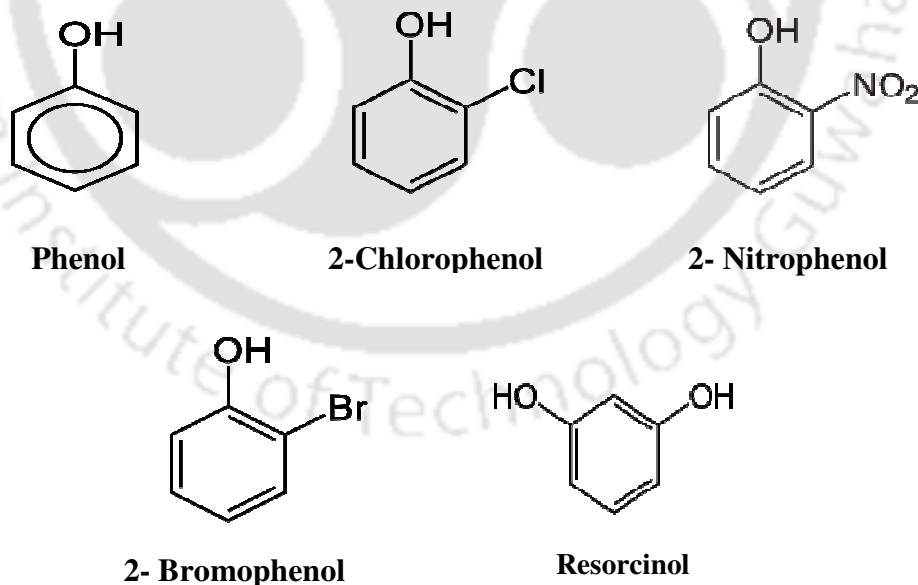


**Figure 1.6** Chemical structure of some common phenolics causing environmental pollution



Phenol produced annually at around 7 billion kg is used as a raw material in various industries as oil refining, pharmaceuticals, pesticides, coking plants, pesticide plants as well as leather industries (Senthilvelan et al. 2014). It is released in wastewaters of various industrial processes of petrochemicals, coal industries, resin plants, pharmaceuticals, dyeing, pulp mill etc. The concentration of phenols in wastewater may vary from 10 to 300 mg/l, but this can rise to 4.5 g/l in highly polluted wastewaters (Al-Khalid and El-Naas 2012). Phenol is considered as one of the most prevalent pollutants on account of its ecological toxicity even at low concentrations and formation of toxic substituted compounds during oxidation and disinfection process. The acute toxic nature of phenol combined with numerous industrial processes serving as point source for phenol pollution qualifies it to be included as a priority pollutants requiring efficient technologies for minimizing its environmental risk. Apart from point sources, phenol pollution from non point sources with accumulated xenobiotics is of more serious concern. Phenol can act as a pollutant in liquid form in factory effluent or even in solid form from water runoff or heavy raining. Phenol pollution related to aquatic ecosystem poses major impact on humans as well as ecological flora and fauna. Phenol is known to pollute soil and food by means of water. In water bodies, phenol desorbs from soil sediment and re-enters the water phase finally accumulating in aquatic organisms as fishes. There are numerous reports on phenol contamination beyond permissible limits in water bodies worldwide as well as in India indicating the seriousness of the problem. Dewani et al. (2003) reported presence of 0.23-0.25 mg/l phenol in sewage water of Hyderabad city. Ayeni (2014) analyzed industrial wastewater samples from point of discharge and water samples of Isebo river near industrial area in Ibadan, Nigeria to determine chemical status of river with respect to phenol pollution. They reported concentration of phenol in industrial wastewater within the range 2.55-14.15 mg/l. The phenol concentration in Tsebo river water was found to vary within the range of 0.05-2.11 mg/l across geographic spread of the study area. Phenol concentration beyond the permissible limits found in Isebo river indicates its potential to pose enormous ecological hazard. Nomani et al. (1996) studied phenolic pollution in four major rivers of four major rivers of Northern India namely Ganges, Yamuna, Hindon and Kali. 2,3-

Dichlorophenol was detected in river Ganges and Yamuna at concentrations of 0.40  $\mu\text{g/l}$  and 0.56  $\mu\text{g/l}$  respectively. Presence of dibromophenol, 4-chlorophenol, trichlorophenol and pentachlorophenol was also reported in both the rivers. The rivers Hindon and Kali was reported to be most unpolluted with respect to phenolic pollution. The Central Pollution Control Board, India reported critical sites of ground water pollution in India in a report published in 1995. They reported that industrial and urban fringe zones of cities sub-soil water has been polluted toxic wastes released by industries. They reported that ground water of Korba (Madhya Pradesh), Singrauli (Uttar Pradesh), Mandi Gobindgarh (Punjab), Kala Amb (Himachal Pradesh) and Parwanoo (Himachal Pradesh) was polluted with phenolics above toxic limits owing to pollution from industries as thermal power plants, aluminium industries, chemical industries, pesticides, steel metal units and paper mills etc. (<http://www.nih.ernet.in>). Traces of phenol contamination within prescribed limits were observed in groundwater of Durgapur (West Bengal), Howrah (West Bengal), Vapi (Gujarat) and surface waters of Godavari canal mainly due to industrial activities (<http://www.nih.ernet.in>, Kumar and Pacha 2015). Even though levels of phenolic compounds are lower than toxic limits, it calls for efficient monitoring as continuous emission of phenolic compounds results in their deposition and increase in the soil sediments (Kumar and Pacha 2015). Soil pollution by phenol is also a matter of grave concern since they are good absorbents of phenolic pollutants owing to high surface area and surface activity (Kumar et al. 2014). Long disposal of phenol on land leads to negative effects on soil fertility (Senthivelan et al. 2014). Kahru et al.(2002) reported presence of 43 mg monobasic phenol per gram dry weight in semi-coke dump leachate polluted soil in North East of Estonia. Cordova-Rosa et al. (2009) reported phenol concentration of 19.48 mg/kg in soil contaminated with textile sludge. Pei et al. (2012) studied phenolic pollution in a retired refinery site and reported presence of 2-chlorophenol, 2-nitrophenol, 2,4-xyleneol, 2,4-dichlorophenol and 2,4,6-trichlorophenol, 2,4-dinitrophenol and 2-methyl-4,6-dinitrophenol in the soil. They also reported contamination of ground water in the refinery site by phenolic pollutants beyond toxic limits. The pollution of ground water by phenol contaminated soil is a serious threat since to human health as it is the source of drinking water.

## 1.4 Ecological toxicity of phenol

Phenol of anthropogenic origin penetrates the natural ecosystem owing to drainage of municipal or industrial sewage to surface wastewater. The three organism groups in an aquatic ecosystem (crustaceans, algae, fish) represent different trophic levels of an aquatic food chain and thus needs to be protected (Aruoja et al. 2011). The toxic phenol levels range between concentrations of 10-24 mg/l for human and between 9-25 mg/l for fishes (Kulkarni and Kaware 2013). Phenol toxicity is related to hydrophobicity of the individual compound and formation of free radicals (Michalowicz and Duda 2007). Penetration of phenol to organisms is related with diffusion of the compound across a cell's membrane. Phenol being hydrophobic in nature affects the more effective penetration of cell's membrane enhancing its toxicity. Microorganism is important in aquatic ecosystem for maintenance of web chain and nutrient cycle on earth. The toxicity of phenol lies in its ability to disrupt membrane permeability of the microbe resulting in imbalance of intracellular cell environment finally resulting in cell death (Wasi et al. 2013; Gami et al. 2014). Phenol contamination of water bodies has serious implications on aquatic organisms as algae and spermatophytes. These photosynthetic organisms are responsible for providing food, habitat and nursery grounds for higher trophic level organisms. Insight into effect of phenol toxicity on plant/algal population is important as changes in dynamics of their population can cause major alterations in aquatic ecosystem functions (Park et al. 2012). Aquatic macrophytes being major constituent of aquatic biomass and thus will have vital role as primary producers. The viability of the aquatic ecosystem could be jeopardized by toxic effects of phenol on aquatic macrophytes. Park et al. (2012) reported phenol concentration dependent decline in frond multiplication, browning of fronds, colony disintegration as well as inhibition of photosynthetic efficiency in aquatic macrophyte *Lemna paucicostata*. Song and Huang (2007) reported inhibitory effect of pentachlorophenol on chloroplast activity while the nitrate reductase activity and peroxidase activity was found to be stimulated in duckweed, *Lemna polyrhiza*. Storm and Roth (1981) reported the toxicity of phenols to aquatic plants *Cyclotella cryptica*, *Dunaliella salina*, *Chlamydomonas reinhardtii*, *Lemna minor* and *Euglena*

*gracilis*. They reported that phenols affect unspecific cell proteins, structural proteins in cell organelles as well as cytoplasmic proteins involved in cell motility and cytoplasmic streaming. Chen et al. (2007) reported growth inhibitory effects of phenolics as 2,4-xyleneol, para-cresol and phenol on unicellular green algae *Dunaliella salina*. Phenol reported highest inhibition of growth of *Dunaliella salina* followed by para-cresol and 2,4-xyleneol. R Hunt (2006) investigated the algal toxicity of triclosan (5-chloro-2-(2,4-dichlorophenoxy) phenol) which commonly pollutes surface waters due to its presence in disinfectant hand soaps. They reported growth inhibitory effect of triclosan on *Selenestrum* sp. However, the growth inhibitory effect of triclosan on *Scenedesmus* sp. and diatoms present in triclosan polluted water body was found to be lesser. Phenol may accumulate in bottom sediments upto ten-fold concentrations. Thus, the toxic effect of phenol in many cases may be manifested earlier in bottom dwellers than in pelagic species belonging to higher trophic level (Okasama and Kristoffersson 1979). Ristola (2000) reported the sensitivity of bottom feeder *C. riparius* to 2,4,5-trichlorophenol. They reported that the sensitivity of 2,4,5-trichlorophenol to *C. riparius* decreased with larvae age. In sediment exposure of first instars, the threshold 2,4,5-trichlorophenol concentration of mortality was in range of 200-350  $\mu\text{mol/kg}$ . However, longer exposure to 2,4,5-trichlorophenol to *C. riparius* hastened adult emergence. Liber and Solomon (1994) studied the effects of 2,3,4,6-tetrachlorophenol and pentachlorophenol on daphnids and rotifers which feed on algae, protozoa and bacteria. Daphnids and rotifers in turn being important food source for fishes as well as aquatic invertebrates are important for proper functioning of the aquatic ecosystem. Chronic exposure of the phenolics to Daphnids or rotifers showed significant adult mortality. Phenol has been reported to induce toxic effects on health of higher trophic level animals as fishes. Abdel-Hameid (2007) studied the effect of phenol on *Oreochromis aureus* juveniles and reported hepatosomatic index (HSI) increase while gonadosomatic index (GSI) was significantly reduced. The total liver protein content was reduced indicating tissue proteolysis. The liver of fish subjected to phenol showed high score of histopathological symptoms as inflammation, central necrosis and cell degeneration. Liver glucose and glycogen were also reduced by phenol exposure in the fish juveniles. Saha et al. (1999) reported that

phenol in the aquatic environment reduces fish food consumption, mean weight and fertility. Ibrahim (2011) reported that the median lethal concentration of phenol is 35 mg/l for African catfish *Clarius Gariepinus*. They reported that toxicity of phenol has negative effects related to mortality, behavioral, histopathological change and ability to resist infections. Gad and Saad (2008) reported that sublethal concentration of phenol caused endocrine disruption in fish, liver disfunction, genotoxic effects, growth rate reduction and accumulation of phenol in fish tissues as liver, muscles and lungs. El-Serafy et al. (2009) studied the histological and histochemical alteration induced by phenol on juveniles of *Oreochromis aureus*. They reported that fish subjected to sublethal concentrations of phenol necrosis and degeneration in liver tissues, pyknosis, cellular proliferation, gill hyperplasia, shortening and fusion of gill lamellae and splenic capsule deterioration, carbohydrate depletion in tissues. They also reported enhanced production of mucopolysaccharides in gill as a adaptive response to prevent phenol entrance which in turn impedes fish respiration. Phenol exposure also leads to amplification of liver DNA in *Oreochromis aureus* juveniles suggesting beginning of carcinogenesis. The exact mechanism of phenol toxicity to fishes is not clearly known. Phenol enters in fish blood circulation from water through gills or mucous epithelium of mouth and accumulates in different organs in fish body leading to harmful physiological effects or even death based on concentration (Verma et al. 1980; Mukherjee et al. 1991; Saha et al. 1999). Ponopal and Paunescu (2014) evaluated the effect of 25 mg/l and 50 mg/l phenol on Perch (*Percha fluviatilis*) and marsh frog (*Pleophylax ridibundus*) commonly exposed to pollutants in aquatic ecosystems. They reported that phenol exposure for first 48-72 hours led to stimulation of breathing frequency of perch and marsh frogs. Long term exposure for two weeks causes decrease in respiratory rhythm and erythrocytes in these animals. Phenol exposure resulted in increase in plasma glucose and leukocyte count in perch and marsh frogs. Thus phenol pollution needs to be taken in consideration in the fish farming systems and also in natural aquatic habitat. Phenol by causing toxicity to aquatic organisms can potentially affect humans higher in the food chain. In humans, acute phenol poisoning leads to dryness in throat and mouth, dark-colored urine and strong irritation of mucous membranes. Phenol toxicity is related with donation of free

electrons by phenol from oxidized substrate. Interaction of phenol or its radical metabolites interact with mitochondrion leading to coupling between oxidative phosphorylation and electron transport in respiratory chain. Chronic administration of phenol results in pathological changes in esophagus, lungs, liver, kidneys and also urogenital tract. A dose of 1 g phenol may be lethal for an adult man (Michalowicz and Duda 2007). Phenol is reported to block ion channels in a micromolar concentrations range (Roy et al. 1998; Michalowicz and Duda 2007). Phenol is also known to irritate skin and causes its necrosis by its coagulation with amino acids contained in keratin of epidermis and collagen in inner skin (Clayton and Clayton 1994; Michalowicz and Duda 2007).



**Figure 1.7** Phenol burn on skin (www.answers.com)



**Figure 1.8** Necrosis of mucosa by phenol (www.pocketdentistry.com)

### 1.5 Methods for treatment of phenol pollution

Owing to profound ecological toxicity of phenol, it is considered a priority pollutant. The World Health Organization has set a guideline of 1  $\mu\text{g/l}$  to regulate the phenol concentration in drinking waters (Yan et al. 2006; Al-Khalid and El-Naas 2012). The US Environmental Protection Agency and European Council Directive has set a limit of 1  $\mu\text{g/l}$  and 0.5  $\mu\text{g/l}$  phenol respectively in drinking waters (Tziotzios et al. 2005; Al-Khalid and El-Naas 2012). UAE has set a limit of 0.1  $\text{mg/l}$  phenol in

industrial water discharged to the marine environment. A range of efficient physio-chemical methods are used for treatment of phenol in wastewaters which are discussed below:

### **1.5.1. Solvent extraction**

In this technique, a mixture of two components is treated by a solvent leading to dissolution of one or more components in the mixture (Lakshmi and Sridevi 2009) and get separated from others. Rao et al. (2009) reported phenol removal by 1-hexanol, 1-heptanol and 1-octanol with 1-octanol showing lower phenol removal efficiency. Xu et al. (2006) reported that QH-1 extractant with 15% NaOH led to phenol stripping efficiency of more than 99%. The main disadvantage of this process is that when phenol concentration is less than 2gm/l, the process incurs extra operating and capital costs.

### **1.5.2 Photodecomposition**

Photocatalysis involves acceleration of a photoreaction in presence of catalyst. Ilisz et al. (1999) reported photodecomposition of phenol in near UV-irradiated aqueous TiO<sub>2</sub> suspensions. Akbal and Onar (2003) showed photocatalytic degradation of phenol using UV-irradiated TiO<sub>2</sub> catalyst and H<sub>2</sub>O<sub>2</sub>. Cost associated with downstream catalyst separation is the main disadvantage associated with this process.

### **1.5.3 Advanced oxidation processes (AOPs)**

This process of phenol removal involves use of ozone, UV, ozone in combination with UV, ozone with hydrogen peroxide, hydrogen peroxide in presence of ultraviolet light. Use of AOPs coupled to biological treatment for phenol treatment have been reported by Rubalcaba et al. (2007). Sidlecka et al. (2012) reported application of AOP for treatment of phenol, 2 chlorophenol and 2 nitrophenol. High costs incurred on ozone, hydrogen peroxide or UV-lights are the main drawbacks associated with AOPs.

#### **1.5.4 Adsorption**

In this process, solutes from the liquid media were absorbed on solids. The liquid phase adsorption of phenol from water was carried out using silica gel, activated carbon, activated alumina (Roostaei and Tezel 2004), sawdust, polymerized saw dust, sawdust carbon (Jadhav and Vanjara 2004); hyacinth (Uddin et al. 2007); rice husk adsorbent (Kadhim and Al-Seroury 2012); oil palm shell activated carbon (Lua and Jia 2009). The applicability of adsorption being confined to low concentration of solutes compromises use of this process.

#### **1.5.5 Electro-Fenton method**

This method consists of a cell containing an electrolyte through which an externally generated electric current is passed by an electrode system to produce an electrochemical reaction. Jiang et al. (2012) reported an electro-fenton method using H<sub>2</sub>O<sub>2</sub> amendments and electro generated ferrous ions for treatment of phenol containing wastewater. High costs associated with such process is a major disadvantage.

#### **1.5.6 Biological treatment**

There is utmost necessity of efficient green and sustainable technology for phenol treatment in industrial effluent. However, the conventional physio-chemical techniques incurs high cost, high energy and reagent requirements along with lack of phenol degradation as phenol is removed to another phase resulting in the formation of hazardous byproducts (secondary pollution). Biodegradation has proved to be cost-effective alternative with possibility of complete mineralization of phenol. Thus, biological treatment of phenols is currently being seen as an important process in pollution control (Liu et al. 2009; Wang et al. 2007; El-Naas et al. 2010). Because of widespread occurrence of phenol, aerobic as well as anaerobic microorganisms with ability to utilize phenol as carbon source exists in natural ecosystem (Basha et al. 2010). Thus, on the basis of the type of microbe, the bioremediation process can be aerobic or anaerobic. In aerobic degradation processes, oxygen acts as electron acceptor. Molecular oxygen is a reactant for oxygenase enzymes and incorporated into



degradation products. In anaerobic degradation, inorganic electron acceptors as  $\text{NO}_3^-$ ,  $\text{SO}_4^-$ ,  $\text{CO}_2$ ,  $\text{Fe}_3^+$  are used (Lakshmi and Sridevi 2009). Aerobic processes are generally preferred over anaerobic processes owing to its faster growth rate, transformation of organic compounds to inorganic  $\text{CO}_2$  and  $\text{H}_2\text{O}$  and low costs (Ucun et al. 2010; Dash et al. 2009; Mrozik et al. 2010; Al-Khalid & El-Naas 2012). Anaerobic degradation is preferred only in degradation processes where reduction is preferred over oxidation (e.g. in case of chlorinated compounds) (Lakshmi and Sridevi 2009). For treatment of phenol contaminated wastewater, aerobic biodegradation is preferred as it leads to its complete mineralization of phenol. Alexander (1985) suggested that for microbial transformation of organic compounds, a number of factors must be satisfied as:

- a) **Presence of specific enzymes:** The specific enzyme responsible for biodegradation must be present in the microorganism. Enzymes may specifically catalyze breakdown of a particular compound or unspecific enzymes with ability to transform a range of substrates. Depending on type of enzyme used, different microbes may degrade the same compound following various degradation patterns (Duetz et al. 1994).
- b) **Availability of organic compound to the microbe:** The organic compound must be available to the microbe for degradation. If the organic compound exists in a different phase from that of the microbe as in a liquid phase which is not miscible in water or when the compound is sorbed to a solid phase (Lakshmi and Sridevi 2009).
- c) **Growth of microbial strain:** Growth of microbial strain is another important factor determining efficiency of degradation process. The microbes growth potential depends on its ability to compete for the organic compound, oxygen or other environmental factors (Lakshmi and Sridevi 2009).

Phenol-polluted wastewater and soil are main sources of phenol-degrading strains belonging to bacteria, fungi and algae. Table 1.1 describes various different microbial species reported to possess phenol degradation ability. *Pseudomonas* genus are commonly utilized for phenol degradation and believed to possess enormous potential

for phenol biodegradation. From Table 1.1, it can be seen that algal phenol degradation capability is much less studied as compared to bacterial and fungal strains and thus deserves special attention. The biodegradation of phenol by microalgae occurs only under aerobic conditions.

**Table 1.1** Various microorganisms reported for phenol degradation

| Microorganism<br>(Bacteria)  | Phenol<br>degraded<br>(mg/l)               | Source  | Reference                    |
|--|--|---|------------------------------|
| <i>Streptococcus epidermis</i>   | 200  | Oil contaminated soil                         | Mohite et al. 2010           |
| <i>Pseudomonas</i> sp., <i>Acinetobacter</i> sp., <i>Kelibsiella</i> sp., <i>Citrobacter</i> sp., <i>Shigella</i> sp.                              | 200-900                                    | Phenol polluted waters of Lake Parishan, Iran | Kafilzadeh et al. 2010       |
| <i>Pseudomonas flourescens</i> PU1   | 1000                                       | Soil samples                                  | Mahiuddin et al. 2012        |
| <i>Pseudomonas putida</i> , <i>Acinetobacter</i> sp., <i>Bacillus thuringiensis</i> , <i>Brevibacterium iodinum</i> , <i>Staphylococcus aureus</i> | 400  | Mangrove sediments in Persian gulf            | Kafilzadeh and Mokhtari 2013 |
| <i>Bacillus cereus</i> strain B3   | Complete degradation below 500 mg/l phenol | Coking wastewater                             | Yu et al. 2011               |

(Continued)

(Continued)

| Microorganism<br>(Bacteria)   | Phenol<br>degraded<br>(mg/l)  | Source  | Reference               |
|---|---|---|-------------------------|
| <i>Pseudomonas</i> sp., <i>Bacillus</i> sp.   | 750-900   | Municipal and petroleum wastewater                  | Dabbagh et al. 2012     |
| <i>Pseudomonas aeruginosa</i>   | 80  | Urban wastewaters                                   | Razika et al. 2010      |
| <i>Ralstonia</i> sp.  | 100-1100  | Oil contaminated soil                               | Tabib et al. 2012       |
| <i>Pseudomonas</i> sp. WUST-C1  | 50-1200   | Activated sludge                                    | Liu et al. 2012         |
| <i>Micrococcus</i> sp., <i>Pseudomonas</i> sp.                                      | 200-1000  | Textile industry effluent                           | Rajani and Vijayan 2015 |
| <i>Pseudomonas aeruginosa</i> ,<br><i>Pseudomonas</i> sp., <i>Bacillus subtilis</i> | 400<br>( <i>P.aeruginosa</i> )<br>700<br>( <i>Pseudomonas</i> )<br>500<br>( <i>B.subtilis</i> ) | Activated sludge of treatment plant of a steel mill | Hasan and Jabeen 2015   |

(Continued)

(Continued)

| Microorganism<br>(Fungi)  | Phenol<br>degraded<br>(mg/l)  | Source   | Reference                     |
|---|---|--|-------------------------------|
| <i>Fusarium</i> sp., <i>Aspergillus</i> sp.,<br><i>Penicillium</i> sp., <i>Graphium</i> sp. | 138-1381  | Stainless steel<br>industry<br>effluent        | Santos and Linardi<br>2004    |
| <i>Paecilomyces variotii</i> JH6  | 100-1800  | Activated sludge                               | Wang et al. 2010              |
| <i>Alternaria</i> sp., <i>Penicillium</i> sp.   | 0.0186<br>( <i>Alternaria</i> ),<br>0.0054<br>( <i>Penicillium</i> sp.) | Indoor<br>environment                          | Jacob and<br>Alsohaili 2010   |
| <i>Penicillium chrysogenum</i>  | 6-400   | Soil   | Wolski et al. 2012            |
| <i>Trametes versicolor</i>  | 100-200   | Paper mill<br>effluent<br>enriched soil        | Udaysoorian and<br>Prabu 2005 |
| <i>Aspergillus niger</i>  | 100-500   | NCIM, Pune                                     | Supriya and<br>Neehar 2014    |
| <i>Aspergillus awamori</i> NRRL 3112  | 0.3-1   | US Department<br>of Agriculture                | Stoilova et al.<br>2006       |
| <i>Fusarium flocciferum</i>   | 1000  | Phenol<br>containing<br>industrial<br>effluent | Mendonca et al.<br>2004       |

(Continued)

(Continued)

| <b>Microorganism<br/>(Fungi)</b>   | <b>Phenol<br/>degraded<br/>(mg/l)</b> | <b>Source</b>                    | <b>Reference</b>           |
|--|---------------------------------------|----------------------------------|----------------------------|
| <i>Fennellia Flavipeps</i> , <i>Aspergillus</i> sp., <i>Penicillium</i> sp, <i>Fusarium</i> sp.  | 250-1000                              | Suez gulf and mangrove ecosystem | Farag and Abd-Elnaby 2014  |
| <i>Syncephalastrum racemosum</i>   | 50-300                                | Tannery effluent                 | Srivastava and Sharma 2014 |
| <i>Penicillium commune</i> AL 2,<br><i>Aspergillus fumigatus</i> AL 3,<br><i>Penicillium commune</i> AL 5,<br><i>Penicillium rugulosum</i> AL 7,<br><i>Lecanicillium</i> sp. AL 12 and<br><i>Aspergillus fumigatus</i> AL 15 | 300                                   | Antarctic soils                  | Litova et al. 2014         |
| <i>Aspergillus Niger</i>   | 250                                   | Paper industry effluent          | Sharma and Gupta 2012      |

| <b>Microorganism<br/>(Algae)</b>   | <b>Phenol<br/>degraded<br/>(mg/l)</b> | <b>Source</b>                            | <b>Reference</b>         |
|--|---------------------------------------|--|--------------------------|
| <i>Scenedesmus obliquus</i> , <i>Spirulina maxima</i> , <i>Chlorella</i> sp. | 1000 mg/l                             | Universite Laval, Quebec                 | Kelknar and Kosaric 1992 |
| <i>Ochromonas danica</i>   | 138                                   | Culture Collection of Algae and Protozoa | Semple and Cain 1997     |

(Continued)

| Microorganism<br>(Algae)   | Phenol<br>degraded<br>(mg/l)                                     | Source   | Reference                |
|--|--|--|--------------------------|
| <i>Ankistrodesmus braunii</i> ,<br><i>Scenedesmus quadricauda</i>  | 1000-1500  | Algal Collection at the<br>University of Texas at<br>Austin (UTEX)   | Pinto et al. 2003        |
| <i>Chlorella vulgaris</i> ,<br><i>Chlorella</i> VT-1   | 300<br>( <i>C.vulgaris</i> ),<br>400<br>( <i>Chlorella</i> VT-1) | <i>Chlorella vulgaris</i><br>(Culture Collection of<br>Algae and Protozoa,<br>Ambleside, Cumbria,<br>UK), <i>Chlorella</i> VT-1<br>(pentachlorophenol<br>polluted water) | A.H. Scragg<br>2006      |
| <i>Chlorella vulgaris</i> , <i>Volvox</i><br><i>aureus</i> , <i>Lyngba lagerlerimi</i> ,<br><i>Nostoc linkia</i> , <i>Oscillatoria</i><br><i>rubescens</i> | 166  | Polluted sites   | El-Sheekh et al.<br>2012 |

Biodegradation is a multifaceted process in which many biotic and abiotic factors are involved (Trigo et al. 2009). There are many factors that can affect the degradation ability or metabolism of microorganisms by either preventing or stimulating growth of the organisms. Each of these factors should be optimized for the selected organism to achieve the maximum degradation of the organic compound of choice:

**a) Substrate concentration:** The optimization of the substrate concentration in phenol biodegradation is particularly important because phenol biodegradation by microbial cells is inhibited in potent phenol degrading organisms by phenol itself, especially at higher concentrations (Nair et al. 2008; Nuhoglu et al. 2005).

**b) pH:** Extreme pH values of the medium (less than 3 or greater than 9) as well as sudden changes in pH in which the microbe is present can inhibit its growth (Al-Khalid and El-Naas 2012). Chemical structure and compound toxicity can affect biodegradation of phenols. The chemical structural effect is reflected by the number of substituents, type of substituents, position of substituents and degree of branching. The greater the number of substituents in the structure, the more toxic and less degradable it becomes. For example, substituted phenols such as mono, di-, tri-, and pentachlorophenol are less degradable than unsubstituted phenol. In addition, o- and p-substituted phenols are more degradable than m-substituted phenols (Agarry et al. 2008).

**c) Substrate toxicity:** Toxicity prevents or slows metabolic reactions. This depends on the exposed microorganisms and the concentrations of specific toxicants. Toxicity may result from gross physical disruption of the microbial cell structure or hindrance in its enzymatic activity (Agarry et al. 2008).

**d) Microbial inoculum concentration:** Microbial abundance is another factor in determining biodegradation efficiency. An high microbial concentration could result in more efficient phenol biodegradation process.

**e) Presence of metabolic inhibitors:** The performance of a biodegradation system may be affected by the presence of metabolic inhibitors or competing substrates (Tsai and Juang 2006; Al-Khalid and El-Naas 2012). There are constraints imposed by the occurrence of the environmental contaminants in mixtures as the degradation of one component can be inhibited by other compounds in the mixture, and because different

compounds within the mixture may require different treatment conditions (Stoilova et al. 2006).

**f) Presence of carbon sources:** The ability of microbial communities to degrade pollutants is affected by the presence of naturally occurring carbon sources. In general, adaptation to variations in the concentration of nutrients such as glucose, yeast extract, and  $(\text{NH}_4)_2\text{SO}_4$  enhances the ability to degrade phenols.

**g) Cometabolism:** The process of cometabolism is an important example of the influence of substrate interaction during the biodegradation of pollutants. Cometabolism is defined as the degradation of a compound only in the presence of another organic material that serves as the primary growth substrate. This phenomenon has been attributed to the production of broad-specificity of enzymes, where the primary substrate and the other compound compete for the same enzyme (Annadurai et al. 2008; Bhatt et al. 2007; Al-Khalid and El-Naas 2012).

For process development of phenol bioremediation it is necessary to know the kinetics of growth and phenol degradation. Microbial biodegradation rate is dependent on biomass growth rate. A higher biomass growth rate results in increased biodegradation rate (Agarry et al. 2008). Thus, evaluation of microbial growth kinetics will bring forward its potential for biodegradation of organic compounds. Phenol-degrading microorganisms have been observed to display substrate inhibition at high phenol concentrations. The biokinetic parameters of maximum specific cell growth rate  $\mu_{\max}$ , substrate-affinity constant  $K_s$  and substrate-inhibition constant  $K_I$  vary over a wide range depending on cell type and culture environments (Banerjee and Ghoshal 2010). The value of  $K_s$  (half saturation coefficient) shows the affinity of the microorganism to the substrate.  $K_s$  being inversely related to affinity of microbial system for substrate, a higher  $K_s$  value indicates its lower affinity to the substrate (Firozaee et al. 2011). The value of  $K_I$  (substrate inhibition constant) denotes the resistance of microorganism to the toxic effect of the substrate (Sahoo et al., 2011). Thus, the biokinetic parameters for phenol biodegradation process is analyzed by



modeling the experimental specific growth rate using various substrate inhibitory models. Table 1.2 shows the various growth kinetic models available in literature widely used to represent microbial growth pattern in presence of inhibitory substrates.

**Table 1.2** Growth kinetic models available in literature

| Authors | Growth kinetic models  | Reference        |
|---------|--|------------------|
| Haldane | $\mu = \frac{\mu_{max} S}{K_S + S + (S^2/K_I)}$  | Haldane 1965     |
| Yano    | $\mu = \frac{\mu_{max} S}{K_S + S + \left(\frac{S^2}{K_I}\right) \left[1 + \left(\frac{S}{K}\right)\right]}$ | Yano et al. 1966 |
| Webb    | $\mu = \frac{\mu_{max} S [1 + (S/K)]}{S + K_S + (S^2/K_I)}$  | Webb 1963        |
| Edward  | $\mu = \mu_{max} S \left[ \exp\left(-\frac{S}{K_I}\right) - \exp\left(-\frac{S}{K_S}\right) \right]$         | Edward 2004      |
| Aiba    | $\mu = \frac{\mu_{max} S}{K_S + S} \exp(-S/K_I)$   | Aiba et al. 1968 |

Knowledge of the growth kinetic constants in presence of phenol is very important both for the prediction of their fate and for the design of remediation processes. The knowledge of growth kinetics is an essential and mandatory input for optimal design and the operation of biological treatment of wastewater containing phenol. Growth kinetic modeling have been widely used to understand phenol degradation kinetics in

bacteria (Kumar et al. 2005; Abuhameda et al. 2004; Bai et al. 2007; Vijayagopal and Viruthagiri 2005; Monteiro et al. 2010), fungi (Yan et al. 2005; Wang et al. 2010; Wolskii et al. 2012) and mixed cultures (Dey and Mukherjee 2010; Pishgar et al. 2012; Firozjaee et al. 2011). To best of our knowledge, none of the previous works on microalgal phenol degradation have attempted to study the kinetics associated to the degradation process and thus deserves adequate attention. The biokinetic parameters obtained could prove instrumental in verifying process efficiency as well as in designing microalgae based process for phenol remediation.

Biodegradation of a compound in a mixture is strongly impacted by co-metabolism of other components of the mixture. Previous works concerning the biodegradation of phenol dealt with model solutions simulating industrial effluents. Bajaj et al. (2008) studied the aerobic phenol degradation in synthetic wastewater within a fixed bed biofilm reactor. They reported maximal phenol removal rate of 2.92gm phenol/ (ld) at hydraulic retention time of 0.95 days, total organic loading rate of 15.3 gm COD/(ld) with phenol concentration of 4.9 gm/l. Ratpukdi (2014) investigated the treatment of phenolic based pharmaceutical contaminated wastewater using activated sludge. They reported that 0-98% phenol removal from the synthetic pharmaceutical wastewater. Silva and Campos (1996) reported study of aerobic degradation of phenol containing synthetic wastewater in a three phase fluidized bioreactor using *Pseudomonas putida*. The reactor was operated at phenol concentration of 51.3-1588.3 mg/l with hydraulic retention time of 0.54 to 7.04 h. The phenol degradation efficiency for the reactor was estimated to be 87.2-98.8%. Ghannadzadeh et al. (2015) reported the phenol removal efficiency from synthetic wastewater in a fixed bed reactor with fixed bed up flow sludge blanket filtration (FUSBF) compared to that by typical up flow sludge blanket filtration (USBF) system. They showed improved phenol removal efficiency of FUSBF against that of USBF. The average phenol removal at concentration of 312 mg/l was found to be 97.52% for FUSBF as against that of 92.82% for USBF respectively. Wu et al. (2009) treated 2000 mg/l phenol containing synthetic wastewater in an immersed membrane bioreactor using activated sludge. The phenol removal efficiency obtained in the reactor was 99.98% at a hydraulic retention time of 18 hours. Duan (2011) degraded

phenol concentrations upto 1500 mg/dm<sup>3</sup> in synthetic wastewater using activated sludge in a batch reactor. The maximum phenol degradation rate of 0.048 g phenol/(g VSS h) achieved was an optimum pH of around 6 and temperature of 30°C with inhibitory effects observed at phenol concentration higher than 100 mg/dm<sup>3</sup>. Raikar et al. (2015) studied treated phenol contained in synthetic wastewater using microorganisms contained in garden soil with cow dung as seeding material in a sequential batch reactor. They reported maximum phenol removal efficiency of 97% for 200 ppm phenol under aeration rate of 40 ml/min. Hussain et al. (2015) reported treatment of phenol containing synthetic wastewater in an sequential batch reactor (SBR) using phenol acclimatized activated sludge. They reported phenol degradation in the range of 500-3000 mg/l with decrease in biodegradation rates with increasing phenol concentration. The microbial growth pattern showed an increase in lag phase with increased initial phenol concentration at all concentrations preceding 500 mg/l. Only a limited amount of work has been reported on the microbial treatment of industrial wastewater. Agarry et al.(2008)treated refinery wastewater in their study, which investigated the phenol-biodegrading potential of two indigenous *Pseudomonas* species. Preito et al. (2002) reported phenol degradation by immobilized *Rhodococcus erythropolis* UPV-1 in two wastewater samples (WW1 and WW2) obtained from resin industries using an air-stirred reactor. Phenol was biodegraded completely for WW1 and partially (concentration lower than 50 mg/l) for WW2. Sharma and Gupta (2012) studied biodegradation of 268 mg/l phenol in synthetic and paper industry effluent using fungi *Aspergillus niger* immobilized on sodium alginate beads as well as free cells. They reported that immobilized cell degraded phenol to 110 mg/l and 28 mg/l in paper industry effluent and synthetic wastewater respectively. Free cells of *Aspergillus niger* degraded phenol to 119 mg/l and 150 mg/l in paper industry effluent and synthetic wastewater respectively. Analysis of practical applicability of the potent phenol degrading microbial strains is of utmost necessity for developing efficient bioremediation systems. None of the phenol degrading algal strains have been verified for practical applicability to treat phenol in industrial wastewater and thus deserves serious attention.

Efficient phenol degrading strains are used for treatment of organic pollutants in activated sludge process (ASP). It is most common biotreatment process used to treat municipal and industrial wastewater. Typically wastewater after primary treatment i.e. suspended impurities removal is treated in an activated sludge process based biological treatment system comprising aeration tank followed by secondary clarifier. The aeration tank is a completely mixed or a plug flow (in some cases) bioreactor where specific concentration of biomass is maintained along with sufficient dissolved oxygen (DO) concentration (typically 2 mg/l) to effect biodegradation of soluble organic impurities. The aeration tank is provided with fine bubble diffused aeration pipe work at the bottom to transfer required oxygen to the biomass and also ensure completely mixed reactor. In several older installations, mechanical surface aerators have been used to meet the aeration requirement. The aerated mixed liquor from the aeration tank overflows by gravity to the secondary clarifier unit to separate out the biomass and allow clarified, treated water to the downstream filtration system for finer removal of suspended solids. Figure 1.9 shows the diagrammatic representation of an ASP process (Mittal 2011).

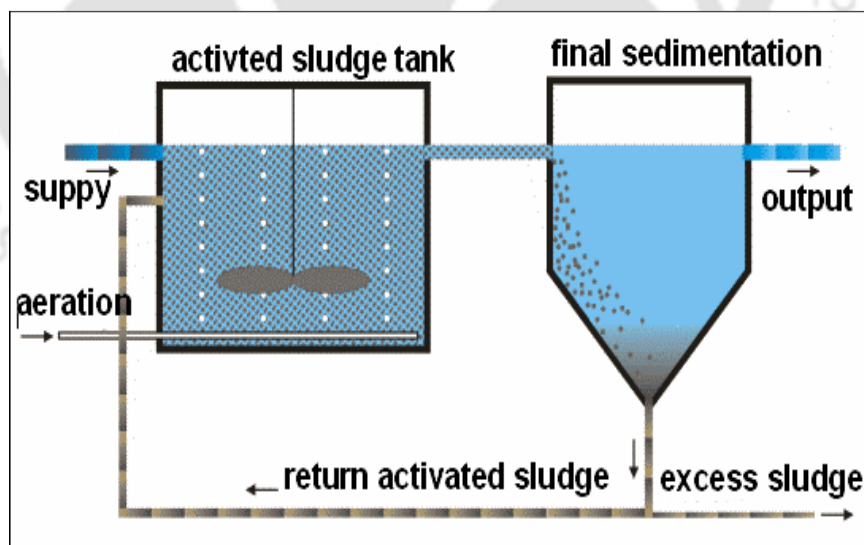


**Figure 1.9** Biological treatment of industrial wastewater using activated sludge process (Mittal 2011).

### 1.6 Microalgal wastewater treatment: Future of sustainable wastewater treatment

The necessity to divert our current research towards understanding microalgae based wastewater treatment arises from its advantages over conventional treatment. The algae based wastewater treatment holds potential to solve problems associated with conventional treatment as follows:

- a) **Self-oxygenation:** Aerobic microorganisms require oxygen to consume organic compounds in wastewater. To provide aeration, traditional wastewater treatment processes employ mechanical aeration accounting for 45 to 75 % of total energy costs of conventional wastewater treatment plants ([www.oilgae.com](http://www.oilgae.com)). Microalgae produce oxygen photosynthetically so it can eliminate the necessity of mechanical aeration in waste water treatment systems, which is costly, limited by poor aqueous solubility of oxygen as well as chances of volatilization of toxic organic compounds during mechanical aeration (Borde et al. 2003). This makes algae based wastewater treatment a cost effective alternative to conventional wastewater treatment systems.
- b) **Carbon negative system:** The conventional wastewater treatment plants as major contributor to greenhouse gases have been identified by US Environmental Protection Agency. The CO<sub>2</sub> produced by algae based wastewater treatment is in turn utilized for algal growth making the entire system carbon negative ([www.oilgae.com](http://www.oilgae.com)).
- c) **Energy rich sludge:** The conventional wastewater treatment system generates huge amount of hazardous sludge which needs to be disposed in landfills. On the contrary, the algal sludge generated in algae wastewater treatment plants is rich in energy. The lipid rich algal sludge can be further processed to make biofuel or other valuable products as bio-fertilizer. Studies have suggested the mixotrophic nature in a number of algal species (i.e. they can grow both autotrophically as well as heterotrophically) leads to enhanced lipid content in algal species cultivated in municipal or industrial wastewater. The basic pathway involved in carbon capture

and lipid biosynthesis during mixotrophic algal cultivation leading to enhanced lipid production is shown in Figure 1.10. The fatty acid precursor are synthesized de novo in chloroplast using both carbon fixed during photosynthesis as well as exogenous organic carbon source. The free fatty acids generated in chloroplast are exported to endoplasmic reticulum (ER) where they are converted to Triacylglyceride (TAG) which bud off into oil bodies in the cytosol (Scott et al. 2010).

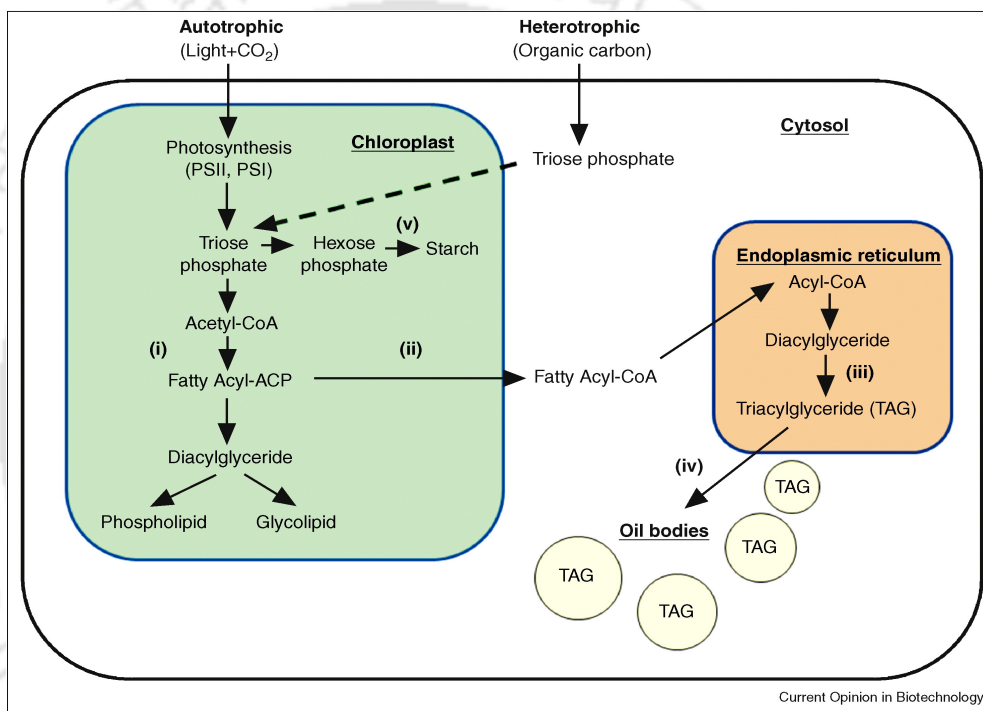


**Figure 1.10** Pathway for carbon capture and enhanced lipid production during mixotrophic growth Key: (i) = acetyl-CoA carboxylase (ACCase) and fatty acid synthase (FAS); (ii) = fatty acid thioesterases and acyl-CoA synthetases; (iii) = TAG biosynthesis enzymes including acyl-CoA:diacylglycerol acyltransferase (DGAT); (iv) = oil body formation; and (v) = ADP-glucose pyrophosphorylase and starch synthase (Scott et al. 2010).

Mahapatra et al. (2014) studied mixotrophic cultivation of algal consortia in municipal wastewater. The reported nutrient removal and remediated total organic carbon from wastewater along with enhanced biosynthesis of lipids in algal biomass from 18% to 28.5% of dry weight. Woertz et al. (2009) studied algae grown on dairy farm and municipal wastewater supplemented with CO<sub>2</sub> as a potential source of low cost biofuels. They reported that a peak lipid productivity of 17 mg/day/L and 24 mg/L/day for dairy and municipal wastewater respectively. The process also resulted in removal of nutrients as ammonium and orthophosphate from both type of wastewaters. Hena et al. (2015) cultured a consortium of native algal strains with high lipid content in dairy farm wastewaters. The native algal strains removed more than 98% nutrients from dairy wastewater with biomass production and lipid content in the algal consortium of 153.54 t ha<sup>-1</sup> year<sup>-1</sup> and 16.89% respectively. Out of the algal lipids obtained 72.70% was converted to biodiesel. Kim et al. (2014) analyzed the nutrient removal and biofuel production efficiency in high rate algal pond using municipal wastewater. They reported an chemical oxygen demand, total nitrogen and phosphate removal efficiency in real municipal wastewater at 85.44 ± 5.10%, 92.74 ± 5.82%, and 82.85 ± 8.63%, respectively in 2 day hydraulic retention time (HRT) by an algal consortium predominantly containing *Chlorella*, *Scenedesmus* and *Stigeoclonium*. The consortium showed biomass and lipid productivity of 0.500 ± 0.03 g/l/day and 0.103 ± 0.0083 g/l/day respectively. The utilization of industrial wastewater as a cultivation medium for algae leading to wastewater treatment and biofuel feedstock generation have not been well studied. However, a few recent studies suggest the enormous prospects of cultivation of algal biodiesel feedstock using industrial wastewaters. Nilsen (2015) studied treatment of industrial and municipal wastewater using microalgal species as *Scenedesmus dimorphus* and *Selenestrum minutum*. They reported that under mixotrophic growth, microalgae and bacteria together removed 50-60% of dissolved organic carbon (DOC) from municipal wastewater and 68-81% DOC from industrial wastewater mixtures. Along with DOC, microalgae also removed more than 99% ammonium and 82-98% total phosphorus. Their results showed that both the algal species showed highest biomass growth in industrial wastewater resulting in higher removal of DOC. Chinnasamy et al. (2010) studied the feasibility of cultivation of a consortium of algal strains in carpet mill effluents for biodiesel production. They reported maximum biomass production of approximately 9.2-17.8 tons ha<sup>-1</sup> year<sup>-1</sup> with removal of more than 96% nutrients from wastewater. They proposed that the generated algal biomass can be used for biodiesel production. Ascon (2009) has patented a process (WO 2009114752 A1)

leading to production of biofuels using toxic xenobiotics released in industrial wastewaters as substrate. They demonstrated that recalcitrant xenobiotic compound as 3,4-dichlorobenzoic acid and Naproxen could be transformed to usable biofuels by aerobic and anaerobic biofilm bacteria cultured in multiphasic reactors. The aerobic and anaerobic bacteria in multiphasic reactor completely metabolizes the xenobiotics by cooperative metabolisms. About 90% of the substrate was converted to biogas by methanogenic consortium in the anaerobic biosynthesis reactor. The CO<sub>2</sub> produced in the aerobic and anaerobic reactor was captured in a photobioreactor containing blue green algal cells. The waste CO<sub>2</sub> supports algal growth in the photobioreactor and serves as a source of hydrogen or lipids as biofuel products. Thus, the patented technology couples microbial breakdown of xenobiotics to microbial biofuel synthesis thus resulting in supply of cheap energy products while remediating environmental pollution and reducing costs associated to hazardous waste disposal. This technology is of interest as the commercial applicability of the mixotrophic culture process is hindered by high substrate cost which accounts for 50% of the cost of the cultivation medium (Cheng et al. 2009). This bottleneck associated to algal mixotrophic cultivation could be answered by finding out cheap alternative substrates which will reduce the production costs of algal biodiesel feedstock. The use of toxic industrial wastes as mixotrophic culture substrate is a significant development as it will reduce the costs associated to mixotrophic algal cultivation solving a major bottle neck in commercialization of algal biodiesel. However, more algal mixotrophic processes using xenobiotics as substrate needs to be developed in future which will couple the benefits of environmental protection from toxic effects of the xenobiotics and algal biodiesel feedstock. Phenol being a xenobiotic widely found in industrial wastewaters, its utilization as a mixotrophic culture substrate could be highly useful to generate a cheap algal mixotrophic culture process with potential biofuel applications. Figure 1.11 shows a process diagram for wastewater based algae cultivation system combining wastewater remediation, CO<sub>2</sub> sequestration as well as generation of algal feedstock for production of biofuels and other bio-based chemicals. Wastewaters provide not only water medium for algal cultivation but also is a source of organic carbon as well as essential nutrients resulting in high algal biomass productivity. In addition, the CO<sub>2</sub> produced in wastewater treatment plants as well as industrial sources as power industries could be sequestered by algae leading to enhanced biomass growth. Wastewater based algae cultivation system saves large quantities of freshwater as well as nutrients and CO<sub>2</sub> demand required for algal growth thus reducing the associated life cycle burdens. The algal cultivation system is a



economically viable, sustainable process providing dual benefits of environmental protection as well as production of carbon neutral fuel (Zhou 2015).

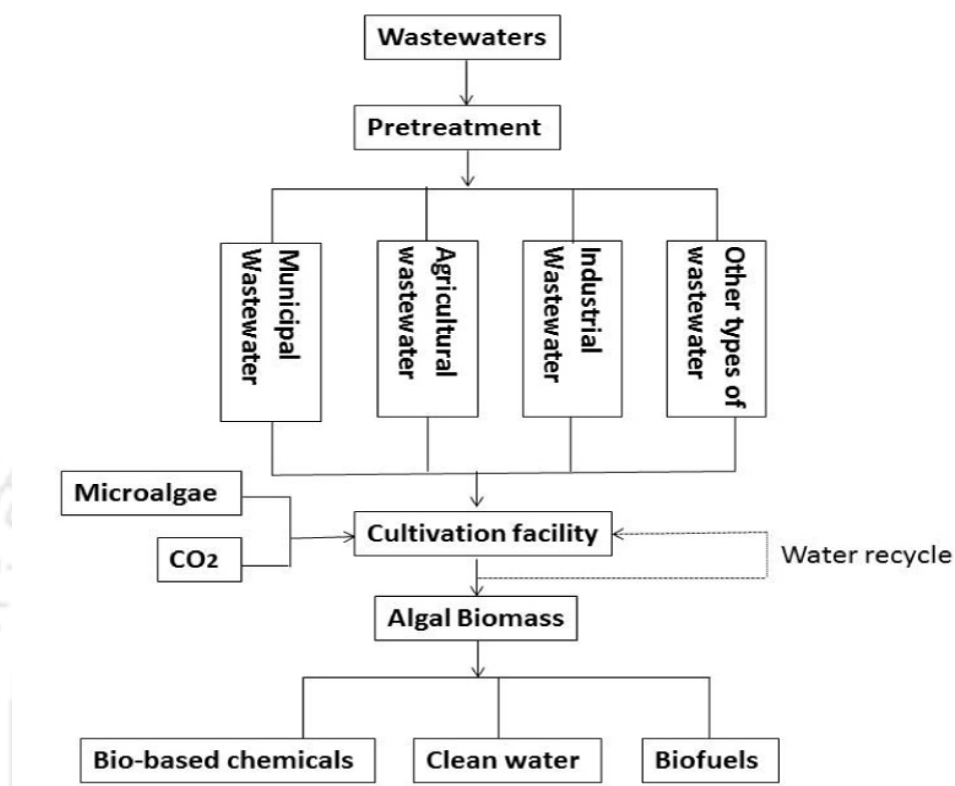


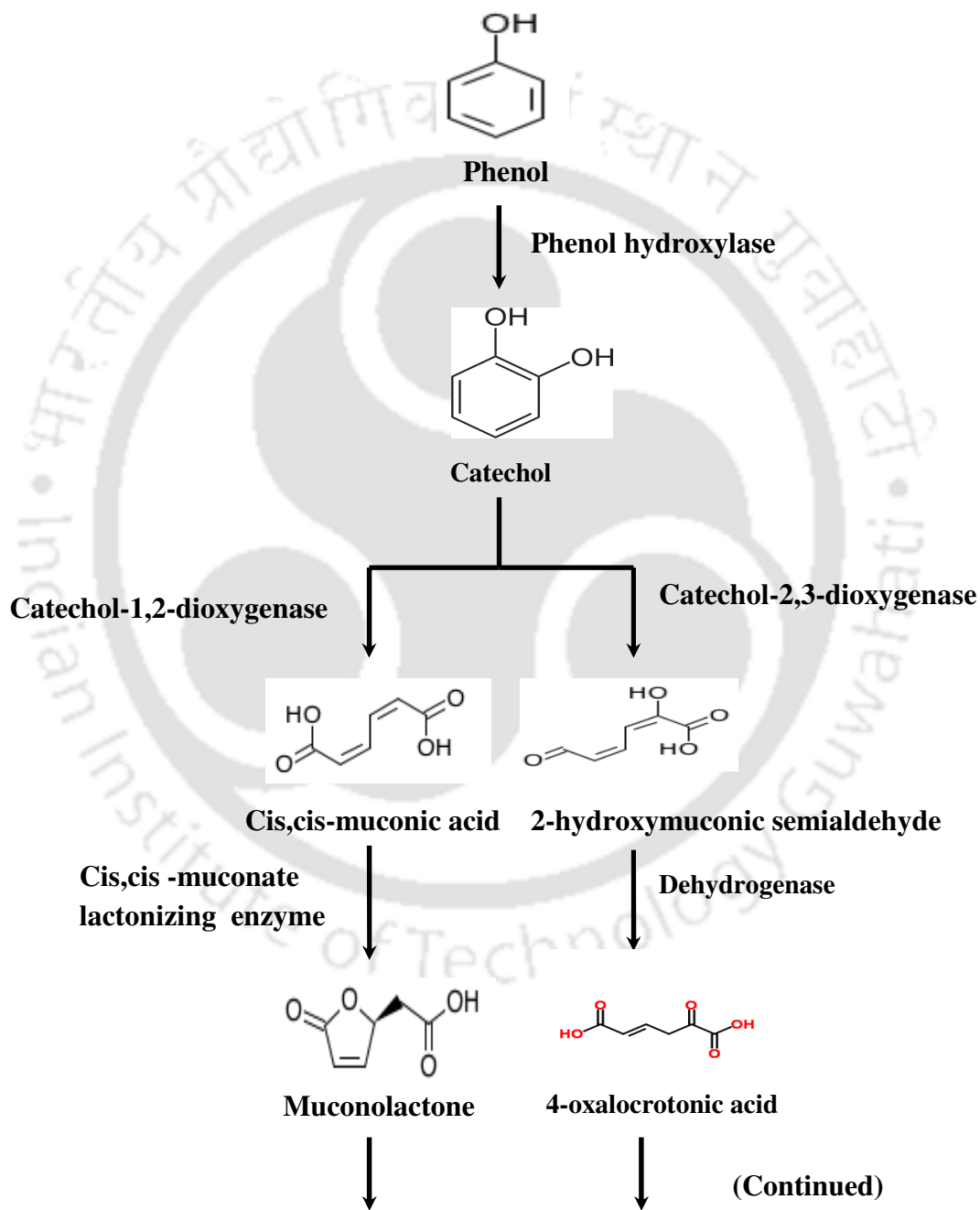
**Figure 1.11** Integrated wastewater based algae cultivation system for wastewater treatment and production of biofuels and bio based chemicals (Zhou 2015).

### 1.7 Mechanism of aerobic phenol biodegradation

Microbial phenol degradation is governed by the action of a cascade of enzymes. There is scarcity of information on enzymatic mechanism involved in algal phenol degradation. The only pathway of algal phenol mineralization has been reported is of *Ochromonas danica* showing activity of meta pathway (Semple and Cain 1996). Complete elucidation of microalgal phenol degradation pathway have not been carried out for any other microalgal strains. This calls for further study to elucidate phenol degradation pathways in microalgae. Presence of molecular oxygen is an important

prerequisite for aerobic phenol degradation. Figure 1.12 shows the general pathway of phenol degradation by aerobic microorganisms. Phenol hydroxylase, the first enzyme of the phenol biodegradation pathway utilizes molecular oxygen to add a hydroxyl group ortho to the hydroxyl group of phenol resulting in catechol. Reduced pyridine nucleotide (NADH<sub>2</sub>) is required for the phenol hydroxylation activity of phenol hydroxylase. Catechol is then be metabolized either by either of the two pathways, ortho ( $\beta$ -keto adipate pathway) or by the meta pathway depending on the organism. In the ortho pathway, the catechol ring is cleaved between two hydroxyl groups by catechol-1,2-dioxygenase. This cleavage mechanism termed intra-diol fission leads to formation of cis,cis-muconic acid. Lactonizing enzyme lactonizes cis,cis-muconic acid to muconolactone. Muconolactone undergoes isomerization by isomerase to form 3-Oxidapate-enol-lactone. 3-Oxidapate-enol-lactonase converts 3-Oxidapate-enol-lactone into 3-oxoadipate which is further metabolized to Krebs cycle intermediates. In the meta pathway, catechol is undergoes extradiol cleavage into 2-hydroxymuconic semialdehyde by catechol-2,3-dioxygenase. The 2-hydroxymuconic semialdehyde is dehydrogenated by NAD<sup>+</sup>-dependent dehydrogenase to 4-oxalocrotonate. 2-keto-4-pentenoate hydratase decarboxylates 4-oxalocrotonate to 4-hydroxy-2-oxovalerate. 4-hydroxy-2-oxovalerate aldolase converts 4-hydroxy-2-oxovalerate to acetaldehyde and pyruvate. The prominence of ortho and meta pathways are distinguishable by measuring their characteristic enzyme activities. Wang et al. (2007) reported that estimated the enzymatic activities for phenol biodegradation by the bacterial strain *Acinetobacter* sp. PD12 which showed catechol-1,2-dioxygenase activity indicating phenol degradation by ortho pathway. Jiang et al. (2007) showed that bacterial strain *Alcaligenes faecalis* proved that phenol was assimilated by ortho pathway. Khleifat (2006) reported that most bacteria uses the meta-pathway for degrading phenol. They reported phenol degradation by *Ewingella Americana* using meta pathway. Active meta pathway for phenol metabolism is also observed in strains of *Bacillus cereus* (Banerjee & Ghoshal 2010). Simultaneous activity of meta as well as ortho pathway were reported in *Pseudomonas fluorescens* PU1 (Mahiuddin et al. 2012). They reported higher meta activity over ortho activity. Cai et al. (2007) also reported similar findings of coexistence of both ortho and meta pathway in *Fusarium* species. Most

eukaryotes generally utilize ortho pathway for phenol degradation (Basha et al. 2010). Involvement of ortho pathway for phenol degradation have been reported in eukaryotes as *Trichosporon cutaneum* (Neujhar and Gaal 1973), *Penicillium* sp. (Hofrichter et al. 1993), *Fusarium* sp., *Aspergillus* sp., *Penicillium* sp. and *Graphium* sp. (Santos and Linardi 2004), *Candida* sp. (Tsai et al. 2005).



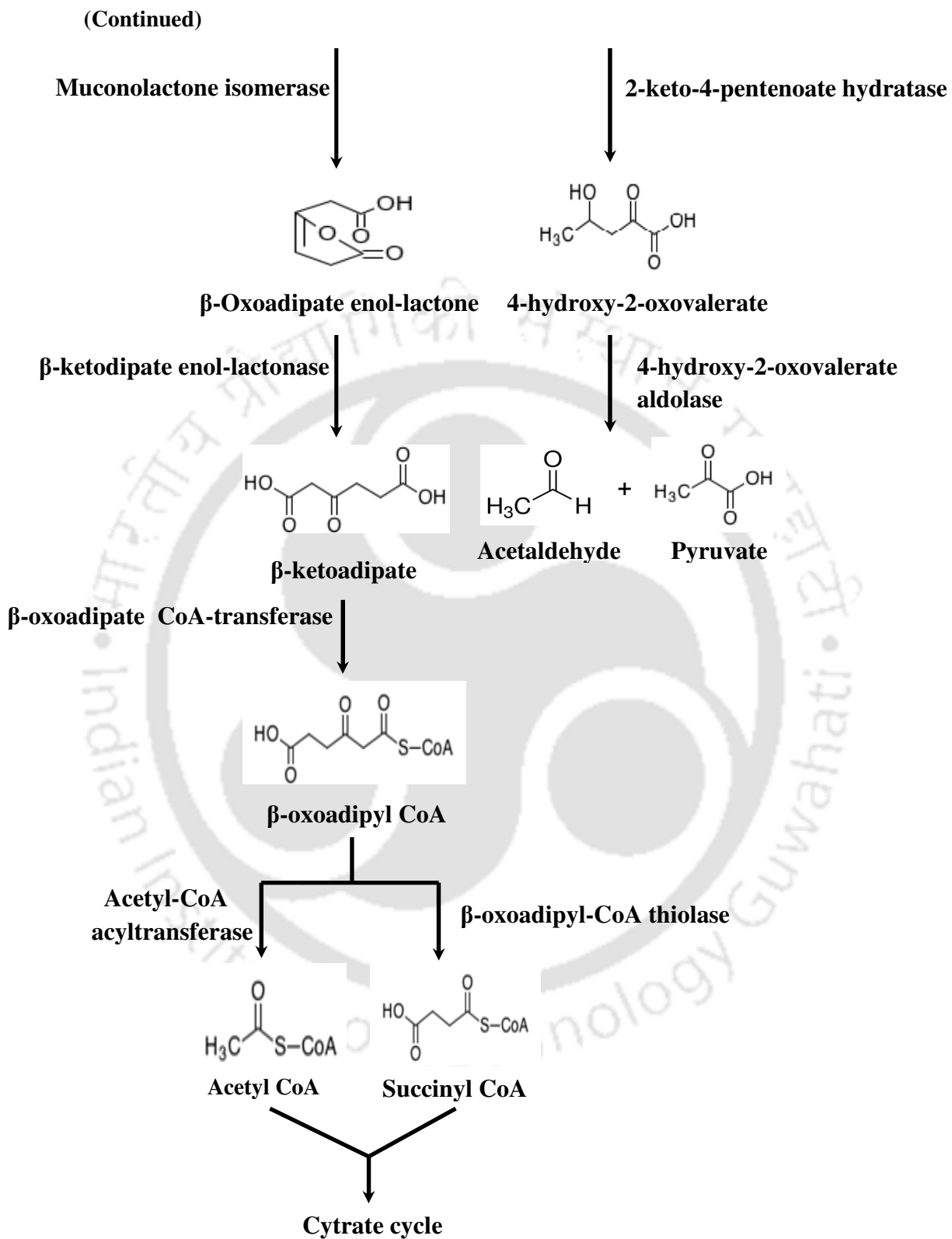


**Figure 1.12** General pathway of phenol degradation in aerobic microbes

## 1.8 Phenol hydroxylase enzymes: Characteristics and potential applications

Phenol being a widely distributed environmental pollutant resulted in strong interest in use of microbial bioremediation for its treatment. As an alternative to use of pure and mixed cultures for bioremediation, the use of purified enzymes for phenol remediation has generated wide interest recently. Since phenol hydroxylase is the first enzyme causing initial attack on phenol in the phenol degradation pathway, the knowledge of its kinetic properties is of utmost importance for its potential applications (Pessione et al. 1999). Phenol hydroxylase (E.C. Number 1.14.13.7) catalyzes NADPH dependent hydroxylation of phenol to catechol which is shown in Figure 1.13. Microorganisms, such as *Pseudomonas* sp. (Kukor and Olsen 1992; Powlowski and Shingler 1994; Dagley and Gibson 1965; Nordlund et al. 1993), *Acinetobacter radioresistens* (Pessione et al. 1999), *Ralstonia eutropha* (Yabuuchi et al. 1995), *T. cutaneum* (Neujahr and Gaal 1973), *Candida tropicalis* (Paca et al. 2007) use flavoprotein monooxygenases to hydroxylate phenol to catechol. Enzymes containing flavins are commonly used by microbes for utilizing aromatic compounds. The role of the flavin in these enzymes is the activation of molecular oxygen. Reduced flavin reacts with oxygen to form a flavin-hydroperoxide, which is an electrophilic, relatively weak oxygenating agent. Oxygenation of the aromatic ring by enzyme-bound oxygen is aided by delocalization of electrons into the ring from the hydroxyl group of phenol (Schie and Young 2007).

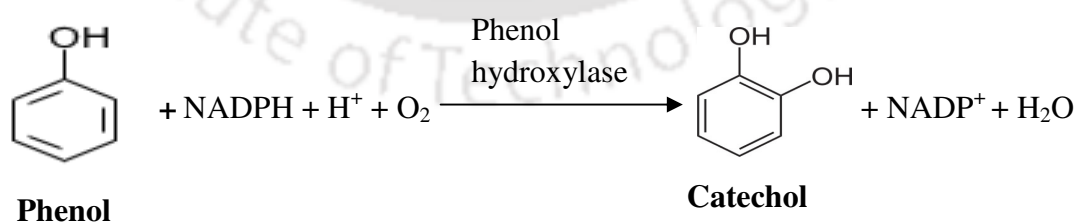


**Figure 1.13** Hydroxylation of phenol to catechol by phenol hydroxylase

The enzyme has been reported to be inducible in nature owing to phenol hydroxylation activity found in enzyme extracts obtained from microbial biomass grown in presence of phenol (Neujahr and Gaal 1973; Paca et al. 2007; Griva et al. 2003; Ahutazi-Chacon et al. 2004; Kagle et al. 2006; Tsai et al. 2005; Greginova et al. 2007). Turek et al. (2011) isolated and characterized the enzyme in *Comamonas testosteroni*. They reported that the enzyme is both cytosolic as well as extracellular with 16 fold higher activity for cytosolic enzymes compared to that in cytosol. Stiborova et al. (2003) reported microsomal location of phenol hydroxylase in *Candida tropicalis*. A number of studies have purified the phenol hydroxylase enzyme and characterized the structural, kinetic as well as molecular properties of the as shown in Table 1.3. As evident from Table 1.3 there is lack of scientific literature that reports the characteristic properties of microalgal phenol hydroxylase and thus deserves further studies in future. This knowledge of about microalgal phenol hydroxylase can instrumental to exploit it for potential application as enzyme based biodegradation, biosensor etc.

Molecular studies have greatly enhanced our knowledge of genes involved in coding of microbial phenol hydroxylases. Genes coding simple flavoprotein phenol hydroxylases have been reported in *Pseudomonas* sp. EST1001 (encoded by *PheA* gene), *P. picketti* PK01 (encoded by *tbuD* gene), *Bacillus stearothermophilus* (encoded by *pheA* gene) and *Trichosporon cutaneum* (encoded by *phyA* gene). On the other hand, multicomponent phenol hydroxylase found in *Pseudomonas* sp. CF600 are encoded by a operon consisting of fifteen structural genes (*dmpB* to *Q*) located in a plasmid encoded operon, *dmp* operon. The operon codes for nine enzymes required for complete phenol and methyl substituted phenol mineralization. Multicomponents of phenol hydroxylase was encoded by the genes *dmp K, L, M, N, O and P*. A ferredoxin like protein is being encoded by *dmpQ*. The gene *dmpB* is encoded by catechol-2,3-dioxygenase which cause ring cleavage. The enzymes necessary for conversion of ring cleavage product to acetyl CoA is encoded by genes *dmpC, D, E, F, G, H* and *I* while the gene *dmpR* encodes a regulatory protein involved in sensing of aromatic substrates. Similar multicomponent phenol hydroxylase is also reported in *Ralstonia eutropha* JMP134 which is encoded by the gene cluster *phlKLMNOP*. The

**Table 1.3** Properties of purified phenol hydroxylase from various microorganisms

| Organism                      | Substrates   | Co factor  | K <sub>m</sub> Value (mM) | K <sub>i</sub> Value (mM) | Specific Activity (μmol/min/mg) | Optimum pH | Optimum temperature (°C) | Molecular Weight (Da) | Storage stability                               | Reference            |
|-------------------------------|--|--|---------------------------|---------------------------|---------------------------------|------------|--------------------------|-----------------------|---|----------------------|
| <i>Brevibacterium fuscum</i>  | Phenol<br>2-aminophenol<br>3-aminophenol<br>2-chlorophenol<br>3-chlorophenol<br>4-chlorophenol<br>3-methylphenol<br>4-methylphenol<br>Orcinol<br>Phlorogucinol<br>Resorcinol | NADPH,<br>NADH<br>(less<br>active<br>than<br>NADH) | -----                     | -----                     | -----                           | 7.5        | -----                    | -----                 | Loses activity upon dilution, dialysis or aging | Nakagawa et al. 1962 |
| <i>Comamonas testosteroni</i> | Phenol   | NADPH  | -----                     | -----                     | -----                           | 7.6        | -----                    | 240000                | -----   | Turek et al. 2011    |

(Continued)

| Organism                            | Substrates  | Co factor    | K <sub>m</sub> Value (mM) | K <sub>i</sub> Value (mM) | Specific Activity (μmol/min/mg) | Optimum pH  | Optimum temperature (°C) | Molecular Weight (Da)                                    | Storage stability   | Reference             |
|-------------------------------------|---|--------------|---------------------------|---------------------------|---------------------------------|---|--------------------------|--|---|-----------------------|
| <i>Bacillus thermoglucosidasius</i> | Phenol  | NADH<br>FAD  | ----                      | -----                     | 0.32                            | 6.7   | 55                       | 120000 (Oxygenase component)<br>35000 (flavin reductase) | -70°C<br>No loss of activity of flavin reductase component after 4 months | Kirchner et al. 2003  |
| <i>Trichosporon cutaneum</i>        | Phenol, Quinol<br>2-aminophenol<br>3-aminophenol<br>4-aminophenol<br>2-chlorophenol<br>3-chlorophenol<br>4-chlorophenol | FAD<br>NADPH | 0.018                     | -----                     | 8.3                             | 7.6 (in phosphate buffer),<br>8.2 (in Tris-Cl buffer) | -----                    | 148000   | Stable for 4-6 weeks at 20°C  | Neujhar and Gaal 1973 |

(Continued)



| Organism                             | Substrates  | Co factor | K <sub>m</sub> Value (mM) | K <sub>i</sub> Value (mM) | Specific Activity (μmol/min/mg)       | Optimum pH | Optimum temperature (°C) | Molecular Weight (Da)   | Storage stability | Reference            |
|--------------------------------------|---|-----------|---------------------------|---------------------------|---------------------------------------|------------|--------------------------|---|-------------------|----------------------|
| <i>Acinetobacter radioresistens</i>  | Phenol,<br>o-cresol, m-cresol<br>p-cresol,<br>4-methylphenol,<br>3,4-dimethylphenol,<br>4-florophenol,<br>3-chlorophenol,<br>4-chlorophenol | NADH      | -----                     | -----                     | -----                                 | 7.5        | 24 °C                    | 207000<br>(oxygenase component)   | -----             | Divari et al. 2003   |
| <i>Pseudomonas</i> sp. strain CF 600 | Phenol  | NADH      | -----                     | -----                     | 0.78<br>(minimum)<br>1.4<br>(maximum) | -----      | -----                    | SDS-PAGE shows three polypeptides of molecular masses of 13000, 39000 and 60000 | -----             | Cadieux et al. 2002  |
| <i>Candida tropicalis</i>            | Phenol  | NADPH     | 0.45                      | -----                     | -----                                 | 7.4-7.6    | -----                    | 240000  | -----             | Paca Jr. et al. 2007 |

genes *phlL*, *N* and *O* encode phenol hydroxylase component, *phlM* encodes ferredoxin like protein, *phlP* encodes electron transfer component and *phlK* leads to transcription of the gene cluster (Schie and Young 2007).

Apart from its application for phenol degradation, phenol hydroxylase have been exploited for a range of other important applications as follows:

**a) Phylogenetic analysis of phenol degrading strains:** Dong et al. (2008) compared the sequences of partial largest subunit of multicomponent phenol hydroxylase (LmPH) gene among strains of genera *Pseudomonas*, *Acinetobacter*, *Comamonas* and *Cupriavidus* respectively. They reported that the physiological groupings in phylogenetic tree formed by 16S rDNA sequences were correlated based on partial amino acid sequences of LmPH of the phenol degrading strains. This suggested possible application of LmPH as molecular marker for phylogenetic analysis of phenol degrading strains.

**b) Organic synthesis of dyes:** Kim et al. (2005) has reported the ability of phenol hydroxylase for organic synthesis of dyes as indole and hydroxyindoles as 7-hydroxyindole from indole and its derivatives (Kim et al. 2005). They expressed multicomponent phenol hydroxylase from from phenol degrading strain of *Pseudomonas* sp. KL33 and n-alkylphenol metabolizing strain *Pseudomonas* sp. KL28 in *Escherichia coli*. *Escherichia coli* strains expressing multicomponent phenol hydroxylase from strain KL28 and strain KL33 catalysed the formation of indigo and 7-hydroxyindole respectively from indole. This provides a new approach for exploiting phenol hydroxylases for organic synthesis of dyes.

**c) Phenol biosensor:** Various spectrophotometric and chromatographic techniques are currently being employed for determination of phenol in environmental samples. Biosensors could be a cheap and easy alternative for phenol detection compared to conventional techniques. Phenol biosensors using whole microorganisms are cost effective and produced easily. However, whole microorganism based biosensor suffers from disadvantage of poor selectivity which could be overcome by enzyme based

biosensor. Kjellen and Neujhar (1980) developed an phenol biosensor using NADPH-dependent phenol hydroxylase isolated from yeast *Trichosporon cutaneum*. They immobilized the phenol hydroxylase on surface of Clark oxygen electrode. They reported linearity between maximal rate of oxygen consumption and phenol concentration in the range of 0.5-50  $\mu\text{M}$ .

The electrode response is independent of pH in the range of pH 6.5-9.5 with a rapid read out of 30 sec after sample addition. Linear increase of electrode response with temperature have been observed in the range of 10-40°C. The phenol biosensor could be used for phenol detection for 150 assays without loss of activity. However, the application of phenol hydroxylase is hampered by high costs of its cofactor NADPH. Metzger et al. (2008) overcame this problem by producing a phenol biosensor based on thermostable phenol hydroxylase from *Bacillus stearothermophilus* which uses a much cheaper cofactor NADH for its activity. The partially purified enzyme was entrapped in sol-gel matrix which was attached to Clark oxygen electrode for phenol biosensor application. The biosensor showed linearity between maximal rate of oxygen consumption and phenol concentration in the phenol concentration range of 2.5-400  $\mu\text{M}$  at 40 °C and pH 7.6. The response time of the biosensor was 10 sec which is relatively short. The sensor exhibited 20% activity loss within 7 days. Thermostability of the enzyme used provided advantages of enhanced stability against chemical denaturation leading to ability of the enzyme to resist harmful conditions as acidic pH encountered during enzyme immobilization.

The variety of other application of phenol hydroxylase along with phenol bioremediation suggest enormous possibility of finding new application for novel characterized phenol hydroxylases. This stresses on the necessity of purification and characterization of novel phenol hydroxylases in the future.

### 1.9 Significance of the work

Biological degradation owing to its advantages of complete mineralization of organic pollutants as well as low costs has gained wide attention for treatment of effluents. Phenol polluted wastewater and soil is a main source of phenol degrading microbial strains (bacteria, fungi and algae). The phenol degradation ability of microalgae is less studied compared to bacterial and fungal strains and thus calls for adequate study. Microbial phenol degradation is a strong function of biomass growth and thus the knowledge of growth kinetics is valuable information leading to understanding the capacity of the microbe for phenol degradation (Kumar et al. 2005). Keeping the necessity to evaluate growth kinetics in mind, growth inhibitory models to describe the microbial growth dynamics in presence of growth inhibitory substrate as phenol have been proposed (Banerjee and Ghoshal 2010). Biokinetic parameters obtained from the growth kinetic modelling is a necessary input for design of biological remediation processes with optimized operational conditions for treatment of phenol polluted wastewater (Sahoo et al. 2011, Banerjee and Ghoshal 2010). The previous works on microalgal phenol degradation have not attempted to study the kinetics associated to the degradation process. This area needs serious attention since the biokinetic parameters could be an essential input in verifying process efficiency as well as in designing microalgae based process for phenol remediation. The microbial phenol mineralization capability is completely dependent on activity of metabolic pathway involving a cascade of phenol metabolizing enzymes. The metabolic pathways involved in phenol biodegradation have been well studied in bacteria and fungi compared to that in algae. The scarcity of information on metabolic mechanism of phenol mineralization in green unicellular algae calls for adequate research in this direction. Apart from bioremediation applications of phenol hydroxylase, it has generated wide interest for use as phylogenetic marker, organic synthesis of dyes as well as phenol biosensor. Thus, the knowledge of kinetic properties of phenol hydroxylase is of utmost importance for its potential applications. There is a serious lack of information on kinetic properties of microalgal phenol hydroxylase and calls for research to fulfill this lacuna in scientific knowledge. Microalgae could serve as a promising source of biodiesel provided there is increased biomass production and lipid

productivity. Mixotrophic cultivation of algae using different substrates as glucose, glycerol, fructose etc. is an ideal cultivation strategy for increased accumulation of lipids within less time (Gracia et al. 2006, Kong et al. 2013). The commercial applicability of the mixotrophic culture process is hindered by high substrate cost which accounts for 50% of the cost of the cultivation medium (Yang et al. 2011). The solution to this the bottleneck of high costs incurred on algal mixotrophic cultivation is to use cheap alternative substrates. Algal mixotrophic cultivation using industrial xenobiotic phenol as cheap substrate has not been previously studied and deserves adequate attention. Successful utilization of industrial toxic waste phenol as mixotrophic culture substrate would bring down production costs of algal biodiesel feedstock along with remediation of phenol pollution. The present work attempts to fulfill the above mentioned lacuna in scientific knowledge concerning microalgal phenol degradation.

The work presented in the thesis is divided into the following parts:

- I:** Screening and characterization of phenol degradation by potent algal strains.
- II:** Generation of a microalgae based process for efficient phenol remediation as well as biofuel production.
- III:** Elucidation of pathway of phenol degradation.
- IV:** Purification and characterization of phenol hydroxylase from *Chlorella pyrenoidosa*.



## **Materials and Methods**

## Chapter II

### Materials and Methods

#### 2.1 Screening and characterization of phenol degradation by potent algal strains

##### 2.1.1 Isolation and identification of algal strains

Filamentous algal strains were isolated as per Schramm (1914) and Vinita and Iyer (2013). The algal samples were collected from sewage water source of IIT Guwahati. Algal filaments were manipulated with sterile needle and washed using sterile nutrient solution. The washed algal filaments were cultured in Fog's media at an illumination of 3500 lux, photoperiod of 14 hours light: 10 hours dark and 140 r.p.m. The algae was identified by microscopic observation. Unicellular algal species was isolated from petroleum refinery wastewater. Wastewater algal species was cultured in Fog's media containing 0.2 g/l MgSO<sub>4</sub>, 0.2g/l K<sub>2</sub>HPO<sub>4</sub>, 0.1g/l CaCl<sub>2</sub>.H<sub>2</sub>O, 1 ml/l micronutrient solution, 5 ml/l Fe-EDTA solution. The micronutrient solution is composed of 2.86 mg H<sub>3</sub>BO<sub>3</sub>, 181.0 mg MnCl<sub>2</sub>.4H<sub>2</sub>O, 22.0 mg ZnSO<sub>4</sub>.7H<sub>2</sub>O, 39 mg Na<sub>2</sub>MoO<sub>4</sub>.2H<sub>2</sub>O, 8 mg CuSO<sub>4</sub>.5H<sub>2</sub>O dissolved in a final volume of 100 ml distilled water. Fog's media was supplemented with 20 mg/l phenol and 5 gm/l ampicillin to avoid any bacterial contamination in culture (Joo and Lee 2007). The algae was cultured at an illumination of 3500 lux, photoperiod of 14 hours light: 10 hours dark and 140 r.p.m. Single algal colonies are isolated by streaking the algal culture in solid Fog's media supplemented with 20 mg/l phenol. Isolated single colony was inoculated to Fog's media containing 20 mg/l phenol and allowed to grow under same culture conditions as mentioned above. Molecular identification of the isolated algal strain was carried out by 16S ribosomal RNA (16S rRNA) sequencing. The sequence obtained was submitted to National Centre for Biotechnology Information (NCBI) Genbank and an accession number was obtained. The gene sequence homology was analyzed using Basic Local Search Alignment (BLAST) tool of NCBI, USA and phylogenetic tree was

constructed using Robust Phylogenetic analysis for the Non-Specialist (Dereeper 2008). Another unicellular algal species *Chlorella pyrenoidosa* (NCIM 2738) was obtained from NCIM, Pune and cultured under culture conditions as mentioned above.

### 2.1.2 Screening of potent phenol degrading algal strains

Algal strains at concentration of 220 mg/l were inoculated to Fog's media containing 20 mg/l phenol and cultured under similar culture conditions as mentioned above. To verify the phenol degradation potential, residual phenol concentration was monitored after an incubation period of 4 days. The analysis of residual phenol was performed by HPLC with UV-Visible detector operating at 270 nm in a C-18 column with mobile phase of acetonitrile:water (70:30) at flow rate of 0.5 ml/min. To determine loss of phenol due to abiotic factors, phenol media without inoculation algae was incubated in same condition for 4 days followed by residual phenol analysis by HPLC.

### 2.1.3 Growth kinetics and phenol degradation by potent algal strains

Microalgal strains was cultured in Fog's medium (pH 7.5) containing 0.2 g/l  $MgSO_4$ , 0.2g/l  $K_2HPO_4$ , 0.1g/l  $CaCl_2 \cdot H_2O$ , 1 ml/l micronutrient solution, 5 ml/l Fe-EDTA solution. The micronutrient solution is composed of 2.86 mg  $H_3BO_3$ , 181.0 mg  $MnCl_2 \cdot 4H_2O$ , 22.0 mg  $ZnSO_4 \cdot 7H_2O$ , 39 mg  $Na_2MoO_4 \cdot 2H_2O$ , 8 mg  $CuSO_4 \cdot 5H_2O$  dissolved in a final volume of 100 ml distilled water. Cultures were maintained on an orbital shaker operated at 140 rpm with illumination of 3500 lux for a photoperiod of 14 hrs light: 10 hrs dark in order to simulate the natural light:dark cycle.

The biomass growth was analyzed at equal intervals of 24 hours by carrying out dry weight analysis. The residual phenol at equal intervals of 24 hours was analyzed by HPLC with UV-Visible detector operating at 270 nm in a C-18 column with mobile phase of acetonitrile: water (70:30) at flow rate of 0.5 ml/min. To determine loss of phenol due to abiotic factors, phenol media without



inoculation of algal strains was incubated in same condition followed residual phenol analysis by HPLC. The specific growth rate ( $\mu$ ) at different phenol concentrations was determined by fitting a linear function to exponential phase of  $\ln x(t)$  vs time curve, where  $x$ = biomass (mg/l) and  $t$ =time (days) (Baranyi 2010). The experimental data were analyzed with several available growth kinetic models like Haldane (Haldane 1965), Yano (Yano et al. 1966), Webb (Webb 1963), Aiba (Aiba 2004), Edward (Edward 1970) to select a suitable kinetic model that can represent growth pattern of algal strains in presence of phenol. From the experimental data of specific growth rate ( $\mu$ ) at various initial concentration of phenol ( $S$ ), the model equations were solved using nonlinear regression method (Excel, Microsoft office) and the values of kinetic parameters of different models were determined based on highest regression coefficient ( $R^2$ ) and least standard deviation (SD) value (Saravanan et al. 2008; Duan 2011; Hasan and Jabeen 2015). The specific degradation rate was determined from the gradient of a semi logarithmic plot of substrate concentration,  $S$  vs time for each initial phenol concentration under study ( $S$ ) (Banerjee and Ghoshal, 2010).

In order to analyze the practical applicability of the microalgal strains, the growth and phenol degradation kinetics was studied in petroleum refinery wastewater. Wastewater from an Indian petroleum refinery was collected and stored at 4 °C for further analysis. The analysis of the oil components in refinery wastewater was carried out by China National Standard Method (Zhao et al., 2006). Both oil and oil products have characteristic absorbance at UV range. Heavy oil contains aromatic compounds which corresponds to absorbance wavelength of 250-260 nm whereas clean oil contains alkanes corresponding to absorbance at 215-230 nm. The amount of phenol in refinery wastewater was analyzed by HPLC as mentioned above. The microalgae was inoculated to petroleum refinery wastewater to verify its phenol degradation efficiency in wastewater. The pH of refinery wastewater was 7.9. It was not adjusted for the degradation experiments. All other growth and culture conditions were similar as mentioned in section above. The biomass growth as well as phenol degradation in refinery wastewater was characterized at regular intervals of 24 hours using dry weight analysis and HPLC respectively. The specific growth and degradation rates were estimated by fitting the experimental growth kinetic data to the growth kinetic models. Following treatment of the wastewater with the microalgae, changes in other oil components of refinery wastewater was characterized by China National Standard Method (Zhao et al., 2006).

### **2.1.4 Analysis of biosurfactant production**

Many microbial species produce biosurfactants which changes the solubility and dispersion of hydrocarbons, thus increasing its availability to the microbial cells. Biosurfactants induce rise in cell surface hydrophobicity which changes the affinity between microbial cell and hydrocarbon, thus leading to increased biodegradation rates (Hassan et al.2014). The biosurfactant production ability was analyzed by the emulsification assay as per Rocha et al.(2007). In this assay, 2 ml of culture was vortex mixed with same volume of kerosene and left to stand for 24 hours. The Emulsification index (E<sub>24</sub>) was calculated as percentage of the height of the emulsified layer (mm) divided by height of the liquid column (mm).

### **2.1.5 Analysis of effect of phenol on cell surface morphology**

The effect of phenol on the cells of microalgae was studied by imaging with scanning electron microscope (1430vp, Leo, Germany). The surface of the algal biomass treated with 200 mg/l phenol for a period of 48 hours were observed by SEM and also compared with control cells. Sample preparation was carried out as per protocol given by Sadiq et al. (2011).

## **2.2. Generation of a microalgae based process for efficient phenol remediation as well as biofuel production**

### **2.2.1 Analysis of growth kinetics and phenol degradation by phenol acclimatized cells of *C. pyrenoidosa***

The best potent microalgal strain was selected and phenol acclimatization of microalgal cells was carried out with the aim of increasing the growth and phenol degradation rates. A strain with high growth and phenol degradation rate is an important requirement for its practical applicability in treatment of phenol in wastewaters. Microbial strains is dependent on activity of phenol metabolism

pathways involving a cascade of phenol metabolizing enzymes. During acclimatization, the phenol degrading enzymes are induced in the cells making the microbial cells compatible to utilize phenol as carbon source thus having positive effects on phenol degradation rates (Dey and Mukherjee 2010; Das et al. 2014). Microalgal phenol acclimatization was carried out by subculturing of the cells at the phenol concentration at which the highest growth as well degradation rate of unacclimatized cells is achieved. Continuous subculturing at an interval two days for a period of two weeks was carried out. The phenol degradation ability of acclimatized cells of microalgae was analyzed in the phenol concentration range of 50-1250 mg/l. The biomass growth at equal intervals of two hours was analyzed by dry weight analysis. The residual phenol at equal intervals of two hours was analyzed by HPLC as described in section 2.1.3.

### **2.2.2 Effect of physical parameters on phenol degradation rate**

Phenol degradation rate is sensitive to many physico-chemical parameters as pH, inoculum size, carbon and nitrogen sources. Optimization of these parameters would lead to enhanced efficiency of phenol degradation as well as decrease the process cost significantly. Thus, a phenol degradation process designed using optimized parameters would be highly instrumental in efficient phenol treatment (Patil and Jena 2015). The three physical parameters of inoculum dose, pH and photoperiodicity optimized in the current study were selected keeping in mind the parameters that could be practically and cost effectively handled to result in an optimized microalgal wastewater treatment system. To determine the effect of physical parameters, the phenol concentration selected for the experiments is the particular concentration at which the induced microalgal cells had highest growth as well as degradation rate as observed in the degradation experiments.

**a) Effect of inoculum dose:** Microbial inoculum dose has been found to significantly affect phenol degradation rates (Kilic and Donmez 2014; Kumar et al. 2015) and optimization of this parameter can be effectively handled in real

wastewater systems. The dynamics of biomass growth and phenol degradation have been evaluated with inoculum concentration in the range of 100-500 mg/l.

**b) Effect of photoperiodicity:** Photodependency on phenol degradation have been reported in algal species as *Scenedesmus obliquus* (Feng et al. 2013) and *Chlorella vulgaris* (Scragg 2006). Thus, knowledge of photoperiod length responsible for optimum phenol degradation will be an invaluable input to develop an efficient microalgal phenol degradation process. To determine the effect of various photoperiod lengths on phenol degradation efficiency, biomass growth and phenol degradation was determined at light: dark photoperiodicity of 6 hours light: 18 hours dark, 8 hours light: 16 hours dark, 10 hours light:14 hours dark, 12 hours light: 12 hours dark, 14 hours light:10 hours dark. The highest length of light duration in photoperiod experiment is chosen to be 14 hours since this is the approximate day length (summer season) in the geographical location of our study. The algal process can be made cheap, environmental friendly and self-sustainable if we can omit the necessity of providing artificial illumination. This is the main idea behind limiting the maximum light period for our study at 14 hours since this is achievable using natural day light.

**c) Effect of pH:** Another, important physical parameter that could affect the efficiency of phenol biodegradation process is pH of the wastewater to be treated. Microbial biodegradation processes are dependent on metabolic pathways involving phenol metabolizing enzymes. pH change can affect enzyme stability leading to decrease in microbial phenol degradation efficiency (Banerjee and Ghoshal 2010). Thus, it is of utmost importance to estimate the pH of the wastewater before employing a microbial biodegradation process for its treatment. To analyze the effect of pH, biomass growth and phenol degradation was studied in pH range 4-9 of the culture media.

### 2.2.3 Growth kinetics and phenol degradation by pre adapted cells

To obtain microalgal cells induced with phenol degrading enzymes which renders it useful for an optimized phenol degradation process, the previously

acclimatized cells were pre adapted to the concentration where highest growth and degradation rate is achieved in phenol degradation experiment (50-1250 mg/l phenol) described in section 2.2.1. For phenol acclimatization, the cells were subcultured at regular intervals of 1 day for a period of seven days in phenol containing media. To evaluate the kinetics of phenol degradation, phenol degradation is being carried out in optimal phenol concentration (i.e. the concentration with highest growth and phenol degradation rate) using optimal biomass concentration, pH and photoperiodicity as obtained from the previous experiments described in section 2.2.2. Biomass growth, residual phenol concentration, specific growth and degradation rate determination and growth kinetic modeling were performed using the same methodology as described in the section 2.1.3.

#### **2.2.4 Practical application of pre adapted microalgae for phenol degradation**

To determine the practical applicability, the pre adapted microalgae was applied for phenol degradation in real refinery wastewater. Collection of wastewater samples and phenol determination was carried out as mentioned in the section 2.1.4. For phenol degradation analysis, phenol acclimatized log phase cells of *C.pyrenoidosa* was inoculated in refinery wastewater and cultured under same condition as mentioned in the section 2.1.3. pH of the wastewater was not adjusted to maintain conditions similar to that of wastewater for the experiment. Determination of biomass growth, residual phenol, specific growth and degradation rate and growth kinetic modeling were performed as in section 2.1.3.

#### **2.2.5 Biochemical characterization of phenol degrading biomass**

The biochemical composition changes in microalgae involved in phenol degradation process was analyzed by FTIR (Perkin Elmer Spectrum 2, USA) as per protocol of Feng et al (2013). The characteristic peak area of lipids, protein and carbohydrates were obtained at 2800-3000  $\text{cm}^{-1}$ , 1500-1700  $\text{cm}^{-1}$  and 1000-1200

cm<sup>-1</sup> respectively was obtained using Spectrum 10 FTIR software (Perkin Elmer Spectrum 2, USA). The total weight of lipids, proteins and carbohydrates were obtained from the characteristic peak area as per Pistorins et al. (2009). Assuming microalgae to be composed mainly of lipid, protein and carbohydrates the biochemical molecule content was obtained as per Feng et al (2013). Productivity of lipids, protein and carbohydrates were calculated as a product of biomass productivity and lipid content as per Lv et al. (2010). High neutral lipid productivity is the main factor success of a microalgal system to serve as an efficient biodiesel feedstock. For analyzing neutral lipids, algal cells were stained with Nile red staining method as per Chen et al (2009). Cell density chosen for Nile red staining was 0.06 (OD<sub>750</sub>) as optimized for the staining protocol by Chen et al. (2009). Fluorescence analysis of Nile red stained algal cells were measured on multimode microplate reader (Infinity, Tecan, Switzerland) at excitation and emission wavelengths at 490 nm and 580 nm respectively. The excitation and emission standards were selected based on pre scan of neutral lipid standard, trilolein (Himedia, India). A trilolein standard curve ( $R^2=0.99$ ) in the concentration range of 5-100 µg/ml was used for neutral lipid quantification. The total lipids from 1 gram of algal biomass was extracted using the protocol of Bligh and Dyer (1959). The chloroform layer containing lipid was collected and vaporized in an evaporator. The crude lipid content is quantified by weighing the dried crude lipid residue and expressed as percentage of dry weight.

### **2.2.6 Bioethanol fermentation of lipid extracted residual biomass**

Dilute acid saccharification of the lipid extracted biomass was performed following the protocol of Lee et al. (2015). The dilute acid saccharification of the defatted biomass (lipid extracted) was performed under the optimized condition of autoclaving at 121°C for 15 minutes in presence of 0.3 N HCl. The dilute acid hydrolysate was centrifuged and the reducing sugar content in the supernatant was determined by Phenol Sulphuric Acid assay (Dubois et al. 1956). The supernatant was then neutralized to pH 7 and autoclaved before employing it for fermentation. The bioethanol fermentation of the lipid extracted biomass using Baker's yeast *Saccharomyces cerevisiae* as suggested by Kavitha et al. (2014). Briefly, a 3 %

yeast inoculum was cultured in LB medium at 30 °C for 24 hours at 200 rpm orbital shaking. The yeast cells were then harvested, residual sugars washed and added to air tight bottles containing algal hydrolysate and incubated in dark at 30 °C for 4 days with 200 rpm orbital shaking. The bioethanol produced in the fermentation process was estimated using spectrophotometric micromethod as per Magri et al.(1997).

## 2.3 Elucidation of pathway of phenol degradation

### 2.3.1 Preparation of crude enzyme extract

Axenic culture of *C.pyrenoidosa* (NCIM 2738) obtained from NCIM, Pune was cultured in Fog's medium (pH 7.5) composed of 0.2 gm/l MgSO<sub>4</sub>, 0.2 g/l K<sub>2</sub>HPO<sub>4</sub>, 0.1 g/l CaCl<sub>2</sub>.H<sub>2</sub>O, 1 ml/l micronutrient solution and 5 ml/l Fe-EDTA solution. The micronutrient solution is composed of 2.86 mg H<sub>3</sub>BO<sub>3</sub>, 181.0 mg MnCl<sub>2</sub>.4 H<sub>2</sub>O, 22.0 mg ZnSO<sub>4</sub>.7 H<sub>2</sub>O, 39 mg Na<sub>2</sub>MoO<sub>4</sub>.2 H<sub>2</sub>O and 8 mg CuSO<sub>4</sub>.5 H<sub>2</sub>O dissolved in 100 ml of distilled water. *C.pyrenoidosa* was cultured in 125 mg/l phenol containing Fog's medium with continuous orbital shaking of 140 rpm under illumination of 3500 lux for a photoperiod of 14 hours light/10 hours dark. The residual phenol concentration was determined by HPLC (Prostar, Varian, USA) with the UV-Visible detector operating at 270 nm using a C-18 column with mobile phase of acetonitrile: water (30:70) at a flow rate of 0.5 ml/min. *C.pyrenoidosa* cells were harvested for preparation of crude enzyme extract after 70 % phenol consumption as suggested by Bastos et al. (2009). The cells were harvested by centrifugation at 3000 rpm for 10 min (4°C) and washed thrice with potassium phosphate buffer (50 mM). The washed cells were ground in 50 mM potassium phosphate buffer (1 gm biomass/ml) using mortar-pestle in ice bath, extract was centrifuged (10,000 r.p.m. at 4°C) and the supernatant obtained was used for enzyme activity analysis. The total protein in the crude enzyme extract was analyzed as per Lowry et al. (1951).

For diatom BD1IITG, the methodology for microbial culture and crude enzyme preparation is same as discussed earlier except that enzyme induction was carried out in 100 mg/l phenol since specific growth and degradation rate was highest at this concentration.

### 2.3.2 Characterization of the phenol degradation pathway

Phenol hydroxylase activity was analyzed in a assay mixture containing 50 mM potassium phosphate buffer solution (pH 7.2), 88 $\mu$ g protein, 1.5  $\mu$ M phenol, 1.5  $\mu$ M NADPH. Heat inactivated enzyme extract served as control. The incubation was stopped at equal intervals with 20  $\mu$ l of 0.6 M perchloric acid. Samples were analysed for phenol utilization and concomitant accumulation of the reaction product catechol by HPLC.

The ortho cleavage of catechol (hydroxylation product of phenol) to cis,cis-muconic acid was carried out by catechol-1,2-dioxygenase. Catechol-1,2-dioxygenase activity was analysed in a reaction mixture containing 50mM potassium phosphate buffer pH 7.2, 88 $\mu$ g protein, 1.5 $\mu$ M catechol. Catechol cleavage to cis,cis-muconic acid was analyzed by HPLC. Catechol-2,3-dioxygenase is responsible for meta cleavage of catechol to 2-hydroxymuconic semialdehyde (2-HMS). Catechol-2,3-dioxygenase activity was determined by increase in absorbance at 375 nm due to accumulation of the reaction product 2-HMS ( $E_{375} = 14,700 \text{ mol/L/cm}$ ).

The breakdown products of cis,cis-muconic acid and 2-HMS were identified by electrospray ionization LC-MS (Make: Agilent, Model: Infinity LC system) in negative charge mode. To characterize the metabolites, the catechol dioxygenase assay was carried out as mentioned above. The LC-MS was operated using acetonitrile:water (60:40) mixture as solvent at a flow rate of 0.5 ml/min with detector at 270 nm. The m/z signals corresponding to the metabolites were identified using the Tandem Mass Spectrum database (open source- Central Drug Research Institute, India).



## **2.4 Purification and characterization of phenol hydroxylase from *Chlorella pyrenoidosa***

### **2.4.1 Purification of phenol hydroxylase**

The crude enzyme extract was subjected to ammonium sulphate fractionation in the salt concentration range of 10-70%. For salt fractionation, various salt concentrations was dissolved in the crude enzyme extract by continuous stirring for 30 minutes with incubation in water-ice slurry. After all salts got dissolved, enzyme extract was centrifuged at 12000 rpm for 20 minutes at 4°C resulting in a pellet containing the fractionated protein. The pellet was resuspended in 50 mM potassium phosphate buffer and then dialyzed overnight at 4°C. Total protein and phenol hydroxylase activity of different ammonium sulphate fractions were analyzed as mentioned in section 2.3.1 and section 2.3.2 respectively.

### **2.4.2 Electrophoresis: Enzyme homogeneity, molecular weight determination**

The homogeneity of the purified enzyme as well as its molecular mass was determined by SDS-PAGE using 12.5 % gel (Laemmli 1970). The different molecular weight markers used as reference were MBP-paramayosin (80 kDa), MBP-CBD (58 kD), CBD-Mxe Intein-2CBD (46 kD), CBD-Mxe Intein (30 kDa), CBD-BmFKBP13 (25 kD) and lysozyme (17 kD). The molecular weight of the purified enzyme was determined by a plot of log of molecular weight vs mobility. For detection of protein bands, the gel was stained with mass spectrometry compatible silver staining protocol (Shevchenko et al. 1996).

### **2.4.3 Peptide mass fingerprinting of the purified protein**

Protein spot corresponding to the purified enzyme in the SDS-PAGE gel was excised followed by in gel digestion by trypsin and peptide mass fingerprinting by MALDI-TOF (UltrafleXtreme, Bruker Daltonics, U.S.A.) as per Shevchenko et al. (1996). The resulting tryptic maps were identified by MASCOT (www.matrixscience.com) using NCBI nr and JGI Chlorella genome portal as per Atteia et al. (2006).

### **2.4.4 Absorption characteristics of flavoproteins**

Phenol hydroxylase is known to show characteristic spectral properties of flavoproteins with maxima around 271 nm, 345 nm (Fe-S clusters), 450 nm (flavins) and shoulder between 465-470 nm (Fe-S clusters). The absorption spectrum of the purified protein was analyzed for characteristic of flavoproteins by UV-Visible spectrophotometry (Cary 100, Agilent Technologies, USA) (Paca et al. 2007; Neujhar & Gaal 1973; Pessione et al. 1999).

### **2.4.5 Effect of NADH as cofactor on phenol hydroxylation activity**

Phenol hydroxylase requires nicotinamide adenine dinucleotide as co-substrate for phenol hydroxylating activity. However phenol hydroxylase shows specific ability to use NADH or NADPH or both as cofactors (Neujhar and Gaal 1973; Metzger et al. 1998; Paca et al. 2007). NADPH being very expensive it is desirable to look for phenol hydroxylase with ability to use NADH as cheaper alternative (Metzger et al. 1998). The assay mixture for phenol hydroxylase activity contained 500 µg protein, 1.5 µM phenol, 1.5 µM NADH in 50 mM potassium phosphate buffer. Heat inactivated enzyme extract was used as control. The assay incubation was carried out at 37 °C. The incubation was stopped at equal intervals of time by 20 µl of 0.6 M perchloric acid. HPLC analysis of the samples were carried out to determine phenol utilization and concomitant production of the reaction product catechol (Paca et al. 2007).

#### **2.4.6 Stoichiometry of reaction with phenol**

Stoichiometry helps determine the optimal ratio of reactants for a chemical reaction so that all reactants are fully used. An understanding of appropriate stoichiometry of phenol hydroxylase reaction will help determine the optimal ratio of phenol and co-substrate NADPH at which complete phenol concentration will be hydroxylated to its reaction product catechol. The appropriate stoichiometry of phenol hydroxylase reaction was determined using various combination of initial concentration of phenol and NADPH as per Neujhar and Gaal (1973).

#### **2.4.7 Substrate affinity of purified enzyme towards phenol**

Measurement of velocity of enzyme catalyzed reaction at different substrate concentration helps us understand the enzymes affinity for the substrate. The substrate affinity of phenol hydroxylase towards various phenol concentration and the values of maximal velocity ( $V_{max}$ ) and apparent michealis constant ( $K_m$ ) for phenol oxidation calculated from Lineweaver Burk plots (Paca et al. 2007; Neujhar and Gaal 1973).

#### **2.4.8 Effect of pH and temperature on enzyme activity**

Several factors as binding of substrate to enzyme, ionization states of amino acid residues in enzymes active site, substrate ionization and enzyme structure variation are effected by pH. Temperature has effects on enzymes reaction rate constant and denaturation of enzymes at high temperature ([www.rpi.edu](http://www.rpi.edu)). The dependence of phenol hydroxylating activity on pH and temperature was studied in the pH range 5.5-8.0 and temperature range 25-80°C and the optimal pH and temperature for enzyme activity was determined.

#### **2.4.9 Effect of chelators, heavy metals, denaturant and oxidizing agent on enzyme activity**

The presence of iron or copper in the enzyme was verified by inhibition of enzyme activity by iron or copper chelators. The effect of phenanthroline and sodium arsenate ( $\text{Fe}^{2+}$  chelator), sodium diethyldithiocarbamate (Cu chelator) on phenol hydroxylating activity was determined. Heavy metals are known to accumulate inside living organisms by biomagnification. Heavy metals effect the tertiary structures of enzymes by catalyzing protein destroying reactions or interfering with sulphur-sulphur cross bridges(www.sd67.com). This brings on the importance to study the effect of heavy metals on phenol hydroxylase activity. The effect of heavy metals as  $\text{CuSO}_4$ ,  $\text{AgCl}_2$ ,  $\text{HgCl}_2$  on enzyme activity was analyzed. Denaturation of enzyme changes the enzyme structure and in the changed conformation substrate may no longer fit optimally to enzymes active site. Thus the effect of denaturants on phenol hydroxylase activity needs study. The effect of denaturants as SDS and Urea on enzyme activity was analyzed. The  $-\text{SH}$  group is essential for many enzymes for their activity. Oxidation of  $-\text{SH}$  group by any oxidizing agent results in loss of activity by forming (S-S) disulphide linkages (Kulkarni 2008). Thus, the effect of oxidizing agent  $\text{H}_2\text{O}_2$  on enzyme activity was analyzed.

#### **2.4.10 Multisubstrate specificity of purified enzyme**

The broad substrate specificity of phenol hydroxylase was determined in addition to phenol against isomeric diphenols (catechol, resorcinol, quinol), isomeric methylphenols (o- cresol, m-cresol, p-cresol), halogen substituted phenols (2-chlorophenol, 4-chlorophenol, 2,4- chlorophenol, 2-aminophenol, 3-aminophenol, p-bromophenol, 4-nitrophenol), p and m-hydroxybenzaldehyde, p-hydroxybenzoic acid and 4-nitrophenol. Phenol hydroxylase activity was analyzed in a assay mixture comprised of 50 mM potassium phosphate buffer solution (pH 7.2), 88 $\mu\text{g}$  protein, 1.5  $\mu\text{M}$  substrate, 1.5  $\mu\text{M}$  NADPH. Phenol hydroxylase activity was analyzed by measuring the disappearance of its specific cosubstrate NADPH at 340 nm in UV-Visible Spectrophotometer (Cary 100, Agilent, USA).

### 2.4.11 Storage stability of phenol hydroxylase

Phenol hydroxylase with good storage stability is required so that it can be used for prospective practical applications as phenol remediation or biosensors. Thus, the effect of storage at room temperature as well as 4°C on phenol hydroxylase activity was determined over a period of seven days.





## **Results and Discussion**

## Chapter III

### Results and Discussion

#### 3.1 Abstract

High ecological toxicity of phenol calls for efficient technologies for removal of phenol in industrial wastewater before it is released into aquatic ecosystems. Biodegradation has gained wide interest owing to its advantages of complete phenol mineralization and low costs over conventional physio-chemical methods of phenol treatment. Phenol degradation capabilities of bacteria and fungi have been profoundly studied compared to that in algae. Thus, the present work deals with isolation and screening of potential phenol degrading algal strains. Two unicellular algal species *Chlorella pyrenoidosa* (NCIM 2738) and diatom BD11ITG (isolated from petroleum refinery wastewater) significant capability for phenol degradation showing prospects for application of these two algal strains for control of phenol pollution. The growth and phenol degradation dynamics of two potent algal strains *C.pyrenoidosa* and diatom BD11ITG was analyzed by growth kinetic modeling. Owing to the complete phenol degradation ability of *C.pyrenoidosa*, the strain was used to develop an efficient phenol degradation process that could remediate a wide range of phenol concentration within a short time period. The practical applicability of the microalgal process for degradation of phenol in petroleum refinery wastewater was also evaluated. The ability of *C.pyrenoidosa* cells to treat phenol in petroleum refinery wastewater with high growth kinetic parameters adds to practical applicability of the process. High lipid as well as neutral lipid productivities obtained in spent biomass after treatment of phenol containing refinery wastewater qualifies the process as a source of algal biodiesel feedstock. The lipid extracted biomass was used for bioethanol fermentation which further enhances its economic feasibility for biofuel applications. The microbial phenol degradation is completely dependent on activity of metabolic pathway involving a cascade of phenol metabolizing enzymes. The metabolic pathways involved in phenol biodegradation have not been well studied in microalgae and deserves serious attention. This present

research attempt reports for the first time the complete pathway of phenol degradation in *Chlorella pyrenoidosa* and diatom BD1IITG using HPLC, LC-MS and UV-Visible spectrophotometry. Both the algal strains degrades phenol by both ortho and meta pathway with prominence of ortho over meta pathway. As an alternative to use microbes for bioremediation, the use of purified enzymes for phenol remediation has generated wide interest recently. Since phenol hydroxylase is the first enzyme causing initial attack on phenol in the phenol degradation pathway, the knowledge of its kinetic properties is invaluable for its potential applications. There is no information regarding characterization of the kinetic properties of any microalgal phenol hydroxylases. In the present research work purification and characterization of microalgal phenol hydroxylase from *C.pyrenoidosa* has been carried out. The characterization of properties of microalgal phenol hydroxylase gains importance as the information could be instrumental in developing enzyme based phenol remediation technology.





### 3.2 Screening and characterization of phenol degradation by potent algal strains

Owing to high ecological toxicity phenol is considered a priority pollutant. Thus, phenol containing industrial wastewater needs to be treated before it is released into natural ecosystem. Biological degradation owing to its advantages of complete mineralization of organic pollutants as well as low cost has gained wide attention for treatment of effluents. Phenol polluted wastewater and soil is a main source of phenol degrading microbial strain (bacteria, fungi and algae). Algal phenol degradation capability is much less studied as compared to bacterial and fungal strains. To fulfill this lacuna the present research work intends to identify phenol degrading algal isolates from wastewater sources.

#### 3.2.1 Identification of the isolated algal strains

Isolation of four of filamentous algal strains was carried out from sewage water (Figure 3.1 a-d) two of which were morphologically identified as *Spirogyra* (Figure 3.1 a) and *Closterium* (Figure 3.1 b) while the other two algal strains (Fig. 3.1 c and d) remain unidentified. A novel unicellular algae was isolated from petroleum refinery wastewater. A unicellular algal strain *Chlorella pyrenoidosa* (NCIM 2738) was obtained from National Collection of Industrial Microorganisms (NCIM), Pune (Figure 3.1 e). A phenol tolerant algal isolate diatom BD1IITG was isolated from petroleum refinery wastewater and identified on basis of 16S rRNA plastid gene sequence. BLAST analysis suggests the isolate BD1IITG to be a diatom based on homology with 99% identity to 16S rRNA plastid sequence of diatom EJ10-B11-11A. The high bootstrap support of the phylogenetic tree (Figure 3.2 b) demonstrated that the isolate BD1IITG belongs to the algal group diatom owing to close evolutionary relationship with diatom EJ10-B11-11A. The 16S rRNA gene sequence of diatom BD1IITG was deposited to NCBI GenBank and an Accession no. KJOO2533 was obtained.

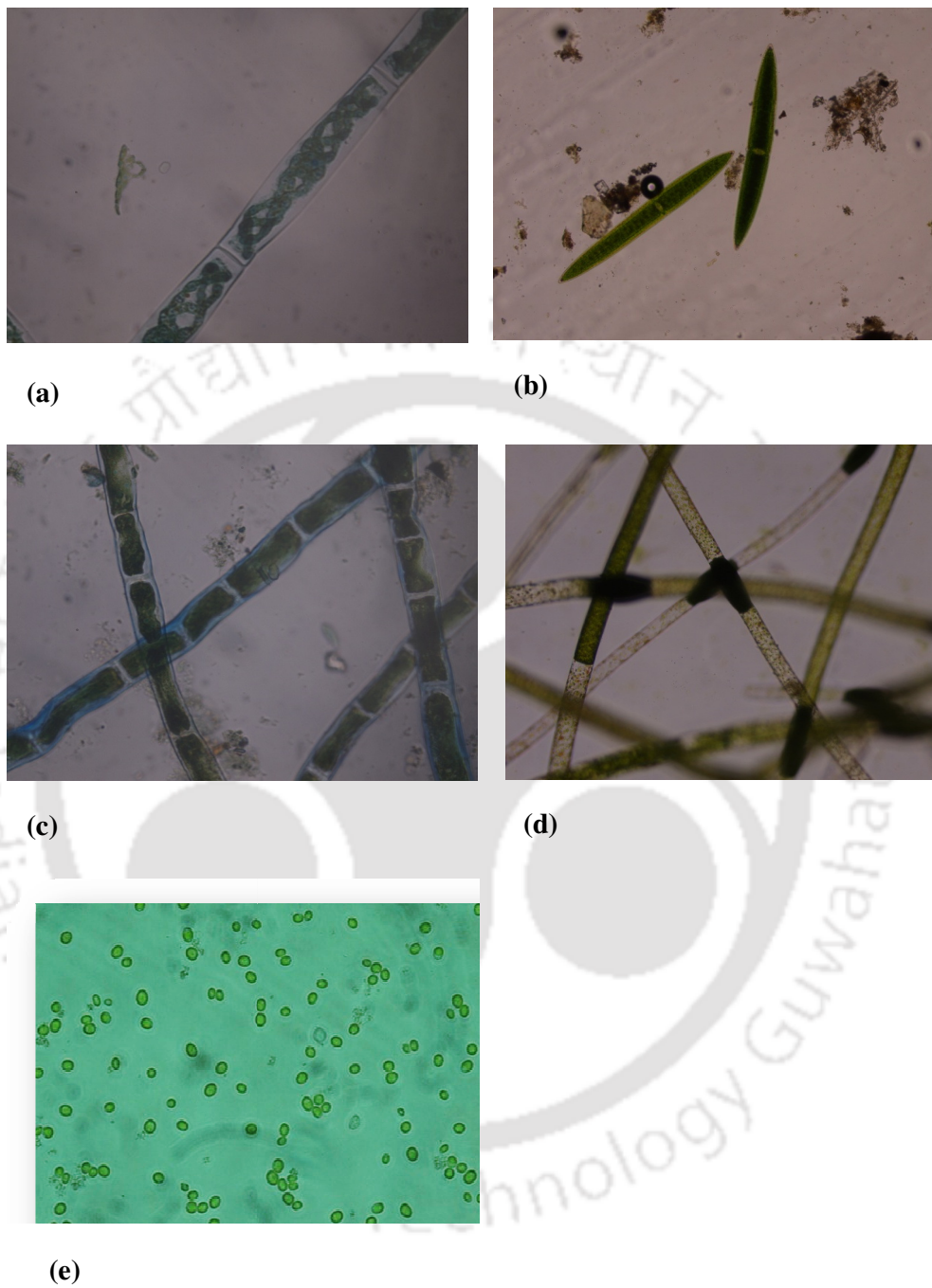


**Figure 3.1** Bright field microscopic images of algal isolates: **a)** *Spirogyra*  
**b)** *Closterium* **c)** Unidentified Sample 1 **d)** Unidentified Sample 2 **e)** *Chlorella*  
*pyrenoidosa*

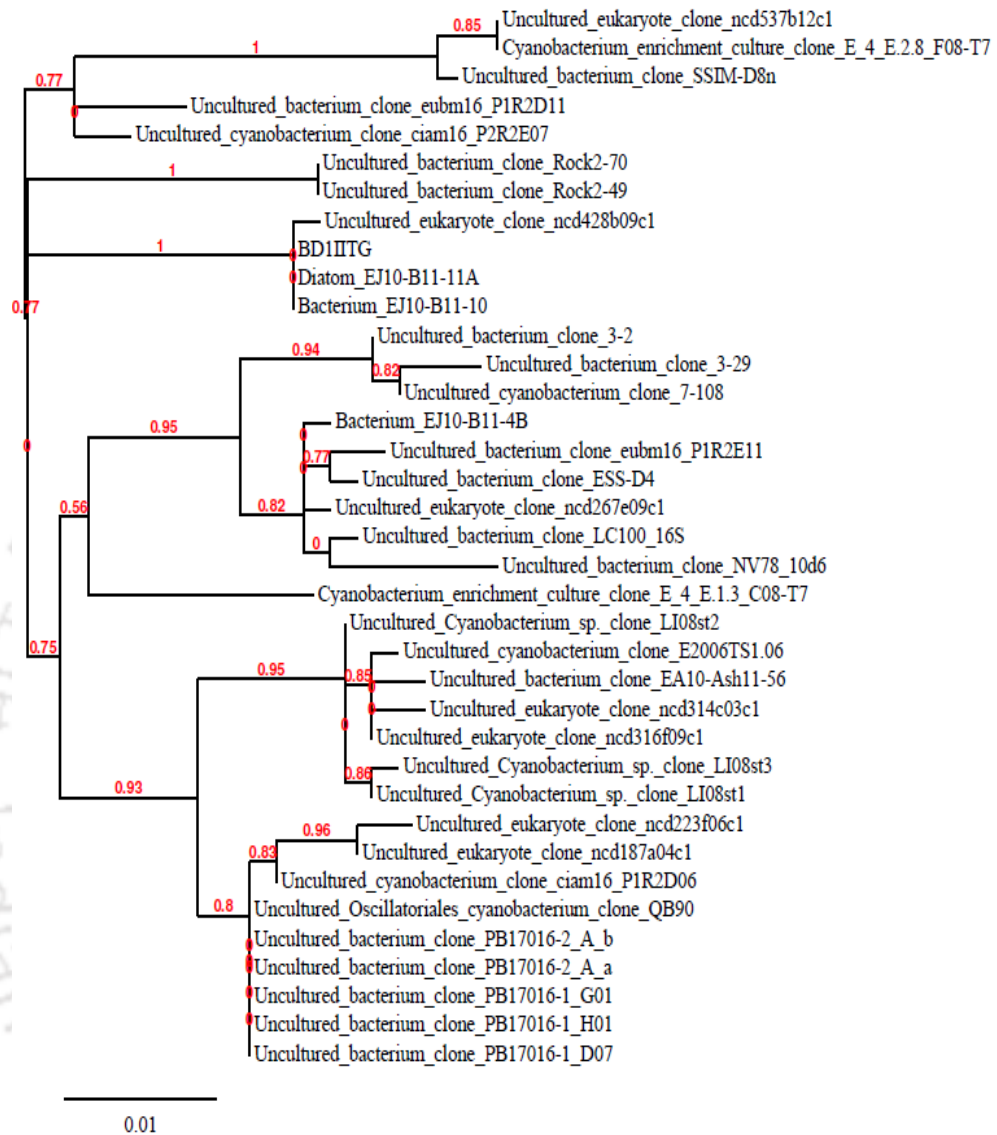


**Figure 3.2** Phylogenetic tree constructed using Robust Phylogenetic tree for the non-specialist

### 3.2.2 Screening of potent phenol degrading algal strains

Table 3.1 shows phenol degradation ability of six microalgal strains after a incubation period of 4 days. It is clear that out of six microalgal species tested, *Chlorella pyrenoidosa* and diatom BD1IITG showed positive phenol degradation ability with complete phenol degradation and 43.95 % phenol degradation respectively within 4 days. To negate the effect of any abiotic factors in phenol removal, the loss of phenol from culture media without algae was determined and a 2.85 % abiotic loss of phenol was found within 4 days. This proves that *C.pyrenoidosa* and diatom BD1IITG was solely responsible for phenol removal from the sample. Table 3.1 shows minimal phenol degradation of 3.45% in *Spirogyra* cultures, 3.85% phenol degradation in *Closterium* cultures, 4.4% phenol degradation in unidentified Sample 1 cultures and 4.2% phenol degradation in unidentified sample 2. Out of this, 2.85% phenol loss is contributed by abiotic loss of phenol (control) thus negating any significant phenol degradation ability. Thus, the findings indicate prospects for application of *C.pyrenoidosa* (NCIM 2738) and diatom BD1IITG for phenol remediation.

**Table 3.1** Phenol degradation potential of the algal isolates

| Algal strain          | Phenol degradation (%) |
|-----------------------|------------------------|
| <i>C.pyrenoidosa</i>  | 100 ± 0.36             |
| Diatom BD1IITG        | 43.95 ± 0.8            |
| <i>Spirogyra</i>      | 3.45 ± 0.17            |
| <i>Closterium</i>     | 3.85 ± 0.27            |
| Unidentified Sample 1 | 4.4 ± 0.51             |
| Unidentified Sample 2 | 4.2 ± 0.30             |
| Control (No algae)    | 2.85 ± 0.15            |

### 3.2.3 Growth kinetics and phenol degradation by potent algal strains

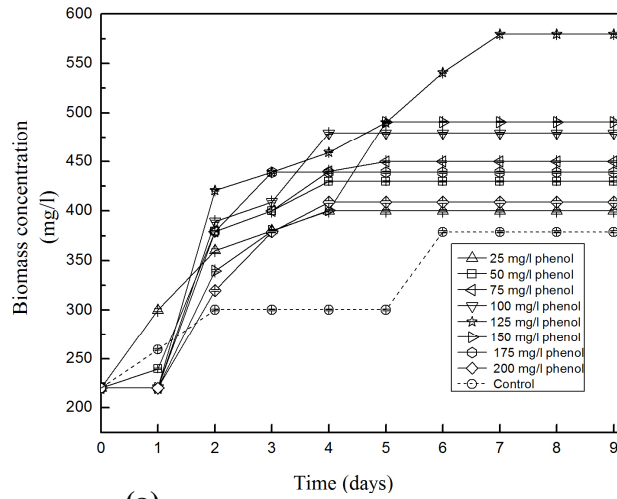
Microbial phenol degradation is a strong function of biomass growth. The knowledge of growth kinetics is valuable information leading to understanding the capacity of the microbe for phenol degradation (Kumar et al. 2005). Keeping the necessity to evaluate growth kinetics in mind, growth inhibitory models to describe the microbial growth dynamics in presence of growth inhibitory substrate as phenol have been proposed (Banerjee and Ghoshal 2010). Biokinetic parameters obtained from the growth kinetic model best fitting to the experimental data is a necessary input for design of biological remediation processes with optimized operational conditions for treatment of phenol polluted wastewater (Sahoo et al. 2011). The previous works on phenol degradation ability by microalgae provides no details of growth kinetics which is essential for designing a microalgae mediated phenol remediation process. The present work attempts to address this lacunae in the area of algal phenol degradation.

#### 3.2.3.1 Biomass growth and phenol degradation in *Chlorella pyrenoidosa*

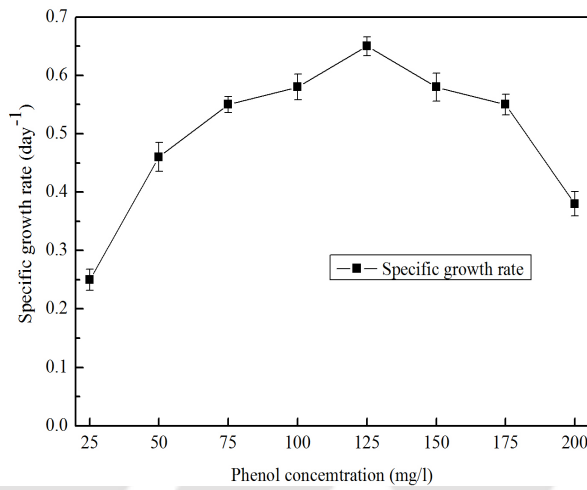
The effect of phenol concentration on biomass growth profile and experimental specific growth rate of *C. pyrenoidosa* have been shown in Figure 3.3 a and Figure 3.3 b respectively. The growth curves show that there is no lag phase in control and low concentration of phenol (25 mg/l) cultures. However, lag phase is observed from 50 mg/l phenol and the phenol concentrations preceding it as seen from Figure 3.3a. Lag phase is followed by exponential growth phase which is simultaneously followed by phenol utilization by the biomass. After the exponential growth period, phenol is depleted and the microalgae enters the stationary phase. The biomass growth even when phenol is depleted may be explained by biotransformation of phenol into its metabolic intermediates which serves as growth substrates until fully utilized Li et al.(2010) worked on phenol degradation by *Pseudomonas putida* LY1 and observed similar results of appearance of lag phase with increased phenol concentration, simultaneous phenol

transformation in the exponential phase, appearance of stationary phase concomitant with phenol depletion and increase in biomass even after complete phenol utilization. From the growth curve, the specific growth rate of  $0.16 \text{ d}^{-1}$  of control culture was found to be comparatively lower as compared to specific growth rate achieved in presence of phenol (Figure 3.3 b). This higher specific growth rate is probably because of phenol utilization as an organic carbon source by *C. pyrenoidosa*. The specific growth rate was found to increase with increase in substrate concentration until the highest value of  $0.65 \text{ d}^{-1}$  was attained at phenol concentration of  $125 \text{ mg/l}$  (Fig. 3.3 b). However, the growth rate was found to decline with increase in phenol concentration beyond  $125 \text{ mg/l}$  suggesting growth inhibition effect of phenol. Utilization of phenol as an organic carbon source by algae has also been reported by Semple and Cain (1996) and Lika and Papdakis (2009). They suggested phenol can be metabolized into organic end products like pyruvate and  $\text{CO}_2$  which can contribute to biomass growth.

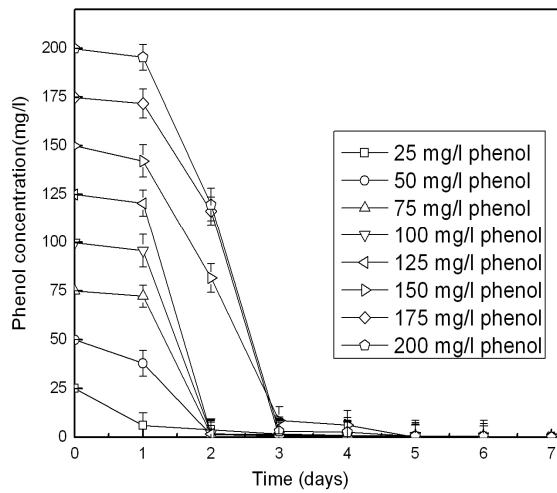
To determine the phenol degradation profile, the residual phenol was estimated by HPLC with a retention time of  $19.4 \text{ min}$ . HPLC data shows complete phenol degradation as shown in Fig. 3.3 c. The specific degradation rate increases with phenol concentration until a maximum rate of  $0.29 \text{ d}^{-1}$  which was achieved at  $125 \text{ mg/l}$  phenol (Fig 3.3 d). It is due to the highest specific growth rate of the microalgae at  $125 \text{ mg/l}$  phenol. Beyond this phenol concentration ( $125 \text{ mg/l}$ ), progressive decrease of specific degradation rate could be well explained by inhibited biomass growth. Mathur and Mazumdar (2010) observed similar phenomena during phenol degradation by *Pseudomonas putida*. They reported that both specific growth and degradation rate increases with increase in phenol concentration until a maximum value of  $100 \text{ mg/l}$ . They also reported that both growth and degradation rate declines due to substrate inhibition of phenol concentration beyond  $100 \text{ mg/l}$ .



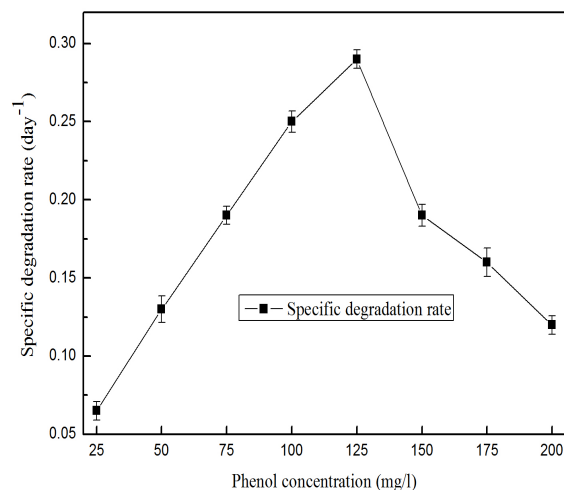
(a)



(b)



(c)



(d)

**Figure 3.3** a) Biomass growth profile of *Chlorella pyrenoidosa* in various initial phenol concentrations b) Variation in specific growth rate of *Chlorella pyrenoidosa* in various initial phenol concentrations c) Phenol degradation profile of *Chlorella pyrenoidosa* d) Specific degradation rate of *C.pyrenoidosa* for different phenol concentrations

### Photo dependent nature of phenol degradation in *C.pyrenoidosa*

To determine if the process of phenol degradation in *Chlorella pyrenoidosa* is a photo dependent, microalgal cells were incubated in phenol under dark condition. During this process, the biomass growth and phenol degradation have been found to be negligible as compared to that in light:dark cycle (Figure 3.4). *C.pyrenoidosa* showed negligible biomass growth of 1.4 mg/l with metabolism of only 7% phenol in 3 days under dark condition, which is almost negligible as compared to light:dark cycle (81.56 % phenol removed within 3 days with a biomass growth of 175 mg/l ). It resembles the observation of Papazi and Kotzabasis (2007). They reported that phenol biodegradation is a photo regulated response in the algae *Scenedesmus obliquus*. They showed that phenol biodegradation by *S. obliquus* was reduced to 5% in dark. Scraag (2006) reported that there is no growth as well



as phenol degradation by *Chlorella vulgaris* under dark condition which is in accord with the present observations.

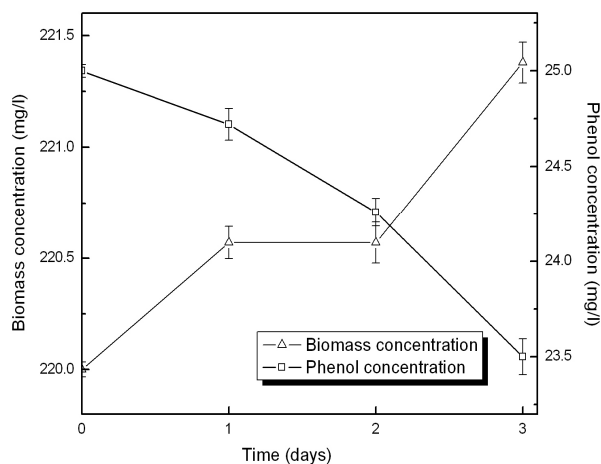
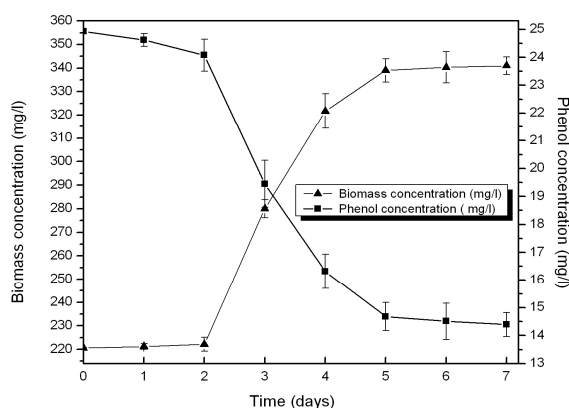


**Figure 3.4** Biomass growth and phenol degradation profile of *C.pyrenoidosa* in dark.

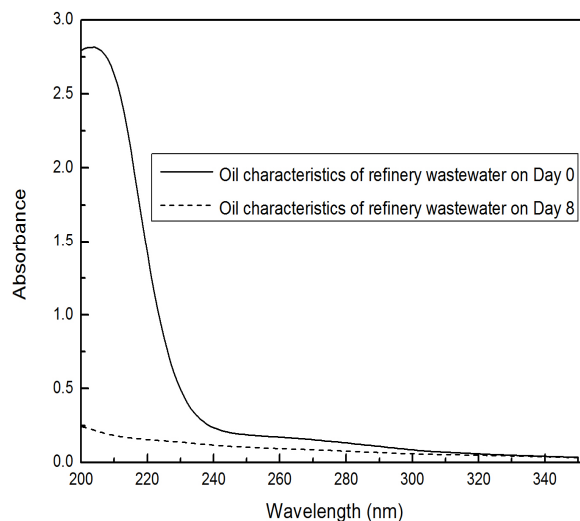
### Application of *C. pyrenoidosa* for degradation of phenol in refinery wastewater

Attempts were also made to understand the dynamics of biomass growth and phenol degradation of *C.pyrenoidosa* in refinery wastewater. The refinery wastewater was quantified to contain 23.33 mg/l phenol. The pH of the refinery wastewater was noted as 7.9. Intending to understand the natural growth and phenol degradation profile of *C.pyrenoidosa*, the experiment in refinery wastewater was carried out without attempting to meet the nutritional requirement of the microalgae and maintaining the actual pH of the refinery waste water. Figure 3.5 a shows the growth and phenol degradation ability of the microalgae in refinery wastewater. The biomass growth profile indicates an initial lag phase of 2 days unlike no lag phase observed in 25 mg/l phenol supplemented Fog's media. After the lag phase, the biomass grows exponentially to 4<sup>th</sup> day and then enters the stationary phase on 5<sup>th</sup> day with a final biomass of 339 mg/l. There is no phenol removal by *Chlorella pyrenoidosa* when it is in the lag phase of growth (till 2<sup>nd</sup> day). After 2<sup>nd</sup> day the microalgae uptakes phenol which is coincident with

exponential growth of the algal biomass. *Chlorella pyrenoidosa* mineralized 38.32 % of phenol in refinery wastewater by 7 day unlike complete mineralization of 25 mg/l phenol concentration by 3<sup>rd</sup> day in Fog's media. Agarry et al. (2008) reported inhibition of complete mineralization of 30 mg/l phenol in refinery wastewater by *Pseudomonas aeruginosa* and *Pseudomonas fluorescens* which correlates well with present finding. *Pseudomonas aeruginosa* mineralized 94.5 % while *Pseudomonas fluorescens* mineralized 69.4% of initial phenol concentration. However, contrary to the present work, they added mineral salt medium to refinery wastewater to meet the nutritional requirement of the microorganism for proper growth. Refinery wastewater may contain other constituents which may prove inhibitory to the phenol degradation potential of the microorganisms (Agarry et al. 2008). Characterization of the nature of oil present in refinery wastewater by UV-spectrophotometry shown in Figure 3.5 b indicates that the refinery wastewater before treatment (day 0) consists of both alkane (absorbance at 215-230 nm) and aromatic compounds (absorbance at 250-260 nm). Since the peak of maximum absorbance is around 215 nm, the nature of oil in refinery wastewater is clean oil. Dotted line (Figure 3.5 b) represents the oil component characteristics in wastewater after treatment with *Chlorella pyrenoidosa* for 8 days, indicating degradation of both alkanes and aromatic compounds. This adds to the potential of the algal candidate. Co-metabolism of other substrates along with phenol may have slowed the phenol degradation rate. Since the refinery wastewater contained clean oil comprising of higher concentration of alkanes as compared to aromatics it is possible that alkanes serve as a primary substrate and phenol as co-substrate leading to decreased phenol degradation rates.



(a)



(b)

**Figure 3.5 a)** Biomass growth and phenol degradation by *C.pyrenoidosa* in refinery wastewater **b)** Oil characteristics of refinery wastewater before (Day 0) and after treatment (Day 8) with *C.pyrenoidosa*

### **Growth and degradation kinetic modeling for *C.pyrenoidosa*: Biokinetic parameter evaluation and performance assessment**

The behavior of biodegradation rate is a strong function of biomass growth rate. Any growth medium where the microbial population can double itself faster will potentially result in higher biodegradation rate (Agarry et al. 2008). Understanding of a microorganism's degradation and growth kinetics will bring out its potential for phenol biodegradation (Arutchelvan et al. 2006). Thus, an attempt has been made to find out the mathematical relationship between (a) growth rate of biomass and substrate concentration and (b) phenol degradation rate and its initial concentration. The results obtained by solving the various growth kinetic models have been tabulated in Table 3.2. From this table it is clear that Yano model yielded comparatively high  $R^2$  value and least SD value confirming that Yano model best fitted the experimental data. A comparative plot of experimental and model predicted specific growth rates have been shown in Figure 3.6. It can be noted from the Figure 3.6 that the experimental data is close to predictions by all growth kinetic models. Previous works have also reported such overlapping of model predictions with experimental data. Juang and Tsai (2006)

predicted phenol biodegradation by *Pseudomonas putida* using Haldane, Yano and Edward model and reported overlapping predictions by each model to experimental data. Onysko et al. (2013) confirmed the same behavior for phenol biodegradation by *P. putida* of overlapping predictions by the different models at phenol levels below 300 mg/l. Banerjee and Ghoshal (2010) reported that growth kinetics of phenol degrading *B. cereus* strains closely fitted by both Yano model and the Edwards model. Such behavior of microbial growth pattern may be strain specific. The value of  $K_S$  (half saturation coefficient) indicates the affinity of the microorganism to the substrate. The value of  $K_I$  (substrate inhibition constant) signifies the degree of resistance of microorganism to the toxic effect of the substrate (Sahoo et al. 2011).

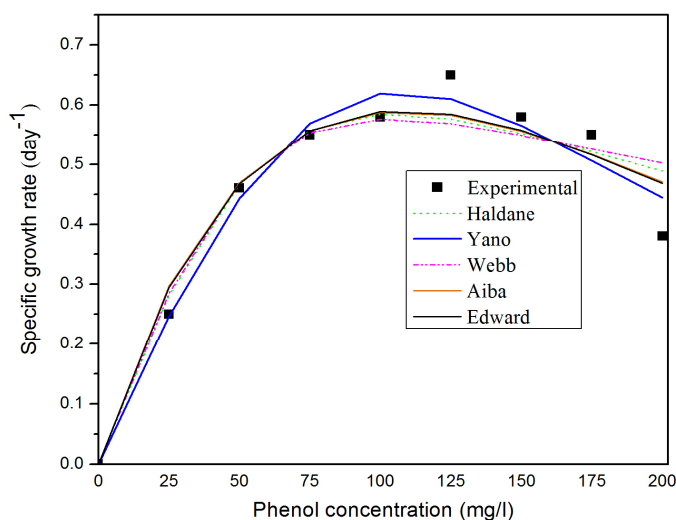


**Figure 3.6** Growth kinetic model fitted to experimental batch growth data of *C.pyrenoidosa*.

On the basis of the encouraging results in cultured condition we attempted to verify the applicability of *Chlorella pyrenoidosa* for phenol removal from refinery wastewater. The kinetic parameters obtained for various growth kinetic models have been shown in Table 3.3. Table 3.3 shows that Haldane model yielded the highest correlation coefficient ( $R^2$ ) and the least standard deviation (SD) and thus best fitted the experimental data.

**Table 3.2** Estimated value of growth kinetic parameters of *C.pyrenoidosa* in phenol

| Model   | $\mu_{\max}$ (d <sup>-1</sup> ) | K <sub>s</sub> (mg/l) | K <sub>I</sub> (mg/l) | K(mg/l) | R <sup>2</sup> | SD <sub>avg</sub> |
|---------|---------------------------------|-----------------------|-----------------------|---------|----------------|-------------------|
| Haldane | 5.57                            | 444.10                | 24.46                 | -----   | 0.94           | 0.049             |
| Yano    | 4.34                            | 410.50                | 214.50                | 32.26   | 0.97           | 0.035             |
| Webb    | 5.39                            | 480.74                | 15.44                 | 519.70  | 0.92           | 0.055             |
| Aiba    | 7.15                            | 472.50                | 132.70                | -----   | 0.95           | 0.045             |
| Edward  | 28.10                           | 111.50                | 105.30                | -----   | 0.95           | 0.044             |

**Table 3.3** Estimated growth kinetic parameters of *C. pyrenoidosa* in refinery wastewater

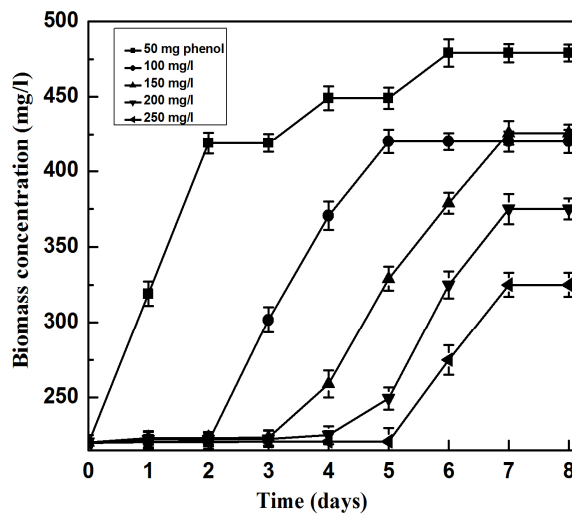
| Model   | $\mu_{\max}$ (d <sup>-1</sup> ) | K <sub>s</sub> (mg/l) | K <sub>I</sub> (mg/l) | K(mg/l) | R <sup>2</sup> | SD <sub>avg</sub> |
|---------|---------------------------------|-----------------------|-----------------------|---------|----------------|-------------------|
| Haldane | 0.017                           | 600.10                | 10.46                 | -----   | 0.96           | 0.025             |
| Yano    | 4.344                           | 600.50                | 150.50                | 10.26   | 0.96           | 0.412             |
| Webb    | 0.356                           | 580.70                | 5.44                  | 530.70  | 0.82           | 0.113             |
| Aiba    | 0.019                           | 572.50                | 70.70                 | -----   | 0.84           | 0.023             |
| Edward  | 0.030                           | 50.94                 | 70.90                 | -----   | 0.34           | 0.05              |

Comparison of the biokinetic parameters may give the indication of how *Chlorella pyrenoidosa* behaved under two significantly different culture conditions of nutrient sufficient media and refinery wastewater. For this reason, a comparison was made between the respective biokinetic parameters of best fit kinetic models representing the biomass growth behavior. Kinetic modeling of the experimental biomass growth data suggests that  $\mu_{\max}$  ( $0.017 \text{ d}^{-1}$ ) and  $K_I$  ( $10.46 \text{ mg/l}$ ) is lower in refinery wastewater as compared to that in nutrient media. The  $K_s$  value ( $600.1 \text{ mg/l}$ ) in refinery wastewater is higher than that in nutrient media. Lower  $\mu_{\max}$  values in refinery wastewater is probably due to the lack of optimal nutrient factors for growth as well as other growth inhibitory constituents which may be present in refinery wastewater. Therefore efficient phenol utilization is less in refinery wastewater as compared to that in nutrient media containing optimal biomass growth conditions. Secondly, cometabolism of alkanes in refinery wastewater along with phenol (aromatic) as discussed above may lead to decreased phenol degradation.  $K_s$  being inversely related to affinity of microbial system for substrate, a higher  $K_s$  value indicates its lower affinity to the substrate (Firozjaee et al. 2011). Higher  $K_s$  value suggests a decreased affinity for phenol of *C.pyrenoidosa* in refinery wastewater compared to that in nutrient media. Higher  $K_s$  value in refinery wastewater explains inhibition of complete phenol mineralization unlike complete mineralization in media. *C. pyrenoidosa* utilizes phenol less efficiently in refinery wastewater due to decreased affinity for phenol.  $K_I$  value is involved in quantification of the effect of toxicity of a compound during the biodegradation process. A higher  $K_I$  value implies less sensitivity of the microbe to substrate inhibition. Lower  $K_I$  value in refinery wastewater suggests high sensitivity of *C.pyrenoidosa* to toxic effect of phenol compared to that in nutrient media. This can be understood from the fact that optimal growth conditions in media helps the microalgae counter the inhibitory effect of phenol in a better way. On the other hand, lack of optimal biomass growth factors and possible presence of other additional inhibitory constituents in refinery wastewater compromises the ability of *C.pyrenoidosa* to resist the inhibitory effect of phenol.

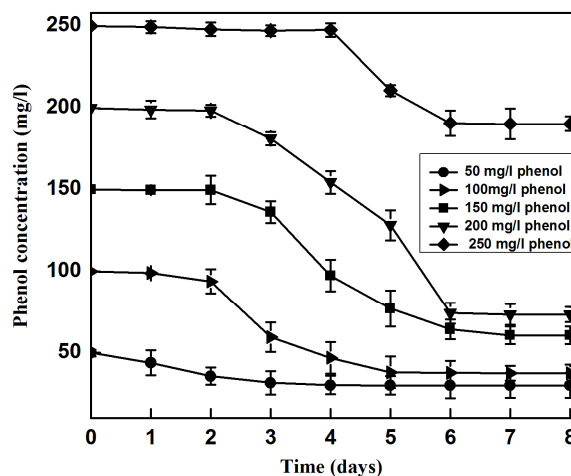
### 3.2.3.2 Biomass growth, phenol degradation and growth kinetic modelling in diatom BD11ITG

The effect of initial phenol concentration on biomass growth profile and phenol degradation by diatom BD11ITG has been shown in Fig. 3.7 a and b. The growth curve shows that there is no lag phase at 50 mg/l phenol culture. A lag phase in the biomass growth profile is evident at 100 mg/l phenol and the phenol concentrations thereafter. Lag phase is followed by exponential biomass growth which is associated with phenol utilization by the biomass. The algal cells then finally enter into stationary phase where there is no more phenol utilization. Li et al. (2010) reported association of lag periods with increased initial phenol concentration and phenol degradation in the exponential growth phase which corroborates with the present findings. The specific growth rate increased with increase in phenol concentration until highest growth rate of  $0.102\text{ d}^{-1}$  was achieved at phenol concentration of 100 mg/l (Figure 3.7 c). With increase in phenol concentration beyond 100 mg/l, the growth rate declines indicating growth inhibition effect of phenol. The phenol degradation profile was determined by HPLC with a retention time of 19.4 min. Figure 3.7b clearly indicates that the diatom degrades 39.88 % (for 50 mg/l phenol), 63% (for 100 mg/l phenol), 59.52% (for 150 mg/l phenol), 51.23% (for 200 mg/l phenol) and 24% (for 250 mg/l phenol). The specific degradation rate increases with increase in phenol concentration until maximum degradation rate of  $0.215\text{ d}^{-1}$  achieved at 100 mg/l phenol (Figure 3.7 c.). It is due to the highest specific growth rate of the microalgae at 100 mg/l phenol. This reflects phenol degradation to be a growth dependent phenomenon. Beyond 100 mg/l phenol concentration, progressive decrease of specific degradation rate could be well explained by inhibited biomass growth. Mathur and Mazumdar (2010) studied phenol degradation by *Pseudomonas putida* and observed a similar phenomenon of increased specific growth and degradation rate with increase in substrate concentration until a maximum phenol concentration of 100 mg/l. They also reported that both growth and degradation rate declines due to substrate inhibition of phenol concentration  $>100\text{ mg/l}$  which accords with findings of present study. Microbial biodegradation rate is dependent on biomass growth rate. A higher biomass growth rate results in increased biodegradation rate (Agarry et al. 2008). Thus, evaluation of microbial growth kinetics will bring

forward its potential for biodegradation of organic compounds. An attempt has been made to find out the mathematical relationship between biomass growth rate and substrate concentration. For this, the biokinetics parameters were estimated using the various substrate inhibitory models. The parameters obtained by solving the various growth kinetic models have been tabulated in Table 3.4. From this table it is clear that Haldane model yielded comparatively high  $R^2$  value and least SD value confirming that experimental data best fitted into the Haldane model. Figure 3.7d shows a comparative plot of experimentally observed variation in specific growth rate of diatom BD11ITG at different initial phenol concentrations as well as the prediction of the experimental data by five different growth kinetic models.

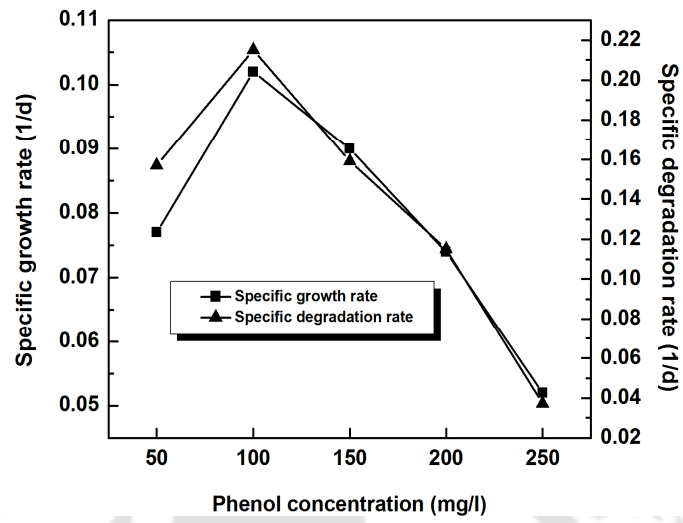


(a)

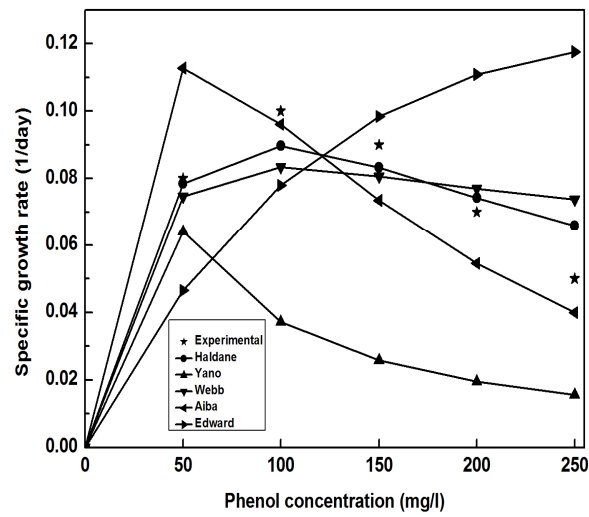


(b)





(c)



(d)

**Figure 3.7** a) Biomass growth profile of diatom BD11ITG b) Phenol degradation profile of diatom BD11ITG c) Specific growth and degradation rate for various concentrations of phenol d) Experimental and growth kinetic model predicted specific growth rates.

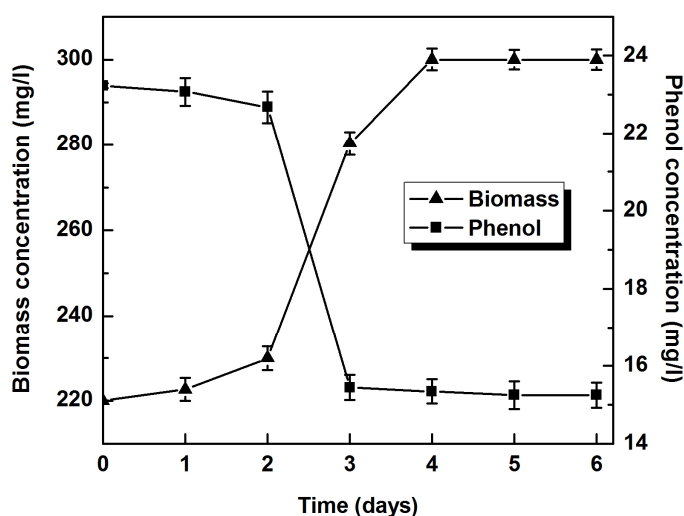
**Table 3.4** Estimated value of growth kinetic parameters of diatom BD1IITG in phenol containing nutrient media

| Model   | $\mu_{\max}$ (d <sup>-1</sup> ) | $K_s$ (mg/l) | $K_I$ (mg/l) | $K$ (mg/l) | $R^2$ | $SD_{\text{avg}}$ |
|---------|---------------------------------|--------------|--------------|------------|-------|-------------------|
| Haldane | 0.30                            | 109.99       | 80.24        | -----      | 0.94  | 0.008             |
| Yano    | 0.22                            | 2.60         | 21.50        | 2000.54    | 0.67  | 0.043             |
| Webb    | 0.27                            | 107.93       | 30.90        | 156.06     | 0.84  | 0.013             |
| Aiba    | 0.23                            | 23.13        | 150.40       | -----      | 0.44  | 0.102             |
| Edward  | 0.25                            | 170.00       | 700.90       | -----      | 0.35  | 0.204             |

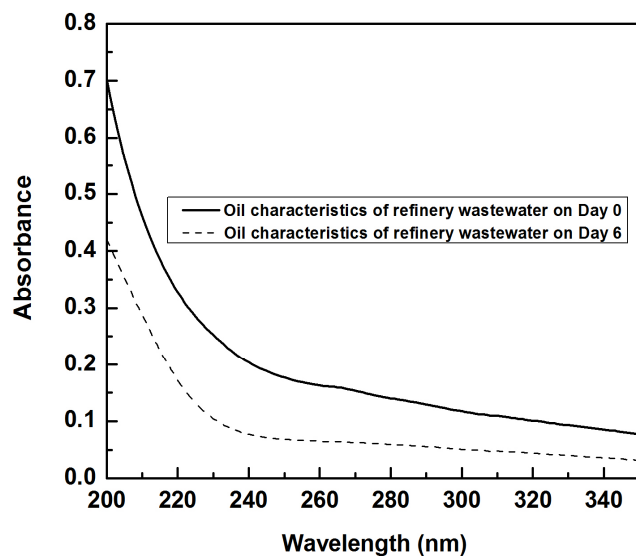
### Application of diatom BD1IITG for degradation of phenol in refinery wastewater

Attempts were also made to analyze the dynamics of biomass growth and phenol degradation of diatom BD1IITG in refinery wastewater. The refinery wastewater was estimated to contain 23.33 mg/l phenol by HPLC. Intending to understand the natural growth and phenol degradation profile of the diatom, the refinery wastewater experiment was carried out without supplementing with any media or media component. Figure 3.8 a shows the growth and phenol degradation ability of the diatom in refinery wastewater. The biomass growth undergoes a lag phase of 2 days unlike absence of lag phase even at 50 mg/l phenol in Fog's media. After the lag phase, there is exponential biomass growth to 4th day and then the biomass enters the stationary phase of growth on 5th day with a final biomass of 300 mg/l. The specific growth rate of biomass in refinery wastewater is 0.17 d<sup>-1</sup>. There is only 2.36 % phenol removal by diatom when it is in the lag phase of growth (till 2<sup>nd</sup> day). After 2<sup>nd</sup> day, the algal phenol uptake rate increases which is

coincident with exponential biomass growth. Diatom BD1IITG mineralized 68.58 % of phenol in refinery wastewater. The specific degradation rate of phenol by diatom BD1IITG in refinery wastewater was  $0.23 \text{ d}^{-1}$ . Analysis of the nature of oil in refinery wastewater by UV-spectrophotometry shown in Fig 3.7 b. indicates that the refinery wastewater (Figure 3.8 b, Day 0, solid line) consists of both alkane (absorbance at 215-230 nm) and aromatic compounds (absorbance at 250-260 nm). Since the high absorbance is observed around 215-230 nm, the nature of oil in refinery wastewater is clean oil. Both alkane and aromatic compounds in refinery wastewater was found to be degraded after treatment with diatom BD1IITG for 6 days (dotted line, Fig.3.8 b). The degradation ability of alkane adds to potential of the diatom strain for bioremediation application. Growth kinetic modeling of diatom BD1IITG in refinery wastewater was also carried out to verify the applicability of diatom BD1IITG for phenol removal from actual refinery wastewater. Table 3.5 shows the kinetic parameters obtained for various growth kinetic models. Table 3.5 indicates that Haldane model yielded the highest correlation coefficient ( $R^2$ ) and the least standard deviation (SD) and thus best fitted the experimental data. Thus, Haldane model best represents the growth behavior of the diatom in refinery wastewater.



(a)



(b)

**Figure 3.8 a)** Biomass growth as well as phenol degradation of diatom BD1IITG in refinery wastewater **b)** Characterization of oil components in refinery wastewater before (Day 0) and after (Day 6) treatment with diatom BD1IITG.

**Table 3.5** Estimated value of growth kinetic parameters of diatom BD1IITG in refinery wastewater

| Model   | $\mu_{\max}$ (d <sup>-1</sup> ) | $K_s$ (mg/l) | $K_I$ (mg/l) | $K$ (mg/l) | $R^2$ | $SD_{\text{avg}}$ |
|---------|---------------------------------|--------------|--------------|------------|-------|-------------------|
| Haldane | 0.40                            | 20.99        | 90.24        | -----      | 0.99  | 0.002             |
| Yano    | 0.17                            | 120.60       | 100.60       | 450.54     | 0.28  | 0.600             |
| Webb    | 0.10                            | 170.93       | 50.90        | 1500.06    | 0.88  | 0.110             |
| Aiba    | 0.23                            | 678.50       | 5.30         | -----      | 0.46  | 0.450             |
| Edward  | 0.23                            | 5.94         | 105.90       | -----      | 0.97  | 0.009             |

Biokinetic parameters comparison could help understand the biomass growth behavior of the diatom under two significantly different culture conditions of nutrient sufficient media and refinery wastewater. For this, the respective biokinetic parameters of best fit kinetic models representing the biomass growth behavior in both the culture conditions were analyzed. The value of  $K_s$  (half saturation coefficient) shows the affinity of the microorganism to the substrate.  $K_s$  being inversely related to affinity of microbial system for substrate, a higher  $K_s$  value indicates its lower affinity to the substrate (Firozaee et al.2011). The value of  $K_I$  (substrate inhibition constant) denotes the resistance of microorganism to the toxic effect of the substrate (Sahoo et al., 2011). Kinetic modeling of the experimental biomass growth data indicates that  $\mu_{max}$  ( $0.4\text{ d}^{-1}$ ) and  $K_I$  ( $90.24\text{ mg/l}$ ) is higher in refinery wastewater (1<sup>st</sup> row in Table 3.5) as compared to that in nutrient media (1<sup>st</sup> row in Table 3.4). The  $K_s$  value ( $20.99\text{ mg/l}$ ) in refinery wastewater (1<sup>st</sup> row in Table 3.5) is lower than that in nutrient media (1<sup>st</sup> row in Table 3.4). A similar study was carried out for degradation of phenol in refinery wastewater ( $30\text{ mg/l}$ ) by two bacterial strains *Pseudomonas aeruginosa* and *Pseudomonas fluorescence* (Agarry et al.2008). The  $K_I$  value ( $90.24\text{ mg/l}$ ) obtained in present study is higher than the  $K_I$  value obtained for *Pseudomonas aeruginosa* ( $29.7\text{ mg/l}$ ) and *Pseudomonas fluorescence* ( $31.7\text{ mg/l}$ ). In contrary to present study, Agarry et al. (2008) added nutrient medium to refinery wastewater to maintain the nutritional requirements for biomass growth. The biokinetic parameters suggest that diatom BD1IITG could prove to be an efficient strain for phenol removal from refinery wastewater due to the following characteristics: a) High  $\mu_{max}$  ( $0.4\text{ d}^{-1}$ ) value obtained (in refinery wastewater) indicates potential of the diatom for efficient biomass growth in refinery wastewater. b) Lower  $K_s$  value ( $20.99\text{ mg/l}$ ) suggests that the diatom has good affinity for phenol in refinery wastewater which would be beneficial in better phenol uptake rates. c) High  $K_I$  value ( $90.24\text{ mg/l}$ ) indicates better tolerance to toxic effect of substrate in refinery waste water. The increased growth rate as well as phenol uptake efficiency of the diatom BD1IITG in refinery wastewater could be related to nature of the refinery wastewater used in the present study. Cometabolism of alkanes present in the wastewater along with phenol (aromatic) as discussed above (Figure 3.8 b) could have positive effect on biomass growth as well as phenol degradation rates. Sun et al. (2012) studied the cometabolism of aromatic phenol and petroleum alkane in

*Acinetobacter* strains and reported enhancement in both biomass growth and phenol degradation rate. Cometabolism of alkanes as well as phenol could provide two parallel carbon sources for the cell which results in more carbon available for cell growth (Sun et al., 2012). An increased biomass growth rate could lead to better phenol degradation rates.

### Biosurfactant production

Emulsification assay suggested that diatom BD1IITG released biosurfactant into the medium which facilitated the phenol degradation process (Figure 3.9). Biosurfactant improve the biodegradation efficiency as well as lower the toxicity of phenol on the cells (Hassan et al., 2014; Rocha et al., 2007). From Figure 3.9, the biosurfactant emulsifying activity is found to be dependent on initial phenol concentration. The highest emulsifying activity has been observed at 100 mg/l phenol (Figure 3.9) where the biomass growth as well as phenol degradation rate of diatom BD1IITG was found to be the highest (Fig 3.7 c). Similar results of biosurfactant production during the process of phenol degradation have been reported for *Candida tropicalis* (Rocha et al., 2007).

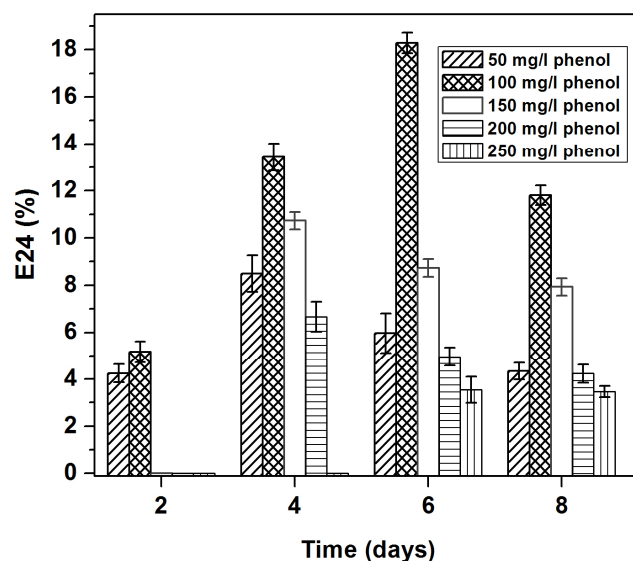


**Figure 3.9** Emulsification index (E 24) of diatom BD1IITG in phenol containing culture.

### **3.3 Generation of a microalgae based process for efficient phenol remediation as well as biofuel production**

On basis of the complete phenol degradation ability of *C.pyrenoidosa*, this strain was chosen for further studies. The successful application of the phenol biodegradation process will depend on a number of factors: a) the strain should possess high resistance to phenol toxicity enabling it to grow efficiently at increased phenol concentration b) the process should be capable of phenol degradation within a wide range of phenol concentration so as to take care of varied phenol levels in industrial wastewater c) the process should possess a higher phenol degradation rate so as to treat phenol in industrial wastewater within shorter time period d) the process should lead to complete phenol degradation e) the process should be completely practically applicable in real wastewater with complete phenol degradation with high degradation rates. Another important aspect of microalgae is its potential application as a biodiesel feedstock. Microalgae could serve as a promising source of biodiesel provided there is increased biomass production and lipid productivity. Mixotrophic cultivation of algae using different substrates as glucose, glycerol, fructose etc. have proved to be an ideal cultivation strategy for increased accumulation of lipids within less time (Kong et al. 2013; Gracia et al. 2006; Hamed and Klock 2014). However, the commercial applicability of the mixotrophic culture process is hindered by high substrate cost which accounts for 50% of the cost of the cultivation medium (Yang et al. 2011). Thus, the bottleneck of high costs incurred on algal mixotrophic cultivation could be answered by finding out cheap alternative substrates. This would reduce the cost of production of algal biodiesel feedstock by mixotrophic cultivation overcoming a main bottleneck in algal biodiesel production (Yang et al. 2011). If the industrial waste phenol could be utilized as a mixotrophic culture substrate for microalgae it would serve as a cost effective substrate reducing the high production cost associated with algal mixotrophic culture. Thus, the generation of environmentally sustainable mixotrophic cultivation process for microalgae in phenol containing refinery wastewater where toxic phenol will be remediated and the generated spent biomass with enhanced lipid content will serve as biodiesel feedstock is the need of the hour. Further any possible application of the residual biomass after lipid extraction could further enhance the economic

feasibility of the process. The present work intends to address the above mentioned issues in microalgal phenol degradation.

### **3.3.1 Growth kinetics and phenol degradation by phenol acclimatized cells of *C. pyrenoidosa***

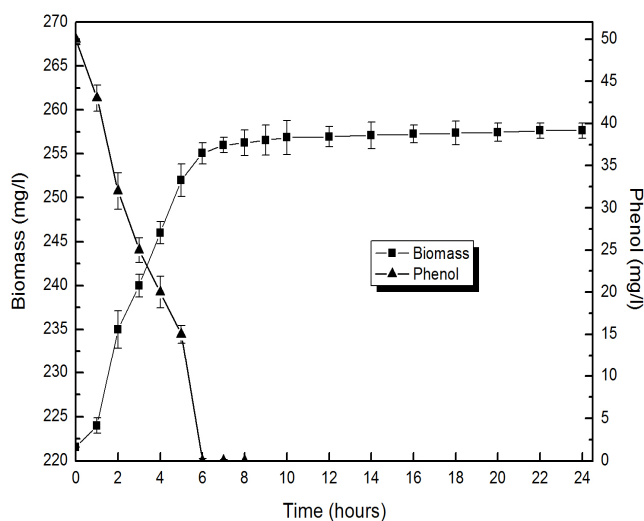
The biomass growth and phenol degradation profile of phenol acclimatized cells of *C.pyrenoidosa* have been shown in Figure 3.10 (a)-(z). As evident from Figure 3.10 (a)-1(c), no lag phase is observed upto phenol concentration of 150 mg/l and in control cultures (Figure 3.10 z) as against no lag phase obtained only in low phenol concentration of 25 mg/l for unacclimatized cells as discussed above. Similar observation of reduction in lag phase in higher phenol concentration on account of acclimatization of cells have been reported in previous works of Mort and Ross (1994) and Ye and Shen (2004). However, lag phase is observed from 200 mg/l phenol (Figure 3.10 d) and the phenol concentrations preceding it (Fig 3.10e-z). The length of lag phase increases with increase in phenol concentration beyond 200 mg/l phenol. Exponential growth phase follows the lag phase which is associated with phenol utilization by the biomass. With phenol depletion, the exponential phase cells enter into stationary phase of growth. The growth of biomass observed even after phenol depletion may be explained by the metabolic intermediates of phenol biotransformation which serve as growth substrates until completely utilized (Li et al. 2010). The specific growth rate of *C.pyrenoidosa* in control cultures ( $0.009 \text{ h}^{-1}$ ) was found to be comparatively lower compared to specific growth rate obtained within the phenol concentration of 50-650 mg/l ( $0.0254\text{-}0.01 \text{ h}^{-1}$ ) (Fig 3.11 a). This higher specific growth rate in phenol incubated cultures is on account of its utilization as an organic carbon source. The potential of algae to utilize phenol as an organic carbon source have been reported by Semple and Cain (1996) and Lika and Papdakis (2009). They suggested that algae metabolizes phenol into organic end products as pyruvate and  $\text{CO}_2$  which contributes to biomass growth. The specific growth rate increases with increase in phenol concentration until the highest growth rate of  $0.06 \text{ h}^{-1}$  is achieved at phenol concentration of 250 mg/l phenol. However, specific



growth rate declines beyond 250 mg/l phenol indicating growth inhibitory effect of phenol.

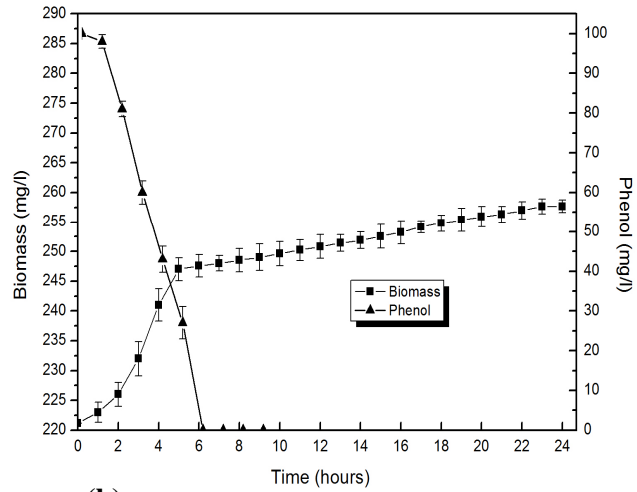
For analyzing the phenol degradation, the residual phenol was quantified using HPLC with the retention time of phenol being 19.4 minutes. Figure 3.10 a-z shows that phenol is being completely degraded in the range of 50-1200 mg/l. However, complete phenol degradation is compromised in 1250 mg/l phenol with 7.2% phenol degradation in 112 hours. The specific degradation rate increases with increase in phenol concentration until maximum degradation rate of  $0.561 \text{ h}^{-1}$  is achieved at 250 mg/l phenol (Figure 3.11 a). Beyond 250 mg/l phenol the specific degradation rate was found to decrease. The specific degradation rate was highest at 250 mg/l phenol since specific growth rate is highest at this concentration reflecting growth dependent nature of phenol degradation. Decreased specific degradation rate beyond 250 mg/l phenol could be explained by inhibited biomass growth beyond this phenol concentration. Phenol acclimatized *C.pyrenoidosa* cells achieved highest specific growth and degradation rate at 250 mg/l phenol which is higher compared to that obtained at 125 mg/l phenol for unacclimatized cells as discussed above. Kwon and Yeom (2009) reported similar observation while studying adaptation techniques for rapid degradation of high phenol concentration in *Pseudomonas fluorescense*. They found that *P.fluorescense* acclimatized to 700 mg/l phenol achieved increased degradation rates adapting cells to efficiently treat high phenol concentration of 1300 mg/l. The phenol degradation capability of a microbe is strongly dependent on biomass growth. A higher degradation rate can be achieved if the microbe has a faster doubling rate (Agarry et al. 2008). Thus, an evaluation of growth kinetics of an microbe will bring to light its potential to serve the purpose of phenol treatment. For this, mathematical relationship between biomass growth and substrate concentration was evaluated using growth kinetic modeling. Table 3.6 shows the biokinetic parameters obtained by solving various growth kinetic models. From Table 3.6 it becomes evident that Yano model with high  $R^2$  value as well as least SD value fits the experimental data compared to other kinetic models. Fig 3.11 b shows a comparative plot of experimental and growth kinetic model predicted specific growth rates at different initial phenol concentrations. From growth kinetic modeling, the maximum specific growth rate ( $\mu_{\max}$ ) of  $0.21 \text{ h}^{-1}$  obtained as per best fitted Yano model falls within the range

reported by previous works (Table 3.7).  $K_s$  value (half saturation coefficient) and  $K_I$  (substrate inhibition constant) value of 400.54 mg/l and 800.41 mg/l respectively obtained from best fitted Yano model is higher compared to values reported in literature (Table 3.7). Phenol acclimatized culture of *C.pyrenoidosa* also has higher  $K_s$  and  $K_I$  value compared to that reported for unacclimatized cells of *C.pyrenoidosa* (Table 3.2). A higher  $K_s$  value indicates that the microorganisms are able to grow efficiently at higher phenol concentrations (Bajaj et al. 2009; Jiang et al. 2002).  $K_I$  (substrate inhibition constant) value indicates resistance of microorganism to toxic effect of the substrate and high  $K_I$  value indicates that biomass is highly resistant to phenol inhibition (Sahoo et al. 2011). Jiang et al. (2002) reported phenol degradation activities with high  $K_I$  and  $K_s$  values for phenol acclimatized microbial granules which accords with our present findings of high  $K_I$  and  $K_s$  values obtained for acclimatized *C.pyrenoidosa* cells.

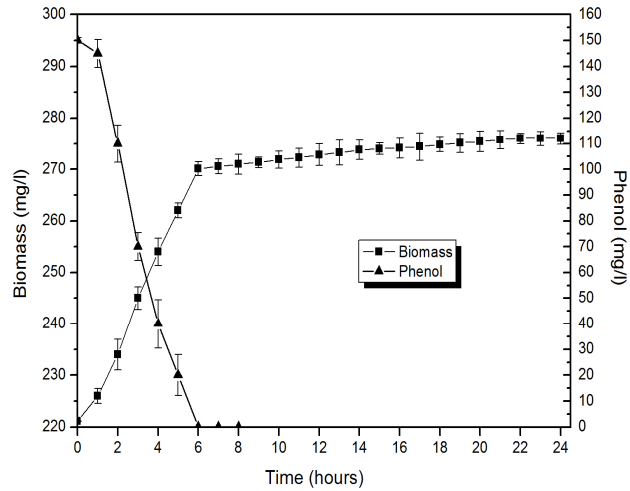


(a)

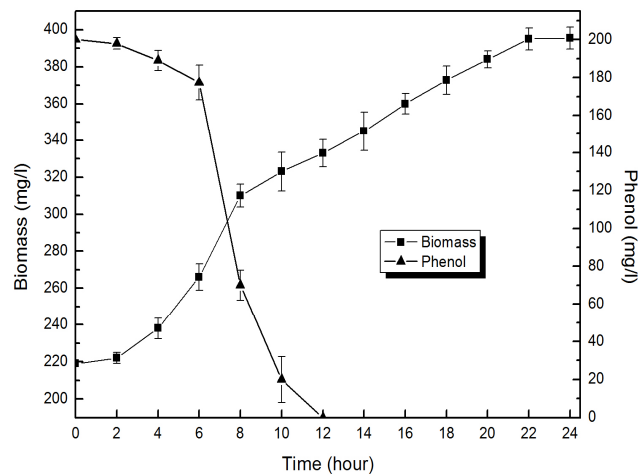
Continued



(b)

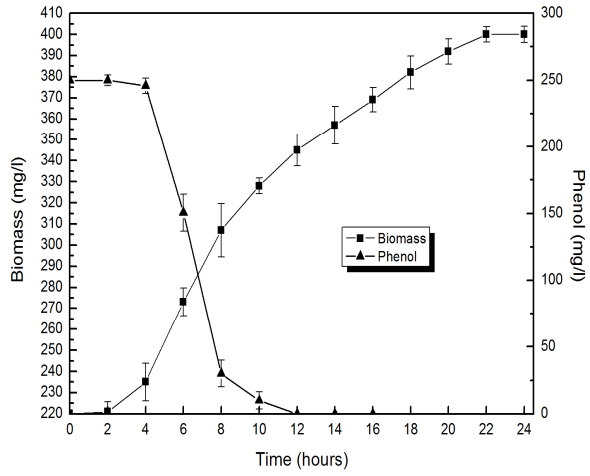


(c)

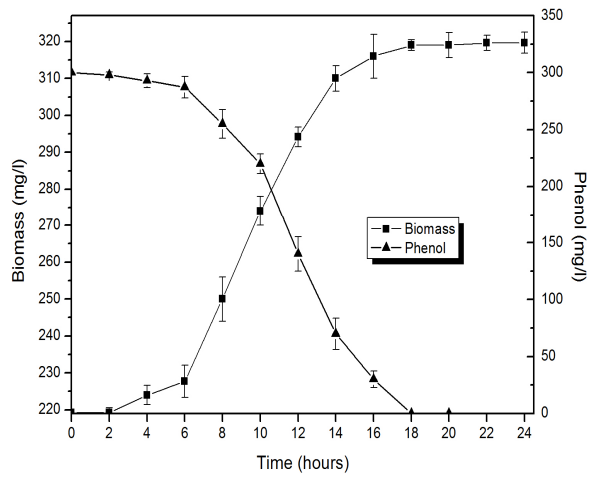


(d)

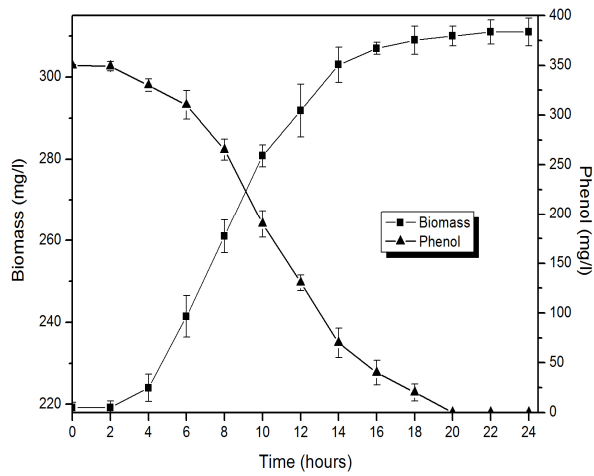
Continued



(e)

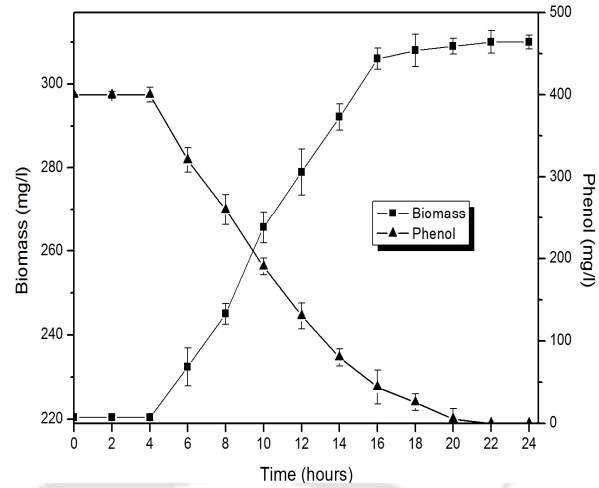


(f)

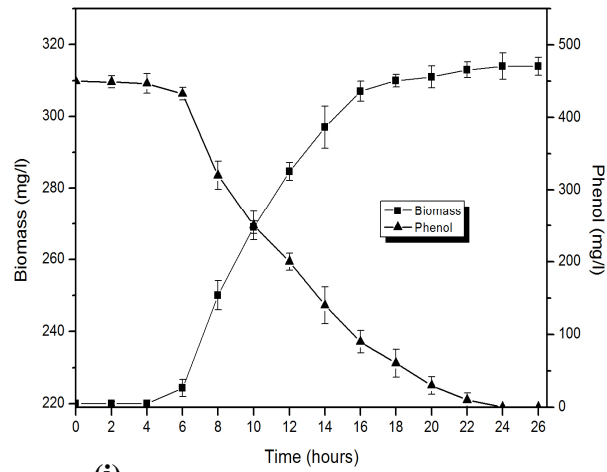


(g)

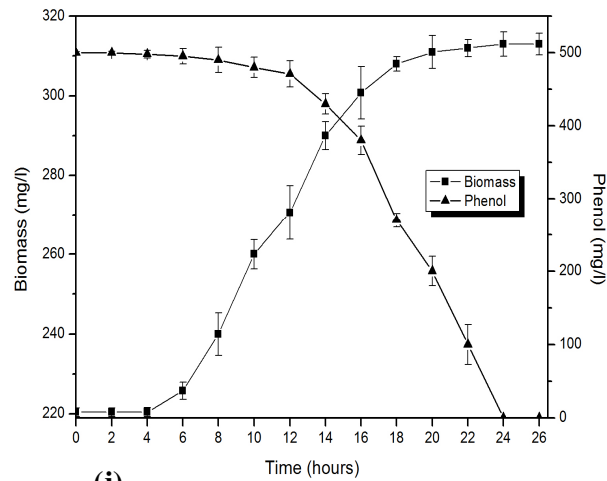
Continued



(h)

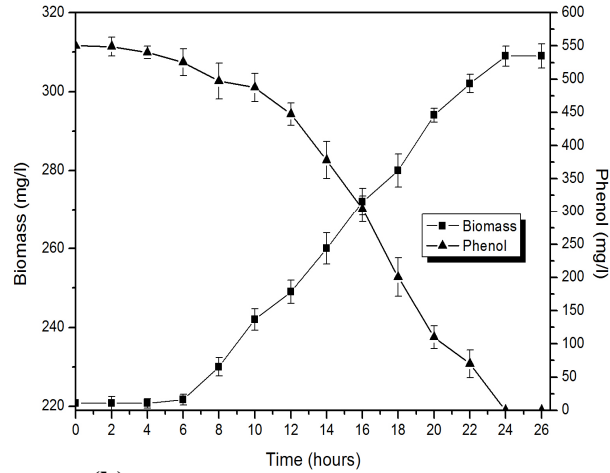


(i)

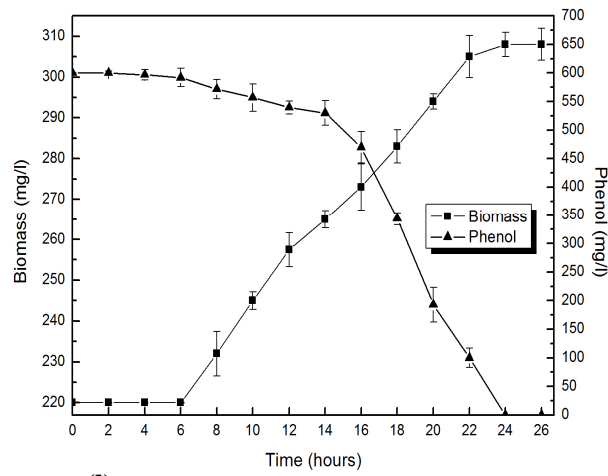


(j)

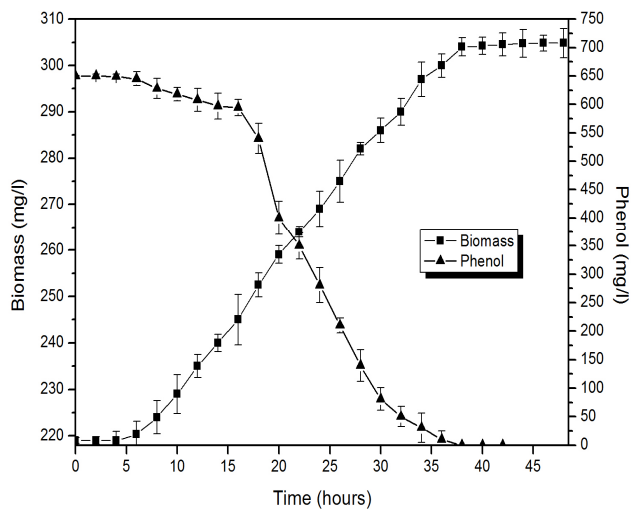
Continued



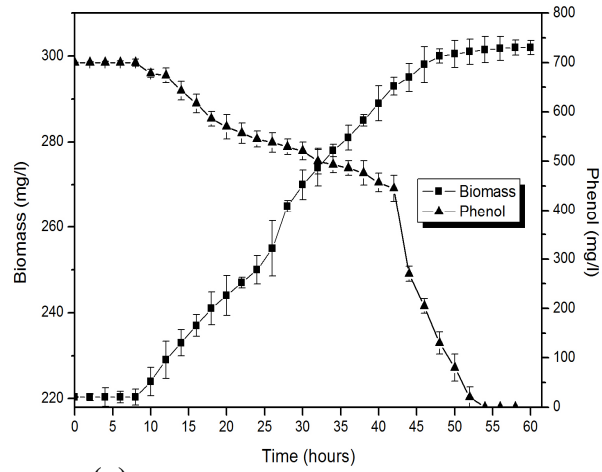
(k)



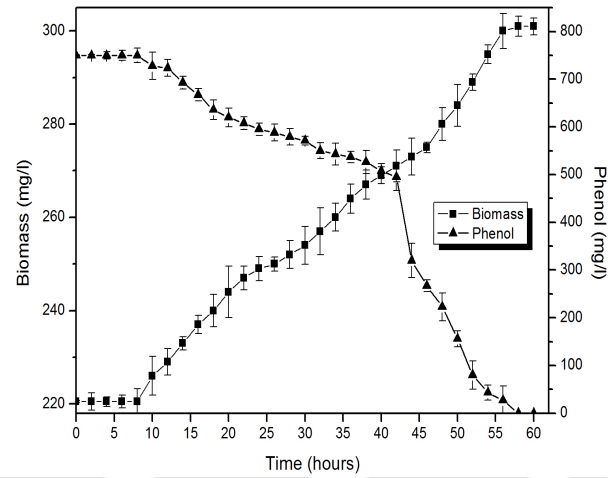
(l)



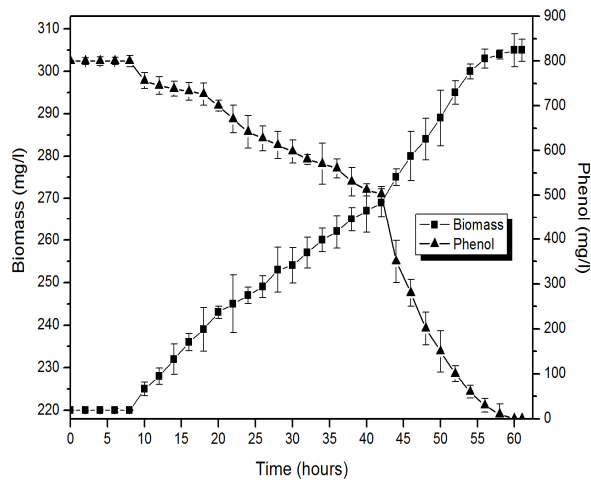
(m)



(n)

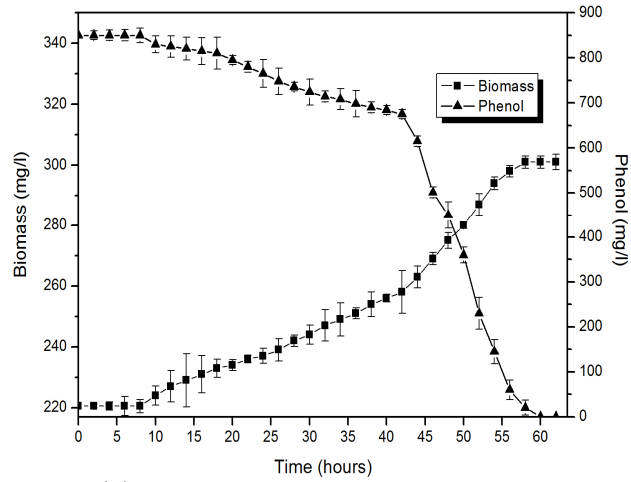


(o)

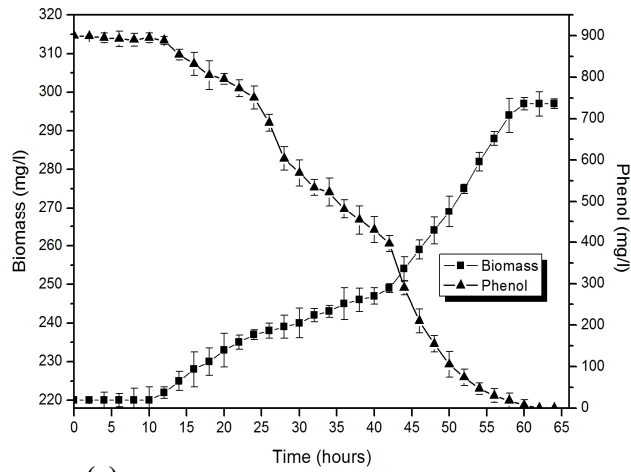


(p)

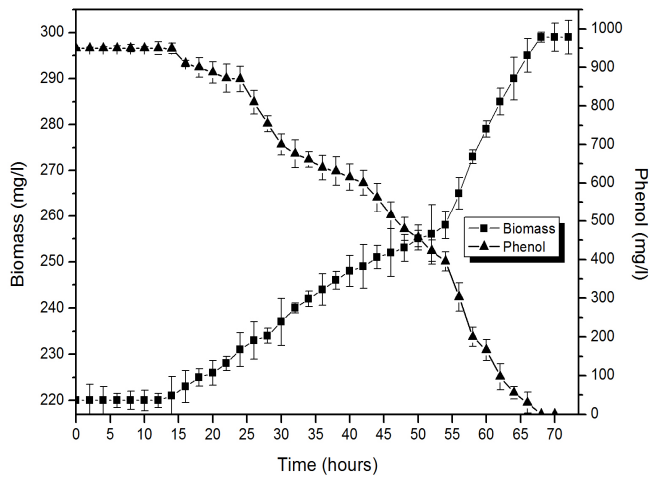
Continued



(q)



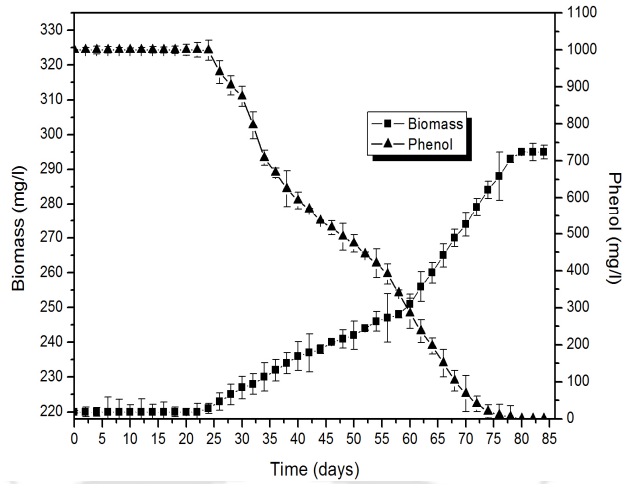
(r)



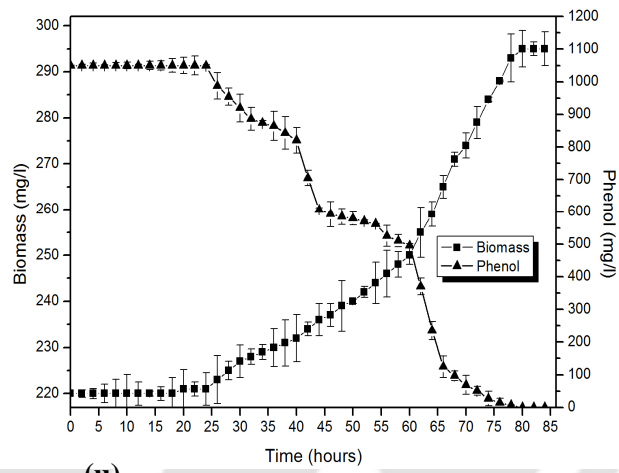
(s)

Continued

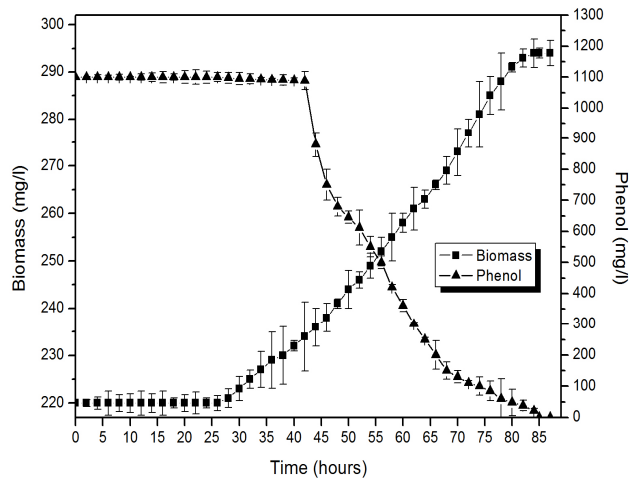




(t)

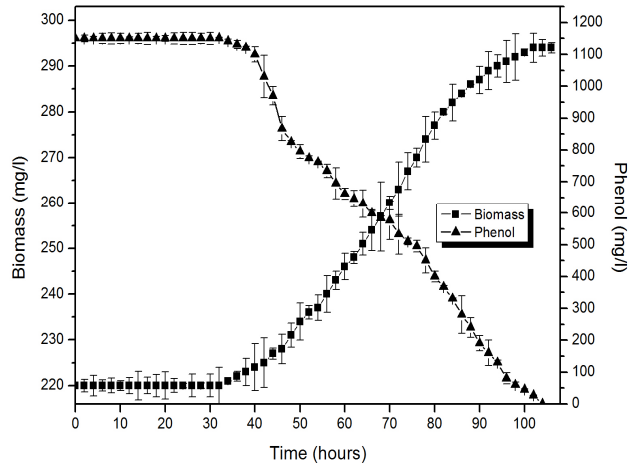


(u)

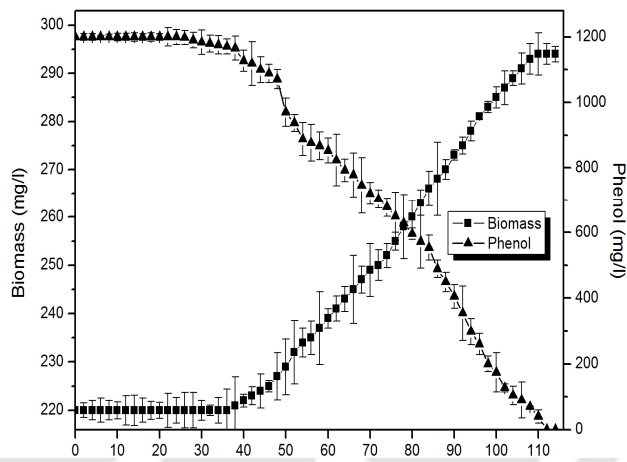


(v)

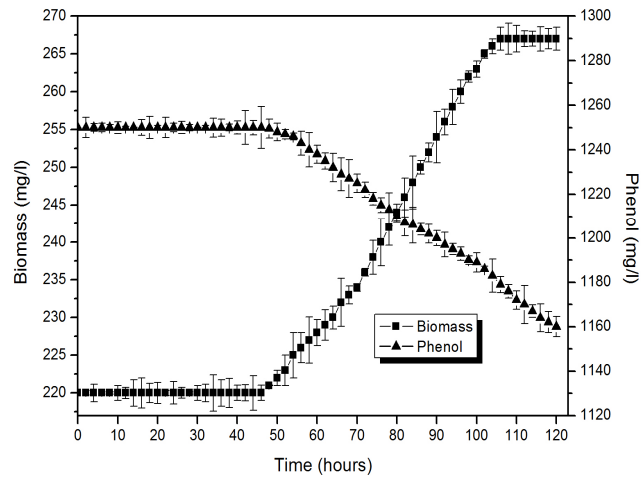
Continued



(w)

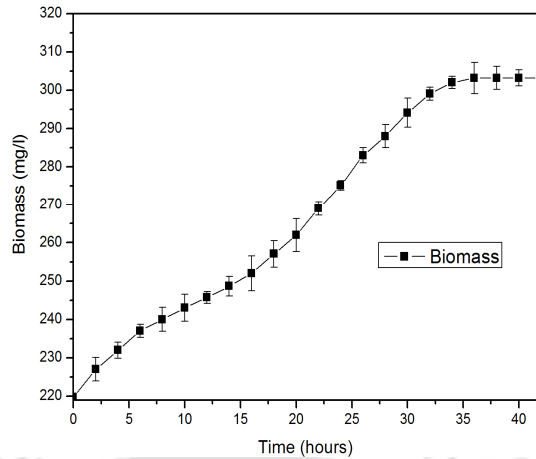


(x)



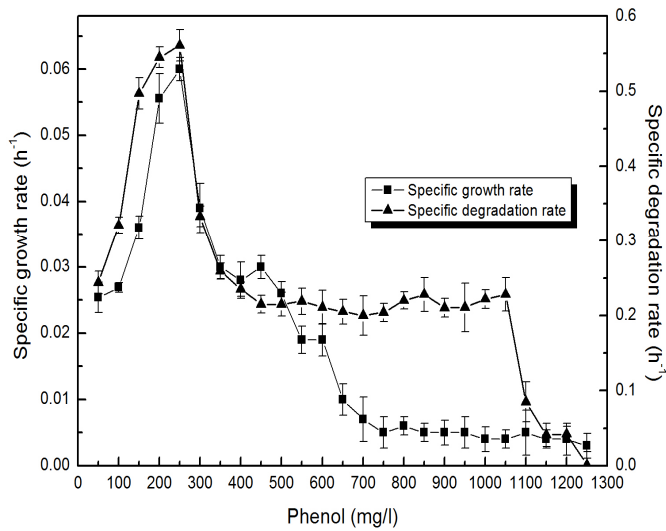
(y)

Continued



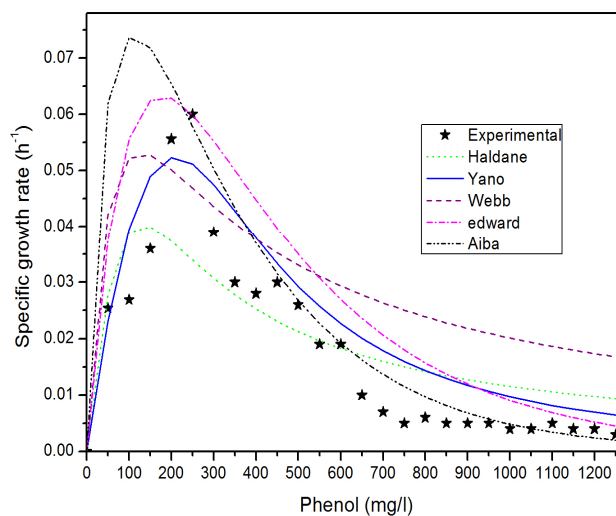
(z)

**Figure 3.10** Biomass growth and phenol degradation profile of *Chlorella pyrenoidosa* in various initial concentrations of phenol: a) 50 mg/l phenol b) 100 mg/l phenol c) 150 mg/l phenol d) 200 mg/l phenol e) 250 mg/l phenol f) 300 mg/l phenol g) 350 mg/l phenol h) 400 mg/l phenol i) 450 mg/l phenol j) 500 mg/l phenol k) 550 mg/l phenol l) 600 mg/l phenol m) 650 mg/l phenol n) 700 mg/l phenol o) 750 mg/l phenol p) 800 mg/l phenol q) 850 mg/l phenol r) 900 mg/l phenol s) 950 mg/l phenol t) 1000 mg/l phenol u) 1050 mg/l phenol v) 1100 mg/l phenol e) 1150 mg/l phenol x) 1200 mg/l phenol y) 1250 mg/l phenol z) Control



(a)

Continued



(b)

**Figure 3.11a)** Experimental specific growth and degradation rate of *C.pyrenoidosa* in various initial phenol concentrations **b)** Growth kinetic models fitted to experimental batch growth data

**Table 3.6** Estimated value of growth kinetic parameters of *C. pyrenoidosa* in phenol

| Model   | $\mu_{\max}$ (h <sup>-1</sup> ) | $K_s$ (mg/l) | $K_1$ (mg/l) | $K$ (mg/l) | $R^2$ | $SD_{\text{avg}}$ |
|---------|---------------------------------|--------------|--------------|------------|-------|-------------------|
| Haldane | 0.315                           | 450.61       | 38.74        | -----      | 0.79  | 0.009             |
| Yano    | 0.21                            | 400.54       | 800.41       | 65.75      | 0.90  | 0.007             |
| Webb    | 0.12                            | 80.00        | 200.00       | 54800.21   | 0.76  | 0.014             |
| Aiba    | 0.18                            | 73.02        | 280.98       | -----      | 0.76  | 0.015             |
| Edward  | 0.14                            | 100.20       | 363.00       | -----      | 0.88  | 0.013             |

**Table 3.7** Growth kinetic parameters obtained by various researchers using eukaryotic, prokaryotic and mixed cultures for phenol degradation

| Authors                            | Strain                                       | System | Phenol (mg/l) | $\mu_{\max}$ (d <sup>-1</sup> or h <sup>-1</sup> ) | $K_s$ (mg/l) | $K_I$ (mg/l) | $K$ (mg/l) | Source of strain                          | Acclimatization status  |
|------------------------------------|--|--------|---------------|--|--------------|--------------|------------|---|---|
| Yan et al., 2005                   | <i>Candida tropicalis</i> (eukaryote)        | Batch  | 0-2000        | 0.48 h <sup>-1</sup>                               | 11.7         | 207.9        | -----      | Municipal gasworks                        | In media containing phenol for 10 weeks                         |
| Wang et al., 2010                  | <i>Paecilomyces variotii</i> JH6 (eukaryote) | Batch  | 100-1800      | 0.312 h <sup>-1</sup>                              | 130.4        | 200          | -----      | Coking wastewater treatment plant         | In media supplemented with 600 mg/l phenol and 100 mg/l glucose |
| Wolskii et al., 2012               | <i>Penicillium chrysogenum</i> (eukaryote)   | Batch  | 6- 400        | 1.3 d <sup>-1</sup>                                | 9.4          | 64.9         | -----      | Isolated from crop soil                   | -----   |
| Das et al. 2015                    | <i>C. pyrenoidosa</i> (eukaryote)            | Batch  | 0-200         | 4.344 d <sup>-1</sup>                              | 410.5        | 214.5        | 32.26      | NCIM                                      | -----   |
| Kumar et al., 2005                 | <i>Pseudomonas putida</i> (prokaryote)       | Batch  | 10-1000       | 0.305 h <sup>-1</sup>                              | 36.33        | 129.79       | -----      | MTCC                                      | In media supplemented with 1000 mg/l phenol with 2% glucose     |
| Abuhameda et al., 2004             | <i>P.putida</i> F1 (prokaryote)              | Batch  | 0-200         | 0.051 h <sup>-1</sup>                              | 18           | 430          | -----      | ATCC                                      | Acclimatized  |
| Bai et al., 2007                   | <i>Alcaligenes faecalis</i> (prokaryote)     | Batch  | 10-1400       | 0.15 h <sup>-1</sup>                               | 2.22         | 245.37       | -----      | Activated sludge from municipal gas works | Acclimatized  |
| Vijayagopal and Viruthagiri , 2005 | <i>Nocardia</i> (prokaryote)                 | Batch  | 50-250        | 0.4227 h <sup>-1</sup>                             | 26.770       | 261.72       | -----      | Isolated from mangrove forest             | Acclimatized  |

| Authors                          | Strain                               | System | Phenol (mg/l) | $\mu_{\max}$ (d <sup>-1</sup> or h <sup>-1</sup> ) | $K_s$ (mg/l) | $K_I$ (mg/l) | $K$ (mg/l) | Source of strain                            | Acclimatization status                              |
|----------------------------------|--------------------------------------|--------|---------------|--|--------------|--------------|------------|---|---|
| Vijayagopal and Viruthagiri 2005 | <i>P.putida</i> (prokaryote)         | Batch  | 50-250        | 0.4378 h <sup>-1</sup>                             | 21.460       | 477.64       | -----      | Isolated from mangrove forest               | Acclimatized  |
| Monteiro et al., 2000            | <i>P.putida</i> DSM 548 (prokaryote) | Batch  | 1-100         | 0.436 h <sup>-1</sup>                              | 6.19         | 54.1         | -----      | Pure culture                                | Acclimatized in phenol containing media             |
| Dey and Mukherjee, 2010          | Mixed                                | Batch  | 100-700       | 0.150h <sup>-1</sup>                               | 51.8         | 404.04       | -----      | Coke oven industry effluent treatment plant | In phenol + glucose + beef extract containing media |
| Pishgar et al., 2012             | Mixed                                | Batch  | 25-1000       | 0.01 h <sup>-1</sup>                               | 27.04        | 127.55       | -----      | Coke oven industrial effluent               | -----   |
| Firozjaee et al., 2011           | Mixed                                | Batch  | 50-1000       | 0.067 h <sup>-1</sup>                              | 2524         | 200          | -----      | Pulp and paper wastewater treatment plant   | In media containing glucose + phenol                |

### 3.3.2 Effect of phenol stress on cell morphology

The effect of phenol stress on the cell morphology have been studied using Scanning Electron Microscopy (SEM). The SEM micrograph (Fig.3.12a and b.) shows that phenol exposure affects the membrane morphology of cells. When cells were exposed to phenol the cell surface was found to be wrinkled. Accumulation of phenol in the hydrophobic part of the membrane leads to disturbance in the interactions between the acyl chain of phospholipids. This causes modification of membrane fluidity and may lead to swelling of the bilayer (Sikkema et al. 1995).

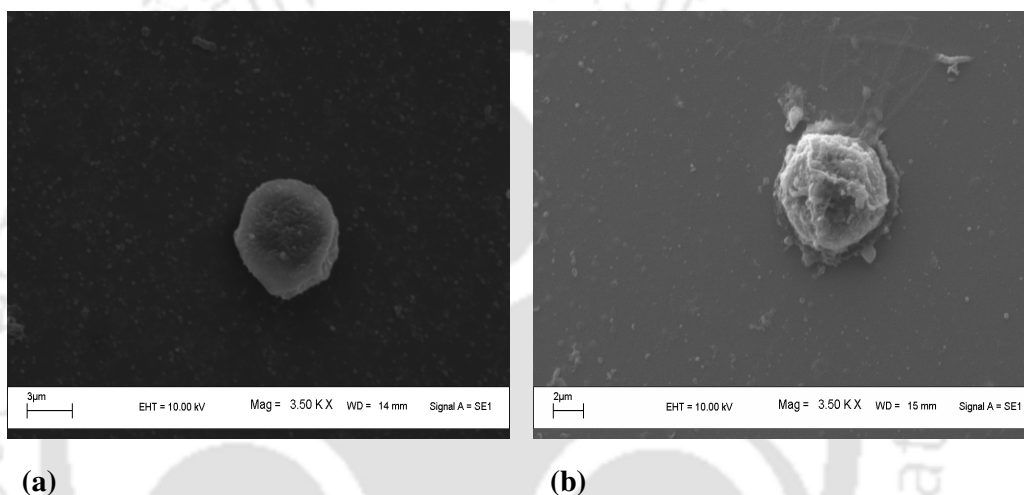


**Figure 3.12** a) SEM image of *C.pyrenoidosa* cell (control) b) SEM image of *C.pyrenoidosa* cell cultured in 200 mg/l phenol

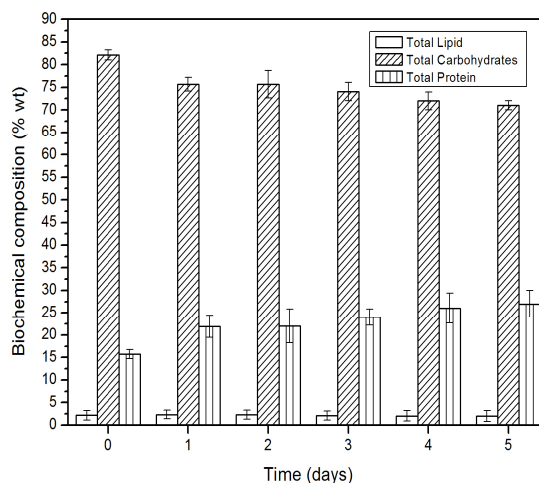
### 3.3.3 Biochemical characterization of the phenol degrading biomass

Biochemical characterization of the phenol degrading biomass to determine commercial applications as biodiesel and animal feed was carried out. Enhanced biosynthesis of both lipid and protein was observed in the phenol degrading biomass (Fig 3.13 a-y). Although an enhanced high protein content in the *C.pyrenoidosa* biomass indicates its potential application as an animal feed its use is compromised by possible concerns of algal biomass toxicity to livestock. Lincoln and Carmichael (1981) reported that dried biomass of *Synechocystis* cultured in swine wastewater are toxic when used as poultry feed. Thus, to propose the spent

biomass of *C.pyrenoidosa* as an animal feed there is utmost necessity to verify for absence of any toxicological properties to livestock. Since, this is out of scope of this work, the study was restricted to analyze the utilizability of spent biomass of *C.pyrenoidosa* as biodiesel feedstock. In a bid to identify the right time for harvesting cells so that high lipid productivity could be obtained, the biochemical variation as a function of culture time was studied (Fig 3.13 a-y). As evident from Fig 3.13 a-y, the highest lipid content is obtained when the cells enter the early stationary phase after phenol is utilized. Successive cultivation of *C.pyrenoidosa* cells following phenol depletion shows a decrease in the cellular lipid content. The results obtained by Feng et al. (2011) while studying lipid production in *Chlorella vulgaris* during wastewater treatment supports our present findings. They observed that *C.vulgaris* obtained the highest lipid content after carbon source in wastewater was completely utilized. However, they reported that further cultivation after carbon source depletion resulted in decrease in the lipid content. Microalgae cultivated under autotrophic condition has lower lipid content compared to that cultured under mixotrophic conditions. With depletion of organic carbon in mixotrophic culture, the microalgae switches from mixotrophic to autotrophic metabolism resulting in decreased lipid content (Feng et al. 2011). Mixotrophic cultivation enhances the lipid productivity i.e. allows microalgae accumulate higher amount of lipids within shorter time which is quintessential for commercial production of biodiesel. Thus, the lipid productivity of *C.pyrenoidosa* cells employed for phenol degradation was analyzed. As mentioned earlier, after complete phenol depletion *C.pyrenoidosa* cells gradually enter into stationary phase of growth and highest cellular lipid content was obtained in the early stationary phase. As the cells reached maximum growth rate at the early stationary phase, the lipid productivity will be maximum at this stage as it is product of biomass productivity and lipid content. On account of this, Lv et al. (2010) working on enhancing lipid production in *Chlorella vulgaris* recommended cells be harvested in the early stationary phase for high lipid productivity. Thus, in present study *C.pyrenoidosa* was harvested in early stationary phase and the lipid and protein productivities obtained has been shown in Figure 3.14. From Figure 3.14, it is clear that the both lipid and protein productivities are higher in phenol degrading *C.pyrenoidosa* cells as compared to control cells. Among the various phenol concentrations studied, the highest lipid productivity of 528.79 mg/l/day

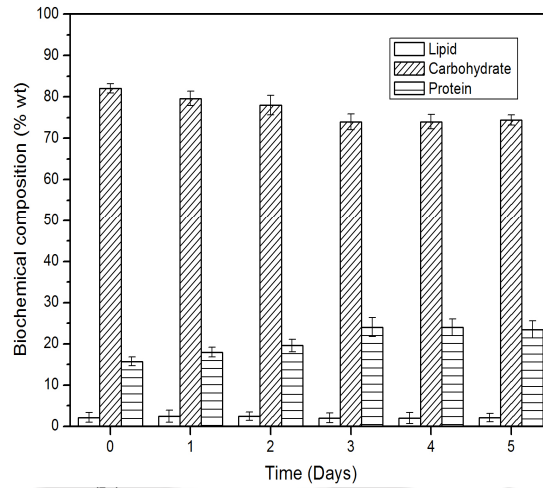


have been obtained at 250 mg/l phenol as compared to low lipid productivity of 47.88mg/l/day in control cultures. Similar results of increased lipid biosynthesis in *Phaeodactylum tricornutum* UTEX-640 (Gracia et al. 2006) and *Chlorella vulgaris* (Kong et al. 2013) cultured mixotrophically with glycerol, fructose and glucose as carbon sources accords with present findings of increased lipid accumulation in presence of phenol as additional carbon source. On basis of high lipid productivity, the spent biomass of *C.pyrenoidosa* from phenol degradation process offers enormous potential as a biodiesel feedstock. Mixotrophic cultivation is known to allow higher lipid production in microalgae within less time (Yang et al. 2011). However, its commercial applicability is hindered by high substrate cost which accounts for 50% of the cost of mixotrophic culture medium. This makes the mixotrophic cultivation of algal biodiesel feedstock costly (Yang et al. 2011). For commercialization of algal biodiesel the cost of biomass feed stock production have to be reduced by utilization of cheap alternative carbon sources for mixotrophic cultivation. The present study shows that *C.pyrenoidosa* biomass has increased lipid biosynthesis while utilizing phenol which is a toxic waste commonly found in industrial wastewaters. Thus, mixotrophic cultivation of *C.pyrenoidosa* using industrial waste phenol could serve as cheap alternative carbon source resulting in decreased production cost of algal biodiesel feedstock. The protein productivity of 3124.17 mg/l/day in phenol degrading biomass of *C.pyrenoidosa* was found to be significantly higher than that of 553.88 mg/l/day obtained in control biomass. As mentioned previously, inspite of high protein productivity in the spent biomass of *C.pyrenoidosa* it potential use as a animal feed cannot be suggested without assessing its probable toxicity to livestock.

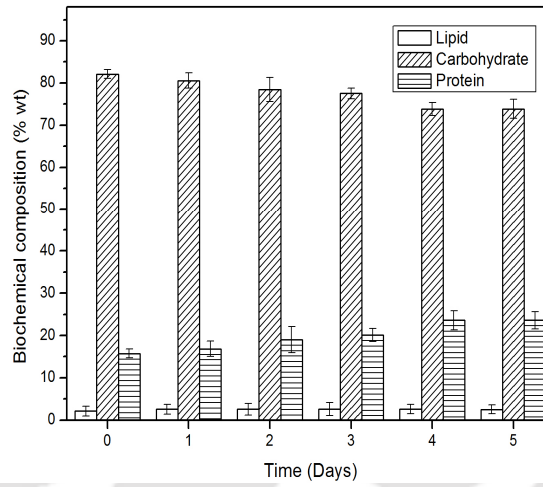


(a)

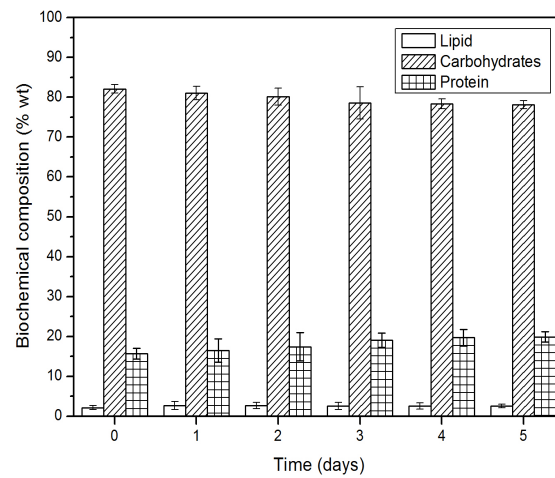
Continued



(b)

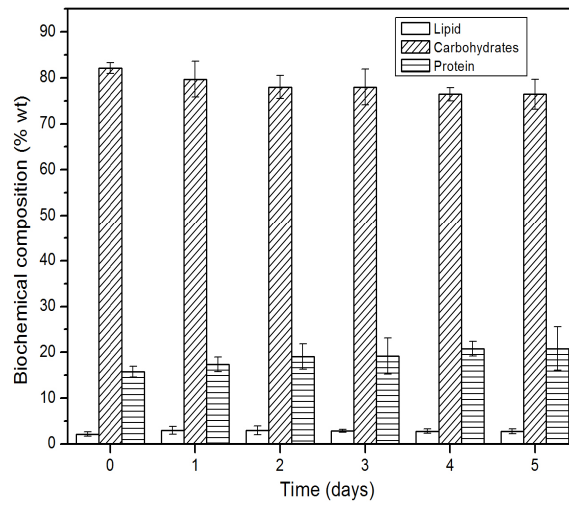


(c)

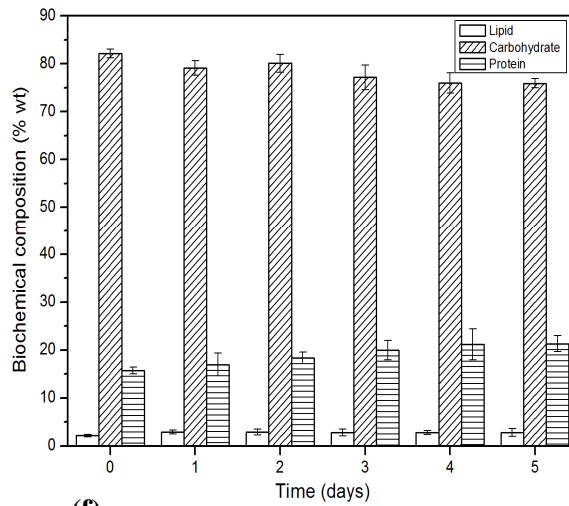


(d)

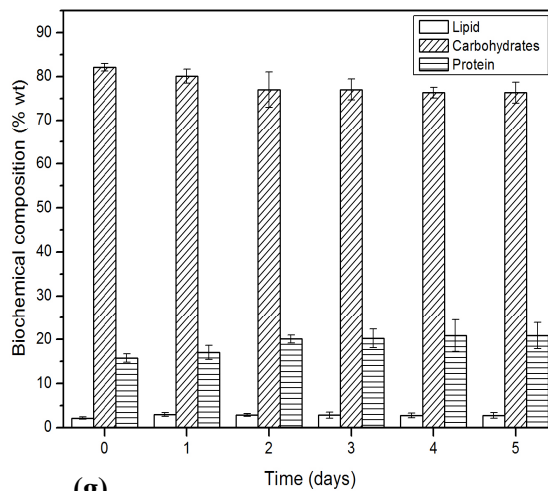
Continued



(e)

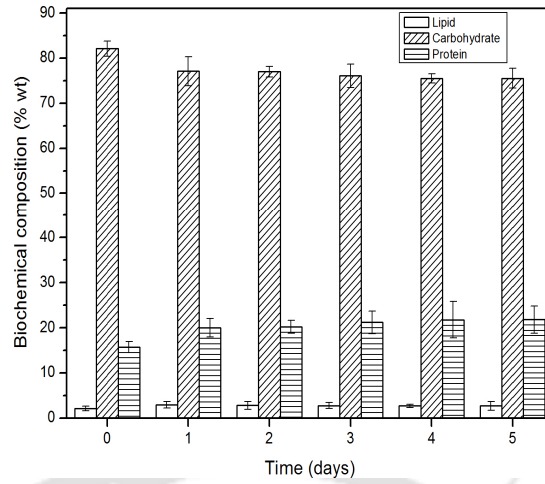


(f)

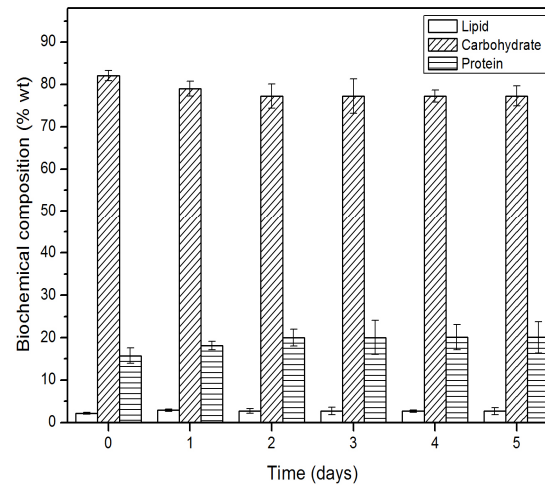


(g)

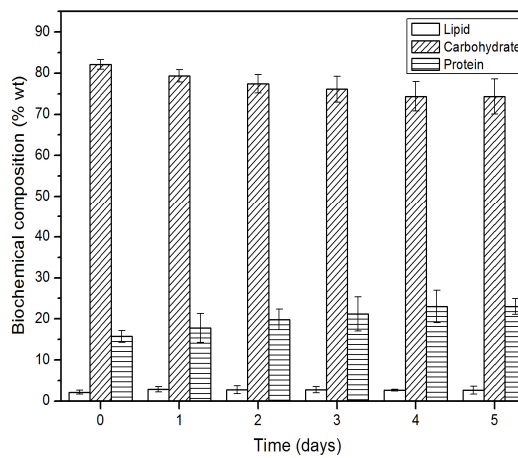
Continued



(h)

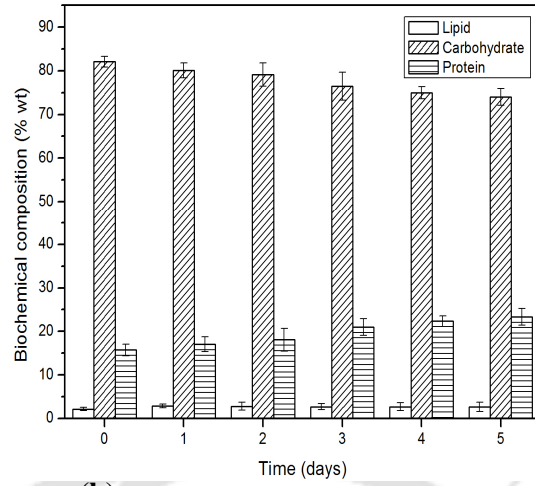


(i)

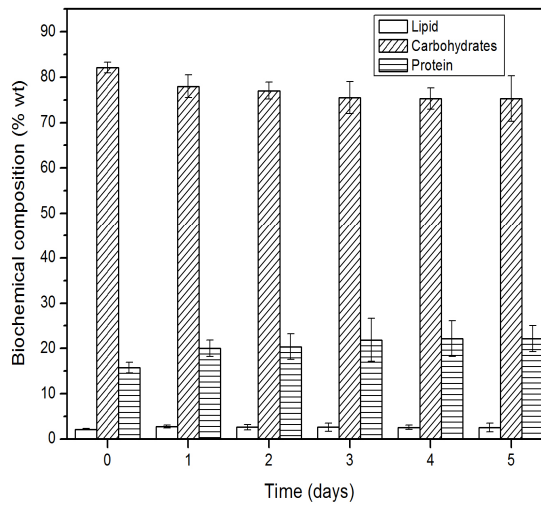


(j)

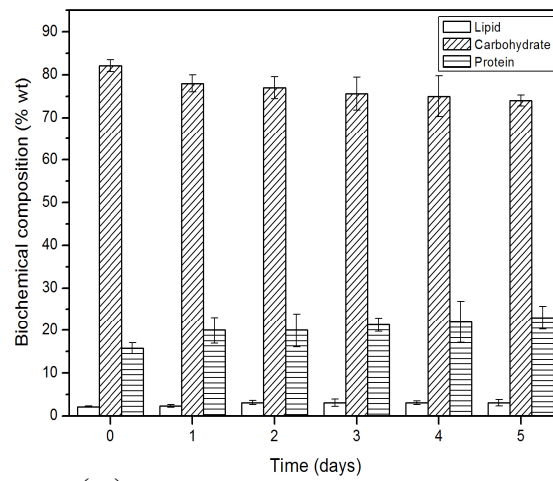
Continued



(k)

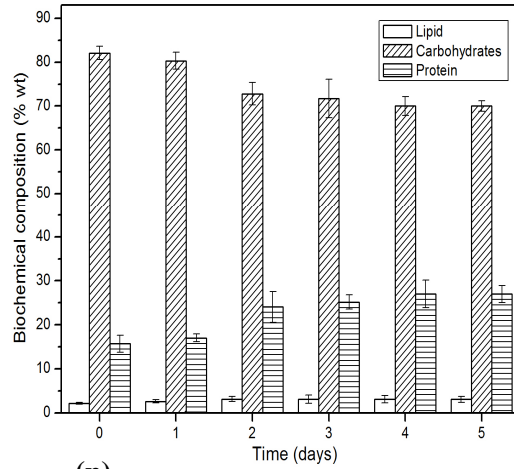


(l)

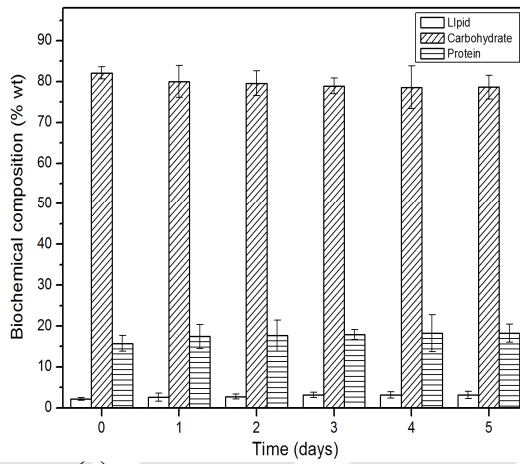


(m)

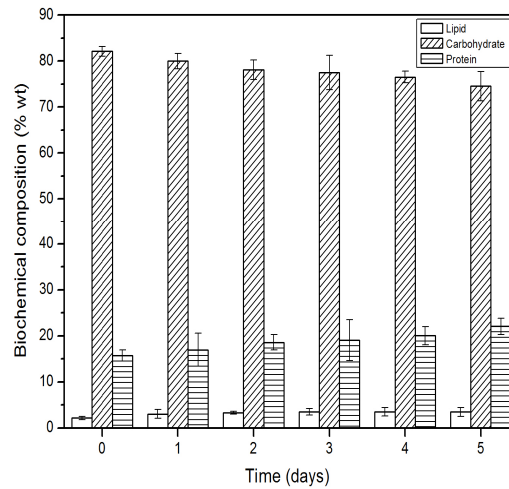
Continued



(n)

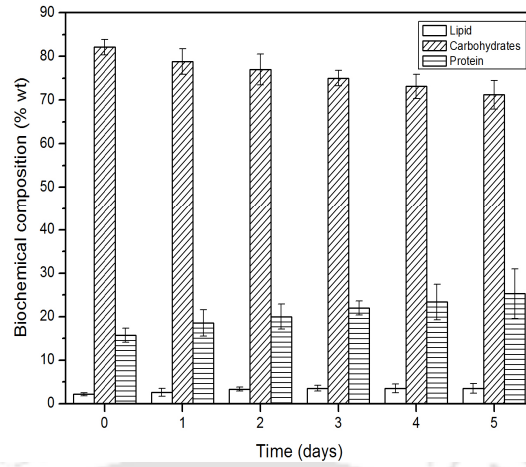


(o)

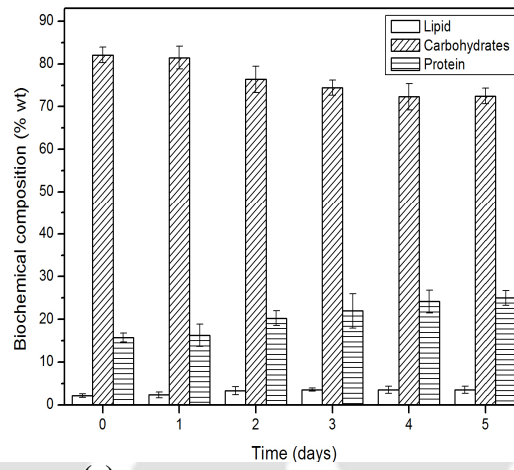


(p)

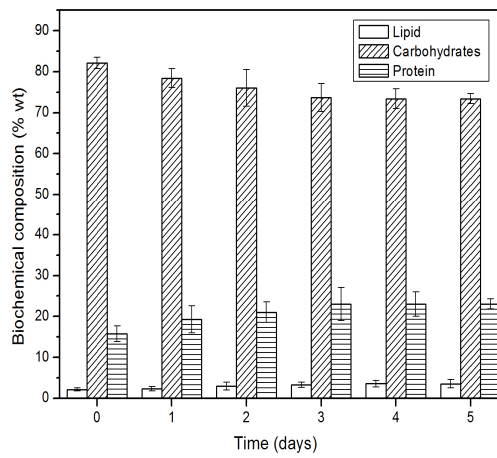
Continued



(q)

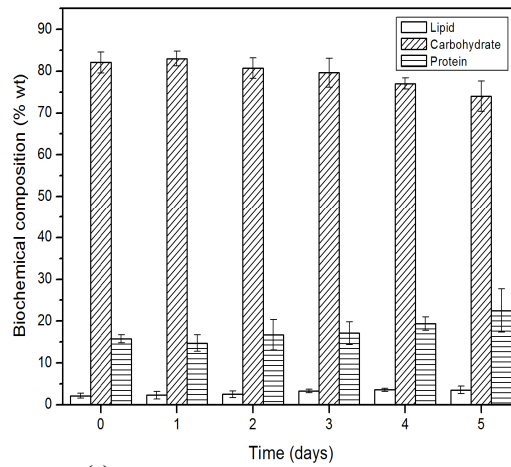


(r)

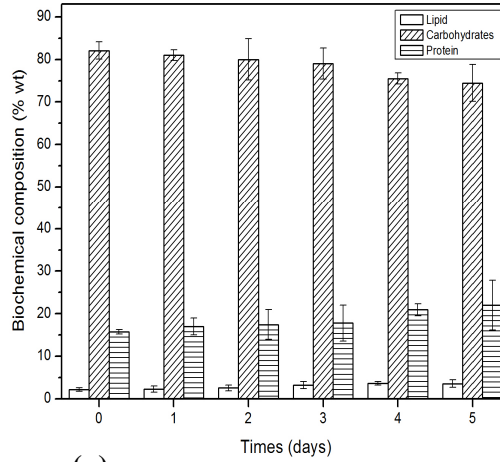


(s)

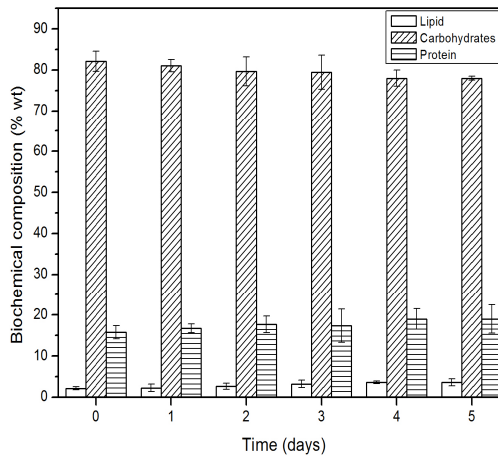
Continued



(t)



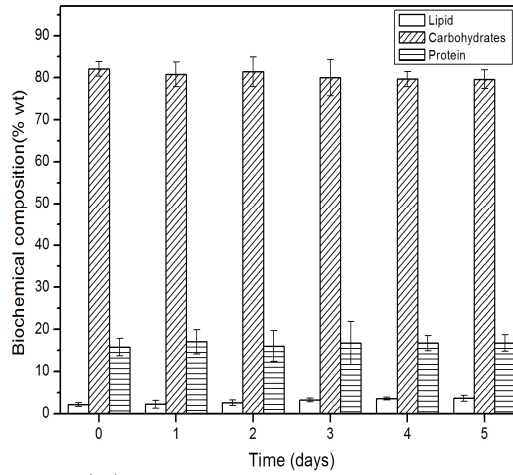
(u)



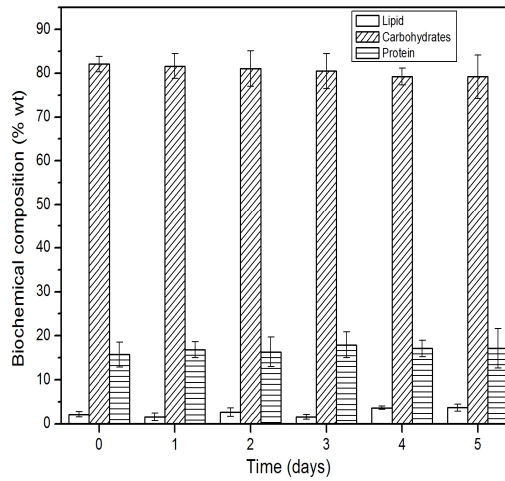
(v)

Continued

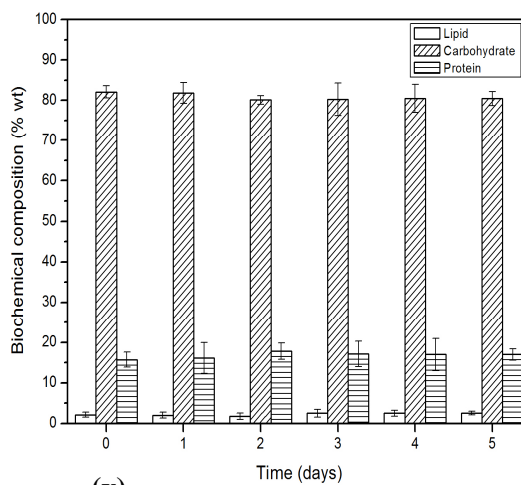




(w)

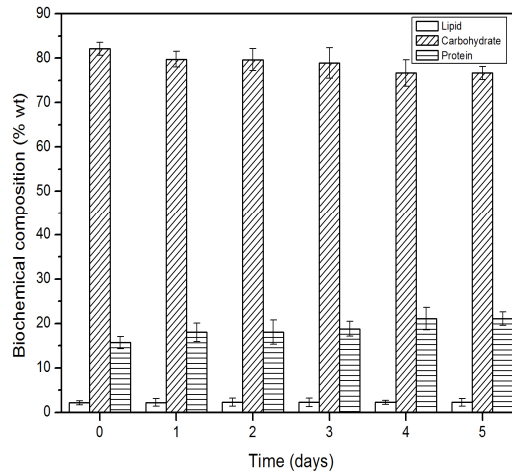


(x)



(y)

Continued



(z)

**Figure 3.13** Biochemical profile of *C.pyrenoidosa* in different initial concentrations of phenol: a) 50 mg/l phenol b) 100 mg/l phenol c) 150 mg/l phenol d) 200 mg/l phenol e) 250 mg/l phenol f) 300 mg/l phenol g) 350 mg/l phenol h) 400 mg/l phenol i) 450 mg/l phenol j) 500 mg/l phenol k) 550 mg/l phenol l) 600 mg/l phenol m) 650 mg/l phenol n) 700 mg/l phenol o) 750 mg/l phenol p) 800 mg/l phenol q) 850 mg/l phenol r) 900 mg/l phenol s) 950 mg/l phenol t) 1000 mg/l phenol u) 1050 mg/l phenol v) 1100 mg/l phenol e) 1150 mg/l phenol x) 1200 mg/l phenol y) 1250 mg/l phenol z) Control

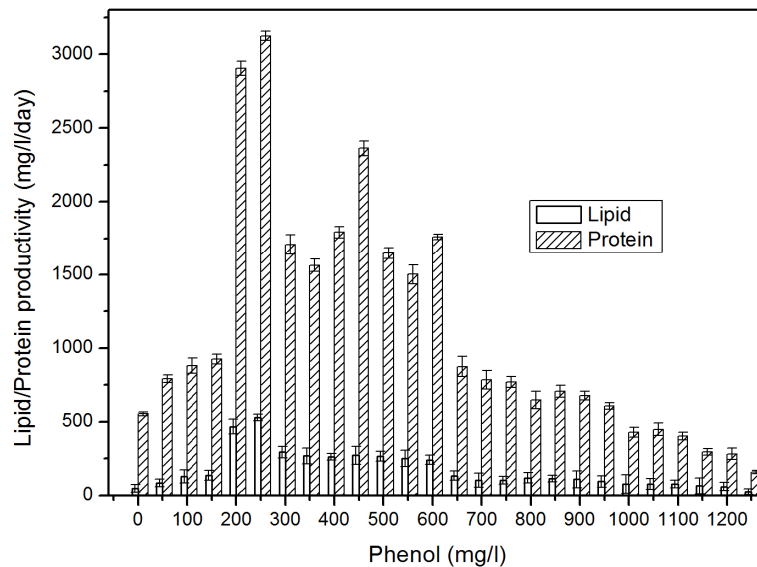
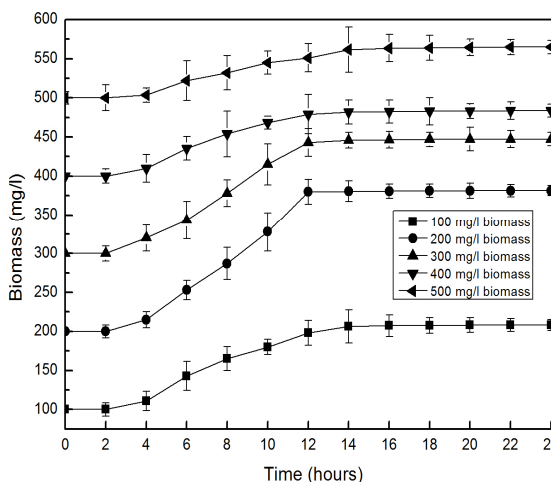


**Figure 3.14** Lipid and protein productivity of *C.pyrenoidosa* in various phenol concentrations

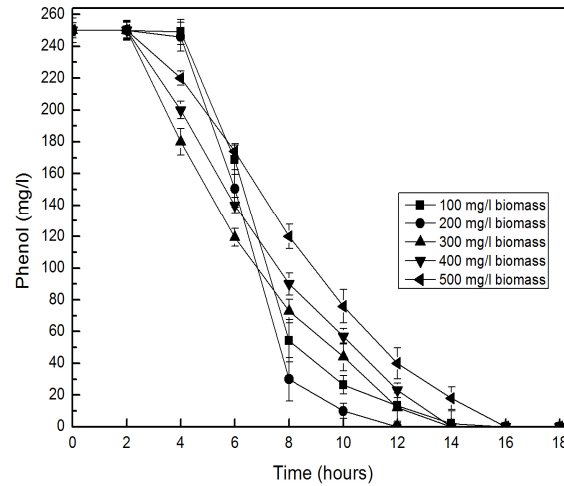
### 3.3.4 Effect of physical parameters on phenol degradation rate

The biomass growth as well as ability of microbes to degrade pollutants are influenced by number of nutritional and physico-chemical parameters and optimization of these parameters is necessary to design process with maximal phenol degradation efficiency (Zhou et al. 2011). With this view in mind, we optimized the physical parameters of inoculum dose, photoperiodicity and pH which could be practically and cost-effectively maintained for *C.pyrenoidosa* based phenol degradation process.

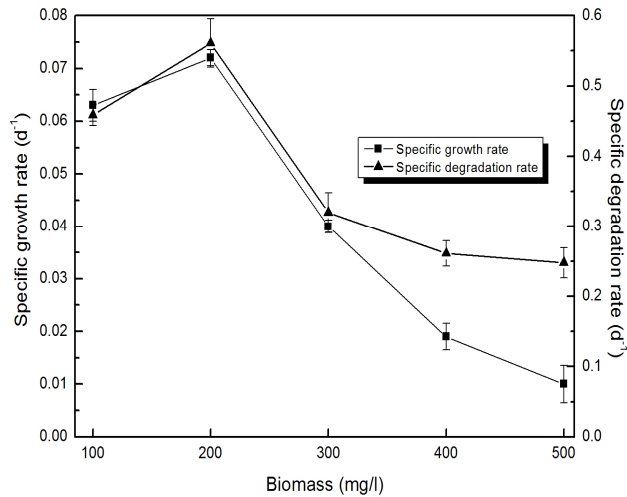
**a) Effect of inoculum dose:** Microalgal pollutant degradation systems are dependent on biomass concentrations for efficient functioning. Application of high concentration of algal biomass could enhance pollutant degradation efficiency and shorten retention time. However, a high cell concentration could lead to self-shading in turn compromising phenol degradation efficiency (Gao et al. 2011). As discussed above phenol degradation is a photo dependent process in *C.pyrenoidosa*. This photo dependent nature calls for optimization of the biomass concentration of *C.pyrenoidosa* at which phenol degradation efficiency will not be hampered. Figure 3.15 a-c shows the effect of inoculum concentration on growth, phenol degradation and specific growth and degradation rates respectively. Among the different biomass concentration ranges tested, the highest specific growth and degradation rate of  $0.072 \text{ h}^{-1}$  and  $0.561 \text{ h}^{-1}$  was obtained at biomass concentration of 200 mg/l.



(a)



(b)

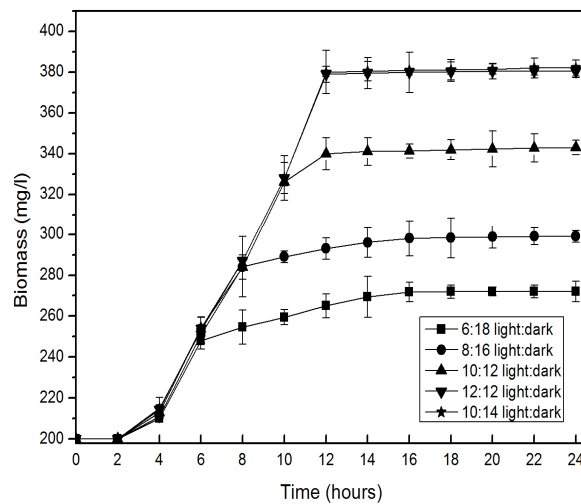


(c)

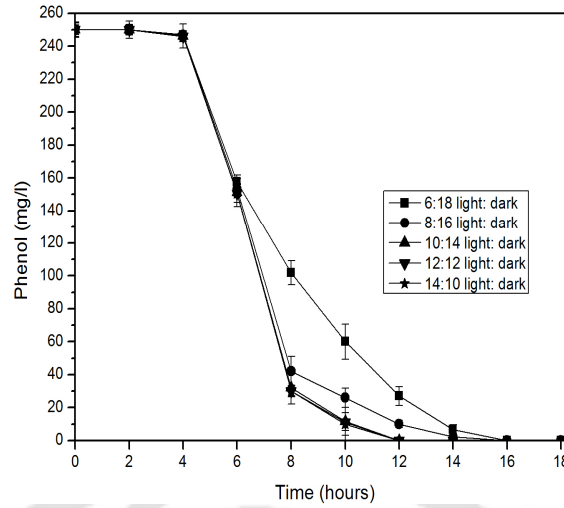
**Figure 3.15 a)** Effect of inoculum concentration on growth profile **b)** Effect of inoculum concentration on phenol degradation **c)** Effect of inoculum concentration on specific growth and degradation profile of *C.pyrenoidosa*

**b) Effect of photoperiodicity:** As phenol degradation process by *C.pyrenoidosa* is photo dependent, determination of optimal photoperiodicity regime could be an essential input for designing phenol degradation process. Papazi et al. (2012) studied the necessity of light illumination for p-cresol biodegradation by alga *Scenedesmus obliquus*. They postulated that initiation of p-cresol bond fission

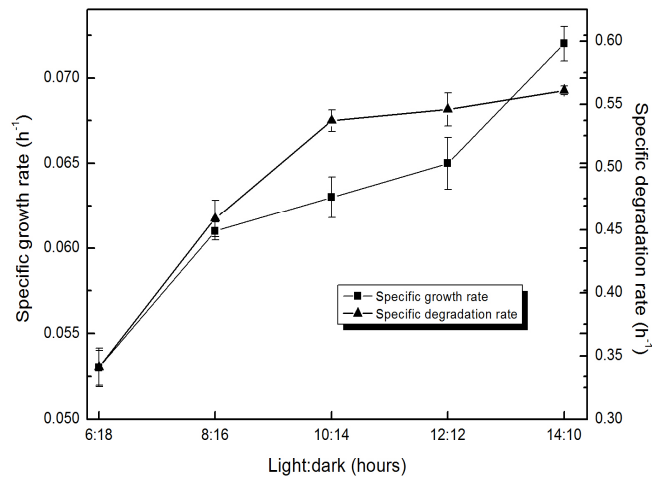
requires extra energy which is provided by the light illumination (through photosynthesis) resulting in utilization of p-cresol as a carbon source. Figure 3.16 a-c indicates the effect of different photoperiodic regimes on growth, phenol degradation and specific growth and degradation rates respectively. Among the different photoperiodic regime tested, the highest specific growth rate of  $0.072 \text{ h}^{-1}$  was achieved at 14 hours light: 10 hours dark photoperiodicity. However, it may be noted that complete phenol degradation is achieved within 12 hours of illumination (Figure 3.16 b) and thus the phenol degradation rates achieved in three photoperiodic regimes of 10 hours light: 14 hours dark, 12 hours light: 12 hours dark and 14 hours light:10 hours dark have fairly close degradation rates of  $0.54 \text{ h}^{-1}$ ,  $0.55 \text{ h}^{-1}$  and  $0.56 \text{ h}^{-1}$  respectively. The average day length is 13 hours 28 minutes in the geographical location (Assam, India) of the current study ([www.assam.climatemps.com](http://www.assam.climatemps.com)). Thus, the light requirement for the phenol degradation process could be fulfilled using natural day light thus adding to cost effectiveness of the system.



(a)



(b)

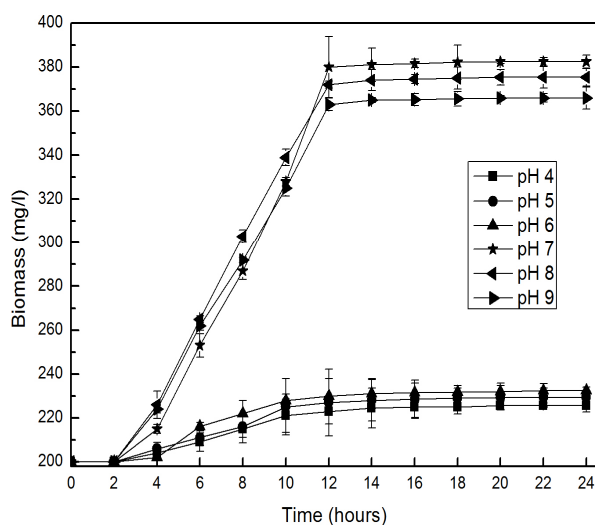


(c)

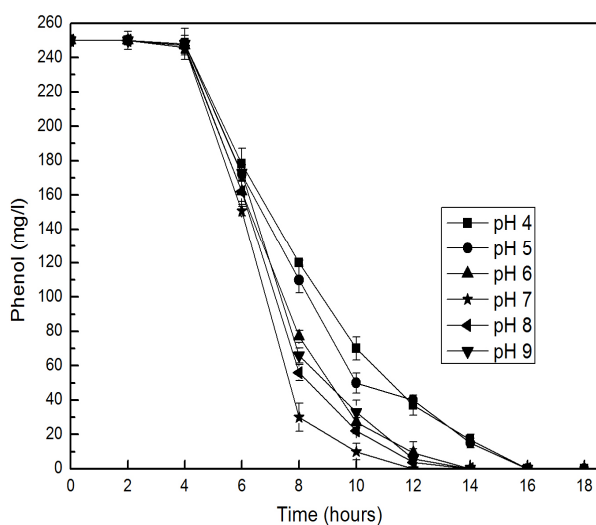
**Figure 3.16** a) Effect of light:dark periodicity on growth profile b) Effect of light:dark periodicity on phenol degradation profile c) Effect of light:dark periodicity on specific growth and degradation profile of *C.pyrenoidosa*

**c) Effect of pH:** Knowledge of the pH of the wastewater to be treated is of utmost importance since microbial degradation is dependent on activity of enzymatic pathways. Each enzyme possesses a particular pH for optimal activity. pH change can affect enzyme stability thus decreasing degradation rates (Banerjee and Ghoshal 2010). As microbes degrade phenol by using enzymatic mechanism and hence its

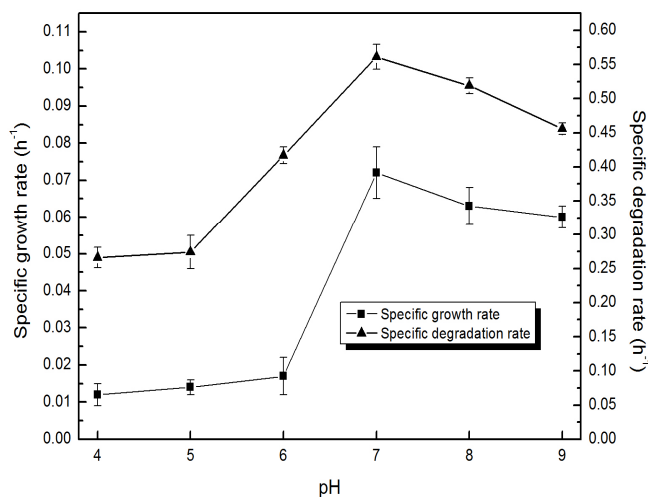
degradation efficiency will also be subject to change in pH. Figure 3.17 a-c shows the effect of pH on growth, phenol degradation and specific growth and degradation rates respectively. Among the different pH ranges tested, the highest growth and degradation rates of  $0.072 \text{ h}^{-1}$  and  $0.561 \text{ h}^{-1}$  was obtained at pH 7 (Figure 3.17 c).



(a)



(b)



(c)

**Figure 3.17** a) Effect of pH on biomass growth profile b) Effect of pH on phenol degradation c) Effect of pH on specific growth and degradation profile of *C.pyrenoidosa*.

### 3.3.5 Pre adaptation as a strategy for rapid phenol degradation

Pre adaptation of cells to the target compound eliminated most of the adaptation period required in subsequent degradation leading to increased degradation rates (Kwon and Yeom 2009). For enhanced degradation rates, the cells should be pre adapted to that concentration of the target compound which is close to the target concentration to be treated (Kwon and Yeom 2009).

#### 3.3.5.1 Growth kinetics and phenol degradation by pre adapted cells

With this view of obtaining enhanced degradation rates, *C.pyrenoidosa* cells pre adapted at 250 mg/l (i.e. the concentration with highest growth and phenol degradation rate) were utilized for degrading 250 mg/l phenol under the optimized



physical conditions obtained above. Figure 3.18 shows the biomass growth and phenol degradation characteristics of preadapted cells of *C.pyrenoidosa*. The lag phase of 2 hours obtained prior to pre adaptation (Figure 3.10 e) was eliminated while utilizing pre adapted cells of *C.pyrenoidosa* for degrading 250 mg/l phenol (Figure 3.16 a). This resulted in enhanced growth rate of  $0.078 \text{ h}^{-1}$  as compared to that of  $0.06 \text{ h}^{-1}$  obtained before pre adaptation of cells. Enhanced growth rate resulted in increased phenol degradation rate of  $0.636 \text{ h}^{-1}$  as compared to  $0.561 \text{ h}^{-1}$  obtained for cells prior to pre adaptation. Thus, pre adapted cells degrade 250 mg/l phenol within comparatively shorter time period of 8 hours compared to 12 hours required by cells before pre adaptation.

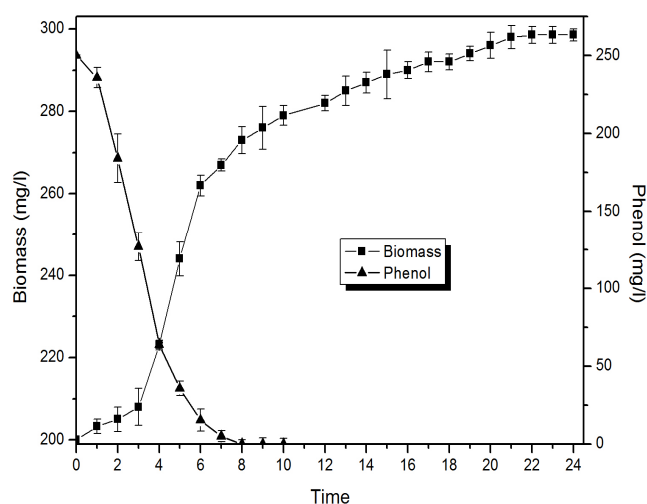


**Figure 3.18** Biomass growth and phenol degradation profile of pre adapted cells (adapted in 250 mg/l phenol) under experimentally derived optimum physical parameters.

As phenol degradation potential of microbe is a growth dependent phenomenon, the growth dynamics of *C.pyrenoidosa* cells pre adapted to the target phenol concentration of 250 mg/l is being analyzed using growth kinetic modeling (Table 3.8). Among the growth kinetic models, Yano model with the highest  $R^2$  value as well as least SD value best fits the experimental growth pattern of pre adapted *C.pyrenoidosa* in 250 mg/l phenol. From growth kinetic modeling, the maximum specific growth rate ( $\mu_{\max}$ ) of  $0.22 \text{ h}^{-1}$  obtained as per best fitted Yano model falls within the range reported in literature (Table 3.7). However as expected, it is slightly higher compared to  $\mu_{\max}$  of  $0.21 \text{ h}^{-1}$  obtained for

*C.pyrenoidosa* prior to the pre adaptation step.  $K_s$  value (half saturation coefficient) and  $K_I$  (substrate inhibition constant) value of 500.54 mg/l and 900.41 mg/l respectively obtained from best fitted Yano model is higher compared to values reported by previous works (Table 3.7). Pre adapted culture of *C.pyrenoidosa* also has higher  $K_s$  and  $K_I$  value compared to that obtained for *C.pyrenoidosa* before pre adaptation treatment (Table 3.2). An enhanced  $K_s$  and  $K_I$  value indicates ability of pre adapted cells of *C.pyrenoidosa* to grow with increased efficiency at higher phenol concentrations and enhancement in resistance to phenol toxicity (Bajaj et al. 2009; Jiang et al. 2002; Sahoo et al. 2011). Thus, pre adapting *C.pyrenoidosa* to the target phenol concentration before actual application for phenol treatment can be efficient way for obtaining a phenol degradation process with optimal activity.

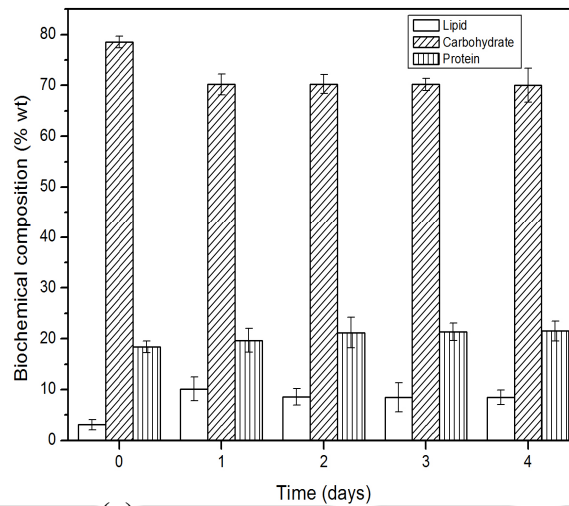
**Table 3.8** Growth kinetic parameters of pre adapted *C. pyrenoidosa* cultures in 250 mg/l phenol

| Model   | $\mu_{max}$ (h <sup>-1</sup> ) | $K_s$ (mg/l) | $K_I$ (mg/l) | K(mg/l)  | R <sup>2</sup> | SD <sub>avg</sub> |
|---------|--------------------------------|--------------|--------------|----------|----------------|-------------------|
| Haldane | 0.997                          | 270.61       | 108.74       | -----    | 0.95           | 0.337             |
| Yano    | 0.220                          | 500.54       | 900.41       | 85.75    | 0.99           | 0.180             |
| Webb    | 0.220                          | 130.00       | 200.00       | 54802.06 | 0.98           | 0.200             |
| Aiba    | 0.252                          | 63.02        | 280.91       | -----    | 0.96           | 0.203             |
| Edward  | 0.250                          | 88.20        | 263.00       | -----    | 0.97           | 0.204             |

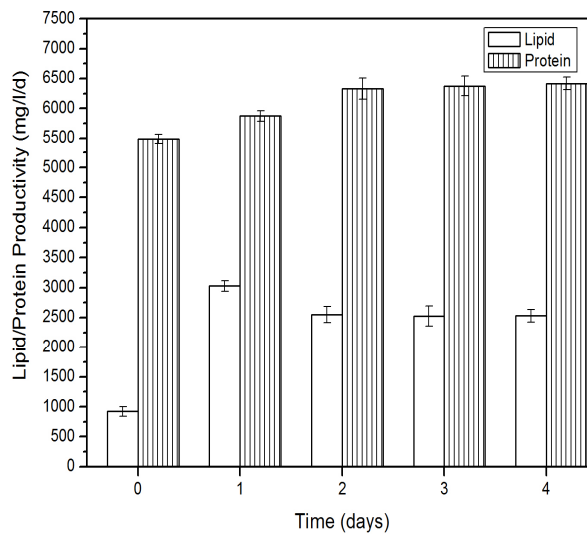
### 3.3.5.2 Analysis of biochemical variation of pre adapted *C.pyrenoidosa* biomass during phenol degradation process

The biochemical variation as a function of culture time was studied to determine the harvesting time for *C.pyrenoidosa* biomass with high lipid productivity. As seen in Figure 3.19 a, contents of biochemical components of preadapted *C.pyrenoidosa* varied during the batch culture in 250 mg/l phenol. A prominent increase in lipid content from 3.08% (Day 0) to 10.14 % (Day 1) when cells enter early stationary phase following complete phenol utilization. However, subsequent culture following phenol depletion lead to a decrease in cellular lipid content. As discussed earlier, our results are in accordance to findings of Feng et al. (2011) who reported *C.vulgaris* obtained the highest lipid content after carbon source in wastewater was completely utilized and further cultivation after carbon source depletion resulted in decreased lipid content. Pre adapted biomass of *C.pyrenoidosa* achieved higher cellular lipid contents faster as compared to that in control cells as well as phenol degrading *C.pyrenoidosa* cells not subjected to pre adaptation step. This is evident from the distinct variation in cellular lipid content on Day 1 in control cells (2.23 %), phenol degrading biomass prior to pre adaptation (2.95 %) and pre adapted phenol degrading biomass (10.14 %). As the cells growth rate reached it maximum at early stationary phase, the maximum lipid productivity of 3026.7 mg/l/day have been obtained in pre adapted biomass of *C.pyrenoidosa* (Figure 3.19 b) as compared to significant low productivities in control (47.88 mg/l/day) and phenol degrading *C.pyrenoidosa* cells prior to pre adaptation (528.79 mg/l/day). The total lipids produced microalgae is composed of non polar or neutral lipids and polar lipids. Out of the two lipid varieties, only neutral lipids can be transesterified for biodiesel production (Sharma et al. 2012). Thus, high quantity of neutral lipids in algal biomass is essential for its application as a commercial biodiesel feedstock. This calls for estimation of neutral lipid content in the spent biomass of *C.pyrenoidosa* to establish its potential as biodiesel feedstock. Figure 3.19 c shows the neutral lipid accumulation profile of pre adapted *C.pyrenoidosa* cells employed for degrading 250 mg/l phenol. As evident from Figure 3.19 c, neutral lipid content increased at a faster rate in the pre adapted cells of *C.pyrenoidosa* employed for phenol degradation as compared to control cells. The marked enhancement in neutral lipid accumulation

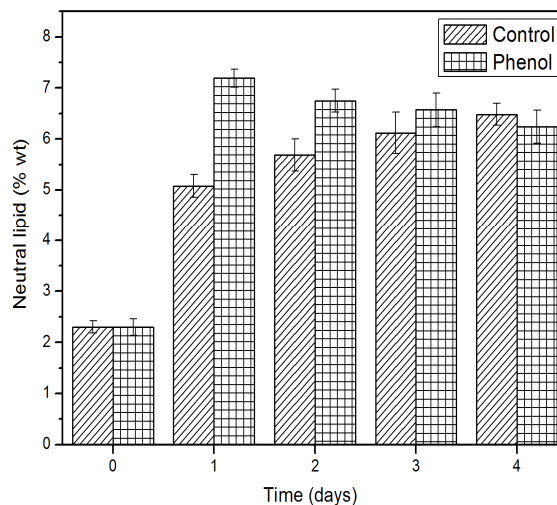
of 7.19 % (day 1) as compared to the low neutral lipid accumulation of 5.08 % (day 1) in control cultures indicates an increased rate of neutral lipid accumulation in pre adapted *C.pyrenoidosa* cells utilized for phenol treatment (Fig 3.19 c). However, further cultivation of *C.pyrenoidosa* cells following phenol depletion leads to slight decrease in neutral lipid content. The prominent enhancement in neutral lipid accumulation in spent biomass of *C.pyrenoidosa* from the phenol degradation process establishes its potential to serve as a biodiesel feedstock.



(a)



(b)



(c)

**Figure 3.19 a)** Biochemical profile of pre adapted cells of *C.pyrenoidosa* in 250 mg/l phenol. **b)** Lipid and protein productivity of pre adapted cells of *C.pyrenoidosa* in 250 mg/l phenol. **c)** Neutral lipid accumulation profile for pre adapted *C.pyrenoidosa* cells in 250 mg/l phenol.

### 3.3.6 Analysis of practical applicability of *C.pyrenoidosa* based process for phenol degradation and biodiesel production

To verify the practical applicability of the process, pre adapted cells of *C.pyrenoidosa* was applied for phenol degradation in petroleum refinery wastewater. The refinery wastewater was quantified to contain 10 mg/l phenol. pH of 7.8 was determined in the refinery wastewater. With the aim of evaluating the natural growth and phenol degradation profile of *C.pyrenoidosa*, the refinery wastewater used for degradation experiment was not supplemented with nutritional requirement of the algae and neither the pH was adjusted to optimal range. Figure 3.20 showed the biomass growth as well as phenol degradation profile of *C.pyrenoidosa* in 10 mg/l phenol containing refinery wastewater. *C.pyrenoidosa* achieves a growth rate of  $0.029 \text{ h}^{-1}$  and completely degrades 10 mg/l phenol in refinery wastewater within 3 hours with a degradation rate of  $0.699 \text{ h}^{-1}$ . Kinetic

modeling (Table 3.9) suggests that Webb model with its highest  $R^2$  value and least SD value could best fit the experimental growth pattern of *C.pyrenoidosa* in 10 mg/l phenol containing refinery wastewater.

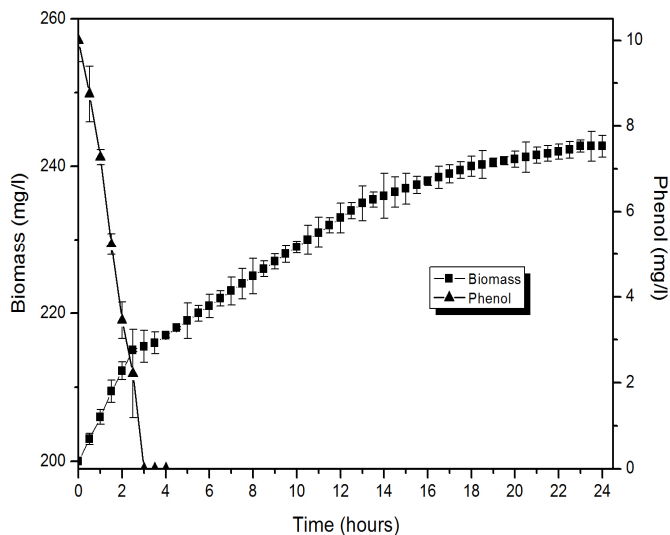


**Figure 3.20** Biomass growth and phenol degradation profile of pre adapted cells (adapted in 250 mg/l phenol) in 10 mg/l phenol containing refinery wastewater.

**Table 3.9** Growth kinetic parameters of *C. pyrenoidosa* in 10 mg/l phenol in refinery wastewater

| Model   | $\mu_{max}$ ( $h^{-1}$ ) | $K_s$ (mg/l) | $K_I$ (mg/l) | $K$ (mg/l) | $R^2$ | $SD_{avg}$ |
|---------|--------------------------|--------------|--------------|------------|-------|------------|
| Haldane | 0.107                    | 360.61       | 128.74       | -----      | 0.650 | 0.221      |
| Yano    | 0.040                    | 600.54       | 1020.41      | 65.75      | 0.510 | 0.240      |
| Webb    | 0.180                    | 50.00        | 202.00       | 53302.06   | 0.998 | 0.120      |
| Aiba    | 0.152                    | 33.01        | 290.98       | -----      | 0.950 | 0.140      |
| Edward  | 0.252                    | 58.20        | 333.00       | -----      | 0.977 | 0.130      |

Since, the cells were pre adapted to 250 mg/l phenol, we also attempted to analyze the growth and phenol degradation dynamics of *C.pyrenoidosa* in 250 mg/l phenol containing refinery wastewater. For this purpose, the 10 mg/l phenol containing refinery wastewater was spiked with phenol to a concentration of 250 mg/l and then used for degradation experiments. Figure 3.21 showed the biomass growth as well as phenol degradation profile of *C.pyrenoidosa* in 250 mg/l phenol containing refinery wastewater. It is observed that *C.pyrenoidosa* attains a biomass growth of  $0.034 \text{ h}^{-1}$  and completely degrades 250 mg/l phenol in refinery wastewater within 11 hours with a degradation rate of  $0.416 \text{ h}^{-1}$ . Among the various growth kinetic models fitted, Webb model with highest  $R^2$  value and least SD value fits experimental growth data the best (Table 3.10).

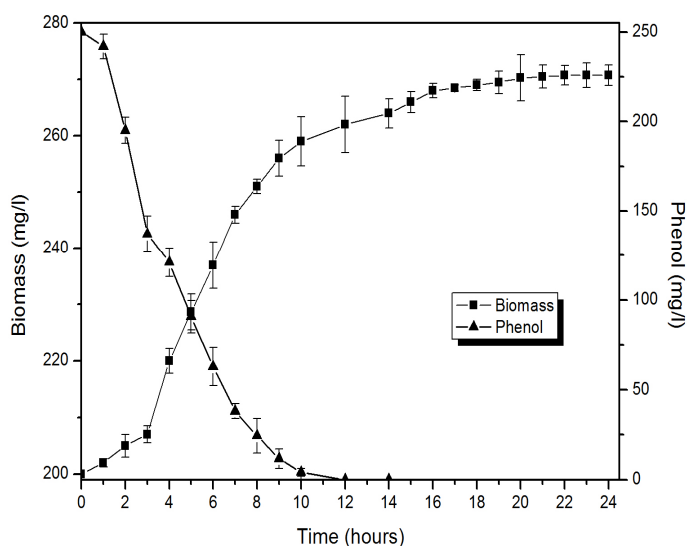


**Figure 3.21** Biomass growth and phenol degradation profile of pre adapted cells (adapted in 250 mg/l phenol) in 250 mg/l phenol containing refinery wastewater.

**Table 3.10** Growth kinetic parameters of *C. pyrenoidosa* in 250 mg/l phenol in refinery wastewater

| Model   | $\mu_{\max}$ (h <sup>-1</sup> ) | K <sub>s</sub> (mg/l) | K <sub>I</sub> (mg/l) | K(mg/l)  | R <sup>2</sup> | SD <sub>avg</sub> |
|---------|---------------------------------|-----------------------|-----------------------|----------|----------------|-------------------|
| Haldane | 0.397                           | 290.61                | 108.74                | -----    | 0.94           | 0.21              |
| Yano    | 0.21                            | 450.54                | 920.41                | 85.75    | 0.98           | 0.19              |
| Webb    | 0.15                            | 50.00                 | 202.00                | 53302.06 | 0.99           | 0.17              |
| Aiba    | 0.20                            | 33.02                 | 280.98                | -----    | 0.98           | 0.19              |
| Edward  | 0.20                            | 68.20                 | 263.00                | -----    | 0.973          | 0.19              |

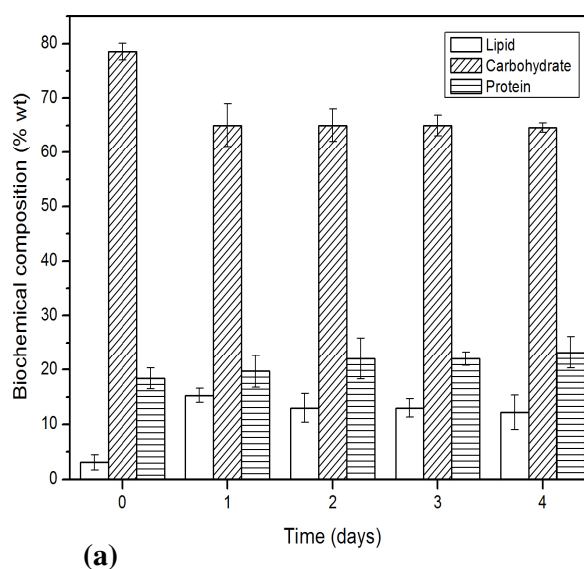
Comparison of biokinetic parameters obtained by growth kinetic modeling in refinery wastewater and in nutrient media could bring to light how *C.pyrenoidosa* behaved under two significantly different culture conditions of nutrient sufficient media and refinery wastewater. The slightly lower  $\mu_{\max}$  values obtained in refinery wastewater (Table 3.9 and 3.10) could be explained by lack of optimal nutrient factors for growth as well as other growth inhibitory constituents which may be present in refinery wastewater. Similarly, an decrease in K<sub>I</sub> and K<sub>s</sub> value in refinery wastewater (Table 3.9 and 3.10) shows decreased efficiency to grow in higher phenol concentrations as well as decreased ability to resist phenol toxicity compared to that of nutrient media. This can be explained by the fact that optimal growth conditions in media allow the microalgae better counteract phenol toxicity. Lack of optimal growth requirements as well as presence of other inhibitory constituents in refinery wastewater compromises the ability of *C.pyrenoidosa* to resist high phenol toxicity leading to decreased efficiency of growth in high phenol concentrations. Agarry et al. (2008) carried out phenol degradation of 30 mg/l phenol containing refinery wastewater using two strains of *Pseudomonas*

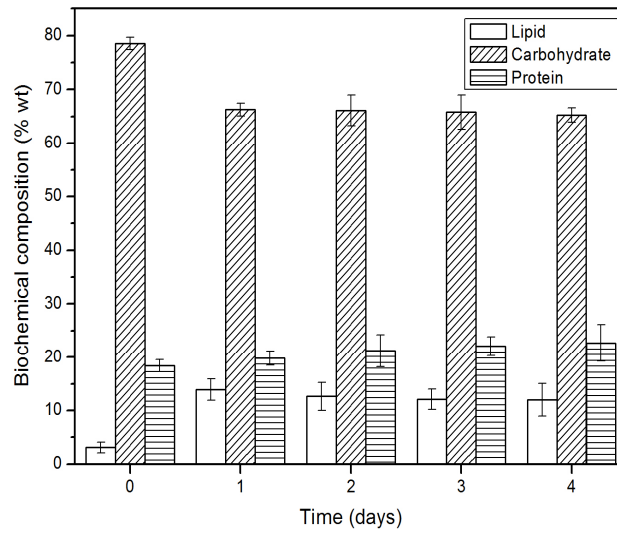


*aeruginosa* and *Pseudomonas fluorescense*. The  $\mu_{\max}$  and  $K_I$  values obtained for *C.pyrenoidosa* in both 10 mg/l and 250 mg/l phenol containing refinery wastewater (Table 3.9 and 3.10) is higher than the values obtained for both *Pseudomonas aeruginosa* ( $\mu_{\max}= 1.65 \times 10^{-2} \text{ h}^{-1}$ ,  $K_I= 29.7 \text{ mg/l}$ ) and *Pseudomonas fluorescense* ( $\mu_{\max}=0.94 \times 10^{-2} \text{ h}^{-1}$ ,  $K_I= 31.7 \text{ mg/l}$ ). They reported that *Pseudomonas aeruginosa* and *Pseudomonas fluorescense* could not completely degrade phenol in refinery wastewater with removal of 94.5% and 69.4% respectively. However, they added mineral salt medium to refinery wastewater to meet the nutritional requirement of the microorganism for proper growth which is in contrary to present work. Thus high values of biokinetic parameters as well as complete phenol degradation by *C.pyrenoidosa* in refinery wastewater suggests the practical applicability of the strain for phenol degradation in refinery wastewater.

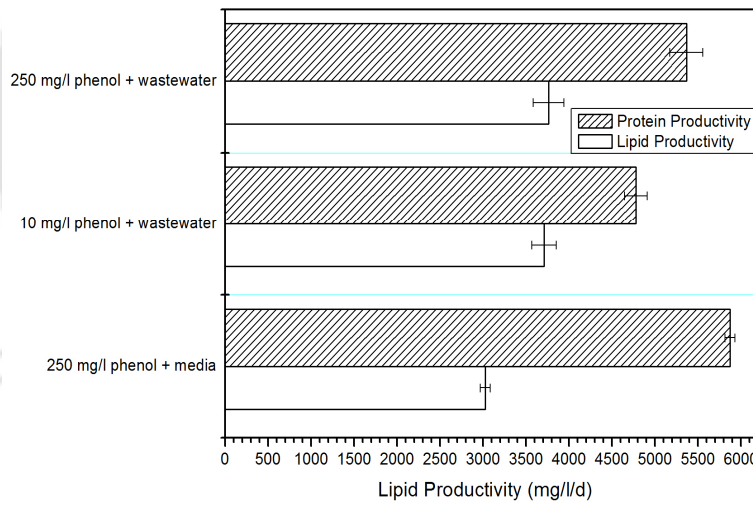
Figure 3.22 a and Figure 3.22 b shows the biochemical variation in *C.pyrenoidosa* cells utilized for treatment of 10 mg/l and 250 mg/l phenol containing refinery wastewater. A significant enhancement in lipid content from 3.08% (Day 0) to 15.28 % (Day 1) was observed when cells enter early stationary phase following complete utilization of 10 mg/l phenol in refinery wastewater. However, further culture following phenol depletion lead to a decrease in cellular lipid content. Similarly, lipid accumulation was found to be enhanced from 3.08% (Day 0) to 13.9 % (Day 1) in early stationary phase obtained after complete degradation of 250 mg/l phenol in refinery wastewater. Also, cellular lipid content decreases with further culture of cells following utilization of 250 mg/l phenol. Fig 3.16 i compares the lipid and protein productivity in pre adapted *C.pyrenoidosa* cells used for degradation of 250 mg/l phenol in nutrient media, 10 mg/l phenol and 250 mg/l phenol in refinery wastewater. The highest lipid productivity of 3763.65 mg/l/day have been obtained in 250 mg/l phenol containing refinery wastewater as compared to slightly lower productivity of 3709.41 mg/l/day in 10 mg/l phenol containing refinery wastewater. The lipid productivity of *C.pyrenoidosa* during phenol degradation process in wastewater was found to be higher than that of 3026.7 mg/l/day obtained in nutrient media (Figure 3.22 c). Farooq et al.(2013) studied lipid production in *Chlorella* sp. during treatment of brewery wastewater. Their reports of enhancement in lipid productivity from 31.1 to 108.0 mg/l/day in *Chlorella* sp. used for wastewater treatment accords with our

present findings. Mahapatra, et al. (2014) reported enhanced lipid productivity of 32 mg/l/day in mixotrophic algal consortium used for bioremediation of municipal wastewater which also supports our present findings. Similarly, Woertz et al. (2009) obtained a lipid productivity of 24 mg/l/day by treating municipal wastewater using an algal consortium. Algae grown in carbon rich wastewater has been observed to possess higher lipid content (Bhatnagar et al. 2010). Due to mixotrophy in carbon rich wastewater, organic carbon gets transformed and gets accumulated as lipids in the algal biomass (Mahapatra et al. 2014). The higher lipid productivity obtained in spent *C.pyrenoidosa* biomass obtained after phenol degradation in refinery wastewater adds to the practical applicability of the process for phenol removal from wastewater along with generation of algal biodiesel feedstock. However, commercial applicability of the wastewater grown *C.pyrenoidosa* biomass will depend on its neutral lipid content. Figure 3.22 d shows the neutral lipid productivity in spent biomass of *C.pyrenoidosa* employed for degradation of 250 mg/l phenol in media, 10 mg/l and 250 mg/l phenol in refinery wastewater. Higher neutral lipid productivities of 3036.8 mg/l/day (10 mg/l phenol containing refinery wastewater) and 2972.84 mg/l/day (250 mg/l phenol containing refinery wastewater) as compared to that of 2146.57 mg/l/day in nutrient media containing 250 mg/l phenol. The high neutral lipid accumulation obtained in *C.pyrenoidosa* cells employed for phenol treatment in refinery wastewater establishes the potential of application of *C.pyrenoidosa* for phenol treatment in wastewaters and utilization of spent biomass as biodiesel feedstock.

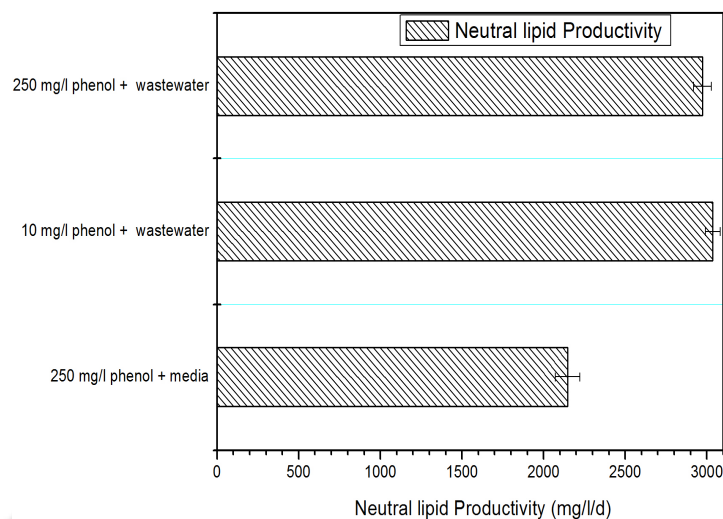




(b)



(c)



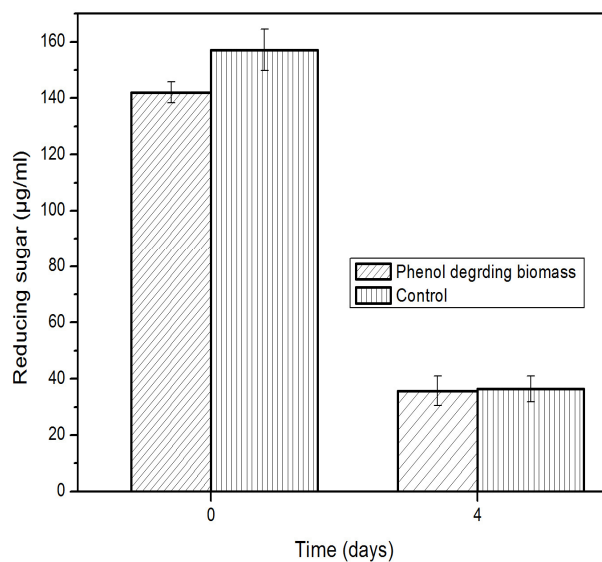
(d)

**Figure 3.22 a)** Biochemical profile of pre adapted cells of *C.pyrenoidosa* in 10 mg/l phenol containing refinery wastewater. **b)** Biochemical profile of pre adapted cells of *C.pyrenoidosa* in 250 mg/l phenol containing refinery **c)** Comparison of lipid and protein productivity of pre adapted cells of *C.pyrenoidosa* in 250 mg/l media, 10 mg/l and 250 mg/l phenol containing wastewater. **d)** Comparison of neutral lipid productivity of pre adapted *C.pyrenoidosa* in 250 mg/l media, 10 mg/l and 250 mg/l phenol containing wastewater.

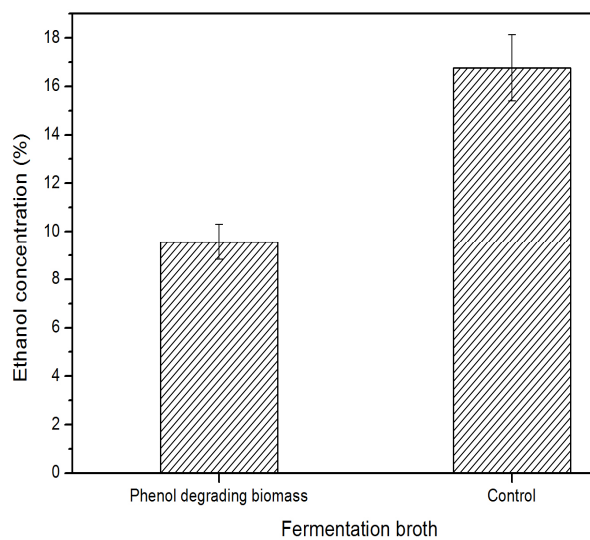
The spent biomass of *C.pyrenoidosa* after degradation of 10 mg/l phenol in refinery wastewater has a high neutral lipid productivity (3036.8 mg/l/day) qualifying it as potential algal biodiesel feedstock. Thus, the total lipid was extracted from the spent biomass and weighed gravimetrically. Total lipid content of 16.3 % dry weight in *C.pyrenoidosa* biomass following phenol degradation was determined by gravimetry in comparison to 2.87 % dry weight in control culture. The slightly higher value determined by gravimetry was also observed by other researchers and was due to chlorophyll dissolved in methanol by ultrasonic extraction which is observed as dark green colour after solvent volatilization (Feng et al. 2013; Cooney et al. 2009; Laurens et al. 2012).

### 3.3.7 Bioethanol fermentation of lipid extracted biomass

Microalgal biomass with carbohydrate content of over 50% of the dry cell weight are important for bioethanol production on a commercial scale using microalgae (Kim et al. 2014). After lipid extraction from *C.pyrenoidosa* as discussed in previous section, the defatted biomass contained 65.03 % and 79.73 % carbohydrates on dry weight in phenol treated biomass and control biomass respectively (Figure 3.22 a). In spite of the decreased total carbohydrate content in phenol cultured *C.pyrenoidosa* biomass, the carbohydrate content of 65.03 % is still high to qualify it as a bioethanol feedstock. Hu and Gao (2003) reported a similar biochemical profile for *Nannochloropsis* sp. grown under acetate added mixotrophic condition. They reported enhancement in content of lipid and protein with a decreased total carbohydrate content in mixotrophically cultured *Nannochloropsis* which supports our present findings. Thus, on account of the high carbohydrate content in *C.pyrenoidosa* biomass, the spent biomass left after lipid extraction was utilized as substrate for bioethanol fermentation using *Saccharomyces cerevisiae*. *Saccharomyces cerevisiae* can produce bioethanol up to 18 % of the fermentation broth and thus widely used for commercial bioethanol production (Kavitha et al. 2014). The hydrolysis of carbohydrates have to be performed to break down complex sugars in biomass to produce simple sugars fermentable by microorganisms (Kavitha et al. 2014; Mosier et al. 2005). Dilute acid saccharification released reducing sugars in the concentration of 142 µg/ml and 157.16 µg/ml for phenol treated and control lipid extracted biomass of *C.pyrenoidosa* (Figure 3.23 a). Bioethanol fermentation of fermentable sugars obtained by saccharification of phenol degrading biomass shows that 74.84 % sugar was consumed within 4 days (Figure 3.23 a) with production of 9.56 % bioethanol in the fermentation broth (Figure 3.23 b). However, 76.84% of fermentable sugar obtained from control culture was consumed within 4 days (Figure 3.23 a) leading to production of 16.77 % bioethanol in the fermentation broth (Figure 3.23 b).



(a)



(b)

**Figure 3.23** Bioethanol fermentation of lipid extracted biomass of *C.pyrenoidosa* :  
 a) Utilization of reducing sugar released by saccharification of lipid extracted biomass b) Production of bioethanol in the fermentation broth

### 3.3.8. Proposed methodology for an environmentally sustainable algal process for remediation of phenol pollution coupled to clean energy generation

On the basis of the experimental findings discussed in previous sections, an algal process for generation of clean energy using industrial waste phenol as a substrate was proposed which is shown in Figure 3.24.

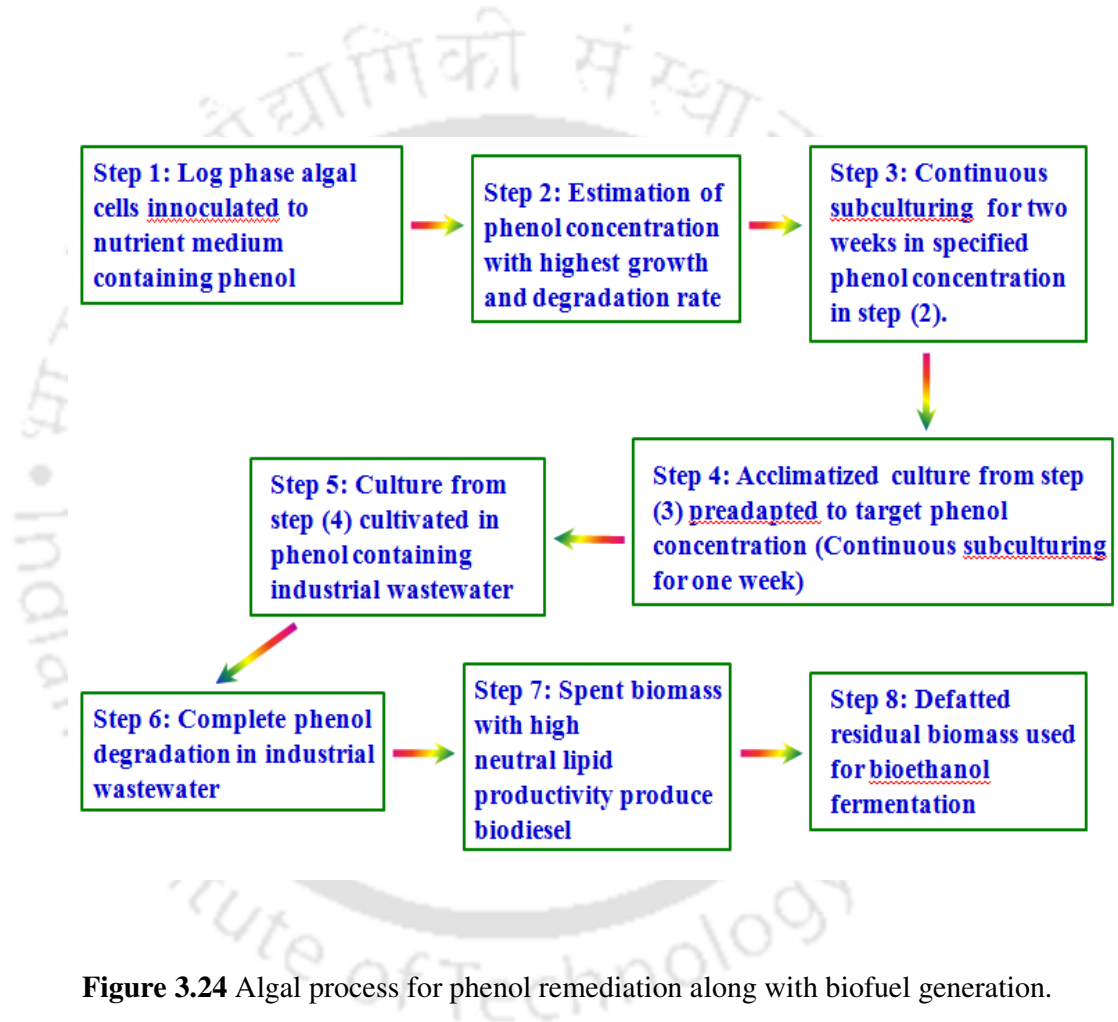


**Figure 3.24** Algal process for phenol remediation along with biofuel generation.

### 3.4 Elucidation of pathway of phenol degradation

The microbial phenol mineralization capability is completely dependent on activity of metabolic pathway involving a cascade of phenol metabolizing enzymes. The metabolic pathways involved in phenol biodegradation have been well studied in bacteria (Mahiuddin et al., 2012; Leonard and Lindley, 1998; Karigar et al., 2006) and fungi (Neujhar and Gall 1973; Krug et al. 1995; Tsai et al. 2005). The only complete pathway of algal phenol mineralization has been reported in batch cultures of achlorophyllus algae *Ochromonas danica* (Semple and Cain 1996). Recently, phenol oxidation to catechol by different green algal species as *Volvox aureus*, *Nostoc linkia*, *Oscillatoria rubescens* have been reported (Sheekh et al. 2012). Oxidation of catechol by *Chlorella vulgaris* and *Volvox aureus* have also been reported however, the product of oxidation was not determined (Sheekh et al. 2012). Similarly, enzymatic mechanism of phenol degradation have not been elucidated in diatoms (a major group of algae). To fulfill this lacuna in literature, the present section deals with elucidation of the complete pathway of phenol mineralization in *Chlorella pyrenoidosa* as well as diatom BD1IITG.

#### 3.4.1. Phenol degradation pathway in *Chlorella pyrenoidosa*

The phenol metabolic pathway was characterized by identifying the different intermediates produced during phenol degradation by using HPLC, UV-Visible spectrophotometry and LC-MS. Figure 3.25 a and b suggests appearance of catechol peak (11.9 min) with progressive decrease in phenol peak (10.69 min), which confirms catechol accumulation in media (extra cellular). The present results also accord with the observation reported by El-Sheekh et al. (2012) for different algal species as *Volvox aureus*, *Nostoc linkia*, *Oscillatoria rubescens*. It proves that phenol is degraded through an enzymatic pathway in *C.pyrenoidosa*.



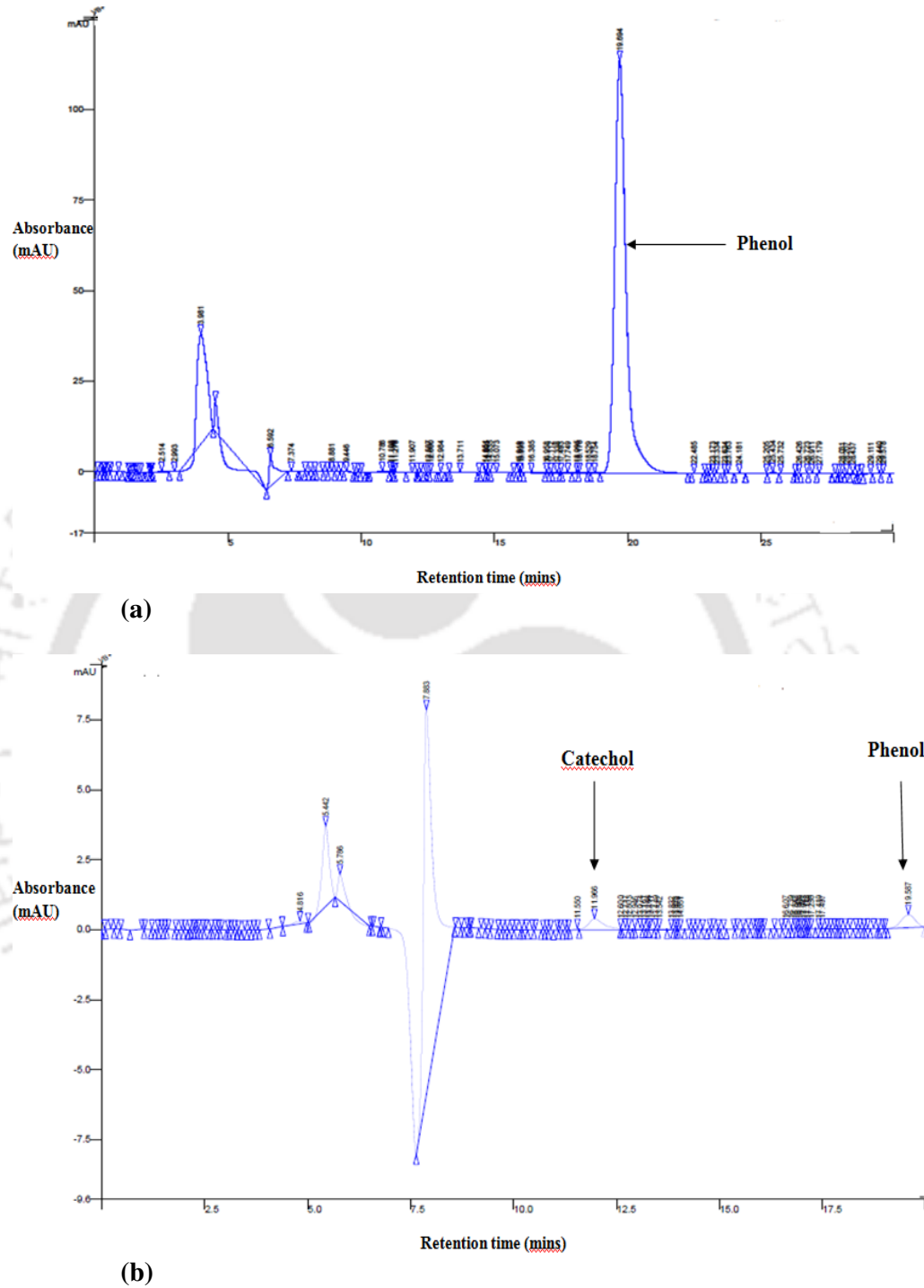
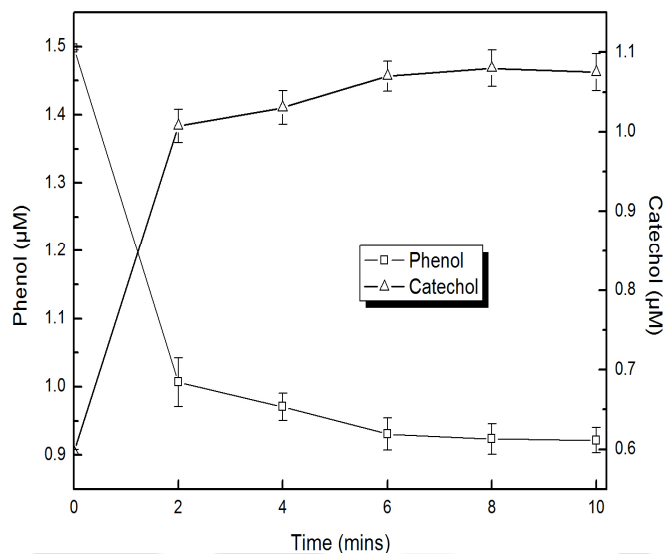


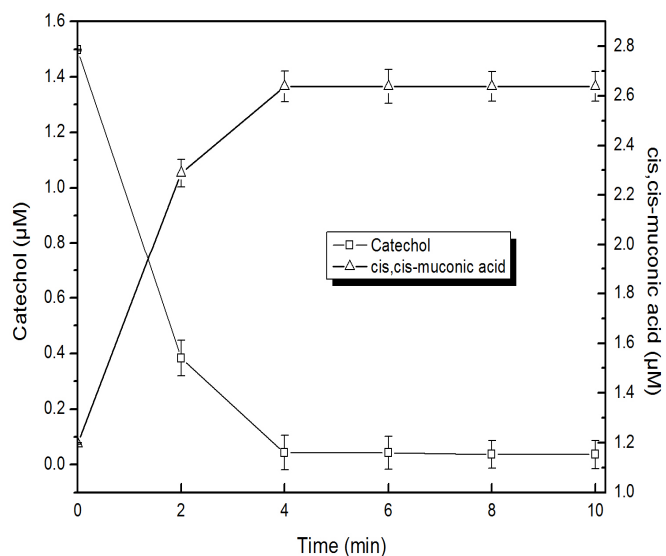
**Figure 3.25** a) HPLC chromatogram day 0 b) HPLC chromatogram at 3<sup>rd</sup> day (phenol degradation and catechol accumulation in media)

Intracellular phenol hydroxylase activity was determined by HPLC (Figure 3.26 a). Control incubations carried out by heat killed enzyme extract showed no phenol hydroxylation activity (no catechol and no phenol utilization). Similar observations have also been reported in literature for algae (Semple and Cain 1996), fungi (Neujhar and Gall 1973; Paca Jr. et al., 2007) and bacteria (Mahiuddin et al., 2012; Ali et al., 1998). Catechol can be ortho cleaved (if it follows ortho pathway) or meta cleaved (if it follows meta pathway) by catechol-1,2-dioxygenase and catechol-2,3-dioxygenase respectively. Catechol-1,2-dioxygenase activity was characterized by identifying its ortho cleavage product namely cis, cis-muconic acid using HPLC as shown in Figure 3.26 b. The reaction product was identified to be cis,cis-muconic based on identical retention time of 4.2 min with that of standard cis,cis-muconic acid. Control incubations carried out by heat killed enzyme extract showed no catechol-1,2-dioxygenase activity. Catechol-2,3-dioxygenase activity was also determined by identifying 2-hydroxymuconic semialdehyde as the meta cleavage product of catechol, using UV-Visible spectrophotometry as shown in Figure 3.26 c. Control incubations by heat killed enzyme extract showed no accumulation of meta cleavage product 2-hydroxymuconic semialdehyde indicating no catechol-2,3-dioxygenase activity. Both catechol-1,2-dioxygenase and catechol-2,3-dioxygenase activity suggests that phenol metabolism involves both ortho as well as meta pathway. The catabolic efficiency of phenol hydroxylase, catechol-1,2-dioxygenase and catechol-2,3-dioxygenase were estimated on basis of specific enzyme activities which is tabulated in Table 3.11. Comparatively higher activity of catechol-1,2-dioxygenase against that of catechol-2,3-dioxygenase suggest efficiency of ortho over meta pathway in *Chlorella pyrenoidosa*. Similar results about simultaneous activity of meta as well as ortho pathway were reported in *Pseudomonas fluorescens* PU1 (Mahiuddin et al. 2012). They reported higher meta activity over ortho activity. Cai et al. (2007) also reported similar findings of coexistence of both ortho and meta pathway in *Fusarium* species. Semple and Cain (1996) reported involvement of meta pathway in golden brown chrysophyte alga *Ochromonas danica* whereas most eukaryotes generally utilize ortho pathway (Basha et al. 2010). Evidence of ortho activity in other eukaryotes as *Trichosporon cutaneum* (Neujhar and Gall 1973), *Penicillium* sp. (Hofrichter et al. 1993), *Fusarium* sp., *Aspergillus* sp.,

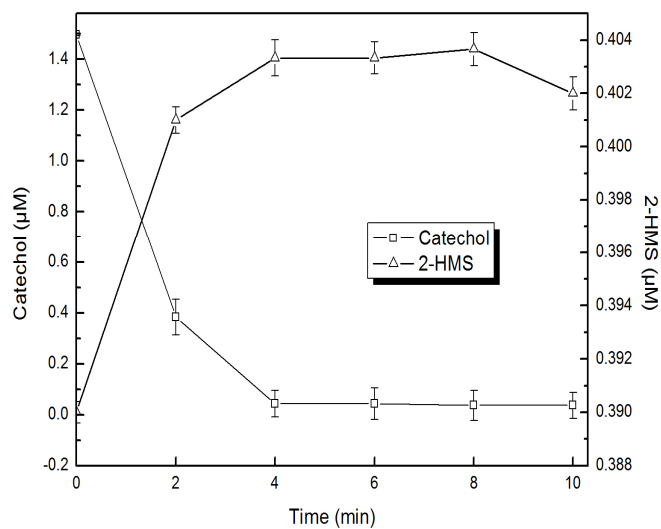
*Penicillium* sp. and *Graphium* sp. (Santos and Linardi 2004), *Candida* sp. (Tsai et al. 2005) correlates with the present finding.



(a)



(b)



(c)

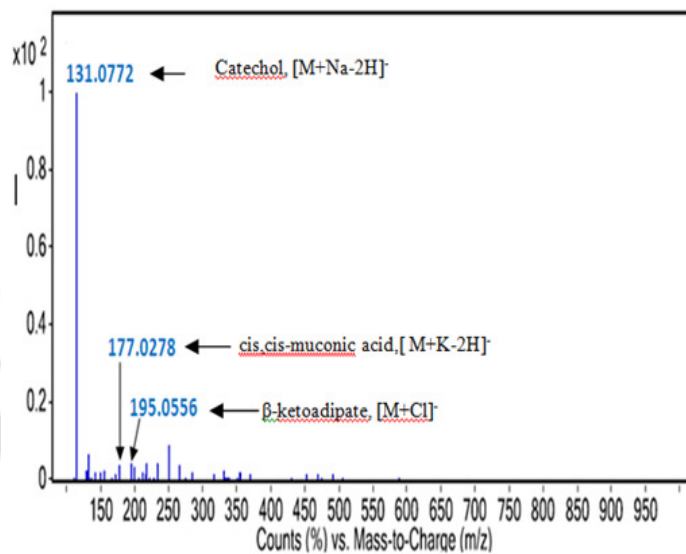
**Figure 3.26** a) Hydroxylation of phenol to catechol by phenol hydroxylase activity. b) Ortho cleavage of catechol to cis,cis-muconic acid by catechol-1,2-dioxygenase activity. c) Meta cleavage of catechol to 2-hydroxymuconic semialdehyde (2-HMS) by catechol-2,3-dioxygenase activity.

**Table 3.11** Enzyme activities in *C.pyrenoidosa* (NCIM 2738) cell lysate grown in phenol containing media.

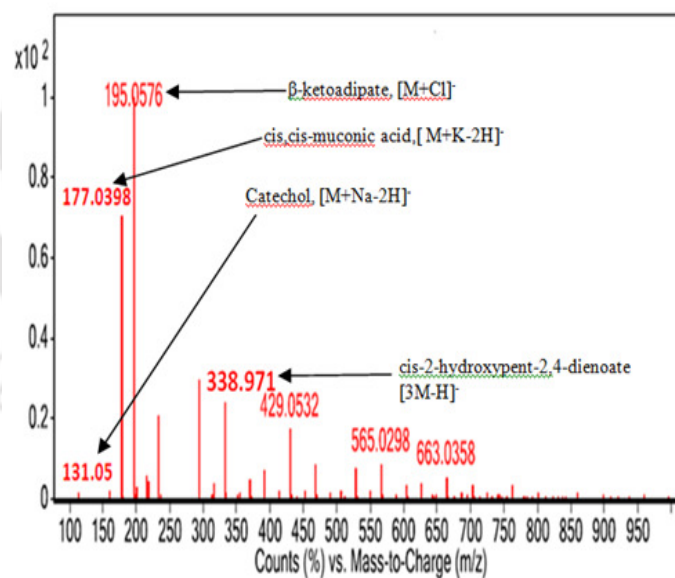
| Enzyme assayed           | Activity (U) | Specific activity (U/mg) |
|--------------------------|--------------|--------------------------|
| Phenol hydroxylase       | 833          | 11.41                    |
| Catechol-1,2-dioxygenase | 514          | 7.04                     |
| Catechol-2,3-dioxygenase | 13           | 0.18                     |

The breakdown products of cis,cis-muconic acid (ortho pathway) and 2-hydroxymuconic semialdehyde (meta pathway) were identified by LC-MS analysis. In order to identify the target metabolites, we are analyzing the catechol dioxygenase assay mixture both at the start and end of the reaction and the chromatograms are shown in Figure 3.20a and b respectively. Figure 3.27 a shows a highly abundant (abundance= 95828) m/z signal of 131. The m/z signal of 131 is consistent with the molecular ion mass of  $[M+Na-2H]^-$  adduct of catechol. Two more m/z signals of low abundance at 177 (Abundance = 2989) and 195 (Abundance = 3060) are also noted. The m/z signal at 177 corresponds the molecular ion mass of  $[M+K-2H]^-$  adduct of cis,cis-muconic acid (ortho cleavage product of catechol). Similarly, the m/z signal at 195 is consistent with the molecular ion mass of  $[M+Cl]^-$  adduct of  $\beta$ -keto adipate, a metabolite of the ortho pathway. The occurrence of adduct ions are common occurrence in LC-MS analysis. Biological samples generally have high endogeneous concentration of various salts while other salts may be added during sample preparation. This justifies the high probability of formation of adduct ions during LC-MS of biological samples ([www.sepscience.com](http://www.sepscience.com)). One probable source of potassium leading to formation of potassium ion adduct in our samples is possibly the utilization of potassium phosphate buffer during cell free extract preparation. The chloride ion adduct formed is one of the commonly formed metal adduct ion during negative ion electrospray analysis ([www.sepscience.com](http://www.sepscience.com)). Figure 3.27 b shows that the abundance of the m/z signal 131 decreases (abundance = 3236) after 20 mins incubation of the reaction mixture, which confirms utilization of catechol. The increase in abundance of m/z signal 177 (abundance= 263655) shows increase in accumulation of ortho cleavage product of catechol i.e. cis,cis-muconic acid. This indicates active ortho pathway for phenol metabolism. Similarly, the increase in abundance of m/z signal at 195 (abundance = 373154) shows increase in accumulation of ortho pathway intermediate,  $\beta$ -keto adipate. Figure 3.20 b shows an additional abundance at m/z 338 (abundance=35223) with a molecular ion mass identical to  $[3M-H]^-$  adduct of cis-2-hydroxypent-2,4-dienoate, a metabolite from the meta cleavage pathway. Identification of adduct ion of cis-2-hydroxypent-2,4-dienoate, suggests presence of meta pathway along with ortho pathway. Literature also supports present observation as Tsai et al. (2005) identified a LC-MS signal at m/z 163 corresponding to molar mass of

sodium adduct of cis,cis-muconic acid in the enzyme activity reaction mixtures, which is due to active ortho pathway in *Candida albicans* TL3.



(a)



(b)

**Figure 3.27** LC-MS analysis of catechol dioxygenase assay mixture **a)** 0 min (before incubation) **b)** 20 min (after incubation)

On the basis of the enzyme activity and metabolite analysis study, the pathway proposed for phenol degradation in *Chlorella pyrenoidosa* has been shown in Figure 3.28. In the pathway, phenol hydroxylase is involved in initial attack on phenol hydroxylating phenol to catechol. The resulting catechol is ortho cleaved by catechol-2,3-dioxygenase as well as meta cleaved by catechol-1,2-dioxygenase. Catechol-1,2-dioxygenase ortho cleaves catechol into its reaction product cis,cis-muconic acid. Determination of 3-oxoadipate, a metabolite downstream of cis,cis-muconic acid in the ortho pathway indicates breakdown of cis,cis-muconic acid. Catechol also undergoes meta cleavage into 2-HMS by catechol-2,3-dioxygenase activity. 2-hydroxymuconate semi-aldehyde hydrolase causes hydrolysis of 2-HMS to cis-2-Hydroxypenta-2,4-dienoate in the meta pathway. Thus, both ortho as well as meta pathway is involved in phenol degradation in *Chlorella pyrenoidosa*. However, ortho pathway is significantly active over meta pathway. The proposed pathway is found to possess similarities with algal (Semple and Cain 1996), fungal (Tsai et al. 2005; Cai et al. 2007; Santos and Linardi 2004) as well as bacterial (Mahiuddin et al. 2012; Ali et al. 1998) catabolic mechanisms.

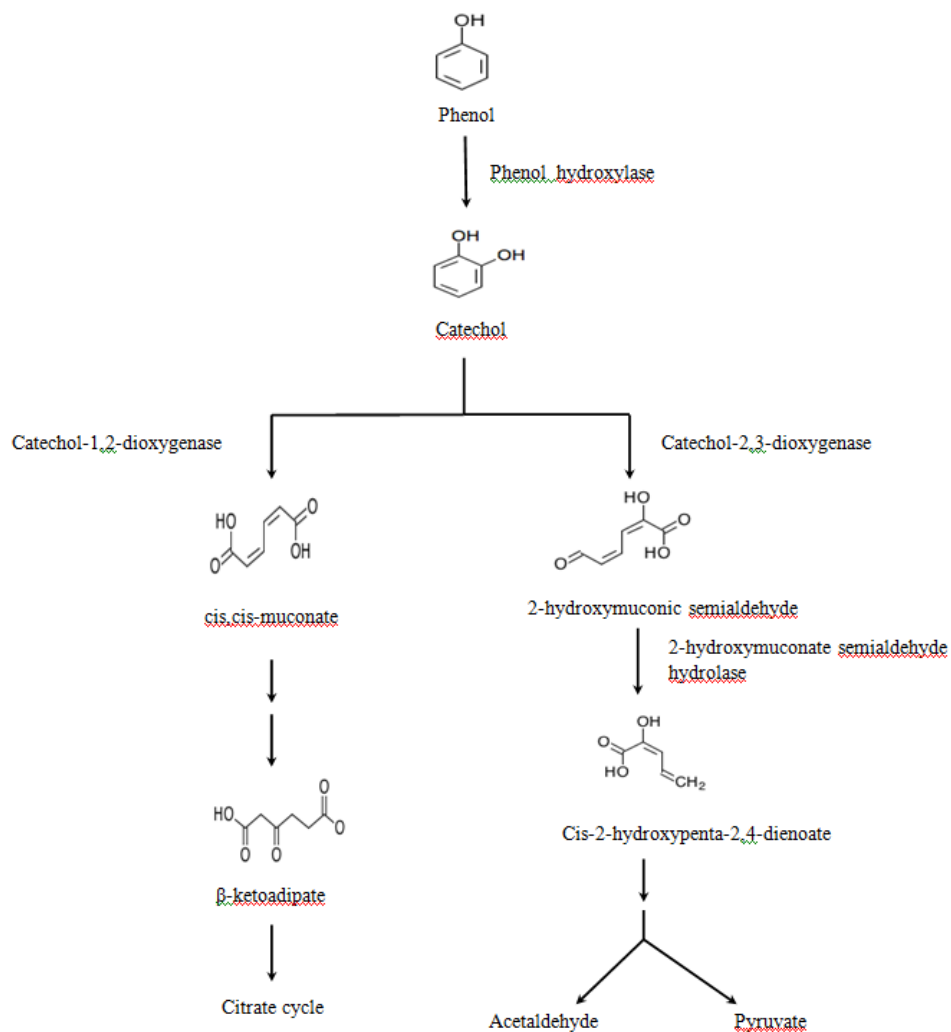
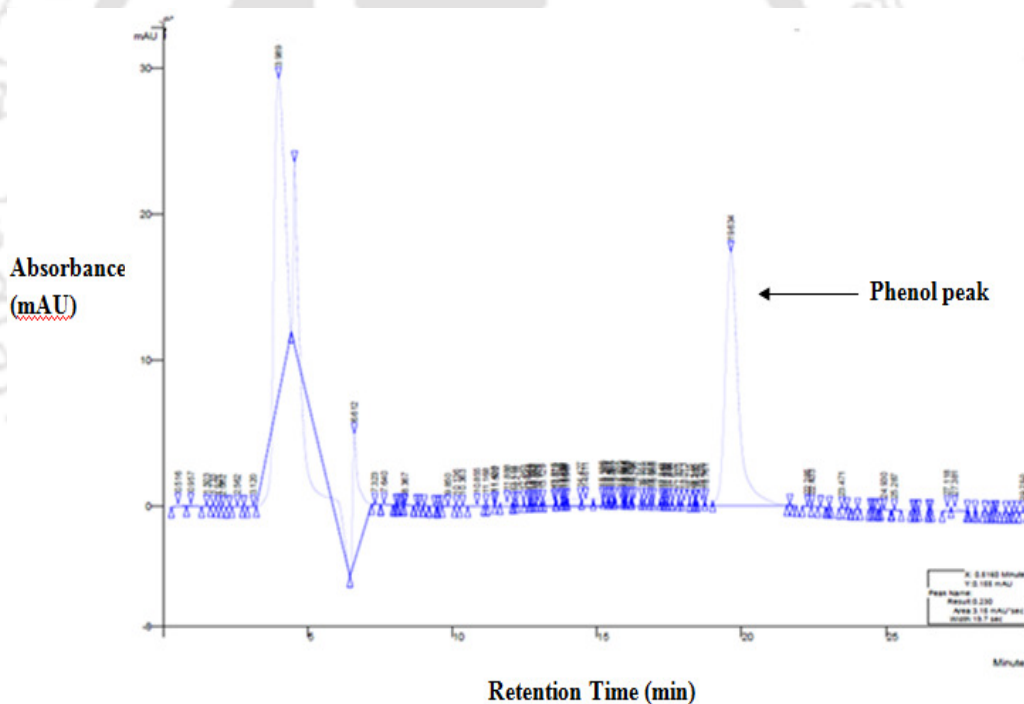


**Figure 3.28** Proposed pathway of phenol degradation in *Chlorella pyrenoidosa* (NCIM 2738).

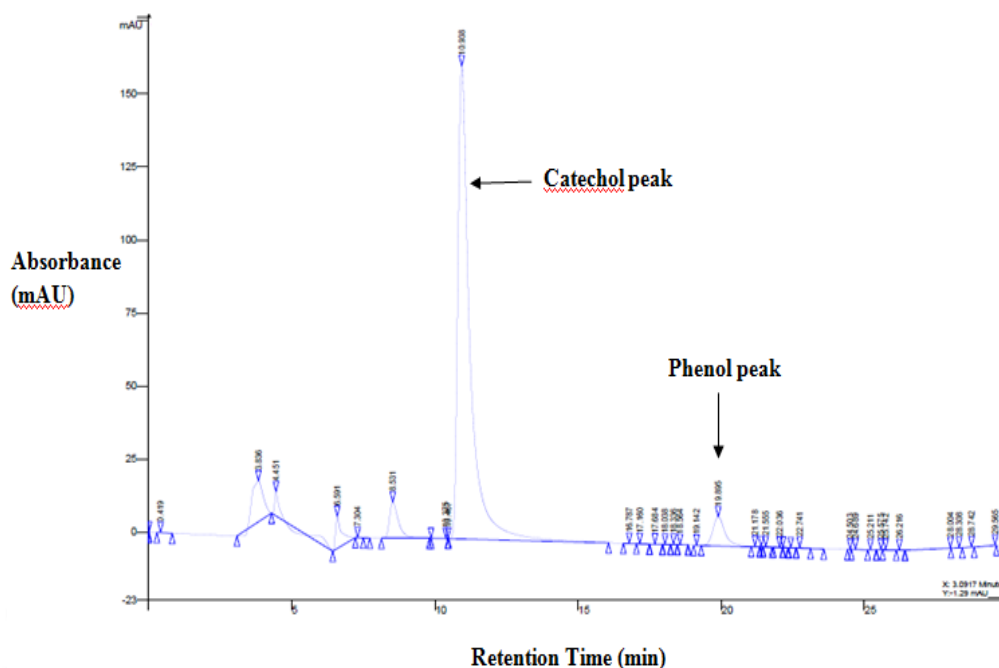


### 3.4.2 Phenol degradation pathway in diatom BD1IITG

The phenol metabolic pathway was elucidated by identifying the different intermediates produced during phenol degradation by using HPLC, UV-Visible spectrophotometry and LC-MS. Analysis of phenol degrading culture media by HPLC (Figure 3.29 a and b) confirms the accumulation of catechol (Retention time: 10.9 min), the first intermediate of phenol degradation pathway. El-Sheekh et al. (2012) reported similar observation of catechol accumulation in culture media during phenol degradation by algal species as *Volvox aureus*, *Nostoc linkia*, *Oscillatoria rubescens*. Catechol accumulation in culture media confirms that phenol is degraded through an enzymatic pathway in the diatom BD1IITG.



(a)

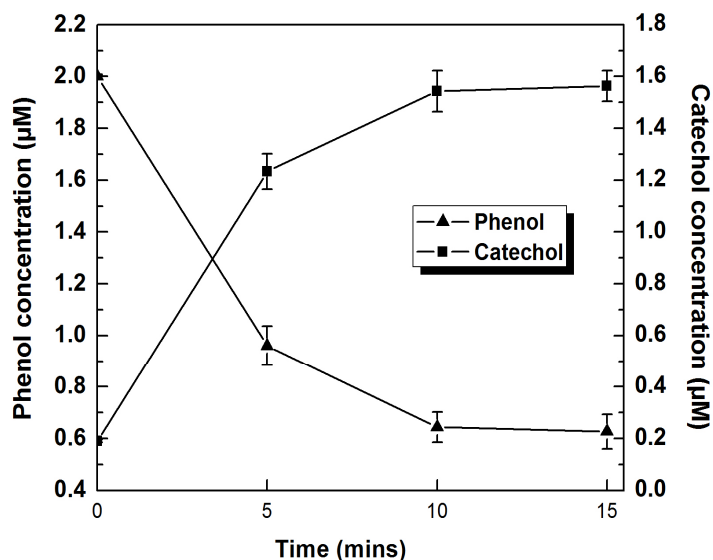


(b)

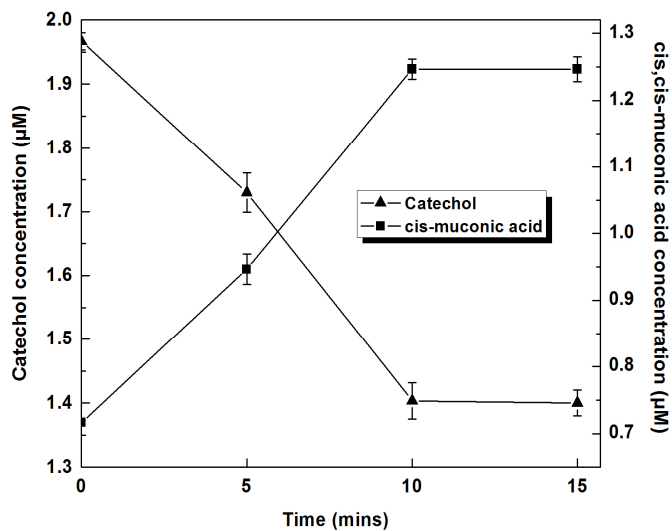
**Figure 3.29** a) HPLC chromatogram at day 0 b) HPLC chromatogram at day 4

Intercellular phenol hydroxylase activity was determined by HPLC (Figure 3.30 a). Phenol hydroxylase was found to hydroxylate phenol to its reaction product catechol. Control incubations were carried out by heat-killed enzyme extract showing no phenol hydroxylation activity (no phenol utilization and no catechol production). Similar observations have also been reported for algae (Semple et al. 1996), fungi (Neujhar and Gaal, 1973; Paca et al. 2007) and bacteria (Mahiuddin et al. 2012; Ali et al. 1998). Catechol can be ortho cleaved (if it follows ortho pathway) or meta cleaved (if it follows meta pathway) by catechol-1,2-dioxygenase and catechol-2,3-dioxygenase respectively. Catechol-1,2-dioxygenase activity was determined by identifying its ortho cleavage product namely *cis, cis*-muconic acid (retention time: 4.2 min) using HPLC (Figure 3.30 b). No catechol-1,2-dioxygenase activity was observed in control incubations carried out by heat-killed enzyme extract. Catechol-2,3-dioxygenase activity was determined by identifying 2-hydroxymuconic semialdehyde as the meta cleavage product of catechol using UV-visible spectrophotometry (Figure 3.30 c). Control incubations by heat-killed enzyme extract showed no accumulation of meta

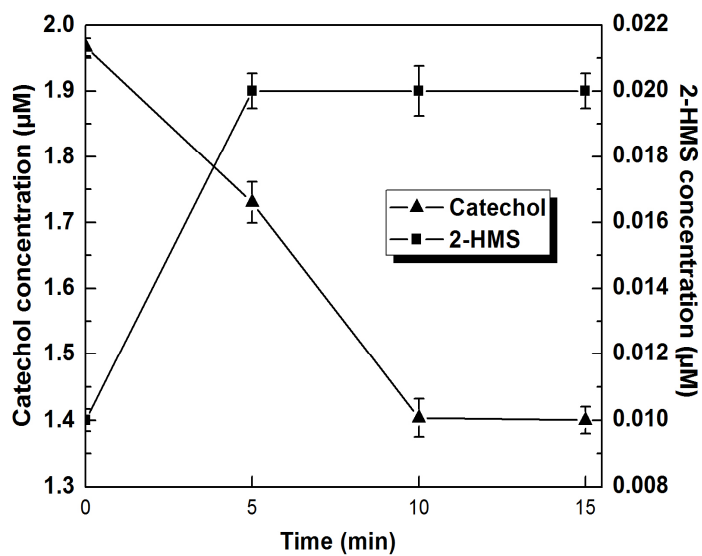
cleavage product 2-hydroxymuconic semialdehyde indicating no catechol-2,3-dioxygenase activity. Both catechol-1,2-dioxygenase and catechol-2,3-dioxygenase activity suggested that phenol degradation involves both ortho and meta pathway. The catabolic efficiency of catechol-1,2-dioxygenase and catechol-2,3-dioxygenase were determined by specific enzyme activities. Comparatively higher activity of catechol-1,2-dioxygenase (0.39 U/mg) against that of catechol-2,3-dioxygenase ( $1.36 \times 10^{-2}$  U/mg) suggest efficiency of ortho over meta pathway in diatom BD11TG. Mahiuddin et al. (2012) reported simultaneous activity of meta as well as ortho pathway in *Pseudomonas fluorescens* PU1. They reported higher meta activity over ortho activity. Cai et al.(2007) also reported similar findings of coexistence of both ortho and meta pathway in *Fusarium* species. Semple and Cain (1996) reported meta pathway activity in golden brown chrysophyte alga *Ochromonas danica* whereas most eukaryotes generally utilize ortho pathway for phenol degradation (Basha et al. 2012). Evidence of ortho activity in other eukaryotes as *Trichosporon cutaneum* (Neujhar and Gaal 1973), *Penicillium* sp.(Hofrichter et al. 1993), *Fusarium* sp., *Aspergillus* sp., *Penicillium* sp. and *Graphium* sp.(Santos and Linardi 2004), *Candida* sp. (Tsai et al. 2005) correlates with the present finding.



(a)



(b)

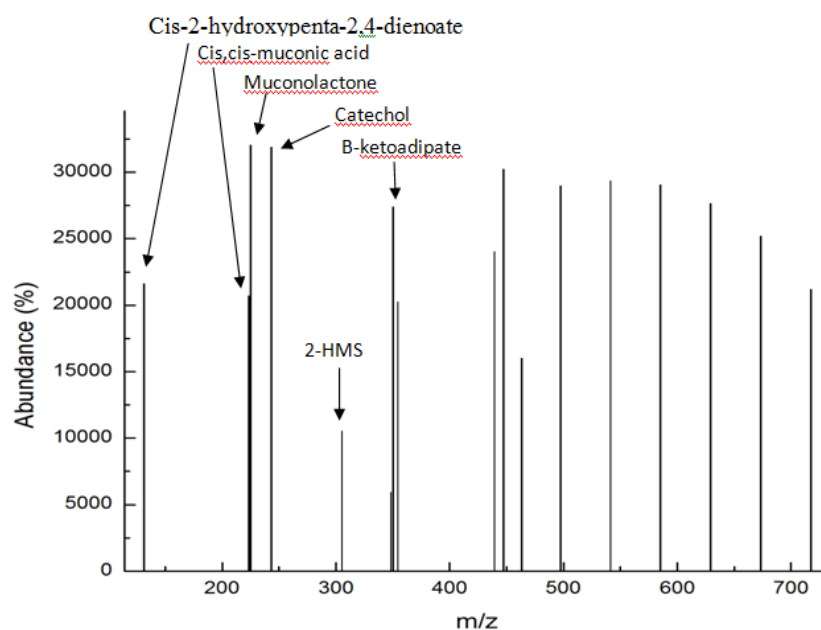


(c)

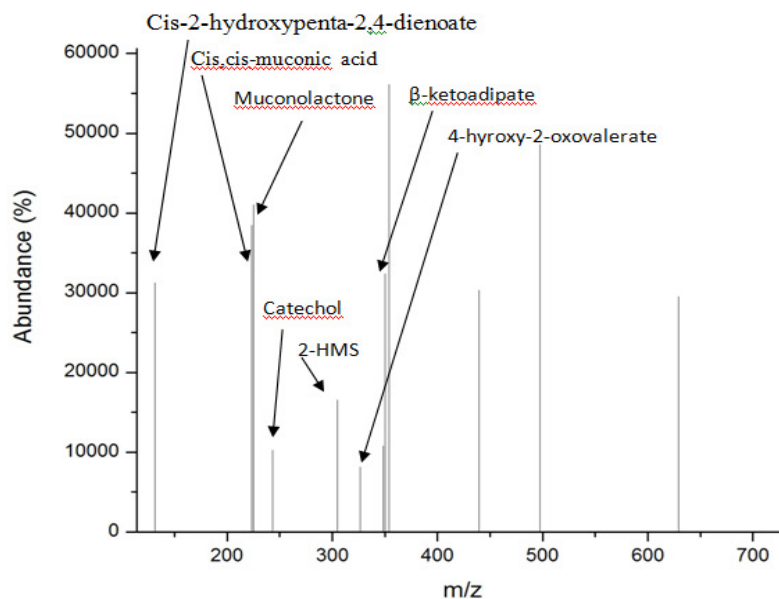
**Figure 3.30** a) Phenol hydroxylase activity assay b) Catechol-1,2-dioxygenase activity assay c) Catechol-2,3-dioxygenase activity assay

The metabolites produced by breakdown of cis,cis-muconic acid (ortho pathway) and 2-hydroxymuconic semialdehyde (meta pathway) were identified by LC-MS analysis. For metabolite identification, catechol dioxygenase assay mixture both at start and end of the reaction was analyzed and the respective chromatograms have been shown in Figure 3.31 a and b. The chromatogram at the start of the assay (Figure 3.31 a) shows a m/z signal at 243.21 high abundance (abundance=31886) consistent with the molecular ion mass of [2M+Na] adduct of catechol. Other m/z signals corresponding to molecular ion mass adducts of ortho pathway metabolites as cis,cis-muconic acid (adduct= M+2ACN+H, m/z value= 223.16, abundance=20721), muconolactone (m/z value=225.17, Adduct= M+2ACN+H, abundance=32048) and  $\beta$ -keto adipate (m/z value=348.27, Adduct= 2M+3H<sub>2</sub>O+2H, abundance=5944). Similarly, the assay mixture (Figure 3.31 a) also contained molecular ion mass adducts of meta pathway metabolites as 2-HMS (m/z value=305.19, adduct=2M+Na, abundance=10541) and cis-2-hydroxypenta-2,4-dienoate (m/z value=131.17, Adduct=M+NH<sub>4</sub>, abundance=21618). The formation of adduct ions are common occurrence in LC-MS analysis. Adduct ions as sodium adduct [M+Na], ammonium adduct [M+NH<sub>4</sub>], adducted solvent molecules as [M+H+H<sub>2</sub>O] are routinely observed in positive ion electrospray analysis. Biological samples generally have high endogenous concentration of various salts while other salts may be added during sample preparation. This justifies the high probability of adduct ion formation during LC-MS of biological samples (www.sepscience.com). After incubation period of 20 min, the LC-MS chromatogram of the assay mixture (Figure 3.31 b) the abundance of the m/z signal at 243.21 corresponding to catechol decreases confirming its utilization during the assay. The increase in abundance of m/z signals corresponding to ortho pathway metabolites as cis,cis-muconic acid (m/z value= 223.16, Abundance=38434), muconolactone (m/z value=225.17, Abundance=41054) and  $\beta$ -keto adipate (m/z value=348.27, Abundance=10794) indicates that catechol is being ortho cleaved by catechol-1,2-dioxygenase to cis,cis-muconic acid. The identification of products found downstream of cis,cis-muconic acid in the ortho pathway indicates breakdown of cis,cis-muconic acid. Cis,cis-muconic acid is lactonized by cis,cis-muconate lactonizing enzyme to muconolactone. Muconolactone isomerase catalyzes the isomerization of muconolactone to 3-oxoadipate-enol-lactone (L.N. Ornston,1966). However, m/z signal corresponding

to 3-oxoadipate-enol-lactone was not identified during LC-MS analysis (Figure 3.23 e) in the present study. Identification of  $\beta$ -keto adipate, the next metabolite in the pathway formed by hydrolysis of 3-oxoadipate-enol-lactone by  $\beta$ -keto adipate enol-lactonase gives an evidence of the existence of oxoadipate-enol-lactone in the phenol degradation pathway. The assay mixture following incubation (Figure 3.31 b) also showed increased abundance for  $m/z$  signal corresponding to meta pathway metabolites as 2-HMS ( $m/z=305.19$ , abundance=16537), cis-2-hydroxypenta-2,4-dienoate ( $m/z$  value=131.17, abundance=31213). Another  $m/z$  signal corresponding to another meta pathway metabolite 4-hydroxy-2-oxovalerate ( $m/z$  signal=326.24, adduct=2M+ACN+Na, abundance=8156) could be detected by LC-MS analysis (Figure 3.31 b). This confirms that catechol-2,3-dioxygenase activity is involved in the meta cleavage of catechol ring to 2-HMS. The identification of products downstream of 2-HMS in meta pathway confirms the metabolism of 2-HMS. 2-hydroxymuconate semialdehyde hydrolase causes hydrolysis of 2-HMS to cis-2-hydroxypenta-2,4-dienoate. 2-oxopent-4-enoate hydratase activity produces 4-hydroxy-2-oxovalerate from cis-2-hydroxypenta-2,4-dienoate.



(a)



(b)

**Figure 3.31** a) Metabolite identification by LC-MS (0 min) b) Metabolite identification by LC-MS (20 min)

On the basis of enzyme activity studies and metabolite identification, the proposed pathway for phenol degradation in the diatom BD1IITG has been shown in Figure 3.32. The proposed pathway was found to have similarities with algal (Semple and Cain 1996), fungal (Tsai et al.2005; Cai et al.2007; Santos and Linardi, 2004) as well as bacterial (Mahiuddin et al.2012; Ali et al.1998) catabolic mechanisms.

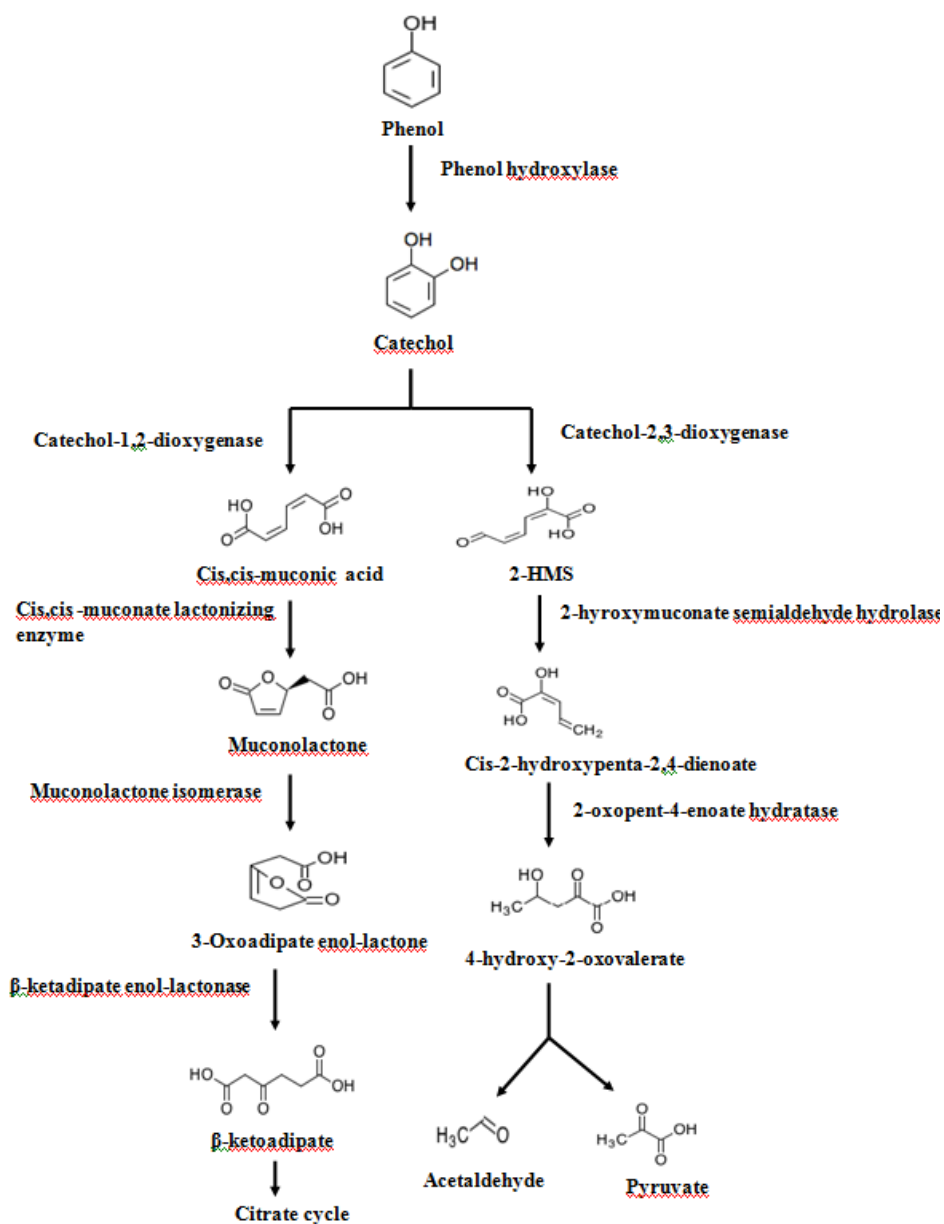


Figure 3.32 Proposed pathway for phenol degradation in diatom BD1IITG.



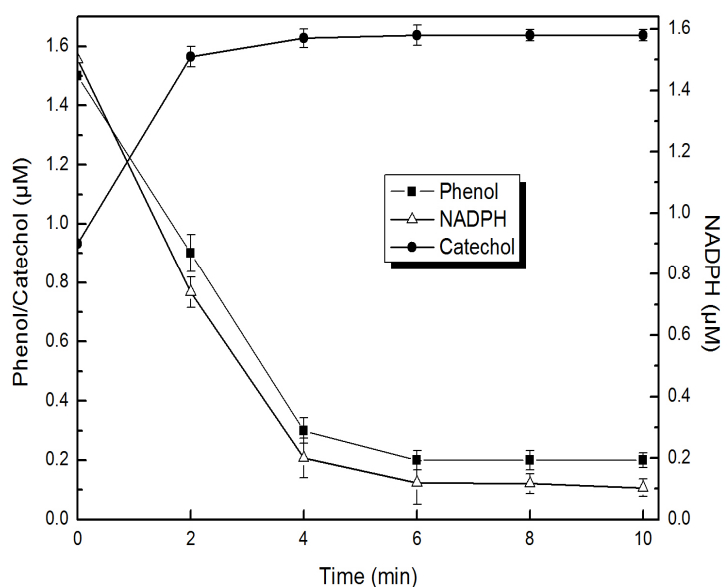
### **3.5 Purification and characterization of phenol hydroxylase from *Chlorella pyrenoidosa***

In the previous section, we have reported the complete pathway of phenol degradation in green algae *Chlorella pyrenoidosa* (NCIM 2738). The first step of the pathway is catalyzed by phenol hydroxylase which causes the initial attack on phenol hydroxylating it to catechol. As an alternative to use microbes for bioremediation, the use of purified enzymes for phenol remediation has generated wide interest recently. Since phenol hydroxylase is the first enzyme causing initial attack on phenol in the phenol degradation pathway, the knowledge of its kinetic properties is invaluable for its potential applications (Pessione et al. 1999). None of the previous studies had characterized the kinetic properties of any microalgal phenol hydroxylase. Thus, to fulfill this lacuna the present section deals with purification and characterization of microalgal phenol hydroxylase from *C.pyrenoidosa*. The study gains importance as the information could be instrumental in developing enzyme based phenol remediation technology in future.

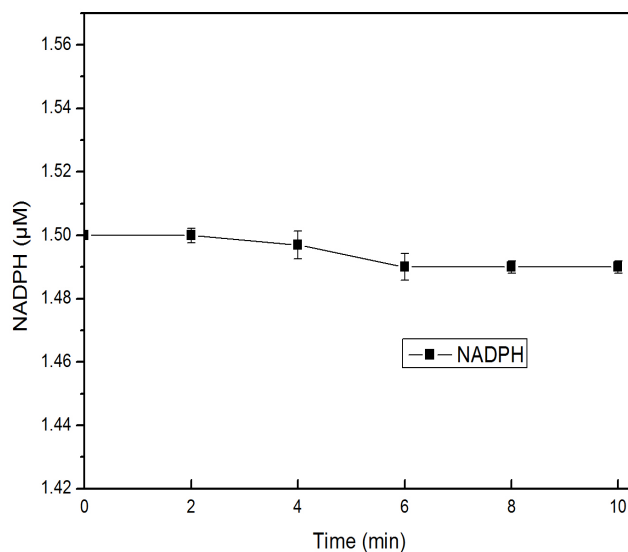
#### **3.5.1 Induction and extraction of crude enzyme extract with phenol hydroxylation activity**

The *C.pyrenoidosa* cells were cultured in 125 mg/l phenol as at this particular concentration the specific growth and phenol degradation rate of *C.pyrenoidosa* was reported to be highest in previous chapter. The crude enzyme extract showed characteristic properties of phenol hydroxylase activity which is shown in Figure 3.33 a. Figure 3.33 a shows that a steep hydroxylation of 1.2  $\mu\text{M}$  phenol to its reaction product catechol by 4 min. After this the phenol hydroxylation slows down considerably with utilization of another 0.1  $\mu\text{M}$  phenol till six minutes. Concomitant accumulation of 0.77  $\mu\text{M}$  of the reaction product catechol till six minutes was observed in Figure 3.33 a. The decreased accumulation of catechol can be contributed to the fact that catechol was cleaved further by the enzymes as catechol-1,2-dioxygenase (ortho cleavage) and catechol-2,3-dioxygenase (meta cleavage) present in the crude enzyme extract. Figure 3.33 a also shows decreased absorbance at 340 nm due to NADPH oxidation concomitantly with phenol hydroxylation suggesting substrate dependent oxidation

of NADPH. Except for crude extract a minimal endogenous oxidation of NADPH of 0.67% was detected (Figure 3.33 b). Control incubation using heat killed enzyme extract showed no characteristic phenol hydroxylation activity. Crude enzyme extract obtained from *C.pyrenoidosa* grown on phenol free media showed no phenol hydroxylation activity indicating inducible nature of phenol hydroxylase in response to phenol. Similar results of NADPH dependent hydroxylation of phenol to catechol by phenol hydroxylases have been reported in a variety of microbes as *Pseudomonas* sp. (Kukor and Olsen 1992; Powlowski and Shingler 1994; Dagley and Gibson 1965; Nordlund et al. 1993), *Acinetobacter radioresistens* (Pessione et al. 1999), *Ralstonia eutropha* (Yabuuchi et al. 1995), *T. cutaneum* (Neujahr & Gaal 1973), *Candida tropicalis* (Paca et al. 2007).



(a)



(b)

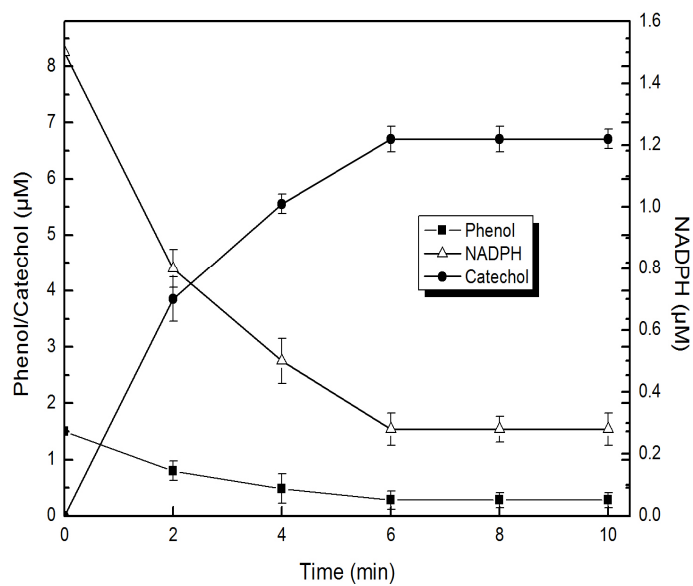
**Figure 3.33 a)** Phenol hydroxylase activity of crude extract **b)** Autooxidation of NADPH

### 3.5.2. Purification of phenol hydroxylase

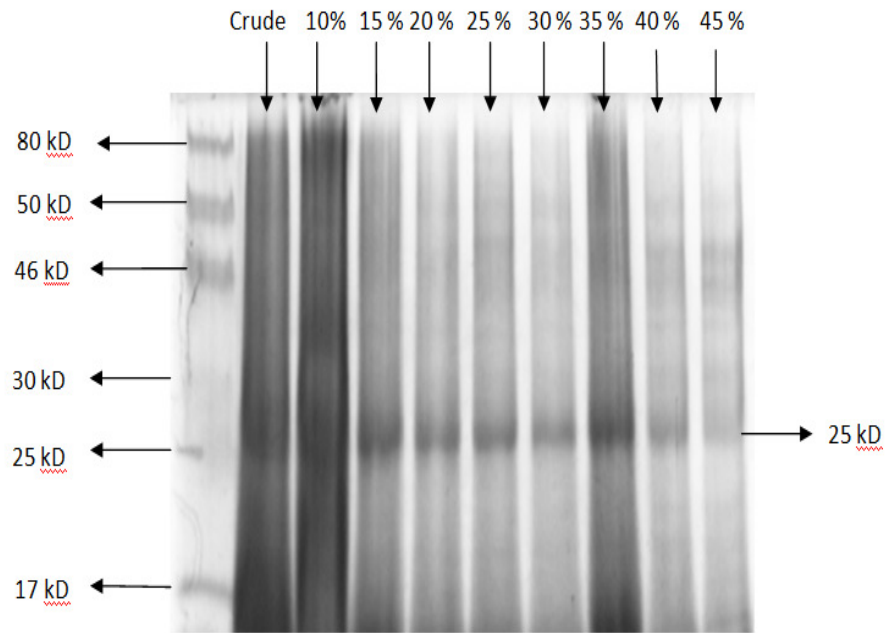
To characterize the phenol hydroxylase it was further purified by ammonium sulphate fractionation. The phenol hydroxylase was purified from crude enzyme extract by ammonium sulphate fractionation. Table 3.12 shows that the ammonium sulphate fractions in the range of 15-40% showed phenol hydroxylase activity with the highest specific activity of 0.39  $\mu\text{mol}/\text{min}/\text{mg}$  obtained at 25% ammonium sulphate fraction. Figure 3.34 a indicates that the 25% ammonium sulphate fraction also showed the characteristic properties of phenol hydroxylase as hydroxylation of phenol to catechol with concomitant oxidation of NADPH during the assay. As judged by SDS-PAGE, the purified enzyme is homogenous and thus shows one single protein band with a molecular mass of 25 kD (Figure 3.34 b and c). The specific activity of 0.39  $\mu\text{mol}/\text{min}/\text{mg}$  of purified enzyme was comparatively higher to that of 0.13  $\mu\text{mol}/\text{min}/\text{mg}$  in crude enzyme extract.

**Table 3.12** Specific activity of active ammonium sulphate fractions

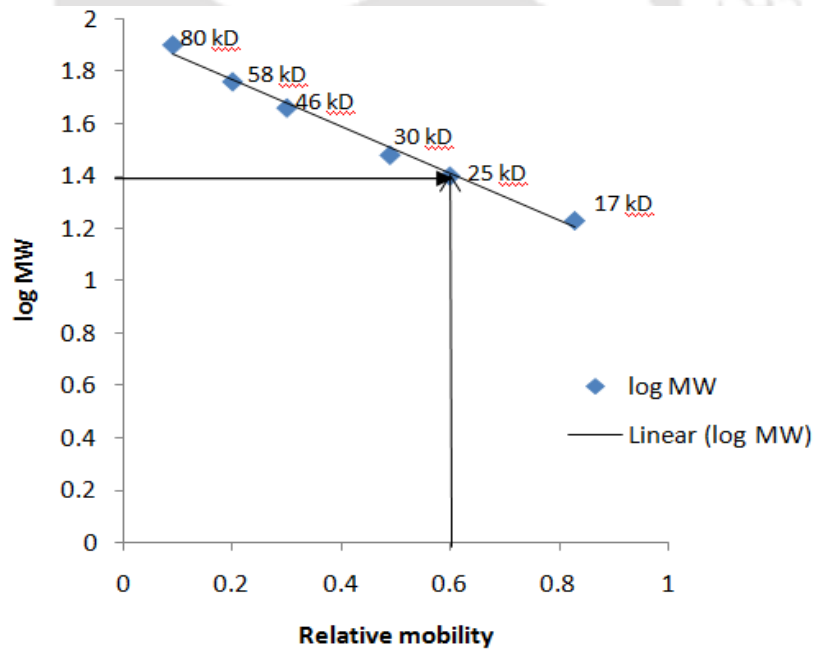
| Purification Step                 | Specific activity<br>( $\mu\text{mol}/\text{min}/\text{mg}$ ) |
|-----------------------------------|---|
| Crude enzyme extract              | 0.13  |
| 15% Ammonium sulphate precipitate | 0.24  |
| 20% Ammonium sulphate precipitate | 0.34  |
| 25% Ammonium sulphate precipitate | 0.39  |
| 30% Ammonium sulphate precipitate | 0.36  |
| 35% Ammonium sulphate precipitate | 0.26  |
| 40% Ammonium sulphate precipitate | 0.14  |



(a)



(b)



(c)

**Figure 3.34** a) Phenol hydroxylase activity of 25% Ammonium Sulphate fraction. b) Silver stained SDS PAGE image of ammonium sulphate fractions (10-45%). c) Molecular weight determination of purified enzyme by log molecular weight (log MW) versus relative mobility plot.

### 3.5.3. Peptide mass fingerprinting of the purified enzyme

Peptide mass fingerprinting of the 25 kDa protein band in SDS- PAGE gel corresponding to the purified enzyme was carried out to identify the enzyme on basis of their constituent peptide masses. MALDI-TOF analysis of the 25 kDa band (Figure 3.35) revealed a protein hit ChINC64A\_1 49348 with protein sequence coverage of 39 % in the *Chlorella* sp. NC64A genome. The protein hit ChINC64A\_1 49348 is a flavoprotein hydroxylase involved in hydroxylation of aromatic rings (Table 3.13). The results correspond well with the phenol hydroxylation ability and flavoprotein nature of the purified protein.

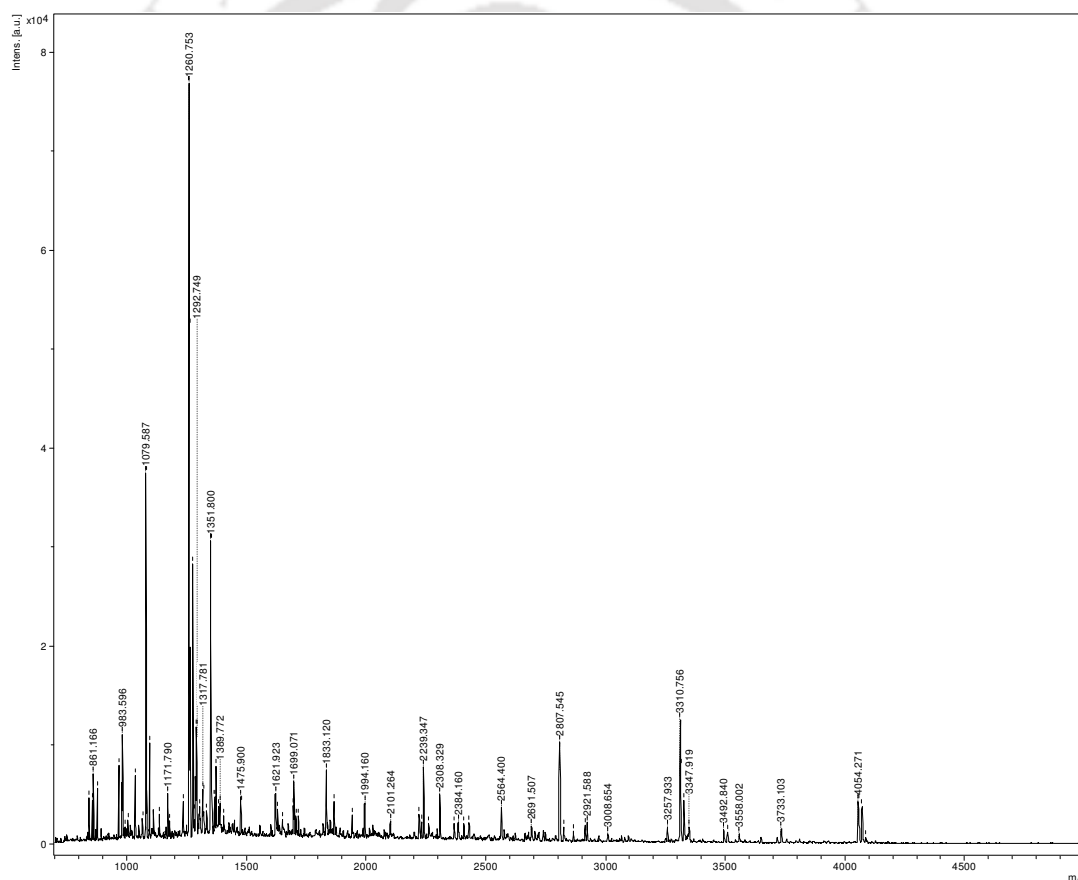


**Figure 3.35** Peptide fragment spectra of Phenol hydroxylase obtained by MALDI TOF.

**Table 3.13** MASCOT search based identification of purified 25 kD protein band using peptide fragment spectra obtained by MALDI TOF.

| Protein Sequence ID hit | Score | E Value   | % Identity | % Coverage | Organism                      | Description  |
|-------------------------|-------|-----------|------------|------------|-------------------------------|--|
| ChINC64A_1<br>49348     | 460   | 1.41E-032 | 46.5       | 39.0       | <i>Chlorella</i> sp.<br>NC64A | Flavoprotein hydroxylase involved in aromatic ring hydroxylation, carries out oxidation reduction reaction |

### 3.5.4 Spectral properties of the purified enzyme

Flavoproteins are known to have a quite distinct UV-Visible spectra (Champman and Reid 1999). The purified enzyme shows characteristic spectral properties of flavoproteins with maxima around 271 nm, 345 nm (Fe-S clusters), 450 nm (flavins) and shoulder between 465-470 nm (Fe-S clusters) (Figure 3.36). This confirms the flavoprotein nature of the protein predicted by protein hit obtained by MASCOT search of the peptide fragment spectra of the purified protein (Table 3.13). The spectra in Figure 3.36 also denotes the presence of Fe-S clusters known for their role in oxidation reduction reactions. The presence of flavin and Fe-S cluster of the type [2Fe-2S] is important for functioning of aromatic hydroxylases. The Fe-S cluster may be present as a separate ferredoxin or as part of an iron sulfur flavoprotein that interacts with NAD (P) directly (Cammack 1992). The spectral characteristics of the purified enzyme is supported by similar spectral properties of phenol hydroxylase from *Candida tropicalis* (Paca et al. 2007), *Trichosporon cutaneum* (Neujhar and Gall 1973) and *Acinetobacter radioresistens* (Pessione et al. 1999).

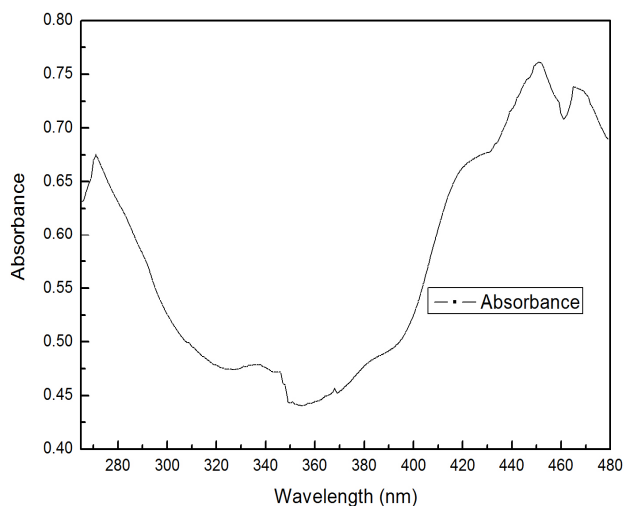


**Figure 3.36** UV-Visible spectrum of purified phenol hydroxylase

### 3.5.5 Effect of NADH as cofactor on phenol hydroxylation activity

Phenol hydroxylases use electrons from cofactor nicotine adenine dinucleotide to activate and cleave a molecule of oxygen through the formation of an intermediate flavin hydroperoxide and enable the incorporation of an oxygen atom into the substrate (Saa et al. 2010). Since phenol hydroxylase shows specific ability to use NADH or NADPH or both as cofactors (Nakagawa et al. 1962; Neujhar and Gaal 1973; Paca et al. 2007) the possibility of utilizing NADH as a cheap alternate was verified. Figure 3.37 shows phenol is being hydroxylated to catechol with concomitant oxidation of NADH. The specific activity of phenol hydroxylase reaction with NADPH as cofactor (0.39  $\mu\text{moles}/\text{min}/\text{mg}$ ) was higher compared to specific activity of 0.14  $\mu\text{moles}/\text{min}/\text{mg}$  with NADH as cofactor suggesting NADPH as better cofactor. The specificity for NADPH or NADH as cofactor has been found to be species specific. Nakagawa et al. (1962) reported reduced activity of phenol hydroxylase obtained from *Brevibacterium fuscum* phenol hydroxylation activity when using NADH as cofactor compared to that with NADPH which accords with our findings. On the other hand, phenol hydroxylase from *Candida tropicalis* (Paca et al. 2007) and *Trichosporon cutaneum* (Neujhar and Gall 1973) was found to be strictly dependent on NADPH for activity. The ability of the purified enzyme to use NADH as a cheap cofactor



could add to application of the enzyme for phenol remediation or biosensor. However, decreased phenol hydroxylation efficiency in NADH is a matter of concern.

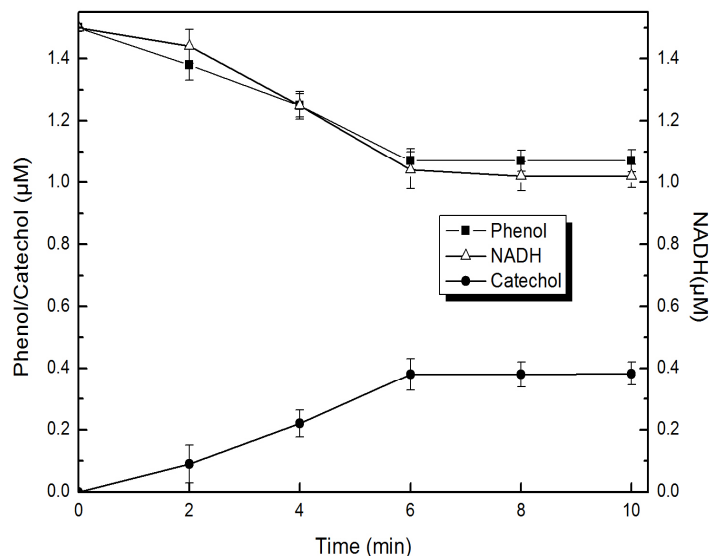


**Figure 3.37** Phenol hydroxylase assay using NADH as cofactor.

### 3.5.6. Stoichiometry of the reaction with phenol

The stoichiometry of reaction of phenol hydroxylase is being shown in Table 3.14. A fairly close equivalence can be seen between the concentration of phenol utilized and its hydroxylation product catechol. The oxidation of NADPH increased with the increasing ratio of NADPH: phenol in the assay mixture. From Table 3.14., it can be concluded that with appropriate concentrations of NADPH (1.5 μM), phenol (1.5 μM) and the enzyme (500 μg) the phenol hydroxylase reaction proceeds with the following stoichiometry:



**Table 3.14.** Stoichiometry of phenol hydroxylase reaction

| Initial concentration phenol/NADPH  | Ratio (NADPH/Phenol) | NADPH ( $\mu\text{M}$ ) | Phenol Utilized ( $\mu\text{M}$ ) | Ratio utilized (NADPH/Phenol) | Catechol produced ( $\mu\text{M}$ ) |
|---|----------------------|-------------------------|-----------------------------------|-------------------------------|-------------------------------------|
| 0.5 $\mu\text{M}$ Phenol/0.5 $\mu\text{M}$ NADPH                              | 1.0                  | 0.25                    | 0.3                               | 0.83                          | 0.30                                |
| 0.5 $\mu\text{M}$ Phenol/ 0.25 $\mu\text{M}$ NADPH                            | 0.5                  | 0.19                    | 0.27                              | 0.70                          | 0.27                                |
| 0.25 $\mu\text{M}$ Phenol/0.5 $\mu\text{M}$ NADPH                             | 2.0                  | 0.29                    | 0.17                              | 1.71                          | 0.16                                |
| 1 $\mu\text{M}$ Phenol/1 $\mu\text{M}$ NADPH                                  | 1.0                  | 0.80                    | 0.70                              | 1.14                          | 0.70                                |
| 1 $\mu\text{M}$ Phenol/0.5 NADPH  | 0.5                  | 0.45                    | 0.69                              | 0.65                          | 0.67                                |
| 0.5 $\mu\text{M}$ Phenol/1 $\mu\text{M}$ NADPH                                | 2.0                  | 0.71                    | 0.43                              | 1.65                          | 0.42                                |
| <b>1.5 <math>\mu\text{M}</math> Phenol/1.5 <math>\mu\text{M}</math> NADPH</b> | <b>1.0</b>           | <b>1.20</b>             | <b>1.20</b>                       | <b>1.0</b>                    | <b>1.20</b>                         |
| 1.5 $\mu\text{M}$ Phenol/0.75 $\mu\text{M}$ NADPH                             | 0.5                  | 0.65                    | 1.10                              | 0.59                          | 0.09                                |
| 0.75 $\mu\text{M}$ Phenol/1.5 $\mu\text{M}$ NADPH                             | 2.0                  | 1.11                    | 0.64                              | 1.77                          | 0.64                                |

Continued

Continued

| Initial concentration phenol/NADPH                | Ratio (NADPH/Phenol) | NADPH ( $\mu\text{M}$ ) | Phenol Utilized ( $\mu\text{M}$ ) | Ratio utilized (NADPH/Phenol) | Catechol produced ( $\mu\text{M}$ ) |
|---|----------------------|-------------------------|-----------------------------------|-------------------------------|-------------------------------------|
| 2 $\mu\text{M}$ Phenol/2 $\mu\text{M}$ NADPH      | 1.0                  | 1.5                     | 1.45                              | 1.03                          | 1.14                                |
| 2 $\mu\text{M}$ Phenol/1 $\mu\text{M}$ NADPH      | 0.5                  | 0.89                    | 1.18                              | 0.75                          | 1.40                                |
| 1 $\mu\text{M}$ Phenol/2 $\mu\text{M}$ NADPH      | 2.0                  | 1.23                    | 0.86                              | 1.43                          | 0.83                                |
| 2.5 $\mu\text{M}$ Phenol/2.5 $\mu\text{M}$ NADPH  | 1.0                  | 1.80                    | 1.63                              | 1.10                          | 1.42                                |
| 2.5 $\mu\text{M}$ Phenol/1.25 $\mu\text{M}$ NADPH | 0.5                  | 0.90                    | 1.53                              | 0.60                          | 1.50                                |
| 1.25 $\mu\text{M}$ Phenol/2.5 $\mu\text{M}$ NADPH | 2.0                  | 1.50                    | 0.94                              | 1.60                          | 0.91                                |
| 3 $\mu\text{M}$ Phenol/ 3 $\mu\text{M}$ NADPH     | 1.0                  | 2.30                    | 1.90                              | 1.21                          | 1.83                                |
| 3 $\mu\text{M}$ Phenol/1.5 $\mu\text{M}$ NADPH    | 0.50                 | 1.18                    | 1.86                              | 0.63                          | 1.82                                |
| 1.5 $\mu\text{M}$ Phenol/3 $\mu\text{M}$ NADPH    | 2.0                  | 1.93                    | 1.13                              | 1.70                          | 1.09                                |

Thus the stoichiometric study helped us determine ratio of the substrate (phenol) and co-substrate (NADPH) at which there will be optimal conversion of all the substrate (phenol) to its reaction product catechol. The enzyme shows monooxygenase behavior since it transfers one oxygen atom to the substrate phenol resulting in production of catechol while the other oxygen atom reduced to water. Similar monooxygenase activity have been reported in phenol hydroxylase of *Trichosporon cutaneum* (Neujhar and Gall 1973), *Acinetobacter radioresistens* (Pessione et al. 1999), *Candida tropicalis* (Paca et al. 2007), *Alcaligenes faecialis* (Zhu et al. 2008), *Trametes versicolor* (Yemendzhiev et al. 2008), *Pseudomonas* sp. (Dong et al. 2008).

### 3.5.7. Substrate affinity of purified enzyme towards phenol

The phenol utilization by the purified enzyme follows Michealis- Menten kinetics (Figure 3.38). The apparent Michealis constant ( $K_m$ ) for oxidation of phenol was estimated to be 1.71  $\mu\text{M}$  and the maximal velocity ( $V_{max}$ ) to be 0.4  $\mu\text{M}/\text{min}$ . The affinity of the purified enzyme for phenol was higher than phenol hydroxylase from *Candida tropicalis* ( $K_m = 450 \mu\text{M}$ ) (Paca Jr. et al. 2007) and *Trichosporon cutaneum* ( $K_m = 18 \mu\text{M}$ ) (Neujhar and Gall 1973).

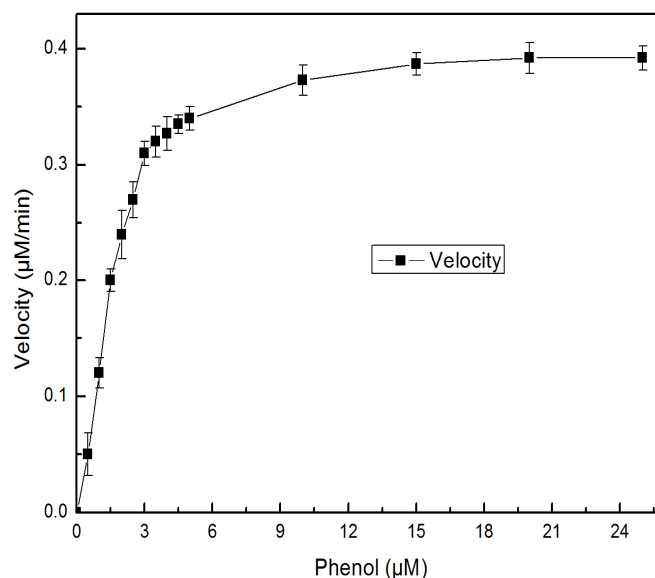


**Figure 3.38** Substrate affinity of purified phenol hydroxylase towards phenol

### 3.5.8 Effect of pH and temperature on phenol hydroxylase activity

Figure 3.39 and Figure 3.40 shows the dependence of phenol hydroxylation on pH and temperature respectively. The optimal pH and temperature for enzyme activity was found to be pH 7 and 35°C respectively. The optimal pH for enzyme activity found in neutral range is comparable to optimal pH range obtained in previous studies as *Brevibacterium fuscum* (pH 7.5), *Comamonas testosteroni* (pH 7.6), *Trichosporon cutaneum* (pH 7.6), *Acinetobacter radioresistens* (pH 7.5), *Candida tropicalis* (pH 7.4-7.6) (Nakagawa et al. 1962; Turek et al. 2011; Neujhar and Gaal 1973; Divari et al. 2003; Paca Jr. et al. 2007).

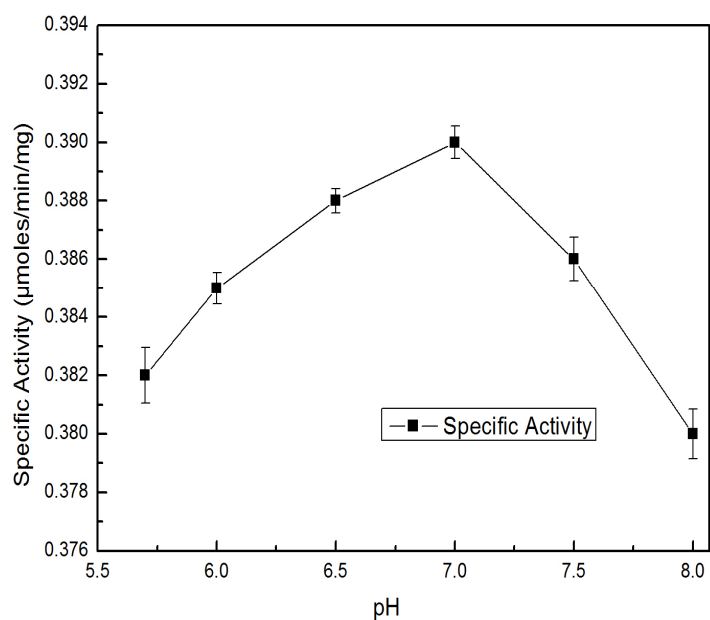


**Figure 3.39** Effect of pH on phenol hydroxylase activity

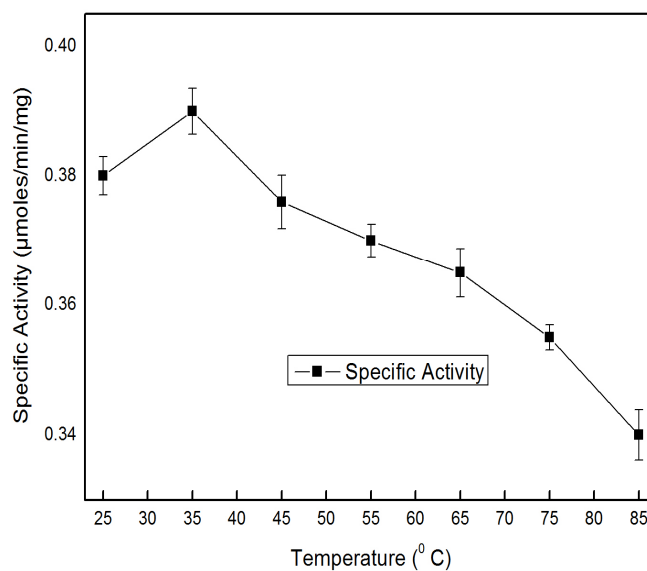
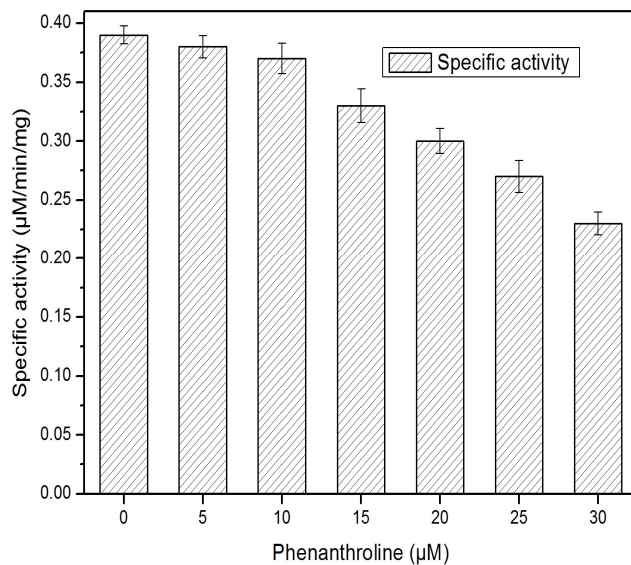


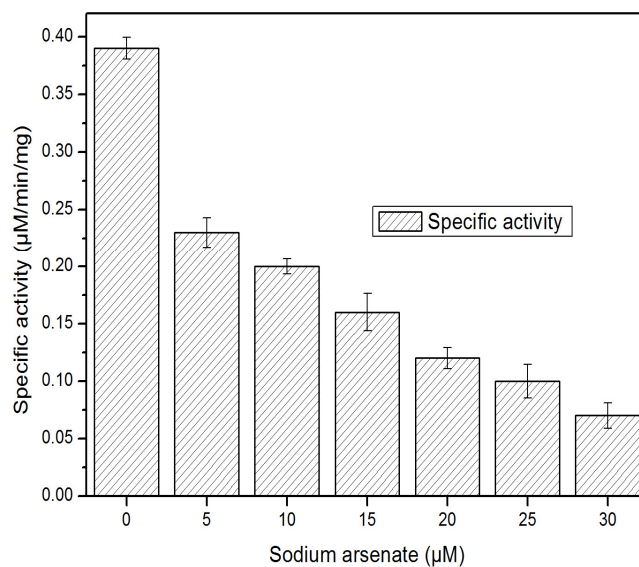
**Figure 3.40** Effect of temperature on phenol hydroxylase activity.

### 3.5.9 Effect of chelators on phenol hydroxylation activity

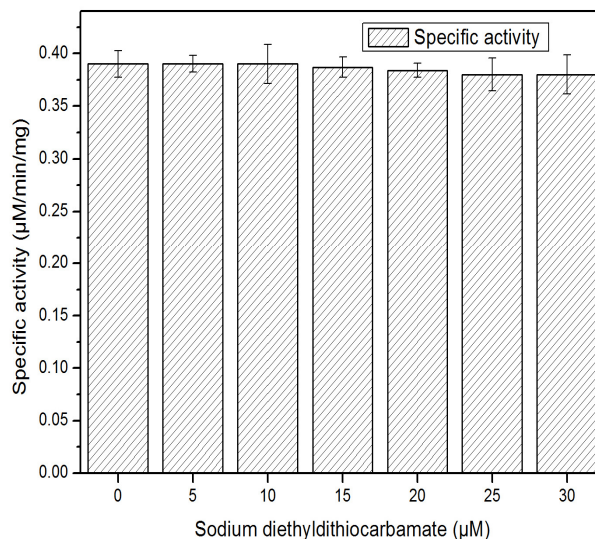
To verify the presence of iron or copper in the purified enzyme, the inhibition of enzyme activity was studied using iron and copper chelators. Phenanthroline and sodium arsenate (chelator  $\text{Fe}^{2+}$ ) shows an increased inhibition of phenol hydroxylation with increase in concentration of both chelators. 30  $\mu\text{M}$  phenanthroline and sodium arsenate depresses the phenol hydroxylation reaction by 42.31% and 84.62% respectively (Fig 3.41 a and b). Sodiumdiethyldithiocarbamate (Cu chelator) has no inhibitory effect on phenol hydroxylation activity (Figure 3.41 c). From these results, it becomes evident that the purified enzyme contains iron and lacks copper. The presence of iron is an important characteristic of phenol hydroxylases. Pessione et al. (1999) studied phenol hydroxylase in *Acinetobacter radioresistens* whose findings support our current results. They reported that phenol hydroxylase contains iron in the Fe-S clusters which support our findings of presence of iron in the purified enzyme.



(a)



(b)



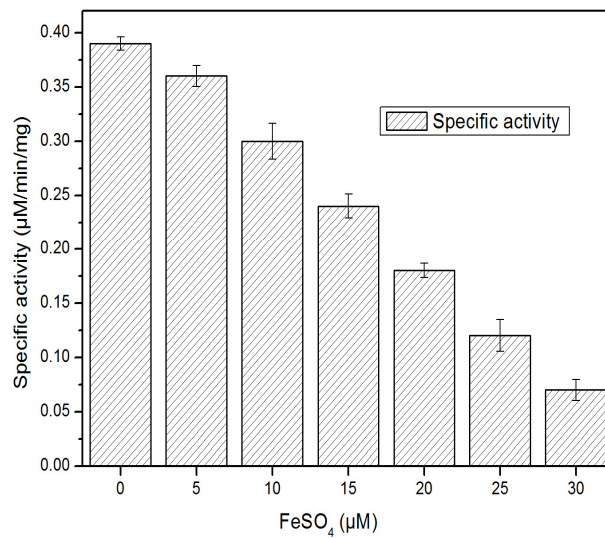
(c)

**Figure 3.41** Effect of chelators on phenol hydroxylase activity: **a)** phenanthroline (chelator of  $\text{Fe}^{2+}$ ) **b)** Sodium arsenate (chelator of  $\text{Fe}^{2+}$ ) **c)** Sodium diethyldithiocarbamate (Cu chealator)

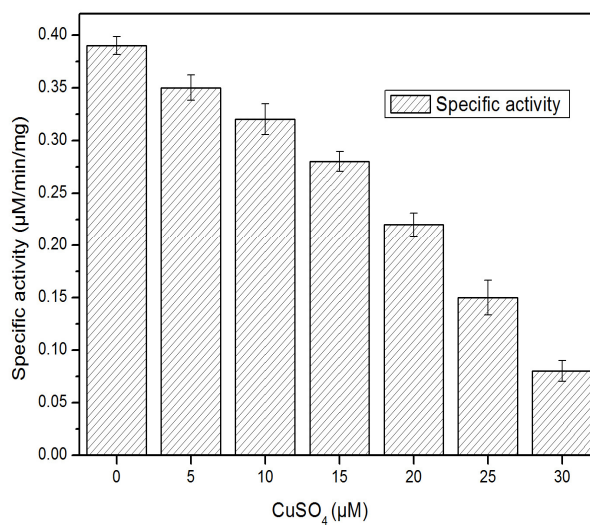
### 3.5.10 Effect of heavy metals on phenol hydroxylation activity

Heavy metals can accumulate in living organisms by biomagnification and can cause harmful effects on tertiary structure of enzymes by catalyzing protein destroying reaction or sulfur-sulfur cross bridge interference (www.sd67.com). This makes it essential to study the effect of heavy metals on enzyme activity. The effect of heavy metals as  $\text{FeSO}_4$ ,  $\text{CuSO}_4$ ,  $\text{AgCl}_2$  and  $\text{HgCl}_2$  on phenol hydroxylase activity was analyzed. Heavy metals as  $\text{FeSO}_4$ ,  $\text{CuSO}_4$ ,  $\text{AgCl}_2$  and  $\text{HgCl}_2$  at a concentration of 30  $\mu\text{M}$  inhibits the enzyme activity by 84.61%, 82.05 %, 74.36% and 82.05 % respectively (Figure 3.42 a, b, c and d). Neujhar and Gall (1973) obtained similar results of inhibitory effect of heavy metals on activity of phenol hydroxylase from *Trichosporon cutaneum*.

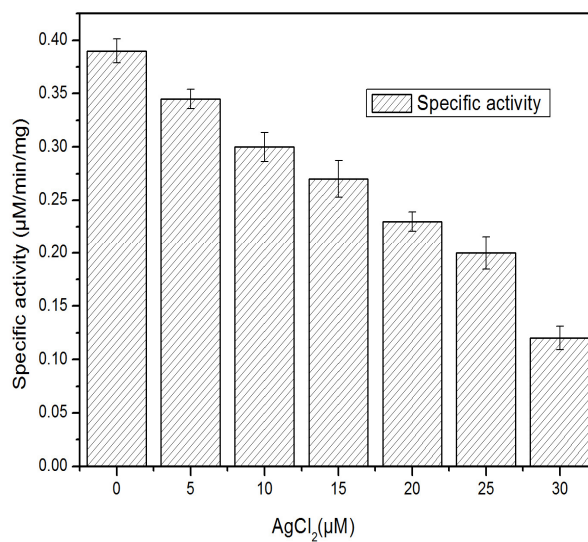




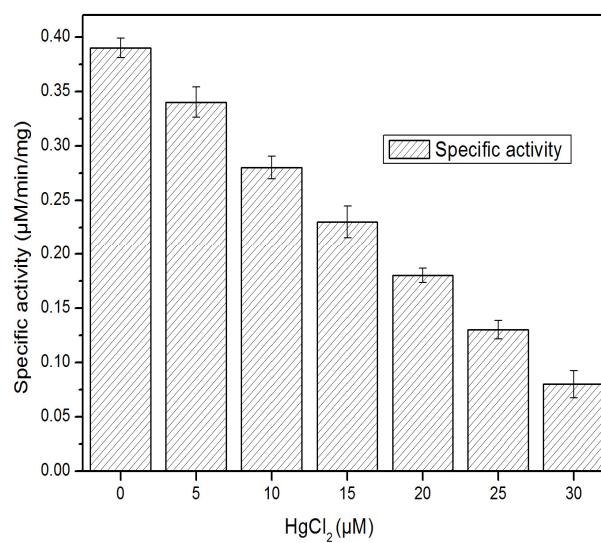
(a)



(b)



(c)

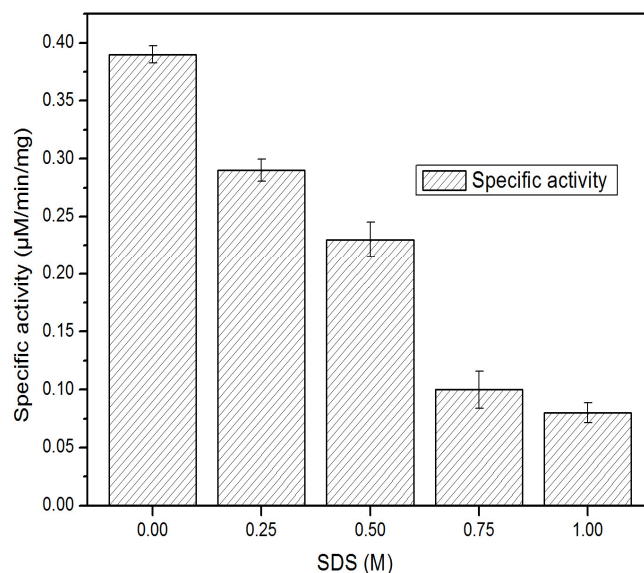


(d)

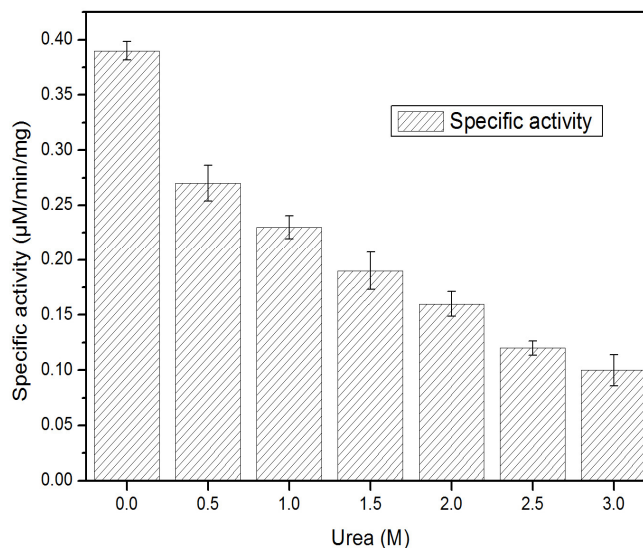
**Figure 3.42** Effect of heavy metals on phenol hydroxylase activity: a) FeSO<sub>4</sub> b) CuSO<sub>4</sub>  
c) AgCl<sub>2</sub> d) HgCl<sub>2</sub>

### 3.5.11 Effect of denaturant on phenol hydroxylation activity

Denaturants change the enzyme structure and an enzyme with changed conformation will have reduced optimal fit of substrate in enzymes active site. Thus, the effect of denaturants on enzyme activity is important. The effect of denaturants as SDS and Urea on phenol hydroxylation was studied. Denaturants as SDS and Urea inhibit phenol hydroxylation activity of the enzyme. 1M SDS while 3M urea inhibit the enzyme activity by 82% and 80.77% respectively (Figure 3.43 a and b). The present results are in accord with the findings of inhibitory effect of denaturants on 3-hydroxybenzoate-6-hydroxylase (Sumathi and Dasgupta 2006). They reported loss of enzyme activity of 90% and 98% by 2M Urea and low concentrations of 0.01% SDS respectively which accords with our present findings. Previous reports of 70-80% inhibitory effect of 2M Urea on activity of phenol hydroxylase from *Trichosporon cutaneum* also support our present findings (Neujhar and Gall 1973).



(a)



(b)

**Figure 3.43** a) Effect of denaturant SDS on Phenol hydroxylase activity b) Effect of denaturant Urea on phenol hydroxylase activity

### 3.5.12 Effect of oxidizing agent on phenol hydroxylation activity

Oxidising agents cause oxidation of –SH group in the enzymes resulting in inhibition of enzyme activity by forming (S-S) disulphide linkages (Kulkarni et al. 2008). The effect of oxidizing agent  $H_2O_2$  on activity of the purified enzyme was analyzed. 20  $\mu M$  of oxidizing agent  $H_2O_2$  depresses the enzyme activity by 83.33% (Figure 3.44). Neujhar and Gall (1973) have reported inhibition of phenol hydroxylase activity by oxidizing agents which correlates with our present findings.

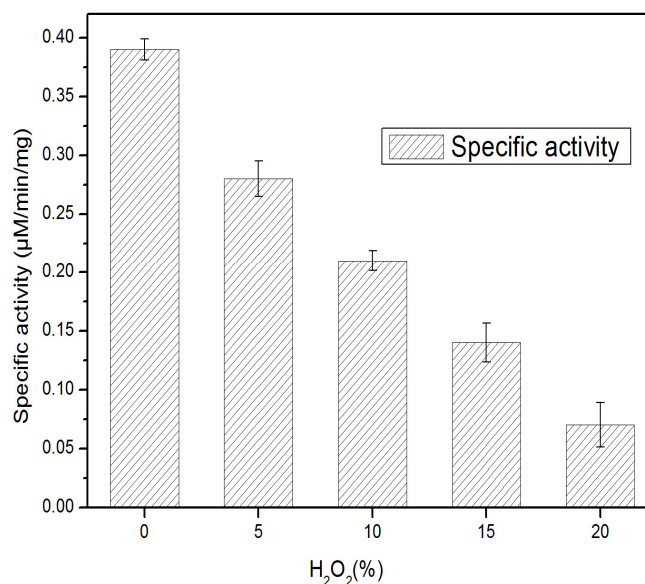


**Figure 3.44** Effect of oxidizing agent H<sub>2</sub>O<sub>2</sub> on phenol hydroxylase activity.

### 3.5.13 Multisubstrate specificity of purified enzyme

The activity of the purified enzyme towards a broad range of phenolics (unsubstituted and substituted phenols) would be beneficial for its application in enzyme based remediation technologies for phenols. Apart from this a broad substrate specificity for a variety of phenolics would further highlight its potential application for developing phenolic biosensors. This makes the study of multisubstrate specificity of phenol hydroxylase important. The purified enzyme has broad substrate specificity acting on isomeric diphenols, isomeric methylphenols, halogen and amino substituted phenols, hydroxybenzaldehydes and hydroxybenzoic acid (Figure 3.45). Similar results of broad substrate specificity of phenol hydroxylase from *Trichosporon cutaneum* supports our present findings (Neujhar and Gall 1973).

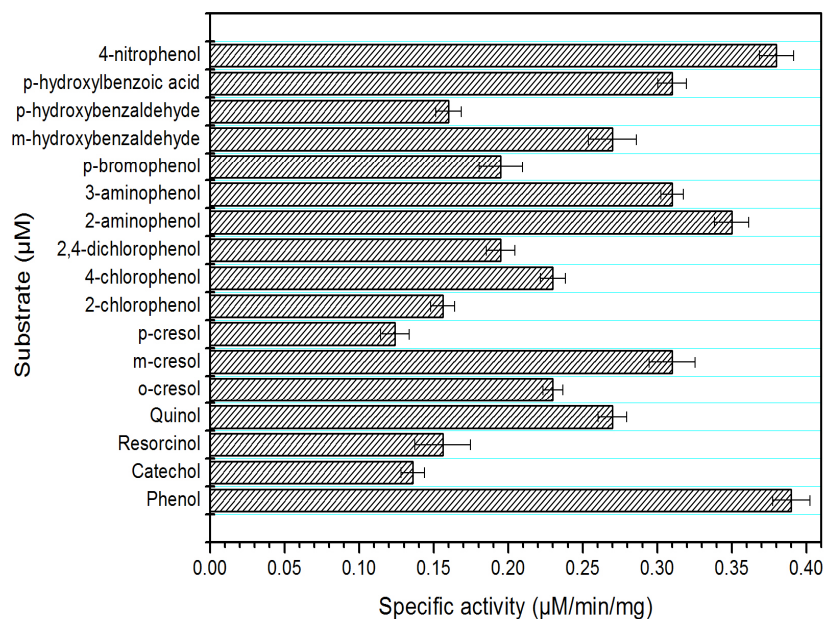


**Figure 3.45** Multisubstrate specificity of Phenol hydroxylase

#### 3.5.14 Storage stability of the enzyme

The enzyme shows remarkable storage stability at room temperature and at 4°C. A minimal loss of phenol hydroxylation activity of 5.13% and 1.28% have been obtained after storage of 7 days at room temperature and 4°C respectively (Figure 3.46). The significant retention of enzyme activity on storage highlights its potential to be used for enzyme based phenol remediation or phenol biosensor applications.

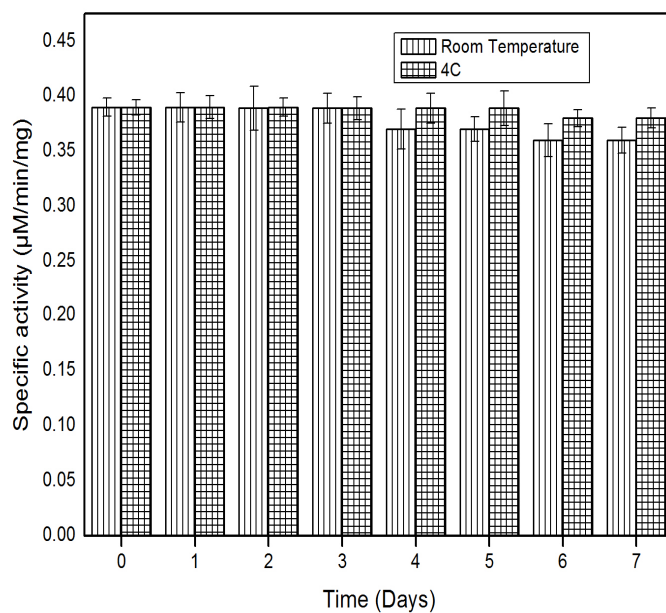
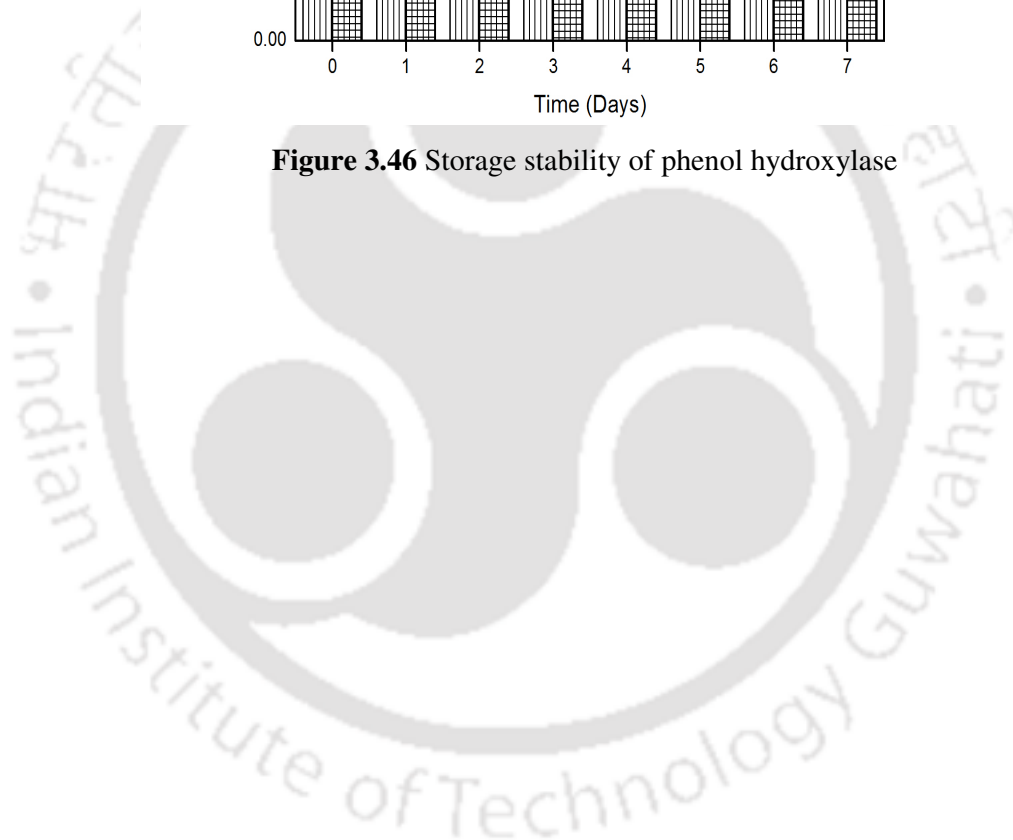


**Figure 3.46** Storage stability of phenol hydroxylase





**Conclusion and Future perspective**



## Chapter IV

### Conclusion and future perspective

#### 4.1 Conclusions

The potential of microalgae for phenol degradation is not well studied as compared to bacterial or fungal phenol degradation. This dissertation work successfully addresses the existing lacunae in the area of microalgal phenol degradation and the conclusion of the research findings have been mentioned as follows:

##### 4.1.1 Introduction and literature review

This section reviewed the current scientific knowledge in the area of biological removal of phenol from wastewaters and highlights the existing knowledge gap that requires further study. Literature survey showed that phenol degradation of microalgae has been less explored compared to other microbial strains and thus deserves further attention. Knowledge of microbial growth kinetics obtained by growth kinetic modeling is an essential input for optimal design and the operation of biological treatment of wastewater containing phenol. Thus, for development of a microalgal phenol bioremediation process using alga it is necessary to know the kinetics of growth and phenol degradation. However, there are no reports concerning growth kinetic modeling of microalgal phenol degradation and thus calls for adequate research in this direction. Phenol metabolizing pathway comprising of a cascade of enzymes is responsible for microbial phenol degradation. There is scarcity of information on the metabolic mechanism of phenol degradation in microalgae and thus requires study in the future. The use of purified enzymes for phenol remediation has generated wide interest recently. Phenol hydroxylase being the first enzyme causing initial attack on phenol in the phenol degradation pathway, the knowledge of its

kinetic properties is of utmost importance for its potential applications. There is no information in literature on kinetic properties of microalgal phenol hydroxylase and calls for research to fulfill this lacuna in scientific knowledge. Microalgae could serve as a promising source of biodiesel provided there is increased biomass production and lipid productivity. Mixotrophic cultivation of algae using different substrates as glucose, glycerol, fructose etc. is an ideal cultivation strategy for increased accumulation of lipids within less time. However, high substrate cost accounting for 50% of the cost of the cultivation medium hinders the commercial applicability of the process. Thus for successful generation of algal biodiesel feedstock requires cheap substrates. Algal mixotrophic cultivation using industrial xenobiotic phenol as cheap substrate has not been previously studied and deserves adequate attention. Successful utilization of industrial toxic waste phenol as mixotrophic culture substrate would bring down production costs of algal biodiesel feedstock along with remediation of phenol pollution. The present research work attempts to fulfill these above mentioned knowledge gaps in scientific knowledge concerning microalgal phenol degradation.

#### **4.1.2 Screening and characterization of phenol degradation by potent algal strains**

Isolation and screening of potent phenol degrading algal strains had been carried out. Six algal strains out of which four multicellular algal strains belonging to genus *Spirogyra*, *Closterium* and two unidentified algae were isolated from sewage water, one unicellular diatom species diatom BD1IITG isolated from petroleum refinery wastewater and another unicellular algae *Chlorella pyrenoidosa* (NCIM 2738) obtained from National Collection of Industrial Microorganisms (NCIM), Pune were screened for phenol degrading ability. However, none of the multicellular algal strains showed any significant phenol degrading ability. Both unicellular algal strains *Chlorella pyrenoidosa* (NCIM 2738) and diatom BD1IITG showed significant phenol degradation ability. The phenol degradation ability of two algal strains *Chlorella*

*pyrenoidosa* and diatom BD1IITG indicates prospects for its application for remediation of phenol pollution.

The present work characterizes the growth and phenol degradation characteristics of two algal strains *C.pyrenoidosa* and diatom BD1IITG. This study showed photodependent phenol degradation capability of *C.pyrenoidosa* with complete degradation till 200mg/l phenol concentration under the optimal nutrient conditions of Fog's medium. The maximum specific rate of degradation was achieved at 125 mg/l phenol due to maximum specific growth rate at this concentration. However, *C.pyrenoidosa* could metabolize 38.32 % of 23.33 mg/l phenol along with removal of aliphatics from petroleum refinery wastewater. Biokinetic parameters obtained by kinetic modeling shows the differences in biomass growth dynamics of *C.pyrenoidosa* in nutrient media and petroleum refinery wastewater. The maximum specific growth rates, phenol affinity as well as phenol toxicity resistance was found to be lower in refinery wastewater than in nutrient media. Cometabolism of alkanes along with phenol decreased the phenol affinity in refinery wastewater. On the contrary, diatom BD1IITG degraded phenol in the range of 50-250 mg/l phenol. However, diatom BD1IITG lacked the complete phenol degradation ability. The specific degradation rate was highest at 100 mg/l phenol due to highest specific growth rate at this concentration. Diatom BD1IITG could mineralize 68.58 % of 23.33 mg/l phenol in refinery wastewater. Biokinetic parameters of  $\mu_{max}$  (0.4 d<sup>-1</sup>),  $K_I$  (90.24 mg/l),  $K_s$  (20.99 mg/l) obtained by growth kinetic modeling suggest that the diatom possess higher maximum specific growth rate, better tolerance to toxicity as well as high affinity for phenol in petroleum refinery wastewater. These kinetic parameters suggest the potential for practical applicability of the strain for phenol remediation in petroleum refinery wastewater. Along with phenol (aromatic compound), the diatom co-metabolised alkanes from refinery wastewater leading to enhanced biomass growth and thus increased phenol uptake rates in petroleum refinery wastewater. Diatom BD1IITG released biosurfactant into the medium which could facilitate improved phenol degradation efficiency and lower phenol toxicity to cells.

### 4.1.3 Generation of a microalgae based process for efficient phenol remediation as well as biofuel production

Owing to the complete phenol degradation ability of *C.pyrenoidosa*, the strain was used to develop an efficient phenol degradation process that could remediate a wide range of phenol concentration within a short time period. This required the strain to possess high resistance to phenol toxicity enabling it to grow efficiently at increased phenol concentration and this issue was addressed by using phenol acclimatized cells of *C.pyrenoidosa*. The phenol acclimatized cells can completely degrade phenol in the concentration range of 50-1200 mg/l with the highest growth ( $0.06 \text{ h}^{-1}$ ) and degradation rate ( $0.561 \text{ h}^{-1}$ ) achieved at 250 mg/l phenol. Biokinetic modeling shows high  $K_s$  value (400.54 mg/l) and  $K_I$  value (800.41 mg/l) indicating that *C.pyrenoidosa* could grow efficiently at higher phenol concentrations by resisting toxicity of high concentration of phenol. Pre adaptation of *C.pyrenoidosa* to the target phenol concentration is being used as a strategy to enhance growth ( $0.078 \text{ h}^{-1}$ ) and phenol degradation rate ( $0.636 \text{ h}^{-1}$ ). Pre adaptation of *C.pyrenoidosa* leads to higher  $\mu_{\max}$  value ( $0.22 \text{ h}^{-1}$ ),  $K_s$  value (500.54 mg/l) and  $K_I$  value (900.41 mg/l) resulting in efficient growth at high phenol concentration. Pre adapted biomass after phenol degradation showed prominent enhancement in total lipid as well as neutral lipid productivity suggesting exciting possibility to be used as biodiesel feedstock. The ability of pre adapted cells to completely degrade 10 mg/l and 250 mg/l phenol in petroleum refinery wastewater with high growth kinetic parameters adds to practical applicability of the process. High lipid as well as neutral lipid productivities obtained in spent biomass after treatment of phenol containing refinery wastewater qualifies the process as a source of algal biodiesel feedstock. Thus, the process is environmentally sustainable as it leads to environmental protection by remediation of toxic phenol in industrial wastewaters along with generation of efficient algal biodiesel feedstock with high neutral lipid content. After lipid extraction from the spent *C.pyrenoidosa* biomass it was used as substrate for bioethanol fermentation on account of its 65.03 % carbohydrate content leading to production of 9.56 % bioethanol in the fermentation broth. The utilization of lipid extracted biomass of

*C.pyrenoidosa* for bioethanol production further enhances its economic feasibility for biofuel applications. On basis of the findings, an environmentally sustainable algal process for remediation of phenol pollution coupled to clean energy generation was proposed.

#### 4.1.4 Elucidation of pathway of phenol degradation

The phenol metabolic pathway was characterized by identifying the different intermediates produced during phenol degradation by using HPLC, UV-Visible spectrophotometry and LC-MS. On basis of the enzyme activity and metabolite analysis study, phenol hydroxylase, the first enzyme of the phenol biodegradation pathway hydroxylates phenol resulting in catechol. Catechol is then be metabolized either by either of the two pathways, ortho ( $\beta$ -keto adipate pathway) or by the meta pathway depending on the organism. In the ortho pathway, the catechol ring is cleaved between two hydroxyl groups by catechol-1,2-dioxygenase. This cleavage mechanism termed intra-diol fission leads to formation of cis,cis-muconic acid. Cis,cis-muconate lactonizing enzyme lactonizes cis,cis-muconic acid to muconolactone. Muconolactone undergoes isomerization by muconolactone isomerase to form  $\beta$ -keto adipate.  $\beta$ -keto adipate enol-lactonase converts 3-Oxidapate-enol-lactone into  $\beta$ -keto adipate which is further metabolized into citrate cycle intermediates. In the meta pathway, catechol is undergoes extradiol cleavage into 2-hydroxymuconic semialdehyde by catechol-2,3-dioxygenase. 2-hydroxymuconate semialdehyde hydrolase causes hydrolysis of 2-HMS to cis-2-hydroxypenta-2,4-dienoate. 2-oxopent-4-enoate hydratase activity produces 4-hydroxy-2-oxoalderate from cis-2-hydroxypenta-2,4-dienoate. 4-hydroxy-2-oxoalderate aldolase converts 4-hydroxy-2-oxoalderate to acetaldehyde and pyruvate. Both the algal strains degrades phenol by both ortho as well as meta pathway with prominence of ortho over meta pathway.

#### 4.1.5 Purification and characterization of phenol hydroxylase from *Chlorella pyrenoidosa*

The microalgal NADPH dependent phenol hydroxylase had been purified to homogeneity from *C.pyrenoidosa* using ammonium sulphate fractionation. It hydroxylates phenol to its reaction product catechol (confirmed by HPLC), substrate dependent NADPH oxidation and has an absorption spectrum typical of flavoproteins. The molecular weight of the purified phenol hydroxylase was found to be 25 kD. MALDI-TOF analysis of the 25 kDa band revealed a protein hit with protein sequence coverage of 39 % in the *Chlorella* sp. NC64A genome of flavoprotein hydroxylase corresponding well with the phenol hydroxylation ability and flavoprotein characteristics of the purified protein. The phenol utilization by the purified enzyme followed Michealis Menten kinetics with apparent Michealis constant ( $K_m$ ) for oxidation of phenol was estimated to be 1.71  $\mu$ M and the maximal velocity ( $V_{max}$ ) to be 0.4  $\mu$ M/min. The optimal pH and temperature for enzyme activity was found to be pH 7 and 35<sup>o</sup> C respectively. Phenanthroline and sodium arsenate (chelator Fe<sup>2+</sup>) showed inhibition of phenol hydroxylation suggesting presence of Fe-S clusters. Heavy metals as FeSO<sub>4</sub>, CuSO<sub>4</sub>, AgCl<sub>2</sub> and HgCl<sub>2</sub> at a concentration of 30  $\mu$ M inhibits the enzyme activity by 84.61%, 82.05 %, 74.36% and 82.05 % respectively. Deanaturants as SDS (1M) while Urea (3M) inhibit the enzyme activity by 82% and 80.77% respectively. The enzyme has broad substrate specificity against isomeric diphenols (catechol, resorcinol, quinol), isomeric methylphenols (o- cresol, m-cresol, p-cresol), halogen substituted phenols (2-chlorophenol, 4-chlorophenol, 2,4-chlorophenol, p-bromophenol,), amino substituted phenols (2-aminophenol, 3-aminophenol), 4-nitrophenol, p and m-hydroxybenzaldehyde and p-hydroxybenzoic acid. The enzyme shows remarkable storage stability at room temperature and at 4<sup>o</sup>C with approximately no loss of activity till 3<sup>rd</sup> day and 5<sup>th</sup> day respectively. The study on characteristics of microalgal phenol hydroxylase gains importance as the information could be instrumental in developing enzyme based phenol remediation technology.

## 4.2 Research Findings

The present research work provided the following significant findings:

1. Characterization of phenol degradation potential for two microalgal strains *Chlorella pyrenoidosa* (NCIM 2738) (NCIM 2738) and diatom BD1IITG.
2. Growth kinetic modeling of microalgal process of phenol degradation for the first time. The biokinetic parameters obtained could be essential inputs for designing microalgae based phenol remediation process.
3. Generation of an environmentally sustainable algal process for remediation of phenol pollution coupled to clean energy generation.
4. Elucidation of complete enzymatic pathway of phenol degradation for *Chlorella pyrenoidosa* (NCIM 2738) and diatom BD1IITG for the first time.
5. Purification and characterization of microalgal phenol hydroxylase for first time.

## 4.3 Future perspective

Growth kinetic modeling of other phenol degrading microalgal strains is required as it can help screen out novel microalgal strains with high phenol degrading efficiency in the future. Further the biokinetic parameters obtained by modeling will be instrumental in development of an efficient microalgae based phenol degradation process. Proteomic studies to identify the key enzymes involved in carbon flux towards lipid accumulation in phenol degrading biomass of *Chlorella pyrenoidosa* could be an exciting area of study. It would lead to identification of novel strain engineering targets for enhanced lipid production. Finding potential application of the phenol hydroxylase from *C.pyrenoidosa* for enzyme based phenol degradation or in phenolic biosensors could be another interesting area of research in future.

## Bibliography

Abdel-Hameid NAH (2007) Physiological and histopathological alterations induced by phenol exposure in *Oreochromis aureus* juveniles. Turk J Fish Aquat Sci 7: 131-138.

Abuhameda T, Bayraktar E, Mehmetoglu T, Mehmetoglu U (2004) Kinetics model for growth of *Pseudomonas putida* F1 during benzene, toluene and phenol biodegradation. Process Biochem 39: 983-88.

Agarry S E, Durojaiye AO, Solomon BO (2008). Microbial degradation of phenols: A review. Int. J. Environ. Pollut. 32:12-28.

Agarry SE, Durojaiye AO, Yusuf RO, Aremu MO (2008) Biodegradation of phenol in refinery wastewater by pure cultures of *Pseudomonas aeruginosa* NCIB 950 and *Pseudomonas fluorescense* NCIB 3756. Int J Environ Pollut 32:3-11.

Ahuatzi-Chacon D, Ordorica-Morales G, Ruiz-Ordaz N, Cristiani-Urbina E, Juarez-Ramirez C, Galindez-Mayer J (2004) Kinetic study of phenol hydroxylase and catechol 1,2-dioxygenase biosynthesis by *Candida tropicalis* cells grown on different phenolic substrates. World J. Microbiol. Biotechnol. 20: 695-702

Aiba S, Shoda M, Nagatani M (1968) Kinetics of product inhibition in alcohol fermentation. Biotechnol Bioeng 10: 845-864.

Akbal F, Onar AN (2003) Photocatalytic Degradation of Phenol. Environ Monit Assess 83: 295-302.

Alexander M (1985) Biodegradation of organic chemicals. Environ Sci Technol 18 : 106-111.

Ali S, Fernandez-Lafuente R, Cowan DA (1998) Meta-pathway degradation of phenolics by thermophilic *Bacilli*. Enz Microb Technol 23: 462-468.

Al-Khalid T, El-Naas M (2012) Aerobic biodegradation of phenols: A comprehensive review. Crit Rev Environ Sci Technol 42: 1631-1690.



Al-Sultani Kadhim F, Al-Seroury FA (2012) Characterization the Removal of Phenol from Aqueous Solution in Fluidized Bed Column by Rice Husk Adsorbent. Res J Recent Sci 1: 145-151.

Annadurai G, Ling LY, Lee JF (2008). Statistical optimization of medium components and growth conditions by response surface methodology to enhance phenol degradation by *Pseudomonas putida*. J Hazard Mat 151: 171–178.

Aruoja V, Shitmae M, Dubourguier HC, Kahru A (2011) Toxicity of 58 substituted anilines and phenols to algae *Pseudokirchneriella subcapitata* and bacteria *Vibrio fischeri*: Comparison with published data and QSARs. Chemosphere 84: 1310-1320.

Arutchelvan V, Kankasabai V, Elangovan R, Nagarajan S, Muralikrishnan V(2006). Kinetics of high strength phenol degradation using *Bacillus brevis*. J. Hazard. Mater. 129: 216-222.

Atteia A, Lis Rv, Gelius-Dietrich G, Adrait A, Garin J, Joyard J, Rolland N, Martin W (2006) Pyruvate Formate-lyase and a Novel Route of Eukaryotic ATP Synthesis in *Chlamydomonas* Mitochondria. J Biol Chem 281:9909-9918.

Ayeni O (2014) A preliminary assessment of phenol contamination of Isebo River in South Western Nigeria. Greener J Phy Sci 4: 30-37.

Bai J, Wen JP, Li HM, Jiang Y (2007) Kinetic modeling of growth and biodegradation of phenol and m-cresol using *Alcaligenes faecalis*. Process Biochem 42: 510–17.

Bajaj M, Gallert C, Winter J (2008) Biodegradation of high phenol containing synthetic wastewater by an aerobic fixed bed reactor. Bioresour Technol 99: 8376-8381.

Banerjee A, Ghoshal AK (2010) Phenol degradation by *Bacillus cereus*: Pathway and kinetic modeling. Bioresour Technol 101:5501-5507.

Baranyi J (2010) Modelling and parameter estimation of bacterial growth with distributed lag time, Dissertation, University of Szeged.

Basha KM, Rajendran A, Thangavelu V (2010) Recent advances in the Biodegradation of Phenol: A review. Asian J Exp Biol Sci 2: 219-234.

Bastos AER, Tornisielo VL, Nozawa SR, Trevors JT, Rossi A (2000) Phenol metabolism by two microorganisms isolated from Amazonian Forest soil samples. *J Ind Microbiol Biotechnol* 24: 403-409.

Bhatnagar A, Bhatnagar M, Chinnasamy S, Das KC (2010) *Chlorella minutissima*-A promising fuel alga for cultivation in municipal wastewaters. *Appl Biochem Biotechnol* 161:523-536.

Bhatt P, Kumar MS, Mudliar S, Chakrabarti T (2007) Biodegradation of chlorinated compounds-a review. *Crit Rev Env Sci Technol* 37: 165–198.

Bligh EG, Dyer WJ (1959) A rapid method for total lipid extraction and purification. *Can J Biochem Physiol* 37: 911-917.

Borde X, Guieysse B, Delgado O, Munoz R, Hatti-Kaul R, Nugier-Chauvin C, Mattiassori B (2003) Synergistic relationship in algal-bacterial microcosms for treatment of aromatic pollutants. *Bioresour Technol* 86: 293-300.

Cadieux E., Vrajmasu V, Achim C, Powlowski J, Muenck E (2002) Biochemical, Mossbauer, and EPR studies of the diiron cluster of phenol hydroxylase from *Pseudomonas sp.* strain CF 600. *Biochemistry* 41:10680-10691.

Cai W, Li J, Zhang Z (2007) The characteristics and mechanisms of phenol biodegradation by *Fusarium sp.* *J Hazard Mater* 148: 38-42.

Chen J, Jiang JG, Lin QS (2007) Toxicity tests of typical mutagenic phenols on *Dunaliella salina*. *Trans ASAE* 50: 685-688.

Chen W, Zhang C, Song L, Sommerfeld M, Hu Q (2009) A high throughput Nile red method for quantitative measurement of neutral lipids in microalgae. *J Microbiol Method* 77:41-47.

Chinnasamy S, Bhatnagar A, Hunt RW, Das KC (2010) Microalgae cultivation in wastewater dominated by carpet mill effluents for biofuel applications. *Bioresour Technol* 9: 3097-3105.

Clayton GD, Clayton FE (1994) *Patty's Industrial Hygiene and Toxicology*. John Wiley & Sons, New York.

- Cooney M, Young G, Nagle N (2009) Extraction of bio-oils from microalgae. *Sep Purif Rev* 38:291-325.
- Cordova-Rosa, SM; Dams RI; Cordova-Rosa EV; Radetski, MR, Correa, AXR, Radetski, CM (2009) Remediation of bacterial contaminated soil by a bacterial consortium and *Acinetobacter calcoaceticus* isolated from an industrial wastewater treatment plant. *J Haz Mat* 164: 61-66.
- Dabbagh F, Mohkam M, Zamani M, Khalvati B, Sheikhsaran F, Farhadi T, Ghasemi Y (2012) Isolation and physiological characterization of phenol degrading bacteria from municipal and petroleum wastewater samples of Fars province, Iran. *Res Pharm Sci* 7:5.
- Dagley S, Gibson DT (1965) The Bacterial Degradation of Catechol. *Biochem.* 95:466-474.
- Das BC, Sinha P, Mukherjee K, Dutta S, Dutta Banik S, Das M (2014) Studies on removal of Phenol from contaminated water source by microbial route using *Bacillus cereus* *Int.J.Curr.Res.Aca.Rev.* 2:179-184.
- Dash RR, Gaur A, Balomajumder C (2009) Cyanide in industrial wastewaters and its removal: A review on biotreatment. *J Hazard Mat* 163: 1–11.
- Dealing with metal adduct ions in electrospray 2014. Available from: [www.sepscience.com](http://www.sepscience.com). Accessed on: June 2, 2014.
- Dewani, VK, Ansari, IA, Khuhawar (2003) Total phenol as pollution indicator of sewage and sewage contaminate canal. *J Chem Soc Pak* 25: 206-209.
- Dey S, Mukherjee S (2010) Performance and kinetic evaluation of phenol biodegradation by mixed microbial culture in a batch reactor. *Int. J. Wat. Resour. Env. Eng.* 2: 40-49.
- Dey S, Mukherjee S (2010) Performance and kinetic evaluation of phenol biodegradation by mixed microbial culture in a batch reactor; *Int J Water Res Environ Eng* 2: 40-49.
- Dong X, Hong Q, He L, Jiang X, Li S (2008) Characterization of phenol-degrading bacterial strains isolated from natural soil. *Int Biodeter Biodegrad* 62: 257-262.

Donner E, Eriksson E, Holten-Lutzhof HC, Scholes L, Revitt M, Ledin A (2010) Identifying and classifying the sources and uses of xenobiotics in urban environment. In: Fatta-Kassinos et al. (eds) Xenobiotics in Urban water cycle: Mass Flows, Environmental Processes, Mitigation and treatment strategies, Springer, New York, DOI 10.1007/978-90-481-3509-7\_2

Duan Z (2011) Microbial degradation of phenol by activated sludge in batch reactor. Environ Prot Eng 37:53-63.

DuBois M, Gilles KA, Hamilton JK, Rebers PA, Smith F (1956) Colorimetric method for determination of sugars and related substances. Anal Chem 28: 350-356.

Duetz WA, Jong CD, Williams PA, Van Andel JG (1994) Competition in chemostat culture between *Pseudomonas* strains that use different pathways for the degradation of toluene. Appl Environ Microbiol 60: 2858-2863.

Edwards VH (2004) The influence of high substrate concentrations on microbial kinetics. Biotechnol Bioeng 12: 679-712.

El-Sheekh, Ghareib MM, EL-Souod GWA (2012) Biodegradation of phenolic and polycyclic aromatic compounds by some algae and cyanobacteria. J. Bioremed. Biodegrad. 3: 133.

El-Naas M H, Al-Muhtaseb S, Makhlof S (2009). Biodegradation of phenol by *Pseudomonas putida* immobilized in polyvinyl alcohol (PVA) gel. J. Hazard. Mat 164: 720–725.

El-Serafy SS, Abdel-Hameid NAH, El-Daly AA (2009) Histological and histochemical alterations induced by phenol exposure in *Oreochromis aureus* juveniles. Egypt J Aquat Biol Fish 13: 151-172.

Farag AM, Abd-Elnaby HM (2014) Degradation of phenol by a new degradable marine halophilic fungus *Fennellia flavipes* isolated from mangrove sediments. Life Sci J 11:836-845.

Farooq W, Lee YC, Ryu BG, Kim BH, Kim HS, Choi YE, Yang JW (2013) Two-stage cultivation of two *Chlorella* sp. strains by simultaneous treatment of brewery wastewater and maximizing lipid productivity. Bioresour Technol 132,:230-238.

Feng GD, Zhang F, Cheng LH, Xu XH, Zhang L, Chen HL (2013) Evaluation of FTIR and Nile red methods for microalgal lipid characterization and biomass composition determination. *Bioresour Technol* 128: 107-112.

Feng Y, Li C, Zhang D (2011) Lipid production of *Chlorella vulgaris* cultured in artificial wastewater medium. *Bioresour Technol* 102: 101-105.

Firozjaee TT, Najafpour GD, Khavarpour M, Bakhshi Z, Pishgar R, Mousavi N (2011) Phenol Biodegradation Kinetics in an Anaerobic Batch Reactor. *Iran J Ener Environ* 2: 68-73.

Gad NS, Saad AS (2008) Effect of environmental pollution by phenol on some physiological parameters of *Oreochromis niloticus*. *Glob Veterina* 6: 312-319.

Gami AA (2014) Phenol and its toxicity. *J Environ Microbiol Toxicol* 2: 11-23.

Gao QT, Wong YS, Tam NFY (2011) Removal and biodegradation of nonylphenol by different *Chlorella* sp. *Mar Pollut Bull* 63: 445-451.

Gerginova M, Manasiev J, Shivarova N, Alexieva Z (2007) Influence of various phenolic compounds on phenol hydroxylase activity of a *Trichosporon cutaneum* strain. *Z. Naturforsch. C* 62: 83-86.

Ghannadzadeh MJ, Jonidi-Jafari A, Rezaee A, Soltani RDC (2015) Biodegradation of phenol in synthetic wastewater using a fixed bed reactor with up Flow Sludge Blanket Filtration (FUSBF). *Glob J Health Sci* 7: 120-130.

Gobas APC F (2001) Assessing bioaccumulation factors of persistent organic pollutants in aquatic food chains. In: Stuart Harrad (Ed) *Persistent organic pollutants*, Springer US, New York, pp 145-165.

Gracia MCC, Camacho G F, Miron A S, Sevilla JMF, Chisti Y, Grima EM (2006) Mixotrophic Production of Marine Microalga *Phaeodactylum tricoratum* on Various Carbon Sources. *J Microbiol Biotechnol* 16: 689-694.

Gray JS (2002) Biomagnification in marine ecosystem: the perspective of an ecologist. *Marine Poll Bull* 45: 46-52.

Griva E, Pessione E, Divari S, Valetti F, Cavaletto M, Rossi GL, Giunta C (2003) Phenol hydroxylase from *Acinetobacter radioresistens* S13: Isolation and characterization of regulatory component. *Eur J Biochem* 270: 1434-1440.

Haldane JBS (1965) *Enzyme*. MIT Press, Cambridge.

Hamed SM, Klock G (2014) Improvement of medium composition and utilization of mixotrophic cultivation for green and blue green algae microalgae towards biodiesel production. *Adv Microbiol* 4: 167-174.

Hasan SA, Jabeen S (2015) Degradation kinetics and pathway of phenol by *Pseudomonas* and *Bacillus* sp. *Biotechnol Biotec Eq* 29:45-53.

Hassan M, Essam T, Yassin AS, Salama A (2014) Screening of biosurfactant production ability among organic pollutants degrading isolates collected from Egyptian Environment. *Microb Biochem Technol* 6:4

Hena S, Fatimah S, Tabassum S (2015) Cultivation of algae consortium in a dairy farm wastewater for biodiesel production. *Water Res Ind* 10:1-14.

Hofrichter M, Gunther T, Fritsche W (1993) Metabolism of phenol, chloro and nitrophenol by *Penicillium* strain Bi 7/2 isolated from a contaminated soil. *Biodegrad* 3: 415-421.

Hu H, Gao K (2003) Optimization of growth and fatty acid composition of a unicellular marine picoplankton, *Nannochloropsis* sp., with enriched carbon sources. *Biotechnol Lett* 25: 421-425.

Hunt R (2006) Investigation of the algal toxicity of Triclosan and Triclocarban. [www.nature.berkeley.edu](http://www.nature.berkeley.edu) Accessed 5 January 2016.

Hussain A, Dubey SK, Kumar V (2015) Kinetic study of aerobic treatment of phenolic wastewater. *Water Res Ind* 11:81-90.

Ibrahem MD (2012) Experimental exposure of African catfish *Clarias Gariepinus* (Burchell 1822) to phenol: Clinical evaluation, tissue alterations and residue assessment. *J Adv Res* 3: 177-183.

Ilsiz I, Laszlo Z, Dombi A (1999) Investigation of the photodecomposition of phenol in near-UV-irradiated aqueous TiO<sub>2</sub> suspensions. I: Effect of charge-trapping species on the degradation kinetics. *Appl Catal* 180: 25–33.

Jacob HJ, Alsohaili S (2010) Isolation of two fungal strains capable of phenol biodegradation. *J Biol Sci* 10: 162-165.

Jadhav DN, Vanjara AK (2004) Removal of Phenol from Wastewater using sawdust, Polymerized sawdust and sawdust carbon. *Indian J Chem Technol* 1: 35-41.

Jiang HL, Tay JH, Tay STL (2002) Aggregation of immobilized activated sludge cells into aerobically grown microbial granules the aerobic biodegradation of phenol. *Lett Appl Microbiol* 35: 439-445.

Jiang L, Mao X (2012) Degradation of Phenol-containing Wastewater Using an Improved Electro-Fenton Process *Int J Electrochem Sci* 7: 4078 – 4088.

Jiang Y, Wen J, Bai J, Jia X, Hu Z (2007). Biodegradation of phenol at high initial concentration by *Alcaligenes faecalis*. *J Hazard Mater* 147: 672–676.

Juang RS, Tsai SY (2006) Growth kinetics of *Pseudomonas putida* in the biodegradation of single and mixed phenol and sodium salicylate. *Biochem Eng J* 31:133-140.

Kafilzadeh F, Farhangdoost MS, Tahery Y (2010) Isolation and identification of phenol degrading bacteria from Lake Parishan and their growth kinetic assay. *Afr J Biotechnol* 9: 6721-6726.

Kafilzadeh F, Mokhtari S (2013) Isolation and identification of phenol degrading bacteria from mangrove sediments in Persian Gulf (Asaluyeh) and their growth kinetic assay. *Biomed Pharma J.* 6: 189-196.

Kagle J, Hay AG (2006) Phenylacetylene reversibly inhibits the phenol hydroxylase of *Pseudomonas* sp. CF600 at high concentrations but is oxidized at lower concentrations. *Appl Microbiol Biotechnol* 72: 306-315.

Kahru A, Maloverjan A, Sillak H, Pollumaa L (2002) The toxicity and fate of phenolic pollutants in the contaminated soils associated with the oil shale industry. *Environ Sci Poll Res Int* 1: 27-33.

Karigar C, Mahesh A, Nagenhalli M, Yun DJ (2006) Phenol degradation by immobilized cells of *Arthrobacter citreus*. *Biodegr* 17:47-55.

Kavitha C, Ashokkumar V, Chinnasamy S, Bhaskar S, Rengasamy R (2014) Pretreatment of lipid extracted *Botryococcus braunii* spent biomass for bioethanol production. *Int J Curr Biotechnol* 2: 11-18.

Kelkhar V, Kosarnic N (1992) Degradation of phenols by algae. *Environ Technol* 13: 493-501.

Khleifat KM (2006) Biodegradation of phenol by *Ewingella americana*: Effect of carbon starvation and some growth conditions. *Process Biochem* 41: 2010–2016.

Kilic NK, Donmez G (2013) Phenol biodegradation by different mixed cultures and optimization of efficiency of degradation. *Environ Technol* 34: 2251-2258.

Kim BH, Kang Z, Ramanan R, Choi JE, Cho DH, Oh HM, Kim HS (2014) Nutrient removal and biofuel production in high rate algal pond using real municipal wastewater. *J Microbiol Biotechnol* 24: 1123-1132.

Kim JY, Kim JK, Lee SO, Kim CK, Lee K (2005) Multicomponent phenol hydroxylase-catalysed formation of hydroxyindoles and dyestuffs from indole and its derivatives. *Lett Appl Microbiol* 41: 163-168.

Kim KH, Choi IS, Kim HM, Wi SG, Bae HJ (2014) Bioethanol production from the nutrient stress-induced microalga *Chlorella vulgaris* by enzymatic hydrolysis and immobilized yeast fermentation. *Bioresour Technol* 153: 47-54.



Kirchner U, Westphal AH, Muller R, van Berkel W.J (2003) Phenol hydroxylase from *Bacillus thermoglucosidasius* A7, a two-protein component monooxygenase with a dual role for FAD. *J Biol Chem* 278: 47545-47553.

Kjellen KG, Neujhar HY (1980) Enzyme electrode for phenol. *Biotechnol Bioeng* 22: 299-310.

Kong WB, Yang H, Cao YT, Song H H, Xia SF (2013) Effect of Glycerol and Glucose on the Enhancement of Biomass, Lipid and Soluble Carbohydrate Production by *Chlorella vulgaris* in Mixotrophic Culture. *Food Technol Biotechnol* 51: 62-69.

Krug M, Zeigler H, Straube G (1985) Degradation of phenolic compounds by the yeast *Candida tropicalis* HP 15.I. Physiology of growth and substrate utilization. *J Basic Microbiol* 25:103-110.

Kukor JJ, Olsen RH (1990) Molecular Cloning, Characterization, and Regulation of a *Pseudomonas pickettii* PKOIGene Encoding Phenol hydroxylase and Expression of the Gene in *Pseudomonas aeruginosa* PAolc. *J. Bacteriol.* 173:4587-4594.

Kulkarni MV (2008) *Biochemistry*. Nirali Prakashan, India.

Kulkarni SJ, Kaware JP (2013) Review on research for removal of phenol from wastewater. *Int J Scint Res Pub* 3:1-5.

Kumar A, Kumar S, Kumar S (2005) Biodegradation kinetics of phenol and catechol using *Pseudomonas putida* MTCC 1194. *Biochem Eng J* 22: 151-159.

Kumar A, Kumar S, Kumar S (2005) Biodegradation kinetics of phenol and catechol using *Pseudomonas putida* MTCC 1194. *Biochem. Eng. J* 22: 151-159.

Kumar B, Tyagi J, Verma VK, Sharma CS, Akolkar AB (2014) Distribution of eleven priority phenolic compounds in soils from mixed landuse and assessment of health hazard for human population. *Adv Appl Sci Res* 5: 125-132.

Kumar PK, Pacha MM (2015) Assessment of phenolic compounds in surface waters of Godaari canal, Andhra Pradesh, India. *Curr World Environ* 10: 338-342.

Kwon KH, Yeom SH (2009) Optimal microbial adaptation routes for the rapid degradation of high concentration of phenol. *Bioprocess Biosyst Eng* 32:435-442.

Laemmli UK (1970) Cleavage of structural proteins during the assembly of the head of bacteriophage T4. *Nature* 227:680-685.

Lakshmi Chandana MVV, Sridevi V (2009) A review on biodegradation of phenol from industrial effluents. *J Ind Pollut Contr* 25: 13-27.

Langenbach T (2013) Persistent and Bioaccumulation of persistent organic pollutants. In: Dr. Patil Y (Ed) *Applied Bioremediation: Active and Passive approaches*. www.intechopen.com <http://dx.doi.org/10.5772/56418>

Laurens LML, Quinn M, Wychen S, Templeton DW, Wolfrum EJ (2012) Accurate and reliable quantification of total microalgal fuel potential as fatty acid methyl esters by in situ transesterification. *Anal Bioanal Chem* 403: 167-178.

Lee OK, Oh YK, Lee EY (2015) Bioethanol production from carbohydrate enriched residual biomass obtained after lipid extraction of *Chlorella* sp. KR-1. *Bioresour Technol* 196: 22-27.

Leonard D, Lindley ND (1998) Carbon and energy flux constraints in continuous cultures of *Alcaligenes eutrophus* grown on phenol. *Microbiol* 144: 241-248.

Li Y, Li J, Wang C, Wang P (2010) Growth kinetics and phenol biodegradation of psychrotrophic *Pseudomonas putida* LY1. *Bioresour Technol*. 101: 6740-6744.

Liber K, Solomon KR (1994) Acute and chronic toxicity of 2,3,4,6-tetrachlorophenol and pentachlorophenol to *Daphnia* and rotifers. *Arch Environ Contam Toxicol* 26: 212-221.

Lika K, Papadakis IA (2009) Modelling biodegradation of phenolic compounds by microalgae. *J. Sea Res.* 62: 135-146.

Lincoln EP, Carmichael WW (1981) Preliminary tests of toxicity of *Synechocystis* sp. grown on wastewater medium. In: Carmichael WW (ed) *The Water Environment*, Springer US, New York, pp 223-230.

Litova K, Gerginova M, Peneva N, Manaseiv J, Alexieva Z (2014) Growth of Antarctic fungal strains on phenol at low temperatures. *J Biosci Biotech* 43-46.

Liu J, Wang Q, Yan J, Qin X, Li L, Xu W, Subramaniam R, Bajpai RK (2012) Isolation and characterization of a novel phenol degrading bacterial strain WUST-C1. *Ind Eng Chem Res* 52: 258-265.

Liu YJ, Zhang AN, Wang XC (2009). Biodegradation of phenol by using free and immobilized cells of *Acinetobacter* sp. XA05 and *Sphingomonas* sp. FG03. *Biochem. Eng. J.* 44:187–192.

Lowry OH, Rosebrough NJ, Farr AL, Randall RJ (1951) Protein measurement with Folin Phenol Reagent. *J Biol Chem* 193:265-275.

Lua AC, Jia Q (2009) Adsorption of phenol in oil palm shell activated carbons in a fixed bed. *Chem Eng J* 150: 455-461.

Lv JM, Cheng LH, Xu XH, Zhang L, Chen HL (2010) Enhanced lipid production of *Chlorella vulgaris* by adjustment of cultivation conditions. *Bioresour Technol* 101: 6797-6804.

Magri AD, Magri AL, Balestrieri F, Sacchini A, Marini D (1997) Spectrophotometric micromethod for the determination of ethanol in commercial beverages. *Frensenius J Anal Chem* 357: 985-988.

Mahapatra DM, Chanakya HN, Ramachandra TV (2014) Bioremediation and lipid synthesis through mixotrophic algal consortia in municipal wastewater. *Bioresour Technol* 168: 142-150.

Mahiuddin Md, Fakhrudin ANM, Al-Mahin A (2012) Degradation of Phenol via Meta Cleavage Pathway by *Pseudomonas fluorescens* PU1. *ISRN Microbiol.* doi:10.5402/2012/741820

Mathur AK, Majumder CB (2010) Kinetics Modelling of the Biodegradation of Benzene, Toluene and Phenol as Single Substrate and Mixed Substrate by Using *Pseudomonas putida*. Chem Biochem Eng 24:101-109.

Mendonca E, Martins A, Anselmo AM (2003) Biodegradation of natural phenolic compounds as single and mixed substrates by *Fusarium flocciferum*. Electron J Biotechnol, 7, DOI: 10.2225/vol7-issue1-fulltext-3

Metzger J, Reiss M, Hartmeier W (1998) Amperometric phenol biosensor based on a thermostable phenol hydroxylase. Biosens Bioelectron 13: 1077-1082.

Michalowicz J, Duda W (2007) Phenols-Sources and Toxicity. Polish J of Environ Stud 16: 347-362.

Mittal A (2011) Biological wastewater treatment. <http://www.watertoday.org> Accessed 7<sup>th</sup> January 2016.

Mohite BV, Jalgaonwala RE, Pawar S, Morankar A (2010) Isolation and characterization of phenol degrading bacteria from oil contaminated soil. Innovat Rom Food Biotechnol 7:61-65.

Monteiro A, Boaventura R, Rodrigues AE (2000) Phenol biodegradation by *Pseudomonas putida* DSM 548 in a batch reactor. Biochem. Eng. J. 6: 45-49.

Mort SL, Dean-Ross D (1994) Biodegradation of phenolic compounds by sulfate reducing bacteria from contaminated sediments. Microb Ecol 28: 67-77.

Mosier N, Wyman C, Dale B, Elander R, Lee YY, Holtzaple M, Ladisch M (2005) Features of promising technologies for pretreatment of lignocellulosic biomass. Bioreour Technol 96: 673-686.

Mrozik A, Cycon M, Piotrowska-Seget Z (2010). Changes of FAME profiles as a marker of phenol degradation in different soils inoculated with *Pseudomonas* sp. CF600. Int. Biodeterior. Biodegrad. 64: 86-96.

Mukherjee D, Guha D, Kumar V, Chakraborty S (1991) Impairment of steroidogenesis and reproduction in sexually mature *Cyprinus carpio* by phenol and sulfide under laboratory conditions. *Aquat Toxicol* 21:29-40.

Nair CI, Jayachandran K, Shashidhar, S (2008). Biodegradation of phenol. *Afr. J. Biotechnol.* 7: 4951–4958.

Nakagawa H, Takeda Y (1962) Phenol hydroxylase. *Biochim. Biophys. Acta* 62: 423-426.

Neujhar HY, Gaal A (1973) Phenol hydroxylase from yeast. *Eur. J. Biochem.* 35: 386-400.

Nielsen A (2015) Treatment of wastewater with microalgae under mixotrophic growth. Dissertation. Umea University.

Nomani AA, Ajmal M, Ahmad S (1996) Gas chromatography: Mass spectrometric analysis of four polluted river waters for phenolic and organic compounds. *Environ Monit Assess* 40: 1-9.

Nordlund I, Pawlowski J, Hagstrom A, Shingler V (1993) Conservation of Regulatory and Structural Genes for a Multicomponent Phenol Hydroxylase within Phenol-Catabolizing Bacteria that Use the meta-Cleavage pathway. *J. Gen. Microbiol.* 139: 2695-2703.

Nuhoglu A, Yalcin B (2005). Modelling of phenol removal in a batch reactor. *Process Biochem* 40: 1233–1239.

Oksama M, Kristofferson R (1980) Effects of phenol and 4-chlorophenol on ionic regulation in *Mesidotea entomon* (Crustacea) in brackish water. *Ann Zool Fennici* 17: 243-247.

Onysko KA, Budman HM, Robinson CW (2000) Effect of temperature on the inhibition kinetics of phenol biodegradation by *Pseudomonas putida* Q5. *Biotechnol. Bioeng.* 70:291–299.

Ornston LN (1966) The conversion of catechol and protocatechuate to beta-ketoadipate by *Pseudomonas putida*.3. Enzymes of the catechol pathway. *J Biol Chem* 241:3795-3799.

Paca JJ, Kremlackova V, Turek M, Sucha V, Vilimkova L, Paca J, Halecky M, Stiborova M (2007) Isolation and partial characterization of NADPH-dependent phenol hydroxylase

oxidizing phenol to catechol in *Candida tropicalis* yeast. *Enzyme Microb Technol* 40: 919-926.

Papazi A, Assimakopoulos K, Kotzabasis K (2012) Bioenergetic strategy for biodegradation of p-cresol by the unicellular green alga *Scenedesmus obliquus*. *PLoS one*, DOI: 10.1371/journal.pone.0051852.

Papazi A, Kotzabasis K (2007) Bioenergetic strategy of microalgae for biodegradation of phenolic compounds- Exogeneously supplied energy and carbon sources adjust the level of biodegradation. *J. Biotechnol.* 129: 706-716.

Park JS, Brown MT, Han T (2012) Phenol toxicity to aquatic macrophyte *Lemna paucicostata*. *Aquat Toxicol* 106-107: 182-188.

Patil SS, Jena HM (2015) Statistical optimization of phenol degradation by *Bacillus pumilus* OS1 using Plackett-Burman Design and Response Surface Methodology. *Arab J Sci Eng* 40:2141-2151.

Pei F, Luo ZJ, Peng JJ, Qi SH (2012) Phenol pollutants in soil and shallow groundwater of a retired refinery site. *Chinese J Environ Sci* 33: 4251-4255.

Pessione E, Divari S, Griva E, Cavaletto M, Rossi GL, Gilardi G, Giunta C (1999) Phenol hydroxylase from *Acinetobacter radioresistens* is a multicomponent enzyme. *Eur J Biochem* 265: 549-555.

Pinto G, Pollio A, Previtiera, L, Stanzione, M, Temussi, F (2003) Removal of low molecular weight phenols from olive oil mill wastewater using microalgae. *Biotechnol Lett* 25: 1657-1659.

Pishgar R, Najafpour GD, Mousavi N, Bakhsh Z, Khorrami M (2012) Phenol Biodegradation Kinetics in the Presence of Supplementary Substrate. *IJE Trans. B: Applic* 25: 181-91.

Pistorius AMA, DeGrip WJ, Egorova-Zachernyuk TA (2009) Monitoring of biomass composition from microbiological sources by means of FTIR spectroscopy. *Biotechnol Bioeng* 103: 123-129.

Ponepal MC, Paunescu A (2014) Effect of phenol intoxication on some physiological parameters of *Perca fluviatilis* and *Pelophylax ridibundus*. *Curr Trend Nat Sci* 3: 82-87.

Powlowski J, Shingler V(1994) Genetics and Biochemistry of Phenol Degradation by *Pseudomonas* sp. CF600. *Biodegradation* 5:219-236.

Preito MB, Hidalgo A, Rodriguez-Fernandez C, Serra JL, Llama MJ (2002) Biodegradation of phenol in synthetic and industrial wastewater by *Rhodococcus erythropolis* UPV-1 immobilized in air stirred reactor with clarifier. *Appl Microbiol Biotechnol* 58: 853-859.

Raikar RV, Patil R, Virupakshi A (2015) Degradation of phenol using sequential batch reactor. *Int J Res Eng Technol* 4: 542-546.

Rajani V, Neethu V (2015) Isolation and identification of phenol degrading bacteria from effluent treatment plant of textile industry in Kerala. *Int J Pure App Biosci* 3:88-94.

Rao N N, Singh J R, Mishra R, Nandi T (2009) Liquid liquid extraction of phenol from simulated sebacic acid wastewater J. *Scient Indust Res* 68:823-829.

Ratpukdi SS (2014) Phenolic based pharmaceutical contaminated wastewater treatment kinetics by activated sludge process. *J Clean Energ Technol* 2: 150-153.

Razika B, Abbes B, Messaoud C, Soufi K (2010) Phenol and benzoic acid degradation by *Pseudomonas aeruginosa*. *J Water Resource Prot* 2: 788-791.

Ristola T (2000) Assessment of sediment toxicity using the midge *Chironomus riparius* (Diptera: Chironomidae). Dissertation. University of Joensuu

Rocha LL, Cordeiro RDA, Cavalcante RM, Nascimento RFD, Martins SCS, Santaella ST, Melo VMM (2007) Isolation and characterization of phenol degrading yeasts from an oil refinery wastewater in Brazil. *Mycopathol*. 164: 183-188.

Roostaei N, Tezel FH (2004) Removal of phenol from aqueous solutions by adsorption J *Environ Manage* 70:157-64.

Roy G, Bernatchez G, Sauve R (1998) Halide and alkyl phenols block volume sensitive chloride channels in human glial cells (U-138MG) *J Memb Biol* 162: 191 -200.

Rubalcaba A, Sua´ rez-Ojeda M E, Stuber F, Fortuny A, Bengoa C, Metcalfe I, Font J, Carrera J, Fabregat A (2007) Phenol wastewater remediation: advanced oxidation processes coupled to a biological treatment. *Wat Sci Technol* 55 :221–227.

Sadiq IM, Dalai S, Chandrasekaran N, Mukherjee A (2011) Ecotoxicity of Titania NPs on two microalgae species: *Scenedesmus* sp. and *Chlorella* sp. *Ecotoxicol Environ Saf* 74: 1180-1187.

Saha NC, Bhunia F, Kaviraj A (1999) Toxicity of phenol to fish and aquatic ecosystems. *Environ Contam Toxicol* 63: 195-202.

Sahoo NK, Ghosh PK, Pakshirajan K (2011) Kinetics of 4-bromophenol degradation using calcium alginate immobilized *Arthrobacter chlorophenolicus* A6. *Int J Earth Sci Eng* 4: 663-668.

Santos VL, Linardi VR (2004) Biodegradation of phenol by a filamentous fungi isolated from industrial effluents-identification and degradation potential. *Process Biochem* 39: 1001-1006.

Saravanan P, Pakshirajan K, Saha P (2008) Growth kinetics of an indigenous mixed microbial consortium during phenol degradation in a batch reactor. *Bioresour Technol* 99: 205-209.

Schevenko A, Wilm M, Vorm O, Mann M (1996) Mass spectrometric sequencing of proteins silver-stained polyacrylamide gels. *Anal Chem* 68: 850-858.

Schie PMV, Young LY (2015) Biodegradation of phenol: Mechanism and applications. *Bioremediat J* 4:1-18.

Schramm JR (1914) Some pure culture methods in algae. *Ann Mo Bot Gard* 1:23-45.

Scott AS, Davey MP, Dennis JS, Horst I, Howe CJ, Lea-Smith DJ, Smith AG (2010) Biodiesel from algae: challenges and prospects. *Curr Opin Biotechnol* 21:277-286.



Scragg A H (2006) The effect of phenol on the growth of *Chlorella vulgaris* and *Chlorella* VT-1. *Enzym Microb Technol* 39: 796-799.

Semple KT, Cain RB (1996) Biodegradation of phenol by algae *Ochromonas danica*. *Appl Environ Microbiol* 62: 1265-1273.

Senthivelan T, Kanagaraj J, Panda RC, Mandal AB (2014) Biodegradation of phenol by mixed microbial culture: an ecofriendly approach for pollution reduction. *Clean Techn Environ Policy*. 16: 113-126.

Sharma KK, Schuhmann H, Schenk PM (2012) High lipid induction in microalgae for biodiesel production. *Energies* 5:1532-1553.

Sharma N, Gupta VC (2012) Batch biodegradation of phenol of paper and pulp effluent by *Aspergillus niger*. *Int J Chem Eng Apl* 3: 182-186.

Sharma N, Gupta VC (2012) Batch biodegradation of phenol of paper and pulp effluent by *Aspergillus niger*. *Int J Chem Eng Appl* 3:182-186.

Sidlecka EM, Stolte S, Golebiowski M, Nienstedt A, Stepnowski P, Thoming J (2012) Advanced oxidation process for the removal of ionic liquids from water: The influence of functionalized side chains on the electrochemical degradability of imidazolium cations. *Sep Purif Technol* 101: 26-33.

Sikkema J, Bont J.A.M.D, Poolman B (1995) Mechanism of membrane toxicity of hydrocarbons. *Microbiol Rev* 59: 201-222.

Siva E, Campos J. Biological phenol degradation by immobilized cells of *Pseudomonas putida* in a three phase fluidized bioreactor. <http://www.bvsde.paho.org> Accessed on 7<sup>th</sup> January 2016.

Song Z, Huang G (2007) Toxic effects of pentachlorophenol on *Lemna polyrhiza*. *Ecotoxicol Environ Saf* 66: 343-347.

Srivastava N, Sharma N (2014) Bioremediation of phenol from Tannery effluents by *Syncephalastrum racemosum*. Int J Res Chem Environ 4: 31-35.

Stiborova M, Sucha V, Miksanova M., Paca, J.Jr, Paca J (2003) Hydroxylation of phenol to catechol by *Candida tropicalis*: involvement of cytochrome P450. Gen. Physiol. Biophys. 22: 167-179.

Stoilova I, Krastanov A, Stanchev V, Daniel D, Gerginova M, Alexieva Z (2006). Biodegradation of high amounts of phenol, catechol, 2,4-dichlorophenol and 2,6-dimethoxyphenol by *Aspergillus awamori* cells. Enzyme Microb. Technol. 39: 1036–1041.

Storm DI, Roth R (1981) Some effects of polyphenol on aquatic plants: I. Toxicity of phenol in aquatic plants. Bull Environ Contam Toxicol 27: 332-337.

Sumathi S, Dasgupta D (2006) Effect of denaturants on the structure and activity of 3-hydroxybenzoate-6-hydroxylase. Indian J Biochem Biophys 43:148-153.

Sun JQ, Xu L, Tang YQ, Chen FM, Wu XL (2012) Simultaneous degradation of phenol and n-hexadecane by *Acinetobacter* strains. Bioreour Technol 123: 664-668.

Supriya C, Neehar D (2014) Biodegradation of phenol by *Aspergillus niger*. IOSR J Pharm 4:11-17.

Tabib A, Haddadi A, Shavandi M, Soleimani M, Aziznikoo P (2012) Biodegradation of phenol by newly isolated phenol degrading bacterium *Ralstonia* sp. strain PH-S1. J Petrol Sci Eng 2: 58-62.

Trigo A, Valencia A, Cases I (2009). Systemic approaches to biodegradation. FEMS Microbiol.Rev. 33: 98–108.

Tsai SC, Tsai LD, Li YK (2005) An isolated *Candida albicans* TL3 capable of degrading phenol at large concentration. Biosci.Biotechnol. Biochem. 69: 2358-2367.

Tsai SY, Juang RS (2006) Biodegradation of phenol and sodium salicylate mixtures by suspended *Pseudomonas putida* CCRC 14365. J. Hazard.Mater. 138: 125–132.

Turek M, Vilimkova L, Kremlackova V, Paca Jr. J, Halecky M, Paca J, Stiborova M (2011) Isolation and partial characterization of extracellular NADPH-dependent phenol hydroxylase oxidizing phenol to catechol in *Comamonas testosteroni*. Neuroendocrinol. Lett. 32:137-145.

Tziotzios G, Teliou M, Kaltsouni V, Lyberatos G, Vayenas DV (2005). Biological phenol removal using suspended growth and packed bed reactors. Biochem Eng J 26: 65–71.

Ucun H, Yildiz E, Nuhoglu A (2010) Phenol biodegradation in a batch jet loop bioreactor (JLB): Kinetics study and pH variation. Bioresour Technol 101: 2965–2971.

Udaysoorian C, Prabu PC (2005) Biodegradation of phenols by lignolytic fungus *Trametes versicolor*. J Biol Sci 5:824-827.

Uddin MT, Islam MS, Abedin M Z (2007) Adsorption of phenol from aqueous solution by water hyacinth ash ARPN J Engg Appl Sci 2: 11-17.

Varsha YM, Naga CH Deepthi, Chenna S (2011) An emphasis on xenobiotic degradation in environmental clean up. J Bioremed Biodegrad <http://dx.doi.org/10.4172/2155-6199.S11-001>

Verma SR, Rani S, Tyagi AK, Dalela RC (1980) Evaluation of acute toxicity of phenol and its chloro-and nitro-derivatives to certain teleosts. Water Air Soil Pollut 14: 95-102.

Vijayagopal V, Viruthagiri T (2005) Batch kinetics in phenol biodegradation and comparison, Ind J Biotechnol 4: 565-67.

Vinita EM, Iyer PR (2013) Isolation, characterization of algae and production of biodiesel. Int J Res Rev Pharm Appl Sci 3: 321-330.

Wang L, Li Y, Yu P, Xie Z, Luo Y, Lin Y (2010) Biodegradation of phenol at high concentration by a novel fungal strain *Paecilomyces variotii* JH6. J Hazard Mater 183:366-371.

Wang Y, Tian Y, Han B, Zhaw H B, Bi J N, Cai, B L (2007) Biodegradation of phenol by free and immobilized *Acinetobacter* sp. strain PD12. J. Environ. Sci. 19: 222–225.

Webb JL (1963) Enzyme and Metabolic Inhibitors. Academic Press, USA.

Woertz I, Feffer A, Lundquist T, Nelson Y (2009) Algae grown on dairy and municipal wastewater for simultaneous nutrient removal and lipid production for biofuel feedstock. *J Environ Eng* 135:1115-1122.

Wolski EA, Durruty I, Haure P, Gonzalez J (2012) *Penicillium chrysogenum*: Phenol degradation abilities and kinetic model. *Water Air Soil Poll* 223: 2323-2332.

Wu Y, Zhang H (2009) Biodegradation of synthetic high phenol contamination wastewater by an immersed membrane bioreactor Proceedings of International Conference on Environmental Science and Information Application Technology. pp. 143-147. <http://ieeexplore.ieee.org> Accessed on 7<sup>th</sup> January 2016.

[www.assam.climateps.com](http://www.assam.climateps.com). Accessed on 12<sup>th</sup> October 2015.

[www.nih.ernet.in](http://www.nih.ernet.in). Accessed on 5 January 2016

[www.oilgae.com](http://www.oilgae.com). Oilgae guide to algae based wastewater treatment. Accessed on 9<sup>th</sup> January 2016.

[www.response.restoration.noaa.gov](http://www.response.restoration.noaa.gov) Accessed 3 January 2016

[www.s67.com](http://www.s67.com) Affect of heavy metals on enzyme activity. Accessed on 9<sup>th</sup> January 2016.

Xu JQ, Duan WH, Zhou Xz, JZ (2006) Extraction of phenol in wastewater with annular centrifugal contactors. *J Hazard Mat* 131: 98–102.

Yabuuchi E, Kosako Y, Yano I, Hotta H, Nishiuchi Y (1995) Transfer of Two *Burkholderia* and an *Alcaligenes* Species to *Ralstonia* gen. nov.: Proposal of *Ralstonia pickettii* (Ralston, Palleroni and Douderoff 1973) comb. nov., *Ralstonia solanacearum* (Smith 1986) comb. nov. and *Ralstonia eutropha* (Davis, 1969) comb. nov. *Microbiol Immunol* 39:897-904.

Yan J, Jianping W, Hongmei Li, Suliang Y, Zongding H (2005) The biodegradation of phenol at high initial concentration by the yeast *Candida tropicalis*. *Biochem. Eng. J.* 24 : 243–47.

Yan J, Jianping W, Jing B, Daoquan W, Zongding H (2006). Phenol biodegradation by the yeast *Candida tropicalis* in the presence of *m*-cresol. *Biochem. Eng. J.* 29: 227–234.

Yang J S, Rasa E, Tantayotai P, Scow K M, Yuan H L, Hristova K R (2011) Mathematical model of *Chlorella minutissima* UTEX2341 growth and lipid production under photoheterotrophic fermentation conditions. *Bioresour Technol* 102: 3077-3082.

Yang J S, Rasa E, Tantayotai P, Scow K M, Yuan H L, Hristova K R (2011) Mathematical model of *Chlorella minutissima* UTEX2341 growth and lipid production under photoheterotrophic fermentation conditions. *Bioresour Technol* 102: 3077-3082.

Yano T, Nakahara T, Kamiyama, S, Yamada, K (1966) Kinetic studies on microbial activities in concentrated solutions I Effect of excess sugars on oxygen uptake rate of a cell free respiratory system. *Agric Biol Chem* 30: 42-48.

Ye F, Shen D (2004) Acclimation of anaerobic sludge degrading chlorophenols and the biodegradation kinetics during acclimation period. *Chemosphere* 54:1573-1580.

Yemendzhiev H, Gerginova M, Kranstanov A, Stoilova I, Alexieva Z (2008) Growth of *Trametes versicolor* on phenol. *J Ind Microbiol Biotechnol* 35:1309-1312.

Yu C, Fei C, Zhao X, Guo T, Lin R, Qu M, Liu Q (2011) Isolation, purification and degrading characteristics of phenol degrading bacteria B3. *Proceedings of International Conference on Electrical and Control Engineering (ICECE) 2011* doi: 10.1109/ICECENG.2011.6058317.

Zhao X, Wang Y, Ye Z, Borthwick AGL, Ni J (2006) Oil field wastewater treatment in Biological Aerated Filter by immobilized microorganisms. *Process Biochem.* 41: 1475-1483.

Zhou J, Yu X, Ding C, Wang Z, Zhou Q, Pao H, Cai W (2011) Optimization of phenol degradation by *Candida tropicalis* Z-04 using Plackett-Burman design and response surface methodology. *J Environ Sci* 23: 22-30.

Zhou, W (2014) Potential application of microalgae in wastewater treatments. In: Liu et al. (Ed) *Recent advances in microalgal biotechnology*. Omics ebooks Group, Hyderabad pp. 1-9.

Zhu C, Zhang L, Zhao L (2008) Molecular cloning, genetic organization of gene cluster encoding phenol hydroxylase and catechol 2,3-dioxygenase in *Alcaligenes faecalis* IS-46. *World J Microbiol Biotechnol* 24:1687-1695.

## Publications

### Thesis Publications

### Journal Publications

**Bhaskar Das**, Tapas K Mandal, Sanjukta Patra. A comprehensive study on *Chlorella Pyrenoidosa* for phenol degradation and its potential applicability as biodiesel feedstock and animal feed. Applied Biochemistry and Biotechnology, 2015, Springer US, 176, 1382-1401.

**Bhaskar Das**, Tapas K Mandal, Sanjukta Patra. Biodegradation of phenol by a novel diatom BD1IITG-kinetics and biochemical studies. International Journal of Environmental Science and Technology, 2016, Springer Berlin Heidelberg, 13, 529-542.

**Bhaskar Das**, Gowtham Selvaraj, Sanjukta Patra. Exploiting phenol polluted wastewaters for clean energy generation: an environment friendly approach (Communicated).

**Bhaskar Das**, Sanjukta Patra. Multisubstrate specific Flavin containing monooxygenase from *Chlorella pyrenoidosa* with potential application for remediation of phenolic wastewaters and phenolic biosensor (Communicated).

**Bhaskar Das**, Sanjukta Patra. Mixotrophic cultivation of microalgae on wastewater stream: a sustainable strategy for bioenergy generation (Manuscript in pipeline).

### Process Patent

**Bhaskar Das**, Sanjukta Patra. An environmentally sustainable algal process for remediation of phenol pollution coupled to clean energy production. (Patent application no: 201631023382, dated: 8/7/2016, Govt. of India)

### Conference Papers

**Bhaskar Das**, Tapas K Mandal, Sanjukta Patra. Pathway of phenol degradation in *Chlorella pyrenoidosa*. Young Ecologists Talk and Interact, IIT Guwahati, December 13-15, 2011 (Poster presentation).

**Bhaskar Das**, Tapas K Mandal, Sanjukta Patra. Microalgae in bioremediation of organic pollutants. One day symposium on Environment and Us. IIT Guwahati. 5th June 2012 (Poster Presentation).

**Bhaskar Das**, Tapas K Mandal, Sanjukta Patra. Phenol degradation by *Chlorella Pyrenoidosa*. Proceedings of International Conference on Algal Biorefinery: A potential source of Food, Feed, Biochemicals and Biofertilizers, Pg. 32. January 10-12, 2013, IIT Kharagpur (Poster presentation).

**Bhaskar Das**, Tapas K Mandal, Sanjukta Patra. Characterization of phenol degradation by a novel diatom species BD1IITG isolated from petroleum refinery wastewater. Proceeding of National Conference on sustainable development of environmental systems. Pg-30. IIT Guwahati. June 20-21, 2014 (Oral Presentation).

**Bhaskar Das**, Gowtham Selvaraj, Tapas K Mandal., Sanjukta Patra. Biodegradation of phenol by microalgae. Proceeding of National Conference on sustainable development of environmental systems. Pg-75. IIT Guwahati. June 20-21, 2014 (Poster Presentation).

**Bhaskar Das**, Tapas K Mandal, Sanjukta Patra. Isolation and growth kinetics of a phenol degrading novel diatom species BD1IITG. 64th Canadian Chemical Engineering Conference. Niagara Falls, Canada, October 19-22, 2014 (Oral Presentation).

**Bhaskar Das**, Tapas K Mandal, Sanjukta Patra. Performance evaluation of phenol degradation by *Chlorella pyrenoidosa* in nutrient sufficient media and refinery wastewater through kinetic modeling. 64<sup>th</sup> Canadian Chemical Engineering Conference. Niagara Falls, Canada, October 19-22, 2014 (Oral Presentation).

**Bhaskar Das**, Sanjukta Patra. Mechanism of phenol degradation in *Chlorella Pyrenoidosa*. Asian Plant Science Conference. 1-3rd November 2014, Lumbini, Nepal. (Oral Presentation).

Gowtham Selvaraj, **Bhaskar Das**, Sanjukta Patra. Recent advances in algal biodiesel production. Asian Plant Science Conference. 1-3rd November 2014, Lumbini, Nepal. (Oral Presentation).

**Bhaskar Das**, Tapas K Mandal, Sanjukta Patra. Characterization of phenol degradation in *Chlorella Pyrenoidosa*. Research Scholars Day 2015, 19th January, IIT Guwahati. (**Best Oral Presentation**).

**Bhaskar Das**, Tapas K Mandal, Sanjukta Patra. Kinetics and enzymatic mechanism of microalgal phenol degradation. Proceedings of National Conference on Challenges in Environmental Research, Pg. 30, June 4-6, 2015, IIT Guwahati. (Oral Presentation).

### **Award**

**1st Prize for oral presentation** of research paper entitled “Characterization of phenol degradation by microalgae” at Research Scholar Day 2015, 19<sup>th</sup> January 2015, IIT Guwahati .

### **Journal Papers (Other than thesis work)**

Swagata Patra, **Bhaskar Das**, Sanjukta Patra. Natural compounds as scaffold for screening of MMP1 inhibitors for therapeutics. (Communicated).

**Bhaskar Das**, Debasree Kundu, Karthikeya Gupta, Sanjukta Patra. Nitrate limited phenol remediation and generation of biodiesel feedstock (Manuscript in pipeline).

**Bhaskar Das**, Karthikeya Gupta, Sanjukta Patra. Stress induced generation of algal biodiesel feedstock with high neutral lipid content (Manuscript in pipeline).

Swagata Patra, **Bhaskar Das**, Sanjukta Patra. Virtual Screening for novel MMP 9 inhibitors (Manuscript in pipeline).

### **Book Chapters (Other than thesis work)**

**Bhaskar Das**, Sanjukta Patra. Antimicrobials: Meeting challenges of antibiotic resistance through nanotechnology. In: Grumezescu AM (ed) Therapeutic Nanostructures, Elsevier (Accepted for publication).

Nitendra Yadav, **Bhaskar Das**, Sanjukta Patra. Drug resistance in tuberculosis: nanomedicines at rescue. In: Grumezescu AM (ed) Nanostructures in therapeutic medicine, Elsevier (Accepted for Publication).

Nitendra Yadav, **Bhaskar Das**, Sanjukta Patra. Biosensors for Mycobacteria. In: Grumezescu AM (ed) Pharmaceutical Nanotechnology, Elsevier (Chapter proposal accepted, In pipeline).



### **Conference Paper (Other than thesis work)**

**Bhaskar Das**, Mukesh K. Meher, Sanjukta Patra. Bioinformatics: An Environmental perspective. One day symposium on Environment and Us. IIT Guwahati. 5<sup>th</sup> June 2012.

Swagata Patra, **Bhaskar Das**, Nivedita Singh, Sanjukta Patra. Natural flavonoids as inhibitors for Matrix Metalloproteinase 1. Research Conclave. 17-20<sup>th</sup> March 2016, IIT Guwahati (Poster Presentation).

### **Workshop and Seminars**

Workshop on Environment and Development: New Frontiers of Research in North East India. IIT Guwahati. January 3-4, 2014.

Summer School on Efficient Fossil Energy Technologies. IIT Guwahati. July 4-10, 2012.

Lecture series on Advances in Seribiotechnology. IIT Guwahati 25<sup>th</sup> April 2012.

